Die approbierte Originalversion dieser Dissertation ist an der Hauptbibliothek der Technischen Universität Wien aufgestellt (http://www.ub.tuwien.ac.at).

The approved original version of this thesis is available at the main library of the Vienna University of Technology (http://www.ub.tuwien.ac.at/englweb/).

TECHNISCHE UNIVERSITÄT WIEN

VIENNA UNIVERSITY OF TECHNOLOGY

DISSERTATION

Synthesis, Characterization and catalytic Activity of P-N Bond containing Transition Metal Pincer Complexes

ausgeführt zum Zwecke der Erlangung des akademischen Grades eines Doktors der Naturwissenschaften unter der Leitung von

Ao. Univ. Prof. DI Dr. techn. Karl Kirchner

Institut für Angewandte Synthesechemie 163/AC

eingereicht an der Technischen Universität Wien

Fakultät für Technische Chemie

von

M. Sc. David Benito-Garagorri

Matr. Nr. 0126246

Kampstrasse 8/11

1200 Wien

Wien, am 19. Februar 2007

Abstract

The first part of this work deals with the synthesis of tridentate PNP, PCP and NPN pincer ligands and of bidentate PN ligands with phosphines as two-electron donor groups and secondary amines as spacers between the aromatic backbone and the phosphines. The preparation of the ligands proceeds via a condensation reaction between the amino groups of the aromatic backbone and electrophilic chlorophosphines (and chlorophosphites) resulting in the formation of aminophosphine (or phosphoramidite) moieties. Several chlorophosphites were synthesized from diols and aminoalcohols and PCl_3 in order to dispose of an array of electrophilic phosphines with different steric, electronic and stereochemical properties. By using 2,6-diaminopyridine and 1,3-diaminobenzene as precursors, both neutral PNP as well as anionic PCP pincer ligands are accessible with just a small modification in the aromatic backbone. Furthermore, PN and NPN ligands were prepared starting from 2-aminopyridine.

Following the preparation of the ligands, the second part of this work describes the synthesis and characterization of several iron, nickel, palladium and platinum complexes obtained by the reaction of these ligands with different transition metal precursors.

In the case of iron, diamagnetic, hexacoordinated tris(acetonitrile) PNP complexes were obtained when the PNP ligands and $[Fe(H_2O)_6](BF_4)_2$ were reacted in acetonitrile. The acetonitrile ligands in these complexes are labile, and they can be easily displaced by chelating nitrogen donor ligands and carbon monoxide. Attempts to obtain zerovalent iron PNP complexes were unsuccessful due to the acidity of the amino bridging protons, which hamper the reduction of the metal center. Additionallly, paramagnetic, pentacoordinated iron(II) complexes of the formula $[Fe(PNP)Cl_2]$ were obtained from the reaction of PNP ligands containing basic, bulky phosphines with $FeCl_2$. The two chlorine atoms in these complexes can be abstractedin acetonitrile in the presence of silver salts to give hexacoordinated, diamagnetic, tris(acetonitrile) complexes. The reaction of $Fe(CO)_4Br_2$ with the phenyl substituted ligand PNP-Ph in the presence of $NaBPh_4$ resulted in the formation of the cationic, dicarbonyl complex $[Fe(PNP\text{-}Ph)(CO)_2Br]Br$. The use of a halide scavenger in this reaction is important in order to shift the substitution reaction towards the displacement of a bromine atom rather than of a carbonyl group. Several iron(II) PN complexes were also synthesized from the same metal precursors.

With nickel, palladium and platinum, both cationic and neutral tetracoordinated complexes were obtained with the PNP and PCP ligands, respectively. The characterization of these complexes revealed that they are structurally very similar to analogous pincer complexes reported in the literature. However, in some cases different reactivities were observed, which led to the formation of unexpected products (e.g. nickel(II) pentacoordinated complexes, see Section 3.3.2). Nickel and palladium PN complexes were also prepared; in the case of the

nickel complexes, their characterization revealed that they possess different coordination geometries in the solid state and in solution, a feature that was supported by means of theoretical calculations. Moreover, η^1- and η^3-palladium allyl PN complexes were synthesized by reacting the dimeric precursor $[Pd(allyl)(CH_3CN)_2](BF_4)_2$ with the PN ligands in the absence and in the presence of a silver salt as halide scavenger.

Finally, the catalytic activity of several transition metal pincer complexes was tested in different coupling reactions. The iron PNP pincer complexes were tested as catalysts in the coupling of aromatic aldehydes with ethyl diazoacetate (EDA). They turned out to be extremely effective and chemoselective catalysts, giving 3-hydroxyacrylates as the main products. Mechanistic investigations based on DFT/B3LYP calculations were performed for this catalytic system, which made it possible to discard unlikely mechanisms for the catalytic cycle and to suggest a plausible one. Furthermore, the palladium PNP and PCP pincer complexes were tested as catalysts in the Suzuki-Miyaura coupling of aryl and alkyl bromides with phenylboronic acid; while the PNP complexes turned out to be mediocre catalysts, the PCP complexes showed very high activities and were able to catalyze the coupling of neutral, activated and deactivated substrates with phenylboronic acid even at catalyst loadings as low as 0.00001 mol%.

Kurzfassung

Im Zuge dieser Arbeit wurden neue Tridentat PNP, PCP und NPN Pincer Liganden und Bidentat PN Liganden synthetisiert. Die Liganden wurden im Baukastensystem durch Kondensationsreaktionen von aromatischen Diaminen (2,6-Diaminopyridin und 1,3-Diaminobenzol) und Aminen (2-Aminopyridin) und einer Reihe von Chlorphosphinen und Chlorphosphiten hergestellt. Die nicht käuflichen Chlorphosphine wurden durch Umsetzung von achiralen und chiralen Diolen und Aminoalkoholen mit Phosphortrichlorid erhalten.

Aus den Pincer Liganden wurden durch Umsetzung mit diversen Eisen-, Nickel-, Palladium- und Platin-Komplexen eine Reihe neuer metallorganischer Verbindungen vom Typ [PXPML_n] (X: N, C; M: Fe, Ni, Pd, Pt; Ln: CH_3CN, CO, Cl, Br, CF_3COO^-) erhalten.

In weiterer Folge wurden ausgewählte im Rahmen dieser Arbeit synthetisierte Komplexe auf ihre katalytischen Aktivitäten in diversen Reaktionen getestet. Eisen(II) Pincer Komplexe zeigten sich als ausgezeichnete und chemoselektive Katalysatoren für die Umsetzung von aromatischen Aldehyden mit Diazoessigsäureethylester (EDA) zu 3-Hydroxyacrylaten. Mit Hilfe von DFT/B3LYP Berechnungen wurde ein plausibler Mechanismus für die Reaktion vorgeschlagen.

Darüber hinaus wurden Palladium(II)- PNP- und PCP- Pincer-Komplexe auf ihre Tauglichkeit als Katalysatoren für die Suzuki-Miyaura Kupplung von Aryl- und Alkylbromiden mit Phenylboronsäure untersucht. Während die kationischen [Pd(PNP)Cl]X (X: Cl, OTf) Komplexe nur mittelmässige Ergebnisse lieferten, zeigten die neutralen [Pd(PCP)X] (X: Cl, TFA) Komplexe sehr hohe katalytische Aktivitäten bei der Umsetzung von neutralen, deaktivierten und aktivierten Substraten mit Phenylboronsäure.

Leo: Let’s do this right.

Josh: Not much chance of that.

(The West Wing, Season 1, episode 3, 1999.)

1 INTRODUCTION AND SCOPE 1

2 GENERAL CONSIDERATIONS 4

2.1 PINCER LIGANDS 4
2.2 PHOSPHINES 5
2.3 AMINOPHOSPHINES 8
2.4 TRANSITION METAL PINCER COMPLEXES 11
2.5 APPLICATIONS OF TRANSITION METAL PINCER COMPLEXES 16
2.5.1 CATALYSIS 16
2.5.2 COORDINATION AND ACTIVATION OF SMALL MOLECULES 19
2.5.3 C-H, C-C AND C-O BOND ACTIVATION 22
2.5.4 SUPRAMOLECULAR CHEMISTRY 25

3 RESULTS AND DISCUSSION 27

3.1 LIGANDS 27
3.1.1 INTRODUCTION 27
3.1.2 CHLOROPHOSPHITES 29
Synthesis 29
Characterization 31
3.1.3 PNP LIGANDS 32
Synthesis 32
Characterization 35
3.1.4 PCP LIGANDS 38
Synthesis 38
Characterization 39
3.1.5 PN LIGANDS 41
Synthesis 41
Characterization 42
3.1.6 NPN LIGANDS 43
Synthesis 43
Characterization 44
3.2 IRON COMPLEXES 45
3.2.1 INTRODUCTION 45
3.2.2 PRECURSORS 47
3.2.3 IRON(II) PNP COMPLEXES FROM $[Fe(H_2O)_6](BF_4)_2$ 50
Iron(II) Tris(acetonitrile) PNP Complexes 50
Synthesis 50
Characterization 52

Lability of the Acetonitrile Ligands **56**
Synthesis 56
Characterization 59
Reduction attempts **63**
3.2.4 IRON(II) PNP COMPLEXES FROM $FE(CO)_4BR_2$ 65
Synthesis 65
Characterization 66
3.2.5 IRON(II) PNP COMPLEXES FROM $FECL_2$ AND $FE(PY)_4CL_2$ 67
Synthesis 67
Characterization 68
3.2.6 IRON(II) PN COMPLEXES 71
Synthesis 71
Characterization 73
3.2.7 IRON(II) NPN COMPLEXES 75
Synthesis 75
Characterization 76
3.2.8 IRON (II) CATALYZED COUPLING OF AROMATIC ALDEHYDES WITH EDA 77
3.2.9 SUMMARY 88
3.3 NICKEL, PALLADIUM AND PLATINUM COMPLEXES **89**
3.3.1 INTRODUCTION 89
3.3.2 NICKEL COMPLEXES 93
Tetracoordinated Nickel(II) PNP Complexes **93**
Synthesis 93
Characterization 94
Pentacoordinated Nickel(II) PNP Complexes **97**
Synthesis 97
Characterization 99
Mechanistic Investigations 103
Nickel PCP Complexes **108**
Synthesis 108
Characterization 109
Nickel PN complexes **113**
Synthesis 113
Characterization 113
Mechanistic Investigations 115
3.3.3 PALLADIUM AND PLATINUM COMPLEXES 116
Palladium and platinum PNP Complexes **116**
Synthesis 116
Characterization 118
Palladium and platinum PCP complexes **124**

Synthesis 124
Characterization 126
Palladium PN complexes 132
Synthesis 132
Characterization 137
3.3.4 PALLADIUM(II) CATALYZED SUZUKI COUPLING 137
Catalytic Activity of the Pd(II) PNP Complexes 139
Catalytic activity of the Palladium(II) PCP Complexes 142
3.3.5 SUMMARY 145
3.4 COPPER(I) CATALYZED FORMATION OF OXAZOLINES AND N-SULFONYL-2-IMIDAZOLINES 147

4 EXPERIMENTAL SECTION 152

4.1 ABBREVIATIONS 152
4.2 GENERAL 153
4.3 COMPUTATIONAL DETAILS 153
4.4 METAL PRECURSORS 154
4.5 PHOSPHITES 156
4.6 LIGANDS 159
4.6.1 PNP LIGANDS 159
4.6.2 PCP LIGANDS 164
4.6.3 PN LIGANDS 166
4.6.4 NPN LIGANDS 169
4.7 COMPLEXES 170
4.7.1 IRON(II) PNP COMPLEXES 170
4.7.2 IRON(II) PN COMPLEXES 179
4.7.3 TETRACOORDINATED NICKEL(II) PNP COMPLEXES 182
4.7.4 PENTACOORDINATED NICKEL(II) PNP COMPLEXES 184
4.7.5 NICKEL(II) PCP COMPLEXES 187
4.7.6 NICKEL(II) PN COMPLEXES 189
4.7.7 PALLADIUM (II) PNP COMPLEXES 189
4.7.8 PALLADIUM(II) PCP COMPLEXES 194
4.7.9 PALLADIUM(II) PN COMPLEXES 198
4.7.10 PLATINUM(II) PNP COMPLEXES 202
4.7.11 PLATINUM(II) PCP COMPLEXES 205
4.8 CATALYTIC REACTIONS 206
4.8.1 IRON(II) CATALYZED COUPLING OF AROMATIC ALDEHYDES AND EDA 206
4.8.2 PALLADIUM(II) CATALYZED SUZUKI-MIYAURA COUPLING 209
4.8.3 COPPER(I) CATALYZED SYNTHESIS OF OXAZOLINES AND N-SULFONYL-2-IMIDAZOLINES 209
4.9 CRYSTALLOGRAPHIC DATA 210

1 Introduction and scope

One of the most important goals in inorganic and organometallic chemistry is to design well defined ligand systems with which the different properties of metal centers can be accurately controlled. There are several methods to achieve this goal, one of which is chelation, that is, the binding of a ligand to a metal through two or more bonds. Among the many chelating ligands that can be found in the chemical literature, pincer ligands[1] and their complexes have attracted increasing interest due to the unusual properties of the metal centers imparted by the pincer ligands. The first pincer ligands and complexes were synthesized in the late 1970s[2], but this area remained relatively unexplored for almost twenty years, until in the late 1990s several applications of pincer complexes in the fields of catalysis, molecular recognition and supramolecular chemistry turned this area into one of the most intensively researched subjects nowadays[3].

These so-called pincer ligands, named after their particular coordination mode to metal centers (Figure 1), are tridentate ligands featuring an aromatic backbone (benzene, pyridine) bound to two-electron donor groups (E) by a spacer A. Pincer ligands coordinate to the metal center via the two-electron donor groups and metal-carbon (benzene-based pincer complexes) or metal-nitrogen (pyridine-based pincer complexes) σ bonds.

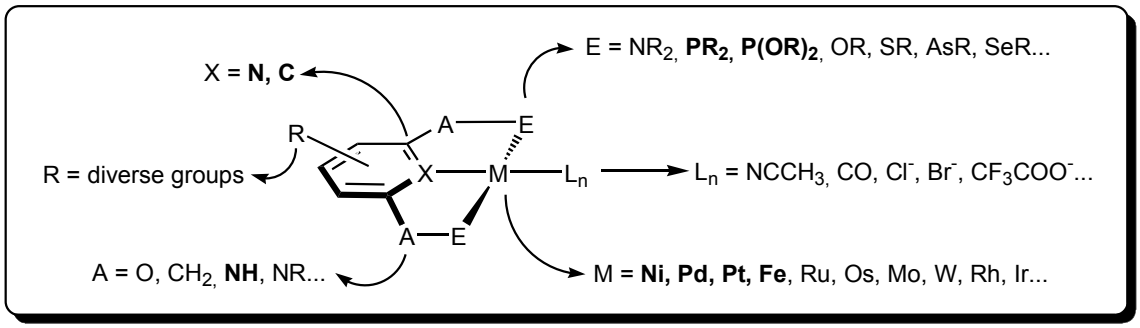

Figure 1. Schematic structure of pincer complexes

---

[1] van Koten, G. *Pure Appl. Chem.* **1989**, *61*, 1681.

[2] (a) Nelson, S. M.; Dahlhoff, W. V. *J. Chem. Soc. A* **1971**, *13*, 2184. (b) Moulton, C. J.; Shaw, B. L.; *J. Chem. Soc. Dalton Trans.* **1976**, 1020. (c) van Koten, G.; Timmer, K.; Noltes, J. G.; Spek, A. L. *J. Chem. Soc. Chem. Commun.* **1978**, 250. (d) van Koten, G.; Jastrzebski, J. T. B. H.; Noltes, J. G. *J. Organomet. Chem.* **1978**, *148*, 233. (e) Creaser, C. S.; Kaska, W. C. *Inorg. Chim. Acta* **1978**, *30*, L325. (f) Rimml, H.; Venanzi, L. *J. Organomet. Chem.* **1983**, *259*, C6.

[3] For reviews concerning pincer ligands and complexes, as well as their different applications, see: (a) Albrecht, M.; van Koten, G. *Angew. Chem. Int. Ed.* **2001**, *40*, 3750. (b) van der Boom, M.; Milstein, D. *Chem. Rev.* **2003**, *103*, 1759. Singleton, J. T. *Tetrahedron* **2003**, *59*, 1837 and references therein.

One of the most important advantages of pincer ligands and their complexes is their variability and the possibility of performing their synthesis via a modular assembly pathway. Thus, by modifying the aromatic backbone (R, X), the donor groups (E), the spacers (A) and even the metal center (M), it is possible to fine-tune the electronic, steric and stereochemical properties of the complexes.

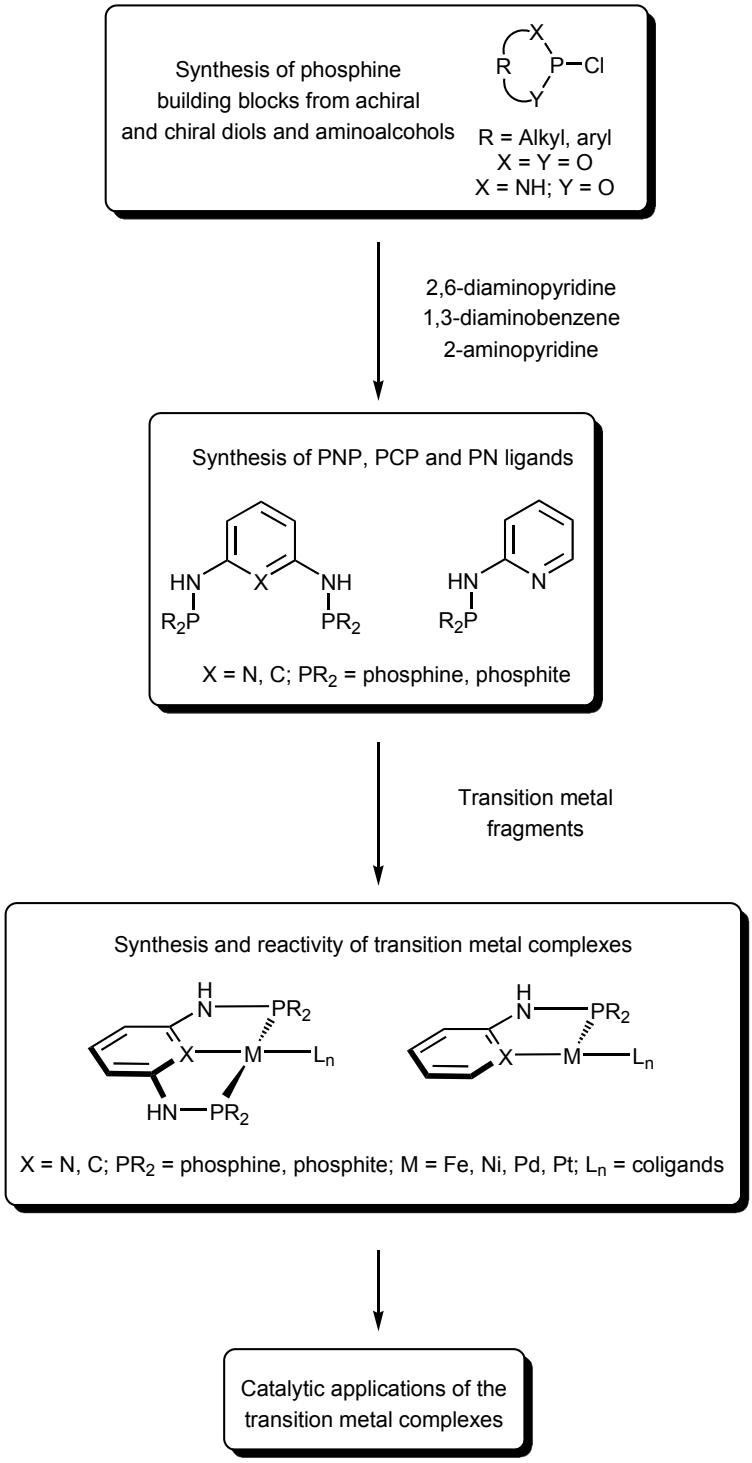

Scheme 1. Goals of this work

The objectives of this work are depicted in Scheme 1; the first one was to prepare the chlorophosphine and chlorophosphite building blocks starting from achiral and chiral diols and aminoalcohols. Using these electrophilic phosphines and different aromatic backbones, such as 2,6-diaminopyridine, 1,3-diaminobenzene and 2-aminopyridine, the goal was to synthesize and characterize an array of tridentate PNP, PCP and NPN pincer ligands and of bidentate PN ligands. Furthermore, the reactivity of these ligands towards different iron, nickel, palladium and platinum precursors, as well as the reactivity of the complexes in several reactions, such as reduction and ligand substitution reactions, was to be investigated.

Finally, the catalytic activity of the pincer complexes was to be investigated in several coupling reactions, such as the Suzuki-Miyaura coupling of aryl halides with phenylboronic acids and the Lewis acid catalyzed coupling of aromatic aldehydes with ethyldiazoacetate (EDA).

2 General Considerations

2.1 Pincer Ligands

Pincer ligands comprise a central aromatic ring, coordinating to the metal *via* the *ipso* atom, which is *ortho, ortho*-disubstituted with heteroatom, two electron donor substituents (E), which coordinate to the metal center (Figure 2). These substituents can be tethered to the central aromatic backbone by different spacers (A), such as methylene groups ($-CH_2-$), amines (-NR-) or oxygen atoms (-O-). The (un)substituted aromatic ring can be either a pyridine ring (X=N) or a benzene ring (X=C); thus, both neutral and anionic pincer ligands can be obtained. As for the neutral lone pair donors E, they are typically amines (NR_2), phosphines (PR_2), phosphites ($P(OR)_2$), ethers (OR), thioethers (SR), and even N-heterocyclic carbenes (NHCs), arsines (AsR_2) and selenoethers (SeR). Both donor groups need not be identical, and systems with two different donor atoms have been reported[4].

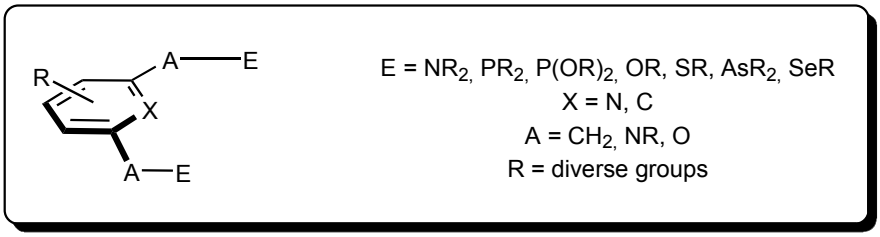

Figure 2. Schematic structure of pincer ligands

Thus, a wide variety of different EXE pincer ligands are accessible by modifying one or more of the parameters in the general structure of the ligand, i.e. the donor groups, the aromatic ring and its substitution and the spacer groups. The nomenclature employed with pincer ligands usually refers to the atoms that coordinate to the metal center: for example, a PNP ligand has phosphines as donor groups and a pyridine ring as backbone, and a NCN ligand coordinates *via* two amino groups and the *ipso* carbon atom of the central benzene ring. Some examples of different kinds of pincer ligands are shown in Figure 3.

---

[4] (a) Castonguay, A.; Sui-Seng, C.; Zaragarina, D.; Beauchamp, A. L. *Organometallics* **2006**, *25*, 602. (b) Danopoulos, A. A.; Tulloch, A. A. D.; Winston, S.; Eastham, G.; Hursthouse, M. B. *Dalton Trans.* **2003**, 1009. (c) Churruca, F.; SanMartin, R.; Tellitu, I.; Domínguez, E. *Tetrahedron Lett.*, **2006**, *47*, 3233. (d) Peveling, K.; Henn, M.; Loew, C.; Mehring, M.; Schuermann, M.; Costisella, B.; Jurkschat, K. *Organometallics* **2004**, *23*, 1501. (e) Yao, Q.; Sheets, M. *J. Org. Chem.* **2006**, *71*, 5384. (f) van Manen, H.-J.; Nakashima, K.; Shinkai, S.; Kooijman, H.; Spek, A. L.; van Veggel, F. C. J. M.; Reinhoudt, D. N. *Eur. J. Inorg. Chem.* **2000**, 2533.

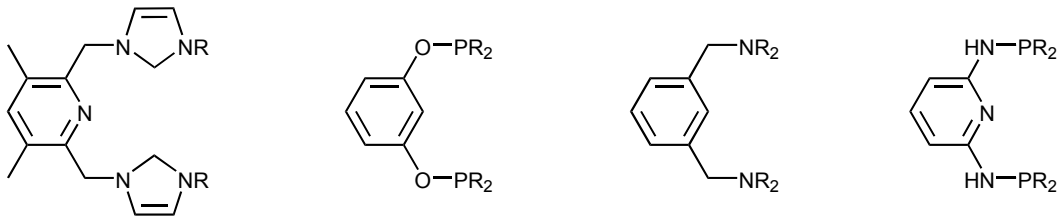

bis-NHC CNC | oxygen bridged PCP | methylene bridged NCN | amino bridged PNP

Figure 3. Examples of different types of pincer ligands

2.2 Phosphines

Tertiary phosphines of the type PR_3 (R = alkyl, aryl, OR', Cl, H) are employed in organometallic chemistry mostly as effective coligands in catalytic reactions. Not only are they easy to synthesize, but their modifiability is almost unending. Thus, their steric, electronic and even stereochemical properties can be readily tuned by an appropriate choice of the substituents.

Phosphines are two electron σ-donor/π-acceptor ligands, which donate electron density from their lone pair to an empty d-orbital of the metal center and simultaneously interact with filled d-orbitals of the metal center via their empty σ* orbitals. This binding mode is similar to that of carbonyl ligands, which allow π-backbonding to their π* orbitals (Figure 4).

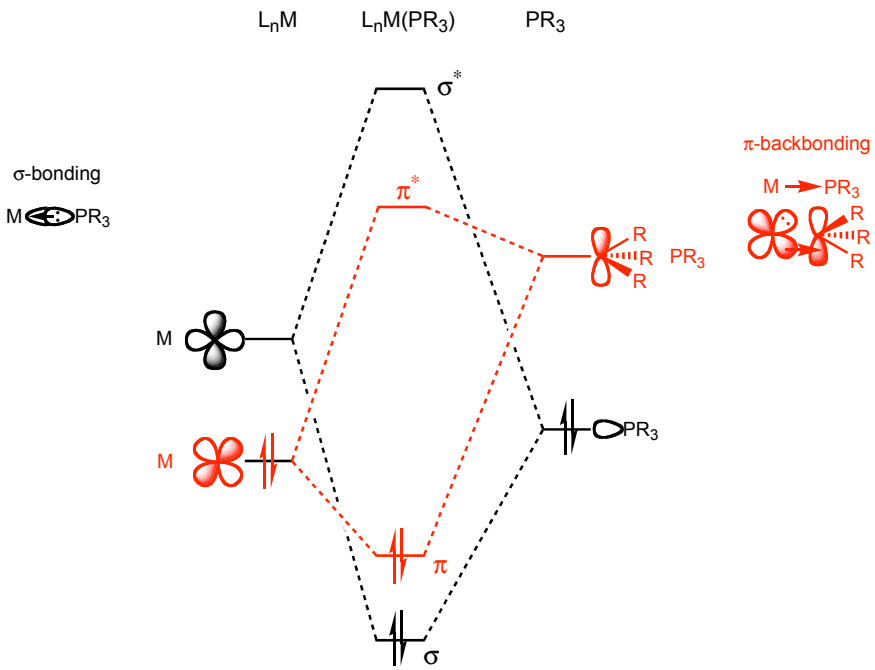

Figure 4. Molecular orbital model of phosphines and phosphine complexes

The donor/acceptor properties of phosphines vary with their electronic properties: electron withdrawing substituents at the phosphine decrease its σ donation and strengthen the σ-backbonding by reducing the energy of the σ* orbital. Thus, it is possible to order phosphines according to their increasing π-acidity and decreasing σ-donating properties (Figure 5). Alkylphosphines form the strongest σ bonds with the metal center, and trifluorophosphine, PF_3, is as strong a π-acceptor as carbon monoxide.

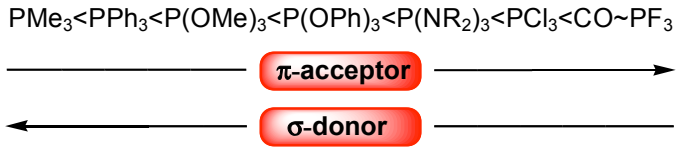

Figure 5. Classification of different phosphines according to their donor/acceptor properties

This classification was published by Tolman in 1977 in an article in which investigated the donor/acceptor properties of a great number of monodentate phosphines[5]. By substituting one carbonyl group of $Ni(CO)_4$ with different phosphines and by comparing the stretquing frequencies of the remaining carbonyl groups with infrared spectroscopy, it is possible to get an idea of the electron density at the metal center, that is, for the π-backbonding. The weaker the backbonding is, the weaker is the C-O triple bond, and the carbonyl stretquing is shifted towards smaller wave numbers.

In this paper, Tolman also reported a parameter to determine the space occupied by a coordinated phosphine (Tolman's cone angle Θ). For symmetric ligands, this parameter is defined as the apex angle of a cylindrical cone, centered 2.28 Å from the center of the phosphorus atom, which just touches the van der Waals radii of the outermost atoms of the model (**A**, Figure 6). For an unsymmetric phosphine $PR_1R_2R_3$, a model has to be used to minimize the sum of half-angles (**B**).

[5] Tolman, C. A. *Chem. Rev.* **1977**, *77*, 313.

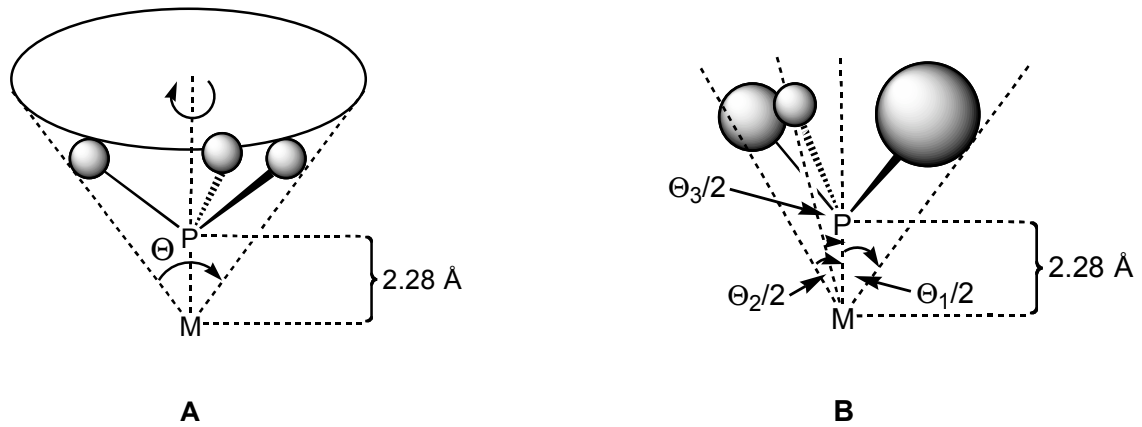

$$\Theta = (2/3)\sum_{i=1}^{3}\theta_i / 2$$

Figure 6. Determination of the steric parameter **Θ** for symmetric (left, **A**) and unsymmetric (right, **B**) phosphines

Another important advantage of phosphines is their detectability by $^{31}P\{^{1}H\}$ NMR spectroscopy. The NMR active isotope is a spin-1/2-nucleus and because of its 100% natural occurrence this method is highly sensitive, despite the fact that the sensitivity of the nucleus is only 6.6% of ^{1}H. Coordination to a metal center normally deshields the phosphorus and in combination with the coupling to ^{1}H and ^{13}C nuclei NMR spectroscopy is a powerful instrument for the characterization of phosphine containing ligands and complexes.

Noticeably, the $^{31}P\{^{1}H\}$ NMR shift of phosphines depends on the steric parameter Θ; the cone angles increase with a downfield shift of $\delta(^{31}P)$. The values of the cone angles and of the $^{31}P\{^{1}H\}$ NMR resonances of several phosphines are summarized in Table 1. This dependence is most significant in the case of phosphines (entries 1-10); in the case of phosphite ligands, the oxygens provide enough flexibility so that the OPO angles remain in the same range (entries 11-14).

Table 1. $^{31}P\{^{1}H\}$ NMR chemical shifts and cone angles of phosphines and phosphites

Entry	Phosphine	$^{31}P\{^{1}H\}$ (δ, [ppm])	Θ (º)
1	PH_3	-240	87
2	PF_3	97	104
3	PMe_3	-62	118
4	PCl_3	220	124
5	PEt_3	-20	132
6	PPr_3	-33	132
7	PPh_3	-6	145
8	$PiPr_3$	17	160
9	PCy_3	11	170
10	$PtBu_3$	61	182
11	$P(OMe)_3$	140	107
12	$P(OEt)_3$	138	109
13	$P(OiPr)_3$	137	130
14	$P(OtBu)_3$	138	172

2.3 Aminophosphines

Aminophosphines are an important part in the structure of the pincer ligands described in this work because amines were chosen as spacers between the central aromatic ring and the phosphines, which act as two-electron donor groups. Over the last years, aminophosphines with one or more P-N bonds have attracted increasing attention, mostly due to the ease of their synthesis and their variability[6]. Their preparation can be achieved by the stoichiometric reaction of a primary or secondary amine with electrophilic phosphines (mostly a chlorophosphine or a dichlorophosphine). Hydrochloric acid, which can be readily removed from the reaction mixture as ammonium hydrochloride, is a by-product of the reaction. Thus, a wide array of aminophosphines with different steric and electronic properties can be easily synthesized starting from inexpensive reagents. Chiral aminophosphines can be prepared by using chlorophosphites derived from chiral alcohols, aminoalcohols or amines. When one or more P-O bonds are present in addition to the P-N bond (as is the case when an amine is condensed with a chlorophosphine derived from an alcohol, for example), the functionality formed receives the name phosphoramidite (Figure 7).

[6] For a review on aminophosphines, see: Ansell, J.; Wills, M. *Chem. Soc. Rev.* **2002**, *31*, 259 and references therein.

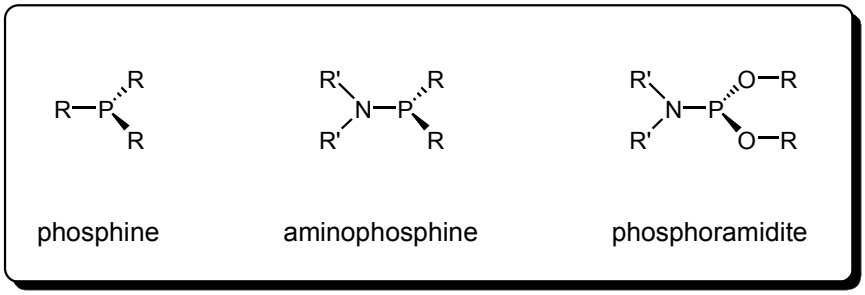

Figure 7. Structure of phosphines, aminophosphines and phosphoramidites

Aminophosphines can act as monodentate ligands, where only the phosphino- group coordinates to the metal center (**A**, Figure 8), but they can also be part of bigger, polydentate ligands. For example, when a primary amine is reacted with two equivalents of a chlorophosphine, bidentate bisphosphinoamine ligands with the amine acting as spacer between the phosphines are obtained (**C**). The phosphinoamines need not be directly bound; in the case of the PNP and PCP ligands described in this work, an aromatic ring is positioned between both aminophosphines, with the amines as spacers (**B**).

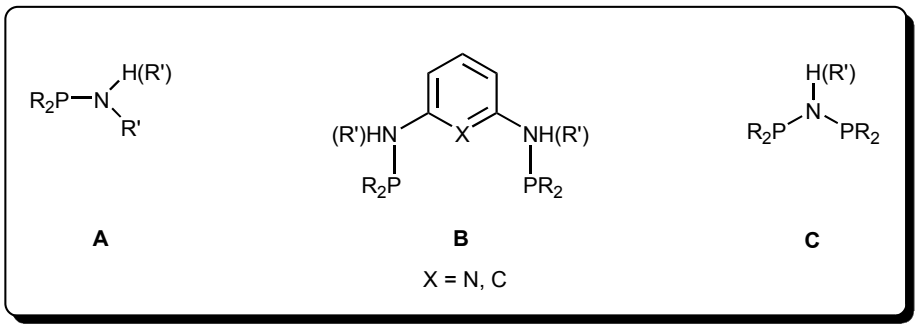

Figure 8. Examples of aminophosphine ligands

The main disadvantage of aminophosphines and phosphoramidites is their lower stability when compared to P-C bond containing phosphines (Figure 9). Due to the higher electronegativity of nitrogen, the P-N bond is more polarized than a P-C bond, making the phosphorus atom more sensitive towards oxidation or the attack of a nucleophile (e.g. oxygen in water or alcohols). In the case of phosphoramidites, the electrophility of the phosphorus atom is increased by the presence of the electron withdrawing oxygen atoms. Aminophosphines and phosphoramidites are not attacked by bases, but the addition of acids causes the cleavage of the P-N bond and the formation of new ligands[7].

[7] (a) Priya, S.; Balakrishna, M. S.; Mague, J. T.; Mobin, S. M. *Inorg. Chem.* **2003**, *42*, 1272. (b) Burrows, A. D.; Mahon, M. F.; Palmer, M. T.; Varrone, M. *Inorg. Chem.* **2002**, *41*, 1695. (c) Balakrishna, M. S.; Krishnamurthy, S. S. *Ind. J. Chem.* **1991**, *30A*, 536. (d) Newton, M. G.; King, R. B. Chang, M.; Gimeno, J. *J. Am. Chem. Soc.* **1978**, *100*, 1632.

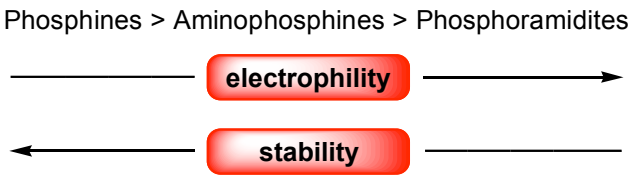

Figure 9. Stability and electrophility of phosphines, aminophosphines and phosphoramidites

To our knowledge, the complexes described in this work are the first catalytically active, aminophosphine containing transition metal pincer complexes that have been reported so far; however, simple, monodentate and bidentate aminophosphines and phosphoramidites have been used since the mid 1990s as powerful additives in several transition metal catalyzed reactions. The most important advantage of this class of ligands in organic synthesis is, apart from their facile preparation, the possibility of introducing chirality fairly easily, which makes them interesting as coligands in transition metal catalyzed enentioselective processes[8]. Some examples of aminophosphine and phosphoramidite ligands, along with the catalytic processes they have been employed in, are depicted in Figure 10[9].

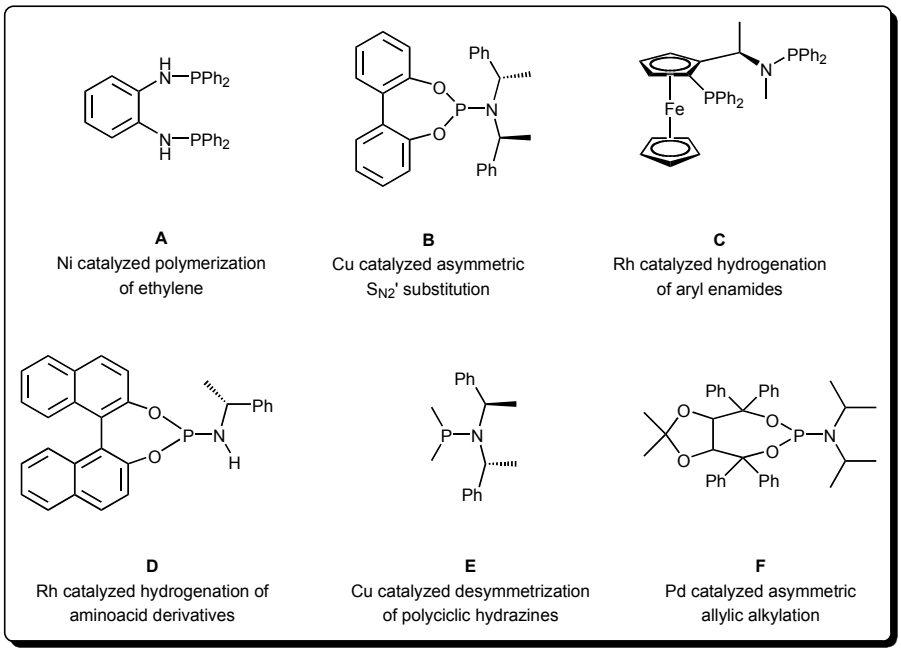

Figure 10. Examples of different aminophosphine and phosphoramidite ligands employed in enantioselective processes.

---

[8] For a review, see: Feringa, B. L. *Acc. Chem. Res.* **2000**, *33*, 346 and references therein.

[9] **A**: (a) Dolindsky, M. C. B.; Lin, W. O.; Dias, M. L. *J. Mol. Cat. A* **2006**, *258*, 267. **B**: (b) Falciola, C. A.; Tissot-Crosset, K.; Alexakis, A. *Angew. Chem. Int. Ed.* **2006**, *45*, 5995. **C**: (c) Li, X.; Jia, X.; Xu, L.; Stanton, H. L. K.; Yip, C. W.; Chan, A. S. C. *Adv. Synth. Catal.* **2005**, *347*, 1904. **D**: (d) Peña, D.; Minnaard, A. J.; de Vries, A. H. M.; de Vries, J. G.; Feringa, B. L. *Org. Lett.* **2003**, *5*, 475. **E**: (e) Bournaud, C.; Falciola, C.; Lecourt, T.; Rosset, S.; Alexakis, A.; Micouin, L. *Org. Lett.* **2006**, *8*, 3581. **F**: (f) Boele, M. D. K.; Kamer, P. C. J.; Lutz, M.; Spek, A. L.; de Vries, J. G.; van Leeuwen, P. W. N. M.; Strijdonck, G. P. F. *Chem. Eur. J.* **2004**, *10*, 6232.

2.4 Transition Metal Pincer Complexes

Pincer ligands, as tridentate ligands, mostly coordinate in a terdentate way to the metal center[10]. In the case of NCN pincer complexes, a large variety of binding modes has been observed, ranging from κ^1-C monodentate over κ^2-N,C bidentate to κ^3-N,C,N tridentate (**A-C**, Figure 11). The tridentate coordination mode is usually meridional, and only in few cases have facial coordination modes been observed (**D**)[10d]. One complex has also been reported in which the NCN ligand acts as a bridging ligand (**E**)[10e]. It seems that this versatility in ECE bonding is, however, a unique feature of the NCN system, since binding modes deviating from a meridional arrangement of the ligand have not been observed for other classes of pincer complexes, such as SCS, PCP or PNP pincer ligands.

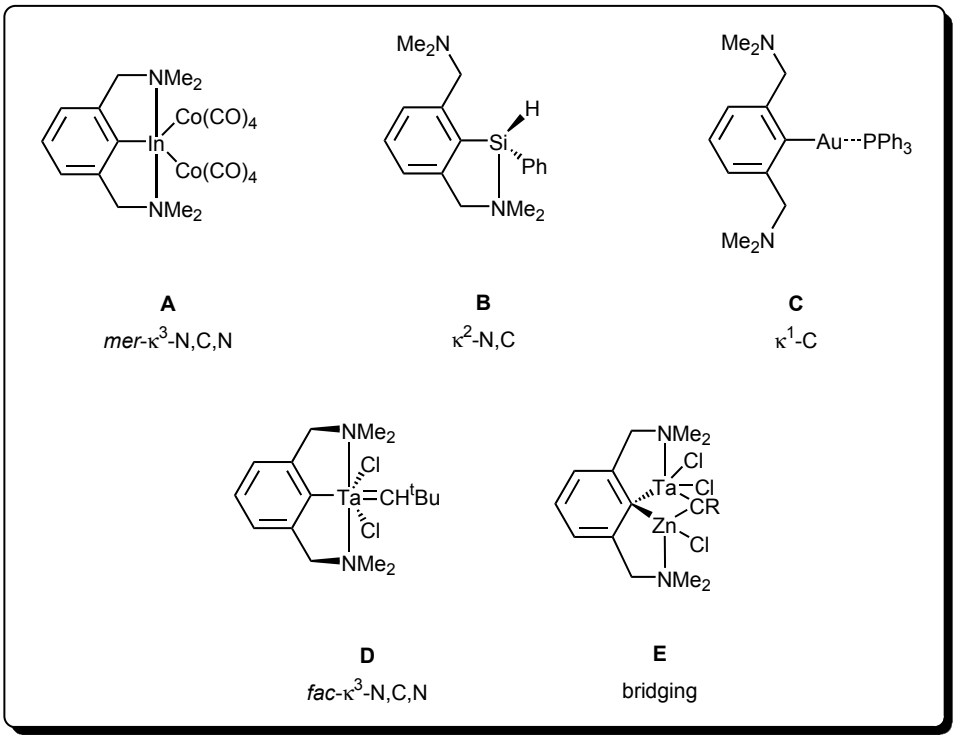

Figure 11. Binding modes of NCN pincer complexes

[10] **A**: (a) Olazábal, C. A.; Gabbaï, F. P.; Cowley, A. H.; Carrano, C. J.; Mokry, L. M.; Bond, M. R. *Organometallics* **1994**, *13*, 412. **B**: (b) Carré, F.; Chuit, C.; Corriu, J. P.; Fanta, A.; Mehdi, A.; Reyé, C. *Organometallics* **1995**, *14*, 194. **C**: (c) Contel, M.; Nobel, D.; Spek, A. L.; van Koten, G. *Organometallics* **2000**, *19*, 3288. **D**: (d) Abbenhuis, H. C. L.; Feiken, N.; Grove, D. M.; Jastrzebski, J. T. B. H.; Kooijman, H.; van der Sluis, P.; Smeets, W. J. J.; Spek, A. L.; van Koten, G. *J. Am. Chem. Soc.* **1992**, *114*, 9773. **E**: (e) Abbenhuis, H. C. L.; Feiken, N.; Haarman, H. F.; Grove, D. M.; Horn, H.; Kooijman, H.; Spek, A. L.; van Koten, G. *Angew. Chem. Int. Ed.* **1991**, *30*, 996. For other coordination modes, see: Rietveld, M. H. P.; Grove, D. M.; van Koten, G. *New J. Chem.* **1997**, *21*, 751.

In the case of PNP and PCP ligands, the most frequently observed coordination mode is the meridional κ^3-PXP one, in which the ligand binds to the metal center in a terdentate manner as a six electron donor with the phosphines *trans* to each other. This binding mode forces the aryl ring of the pincer ligand into a conformation which is approximately coplanar with the coordination plane of d^8 square-planar metal centers (Ni^{II}, Pd^{II}, Pt^{II}) or with the central plane of d^6 octahedral metal geometries (Fe^{II}, Ru^{II}, Rh^{III}, Ir^{III}) (Figure 12).

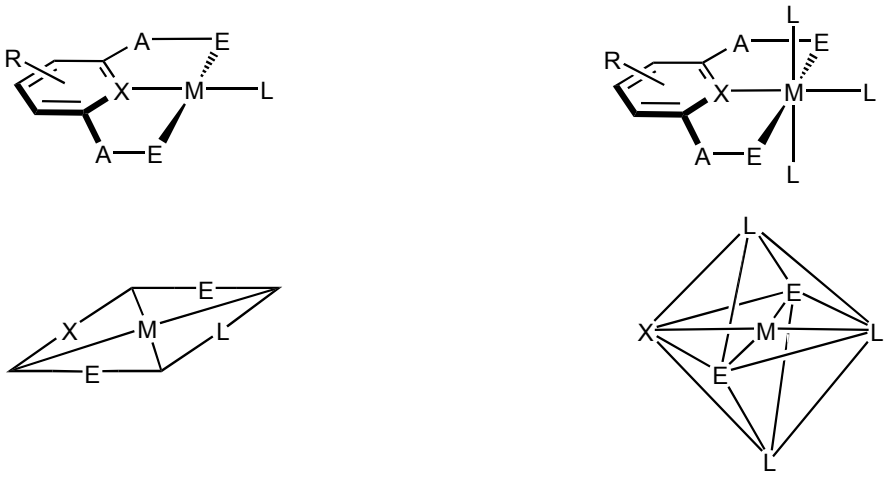

Figure 12. Coordination geometries of pincer complexes

Several methods have been developed for the metalation of pincer ligands, all of which are strongly dependent on the transition metal and the donor groups of the pincer ligand. For some metals, various methods can be applied indistinctively, but for other metals there is only one working metalation procedure. In the case of neutral ENE ligands (such as the PNP ligands), the use of a suitable metal precursor with labile coligands is normally the only requirement; due to the tridentate binding mode of the pincer ligands, the metal precursor coligands are easily displaced and the coordination usuallly takes place in short reaction times at room temperature (Scheme 2).

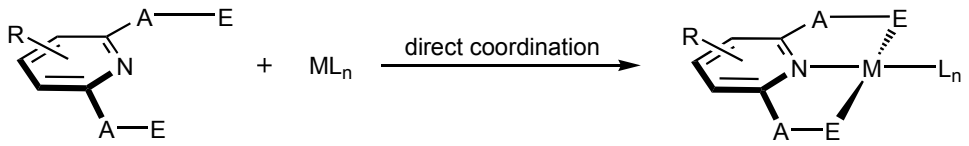

Scheme 2. Direct metalation of PNP pincer ligands

In the case of the complexation of anionic ECE ligands (like the PCP ligands), which require the cleavage of a C-R_1 bond (R_1 = H, CH_3, SiR_3, Li, Cl, Br, I...), the reaction conditions can be harsher; an overview of the different methods that can be used to metalate ECE pincer ligands is given in Scheme 3.

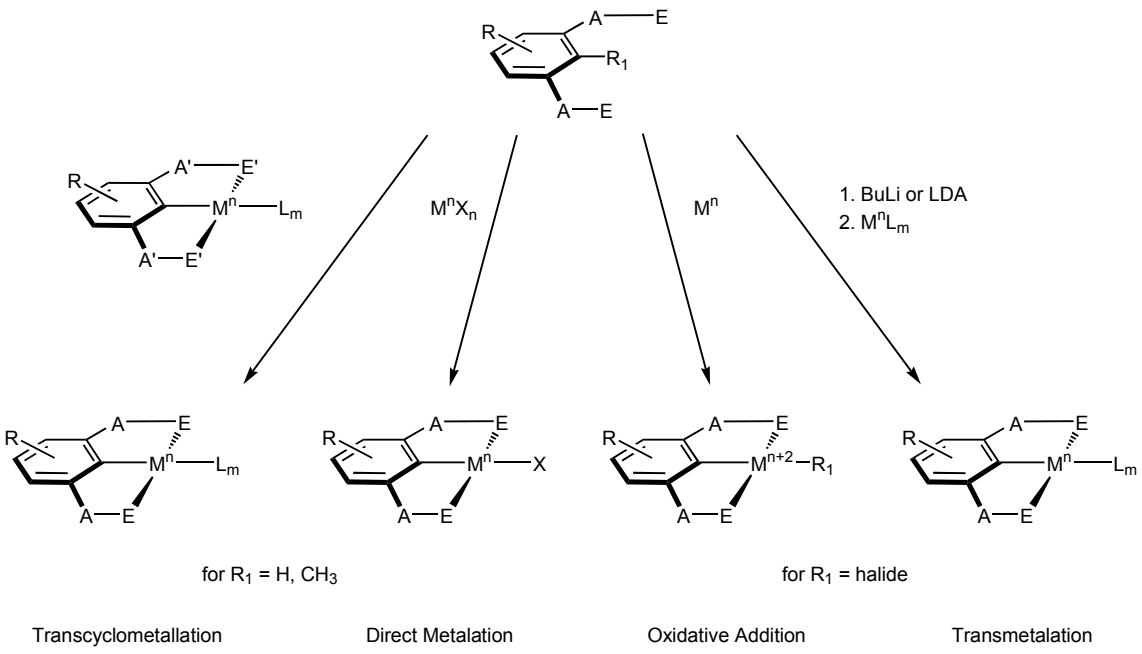

Scheme 3. Synthetic routes to ECE pincer complexes

The direct metalation of pincer ligands is by far the most often used method for the preparation of pincer complexes. Its main advantage is that it does not require the prefunctionalization of the pincer ligand in order to achieve regioselective metalation[11]. The metal precursors are metal halide salts or complexes with labile ligands, such as olefins. Long reaction times and high temperatures are usually required, but the reaction can proceed at milder conditions by choosing the appropriate metal precursor/ligand combination. It has to be noted that if R_1 = H and if a metal halide salt is used as precursor, an acid is formed during the reaction, which might cause problems in the case of acid sensitive ligands. This method was employed as early as 1976 to prepare several transition metal (Ni, Pd, Pt, Rh, Ir) PCP pincer complexes[2a]. However, NCN pincer complexes are more difficult to prepare by direct metalation[11a]: it is generally assumed that the metal has to coordinate to the two electron groups prior to the formation of the M-C bond and since the M-N bond is weaker than other coordinative bonds like M-P or M-S (M = transition metal), this results in kinetically rather than thermodinamically controlled reaction pathways. Thus, *ortho,para* doubly metalated products rather than *ortho,ortho*-biscyclometalated species are obtained[12]. This problem can be

[11] (a) Steenwinkel, P.; Gossage, R. A.; van Koten, G. *Chem. Eur. J.* **1998**, *4*, 759. (b) Ryabov, A. D. Chem. Rev. **1990**, *90*, 403 and references therein.

[12] (a) Trofimenko, S. *J. Am. Chem. Soc.* **1971**, *93*, 1808; (b) Trofimenko, S. *Inorg. Chem.* **1973**, *12*, 1215; (c) Vila, J. M.; Gayoso, M.; Pereira, M. T.; López Torres, M.; Fernández, J. J.; Fernández, A.; Ortigueira, J. M. *J. Organomet. Chem.* **1997**, *532*, 171. (d) Rüttimann, S.; Bernardinelli, G.; Williams, A. F. *Angew. Chem. Int. Ed.* **1993**, *32*, 392; (e) Gayathri,

circumvented in some cases by making R_1 = $SiMe_3$ as a directing (leaving) group on the aromatic ring[13] (Scheme 4).

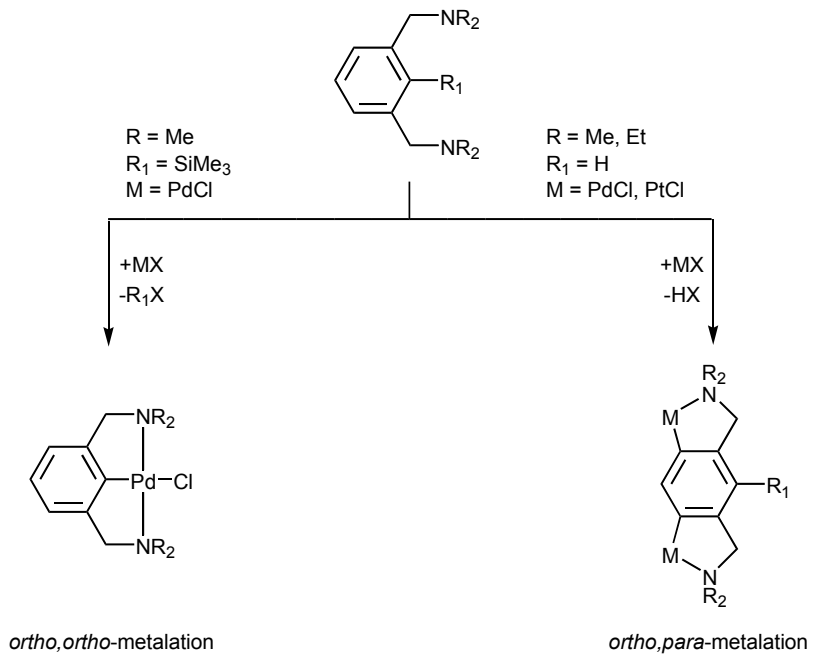

Scheme 4. Site-selective metalation of NCN pincer ligands

The oxidative addition of a metal precursor in a low oxidation state to a carbon-halogen bond is another method to synthesize pincer complexes. In it, the metal changes its oxidation state from M^n to M^{n+2}, with the advantage that the formation of acids is prevented and the reaction proceeds under milder conditions[14]. However, it is necessary to use a metal precursor in a low oxidation state. Suitable precursors are, for example, $Ni^0(COD)_2$, $Pd^0{}_2(dba)_3$ and $[Pt^{II}(4\text{-tolyl})_2(SEt_2)_2]_2$. There are few cases where PCP pincer complexes have been synthesized by this method, most likely because direct metalation was successful with this class of ligands and there was no need to develop alternative synthetic routes.

In the transmetalation method, an organometallic species with the metal coordinated only to the ipso carbon but not to the electron donor groups has to be prepared first and then reacted with a metal precursor to give the fully ligated pincer complex. The organometallic species is

---

V.; Leelamani, E. G.; Gowda, N. M. N.; Reddy, G. K. N. *Polyhedron* **1999**, *18,* 2351. (f) van der Zeijden, A. A. H.; van Koten, G.; Luijk, R.; Vrieze, K.; Slob, C.; Krabbendam, H.; Spek, A. L. *Inorg. Chem.* **1988**, *27*, 1014.

[13] a) Steenwinkel, P.; Gossage, R. A.; Maunula, T.; Grove, D. M.; van Koten, G. *Chem. Eur. J.* **1998**, *4*, 763; b) Valk, J.-M.; Boersma, J.; van Koten, G. *J. Organomet. Chem.* **1994**, *483*, 213.

[14] (a) Myazaki, F.; Yamaguchi, K.; Shibasaki, M. *Tetrahedron Lett.* **1999**, *40*, 7379. (b) Van de Kuil, L. A.; Luitjes, H.; Grove, D. M.; Zwikker, J. W.; van den Linden, J. G. M.; Roelofsen, A. M.; Jenneskens, L. W.; Drenth, W.; van Koten, G. *Organometallics* **1994**, *13*, 468.

commonly prepared by using lithium reagents such as *n*-BuLi or LDA. A problem, which affects mostly to pincer ligands of the PCP type with a methylene bridging between the benzene ring and the phosphines is that if R_1 = H, the lithiation can take place both at the aryl ring and at the activated benzylic positions. If R_1 = X (X = Cl, Br, I), the lithium/halide exchage proceeds quantitatively, but the aryllithium species isomerizes rapidly to the benzyllithium complex. Only when very small phosphines are used (e.g., E = PMe_2) can the lithium migration be prevented[15]. Since there are better alternatives for the metalation of PCP pincer ligands, there are few examples of PCP pincer complexes prepared by this method. However, NCN pincer complexes can be prepared smoothly by transmetalation[16].

Transcyclometalation has been introduced recently as a novel method for the preparation of pincer complexes[17]: the term is adapted from organic chemistry and is used to describe the substitution of one cyclometalated ligand by another without the formation of significant and/or detectable amounts of inorganic compounds (dissociated metal salts). The requirement in these reactions is that the M-E bond must be stronger than the M-E' bond, that is, that the electron donor groups E of the free ligand have to coordinate to the metal center better than those present in the precursor complex (E')[18]. Platinum PCP complexes have been successfully prepared by transcyclometalation using platinum NCN complexes as precursors[17]. However, this method is rather new and still under development.

---

[15] Pape, A.; Lutz, M.; Müller, G. *Angew. Chem. Int. Ed.* **1994**, *33*, 2281.

[16] Ru: (a) Sutter, J.-P.; James, S. L.; Steenwinkel, P.; Karlen, T.; Grove, D. M.; Veldman, N.; Smeets, W. J. J.; Spek, A. L.; van Koten, G. *Organometallics* **1996**, *15*, 941; Ir: (b) van der Zeijden, A. A. H.; van Koten, G.; Luijk, R.; Nordemann, R. A.; Spek, A. L. *Organometallics* **1988**, *7*, 1549; Ni: (c) Kleij, A. W.; Gossage, R. A.; Klein Gebbink, R. J. M.; Brinkmann, N.; Reijerse, E. J.; Kragl, U.; Lutz, M.; Spek, A. L.; van Koten, G. *J. Am. Chem. Soc.* **2000**, *122*, 12112; Pd, Pt: (d) Grove, D. M.; van Koten, G.; Louwen, J. N.; Noltes, J. G.; Spek, A. L.; Ubbels, H. J. C. *J. Am. Chem. Soc.* **1982**, *104*, 6609; (e) Terheijden, J.; van Koten, G.; Muller, F.; Grove, D. M.; Vrieze, K.; Nielsen, E.; Stam, C. H. *J. Organomet. Chem.* **1986**, *315*, 401.

[17] (a) Dani, P.; Albrecht, M.; van Klink, G. P. M.; van Koten, G. *Organometallics* **2000**, *19*, 4468; (b) Albrecht, M.; Dani, P.; Lutz, M.; Spek, A. L.; van Koten, G. *J. Am. Chem. Soc.* **2000**, *122*, 11822. (c) Albrecht, M.; James, S. L.; Veldman, N.; Spek, A. L.; van Koten, G. *Can. J. Chem.* **2001**, *79*, 709.

[18] Maassarani, F.; Davidson, M. F.; Wehman-Ooyevaar, I. C. M.; Grove, D. M.; van Koten, M. A.; Smeets, W. J. J.; Spek, A. L.; van Koten, G. *Inorg. Chim. Acta* **1995**, *235*, 327.

2.5 Applications of Transition Metal Pincer Complexes

Although the applications of transition metal pincer complexes span upon many areas of chemistry, they can be divided into four categories: catalysis, coordination and activation of small molecules, C-H, C-O and C-C bond activation and supramolecular chemistry.

2.5.1 Catalysis

In the field of catalysis, five are the metals whose pincer complexes hoard most of the catalytic applications of pincer complexes: palladium, rhodium, iridium, ruthenium and nickel. Furthermore, it is cyclometalated pincer complexes of the PCP and NCN type that show the highest catalytic activities in many cases[3]. The robust, rigid aromatic backbone of the pincer complexes tolerates structural modifications and limits the number of open (= reactive) sites at the metal center ensuring reaction selectivity and catalyst stability. Reactions with relatively high kinetic barriers may proceed smoothly at elevated temperatures without noticeable catalyst degradation, and the fine tuning of the steric and electronic properties of the complexes has resulted in enhanced catalytic activity with turnover numbers, yields and catalyst lifetimes that approach industrial figures of merit. The high efficiency and selectivity shown by many pincer complexes has given rise to mechanistic studies of the catalytic processes with less reactive substrates, which has helped to understand many of the mechanisms of reactions catalyzed by these complexes. Some examples of catalytically active pincer complexes, along with the processes they mediate are depicted in Figure 13.

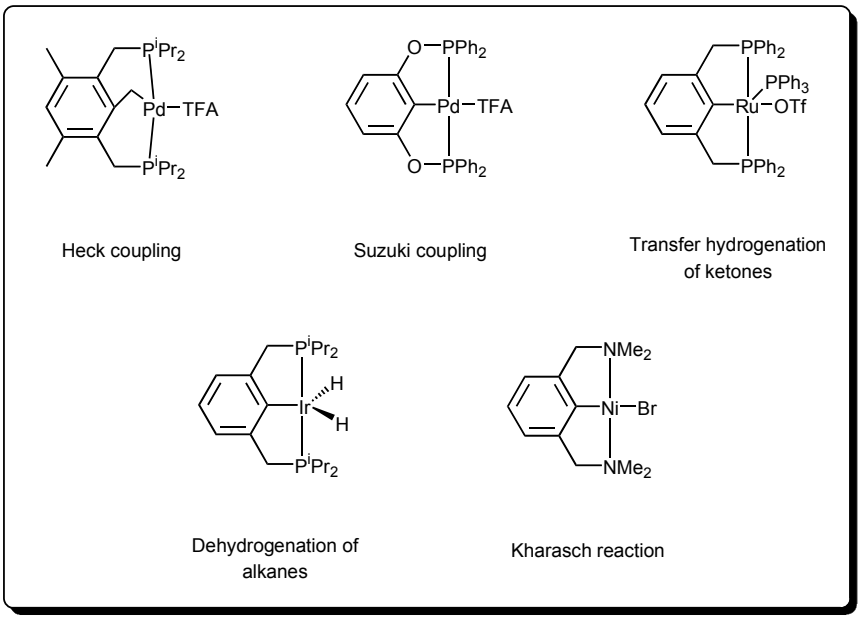

Figure 13. Examples of pincer complexes employed in catalysis

Palladium pincer complexes mediate a number of catalytic reactions, mostly C-C bond forming reactions. Examples include the coupling of aryl halides with boronic acids[19] (Suzuki reaction) and olefins[19a,b,20] (Heck reaction), the hydroamination of olefins[21], the stannation and silation of allyl- allenyl- and propargyl substrates[22] and the aldol condensation of isocyanoacetates with aldehydes[23]. The reaction for which palladium pincer complexes have been employed most successfully is the Heck reaction, and turnover numbers exceeding $5\cdot10^5$ have been reported using phosphine containing PCP complexes[20b,c]. The use of phosphite instead of phosphine groups as electron donors, that is, replacement of the methylene spacer between the aryl ring and the phosphines by oxygen, and the introduction of aryl- and alkyloxy substituents on the phosphorus atoms, had a dramatic influence on the catalyst performance[14a,19a,b]. A catalyst loading as low as 0.1 ppm resulted in astonishing reaction rates (TON: $8.9\cdot10^6$, TOF: $4\cdot10^5$)[14a]. For the Heck reaction, a special mechanism for phosphinito PCP pincer complexes has been proposed involving a Pd(II)/Pd(IV) catalytic cycle instead of the common Pd(0)/Pd(II) cycle[19b]. Alternatively, it has been proposed that palladium pincer complexes are mere precursors for the formation of colloidal palladium nanoparticles, which are the real catalysts[24]. However, the formation of palladium nanoparticles seems to be dependant on the pincer complex employed as catalyst, since they have only been observed in some cases. The most effective catalysts in palladium mediated coupling reactions are pincer complexes of the PCP type; PNP, SCS and NCN pincer complexes show always lower activities[25].

Ruthenium(II) PCP and NCN pincer complexes are effective catalysts in the transfer hydrogenation reaction of ketones using iso-propanol as hydrogen source and KOH as promotor[26]. The PCP complexes show higher activities than the related NCN complexes, and

---

[19] (a) Morales-Morales, D.; Grause, C.; Kasaoka, K.; Redón, R.; Cramer, R. E.; Jensen, C. M. *Inorg. Chim. Acta* **2000**, *300-302*, 958. (b) Morales-Morales, D.; Redón, R.; Yung, C.; Jensen, C. M. *Chem. Commun.* **2000**, 1619. (c) Bedford, R. B.; Draper, S. M.; Scully, P. N.; Welch, S. L. *New. J. Chem.* **2000**, *24*, 745.

[20] (a) Kiewel, K.; Liu, Y. S.; Bergbreiter, D. E.; Sulikowski, G. A. *Tetrahedron Lett.* **1999**, *40*, 8945. (b) Ohff, M.; Ohff, A.; van der Boom, M. E.; Milstein, D. *J. Am. Chem. Soc.* **1997**, *119*, 11687. (c) Beletskaya, I. P.; Chuchurjukin, A. V.; Dijkstra, H. P.; van Klink, G. P. M.; van Koten, G. *Tetrahedron Lett.* **2000**, *41*, 1075. (d) Heck, R. F. *Palladium Reagents in Organic Synthesis*; Benchtop Edition; Academic Press: London, **1990**. (e) Beletskaya, I. P.; Cheprakov, A. V. *Chem. Rev.* **2000**, *100*, 3009. (f) Crisp, G. T. *Chem. Soc. Rev.* **1998**, *27*, 427.

[21] (a) Ryu, S. Y.; Kim, H.; Kim, H. S.; Park, S. *J. Organomet. Chem.* **1999**, *592*, 194. (b) Ryu, S. Y.; Yang, W.; Kim, H. S.; Park, S. *Bull. Korean Chem. Soc.* **1997**, *18*, 1183.

[22] For a review, see: (a) Szabó, K. J. *Synlett* **2006**, 811 and references therein. See also: (b) Kjellgren, J.; Sundén, H.; Szabó, K. J. *J. Am. Chem. Soc.* **2004**, *126*, 474. (c) Kjellgren, J.; Sundén, H.; Szabó, K. J. *J. Am. Chem. Soc.* **2005**, *127*, 1787. (d) Olsson, V. J.; Sebelius, S.; Selander, N.; Szabó, K. J. *J. Am. Chem. Soc.* **2006**, *128*, 4588.

[23] Schlenk, C.; Kleij, A. W.; Frey, H.; van Koten, G. *Angew. Chem. Int. Ed.* **2000**, *39*, 3445.

[24] (a) Sommer, W. J.; Yu, K.; Sears, J. S.; Ji, Y.; Zheng, X.; Davis, R. J.; Sherill, C. D.; Jones, C. W.; Weck, M. *Organometallics* **2005**, *24*, 4351. (b) Eberhard, M. R. *Org. Lett.* **2004**, *6*, 2125.

[25] Bergbreiter, D. E.; Osburn, P. L.; Liu, Y.-S. *J. Am. Chem. Soc.* **1999**, *121*, 9531. (b) Gruber, A. S.; Zim, D.; Ebeling, G.; Monteiro, A. L.; Dupont, J. *Org. Lett.* **2000**, *2*, 1287.

[26] Dani, P.; Karlen, T.; Gossage, R. A.; Gladiali, S.; van Koten, G. *Angew. Chem., Int. Ed.* **2000**, *39*, 743.

they are better catalysts for the hydrogenation of aryl- alkyl-, diaryl- and dialkyl ketones than established monodentate phosphine complexes such as $[RuCl_2(PPh_3)_3]$[27]. Mechanistic investigations have resulted in the isolation of an anionic ruthenium(II)-alkoxyhydrido species, which is believed to be the resting state of the actual catalyst, a neutral d6 ruthenium hydrido complex[28]. Some progress has also been made in the transfer hydrogenation of prochiral ketones using chiral PCP pincer complexes, but although their activities are similar to those of the achiral analogues, the asymmetric induction remains rather low[29].

Dinuclear rhodium(III)-rhodium(I) PCP and NCN complexes of the type $[RhCl(ECE)(\mu\text{-}Cl)_2Rh(COD)]$ have been successfully employed in the polymerization of phenylacetylene to give stereo regular cis-transoidal poly(phenylacetylene) with a molecular weight of about 50.000[30]. The process is probably catalyzed by the (COD)Rh(I) moiety of the complex, since the (ECE)Rh(III) moieties are coordinatively saturated, and dinuclear Rh(III) PCP complexes are not catalytically active.

Several iridium(III) PCP pincer complexes catalyze the alkane dehydrogenation of cycloalkanes, cycloalkenes, tetrahydrofuranes and alkanes to arenes, furanes and alkenes, respectively[31]. A tetrahydrido iridium(V) complex can be prepared in situ by chloride abstraction of the precursor complex [Ir(PCP)(H)Cl] under hydrogen atmosphere; this tetrahydrido species reductively eliminates molecular hydrogen under vacuum to give a dihiydrido iridium(III) complex, which is the active catalyst[32]. Thus, these iridium pincer complexes represent novel organometallic devices for reversible hydrogen storage. However, although the dihydrido iridium(III) catalyst remains active after the reaction is complete, it can be deactivated by high alkene concentration and by traces of inert nitrogen gas[31d]. The performance of these PCP complexes is superior to other dehydrogenation catalysts reported in the literature in terms of turnover numbers, stability and scope. The analogous iridium(III) NCN pincer complexes are less active than their PCP counterparts. Mechanistic investigations have also been performed for the iridium PCP complexes, indicating that a dissociative mechanism rather than an associative one is most likely during the catalytic process[31b-d].

---

[27] Naota, T.; Takaya, H.; Murahashi, S.-I. *Chem. Rev.* **1998**, *98*, 2599.

[28] Gusev, D. G.; Dolgushin, F. M.; Antipin, M. Y. *Organometallics* **2000**, *19*, 3429.

[29] Albrecht, M.; Kocks, B. M.; Spek, A. L.; van Koten, G. *J. Organomet. Chem.* **2001**, *624*, 271.

[30] Yao, J.; Wong, W. T.; Jia, G. *J. Organomet. Chem.* **2000**, *598*, 228.

[31] (a) Gupta, M.; Hagen, C.; Kaska, W. C.; Flesher, R.; Jensen, C. M. *J. Chem. Soc., Chem. Commun.* **1996**, 2083. (b) Gupta, M.; Hagen, C.; Kaska, W. C.; Cramer, R. E.; Jensen, C. M. *J. Am. Chem. Soc.* **1997**, *119*, 840. (c) Jensen, C. M. *Chem. Commun.* **1999**, 2443. (d) Lee, D. W.; Kaska, W. C.; Jensen, C. M. *Organometallics* **1998**, *17*, 1. (e) Liu, F.; Pak, E. B.; Singh, B.; Jensen, C. M.; Goldman, A. S. *J. Am. Chem. Soc.* **1999**, *121*, 4086. (e) Morales-Morales, D.; Lee, D. W.; Wang, Z.; Jensen, C. M. *Organometallics* **2001**, *20*, 1144. (f) Nemeh, S.; Jensen, C. M.; Binamira-Soriaga, E.; Kaska, W. C. *Organometallics* **1983**, *2*, 1442. (g) Xu, W. W.; Rosini, G. P.; Gupta, M.; Jensen, C. M.; Kaska, W. C.; Krogh-Jespersen, K.; Goldman, A. S. *Chem. Commun.* **1997**, 2273.

[32] Wang, K.; Goldman, M. E.; Emge, T. J.; Goldman, A. S. *J. Organomet. Chem.* **1996**, *518*, 55.

Finally, nickel(II) NCN pincer complexes have been used as catalysts in the Kharasch atom-transfer-radical addition (ATRA) of a polyhalogenated alkane (such as CCl_4) to a terminal olefin[33]. Detailed investigations have revealed the formation of the nickel(III) complex [NiX_2(NCN)] (X=Cl, Br) as a persistent radical and [·CCl_3] as the reactive species for the addition to the olefin[34]. The prerequisite for the reaction is that both the polyhalogenated alkane and the olefin need to be present in approximately equal ratios in the reaction mixture; otherwise, atom-transfer radical polymerization is induced and polyolefins are formed[35]. Surprisingly, pincer complexes of the PCP type have not been reported to catalyze this reaction.

The preparation of chiral pincer complexes has only been reported for PCP complexes containing a methylene bridging between the aryl ring and the phosphine groups; in this case, the chirality was introduced in the benzylic positions. Transition metal complexes with these chiral pincer ligands have been employed in the asymmetric aldol condensation of methylisocyanoacetate with aldehydes catalyzed by palladium and platinum[36] and in the alllylic alkylation catalyzed by palladium[37]. Alternatively, NCN C_2 symmetric Phebox pincer complexes in which the nitrogen atom of an oxazoline moiety acts as electron donor have also been prepared and their activity tested with some success in the asymmetric Michael addition[38], in the synthesis of chiral cyclopropanes[39] and in the asymmetric allylation of aldehydes[40]. However, although the chiral induction is good (~80%) in some cases, there is plenty of room for improvement in the area of chiral pincer complexes.

2.5.2 Coordination and activation of small molecules

The reversible coordination of small substrates is a prerequisite for almost any transition metal complex mediated transformation, therefore the importance of investigating the coordination behavior of potential reagents and substrates to transition metal pincer complexes. These have been found to react, depending on the ligand and the metal center, with several small molecules, such as dinitrogen, dihydrogen, carbon dioxide, water, olefines and alkynes. For example, it has been shown that dinitrogen, which is believed to be an inert gas and to not affect reaction outcomes, is certainly not an innocent spectator, and several low valent rhodium(I), iridium(I), osmium(II) and ruthenium(II) dinitrogen PCP pincer complexes have been

---

[33] (a) Grove, D. M.; van Koten, G.; Verschuuren, A. H. M. *J. Mol. Catal.* **1988**, *45*, 169; (b) Grove, D. M.; Verschuuren, A. H. M.; van Koten, G.; van Beek, J. A. M. *J. Organomet. Chem.* **1989**, *372*, C1.

[34] (a) Fischer, H. *Macromolecules* **1997**, *30*, 5666; (b) Fischer, H.; Radom, L. *Angew. Chem. Int. Ed.* **2001**, *40*, 1340.

[35] Granel, C.; Dubois, P.; Jérôme, R.; Teyssie, P. *Macromolecules* **1996**, *29*, 8576.

[36] Gorla, F.; Togni, A.; Venanzi, L. M.; Albinati, A.; Lianza, F. *Organometallics* **1994**, *13*, 1607.

[37] Longmire, J. M.; Zhang, X. *Tetrahedron Lett.* **1997**, *38*, 1725.

[38] Stark, M. A.; Jones, G.; Richards, C. J. *Organometallics* **2000**, *19*, 1282.

[39] Denmark, S. E.; Stavenger, R. A.; Faucher, A.-M.; Edwards, J. P. *J. Org. Chem.* **1997**, *62*, 3375.

[40] Motoyama, Y.; Narusawa, H.; Nishiyama, H. *Chem. Commun.* **1999**, 131.

reported[3b]. In these cases, the dinitrogen molecule can be “end-on” coordinated or act as a bridging molecule between two metal centers.

Some rhodium(III) dihydrogen complexes react with carbon dioxide to give unstable formate species which undergo a secondary transformation to afford carbonyl and hydrido hydroxy species[41] (Scheme 5). This reaction can be seen as a metal mediated reverse water-gas shift process, which is important due to an increasing interest in the reduction of CO_2 and its functionalization to valuable liquid fuels (such as methanol).

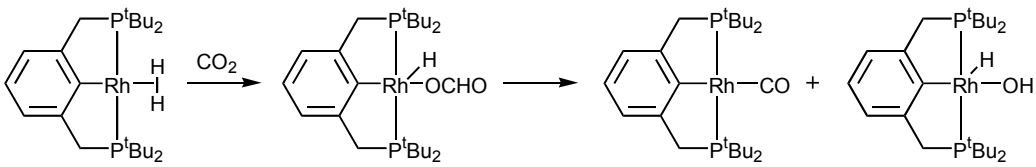

Scheme 5. Reactivity of a rhodium dihydrogen complex towards CO_2

The formation of dihydride iridium(III) complexes is possible by the oxidative addition of dihydrogen to iridium(I) PCP pincer complexes of the type [Ir(PCP)CO][42]. This process is reversible, and dihydrogen can be reductively eliminated to give the original complex. Thus, this is another example for an organometallic species that could be employed for hydrogen storage purposes. These dihydride complexes are also capable of reacting with various electrophilic reagents (carbon disulfide, p-toluenesulfonic acid, methyl iodide, chloroform, etc) to give the corresponding monohydride complexes, which are completely inert towards excess of the electrophiles, demonstrating the unique reactivity of just one hydride moiety. It is also possible to obtain osmium polyhydride complexes and compounds with molecular hydrogen coordinated to the metal center[3b].

Terminal acetylenes are also reactive towards transition metal pincer complexes: when [Ru(PCP)(PPh_3)Cl] is reacted with LiCCPh, the acetylide coordinates “end-on”, while when the same complex is reacted with phenylacetylene, “side-on” coodination takes place[43]. In both cases, the insertion of the terminal acetylene carbon atom into the Ru-C_{aryl} bond is observed (Scheme 6). When phenylacetylene is used, the reaction most likely proceeds through a vinylidene intermediate, which has not yet been isolated. However, analogous vinylidene ruthenium complexes with neutral PNP pincer ligands have been reported[44]. Osmium(IV) vinylidene and carbyne complexes have also been prepared[3b], and a procedure to synthesize

[41] Kaska, W. C.; Nemeh, S.; Shirazi, A.; Potuznik, S. *Organometallics* **1988**, *7*, 13.

[42] Rybtquinksi, B.; Ben-David, Y.; Milstein, D. *Organometallics* **1997**, *16*, 3786.

[43] (a) Jia, G.; Lee, H. M.; Xia, H. P.; Williams, I. D. *Organometallics* **1996**, *15*, 5453. (b) Lee, H. M.; Yao, J.; Jia, G. *Organometallics* **1997**, *16*, 3927.

[44] Katayama, H.; Wada, C.; Taniguchi, K.; Ozawa, F. *Organometallics* **2002**, *21*, 3285.

PCP metal carbene complexes by using sulfur ylides as carbenoid precursors has also been developed[45]. This synthetic route is safer than the one using diazo precursors and is not limited only to pincer complexes; various carbene complexes, including Grubbs' catalysts and new metal alkylidenes have been obtained with this method.

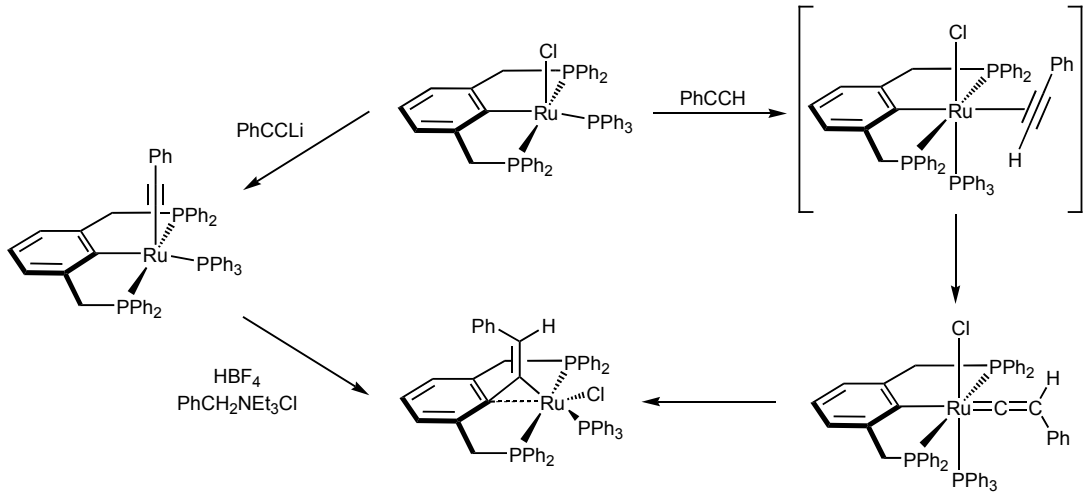

Scheme 6. Reactivity of [Ru(PCP)Cl(PPh_3)] towards terminal acetylenes

An interesting application of pincer complexes in the activation of small molecules is their possible use as gas sensors: a platinum NCN pincer complex has been found to selectively bind atmospheric SO_2, changing its color from colorless to bright orange when switquing between the tetracoordinated complex and the pentacoordinate adduct[46] (Scheme 7).

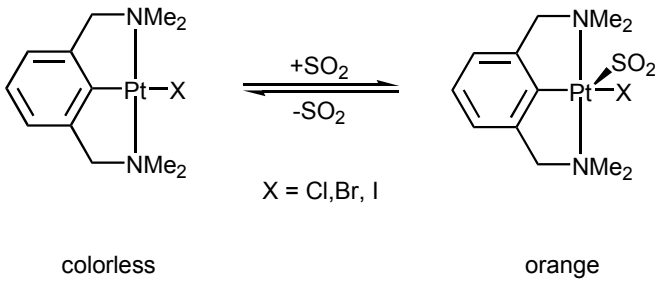

Scheme 7. Reversible binding of SO_2 on platinum NCN pincer complexes

[45] Gandelman, M.; Rybtquinski, B.; Ashkenazi, N.; Gauvin, R. M.; Milstein, D. *J. Am. Chem. Soc.* **2001**, *123*, 5372.

[46] (a) van der Ploeg, A. F. M. J.; van Koten, G.; Brevard, C. *Inorg. Chem.* **1982**, *21*, 2878. (b) Albrecht, M.; Gossage, R. A.; Lutz, M.; Spek, A. L.; van Koten, G. *Chem. Eur. J.* **2000**, 6, 1431. (c) Albrecht, M.; Schlupp, M.; Bargon, J.; van Koten, G. *Chem. Commun.* **2001**, 1874.

2.5.3 C-H, C-C and C-O bond activation

In contrast to the synthesis of transition metal ENE pincer complexes, which is a mere coordinative process, the preparation of ECE pincer complexes proceeds via a C-H bond activation process. There are two generally accepted mechanistic pathways accounting for most metal-based aromatic C-H bond activation processes[11b,47] (Scheme 8).

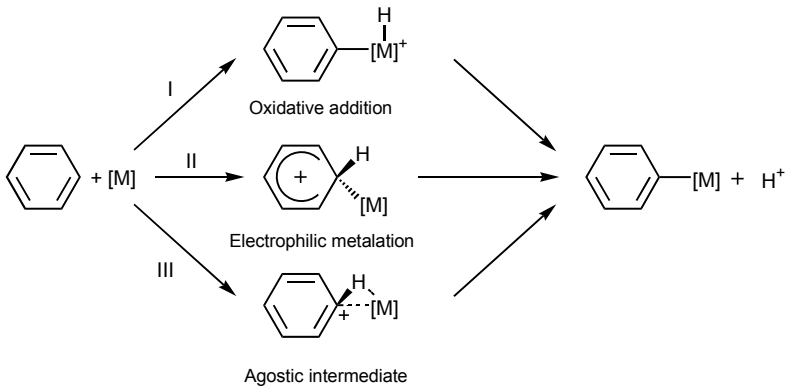

Scheme 8. Mechanistic pathways for aromatic C-H bond activation processes

Route I involves a concerted oxidative addition process via a η^2 metal arene complex with the formation of a metal hydride species. Alternatively, an electrophilic attack of the metal center on the C_{ipso} carbon atom of the aromatic ring may afford a metal arenium complex followed by proton loss (route II). An alternative route, which does not involve the arene π-system, can be considered as well (route III)[48]. Agostic alkyl complexes are known and, although examples of agostic aryl complexes are extremely rare[49], it is most likely that the formation of ECE pincer complexes proceeds via a η^2-C-H agostic intermediate. This is based on the direct experimental observation of such intermediates for aromatic C-H bond activation by van Koten[50], Milstein[48] and Gusev[28] with ruthenium and rhodium complexes. The X-ray structures of such complexes show no distortion of the aromatic ring, which is incompatible with the intermediacy of an arenium complex, and theoretical calculations indicate that there is an insignificant contribution (if at all) of a metal arenium structure in the C-H activation process[48].

---

[47] (a) Sweet, J. R.; Graham, W. A. G. *J. Am. Chem. Soc.* **1983**, *105*, 305. (b) Jones, W. D.; Feher, F. J. *Acc. Chem. Res.* **1989**, *22*, 421. (c) Taylor, R. *Electrophilic Aromatic Substitution*; John Wiley & Sons: New York, **1990**. (d) Aoyama, Y.; Yoshida, T.; Sakurai, K.; Ogoshi, H. *Organometallics* **1986**, *5*, 168.

[48] Vigalok, A.; Uzan, O.; Shimon, L. J. W.; Ben-David, Y.; Martin, J. M. L.; Milstein, D. *J. Am. Chem. Soc.* **1998**, *120*, 12539.

[49] See, for example: Lavin, M.; Holt, E. M.; Crabtree, R. H. *Organometallics* **1989**, *8*, 99.

[50] (a) Dani, P.; Karlen, T.; Gossage, R. A.; Smeets, W. J. J.; Spek, A. L.; van Koten, G. *J. Am. Chem. Soc.* **1997**, *119*, 11317. (b) Dani, P.; Toorneman, M. A. M.; van Klink, G. P. M.; van Koten, G. *Organometallics* **2000**, *19*, 5287. (c) Steenwinkel, P.; Kolmschot, S.; Gossage, R. A.; Dani, P.; Veldman, N.; Spek, A. L.; van Koten, G. *Eur. J. Inorg. Chem.* **1998**, 477. (d) del Rio, I.; Gossage, R. A.; Lutz, M.; Spek, A. L.; van Koten, G. *J. Organomet. Chem.* **1999**, *583*, 69.

An alternative route for the synthesis of PCP pincer complexes involves the use of C_{ipso}-alkyl-functionalized $PC(CH_3)P$ pincer ligands. However, it was found out that both C_{alkyl}-H as well as C_{aryl}-C_{alkyl} bond activation can take place to give benzyl- as well as phenyl- PCP pincer complexes. A series of mechanistic investigations[51] and a theoretical study with rhodium complexes[51e] revealed that C_{alkyl}-H bond activation may be a competitive reaction, but not an intermediate of the C_{aryl}-C_{alkyl} activation process. Instead, the intermediacy of a cyclopropane-type metallacycle is most likely (Scheme 9). The product resulting from the C-H bond cleavage (that is, the benzylic complex) can be converted to the aryl complex, a process which can be induced either thermally or by the addition of molecular hydrogen. This process is presumed to reverse the C-H bond activation and results in the formal release of a methylene fragment[52]. Remarkably, this group can be selectively delivered to an organic substrate under certain reaction conditions, giving, for example, toluene from benzene (Scheme 9)[53].

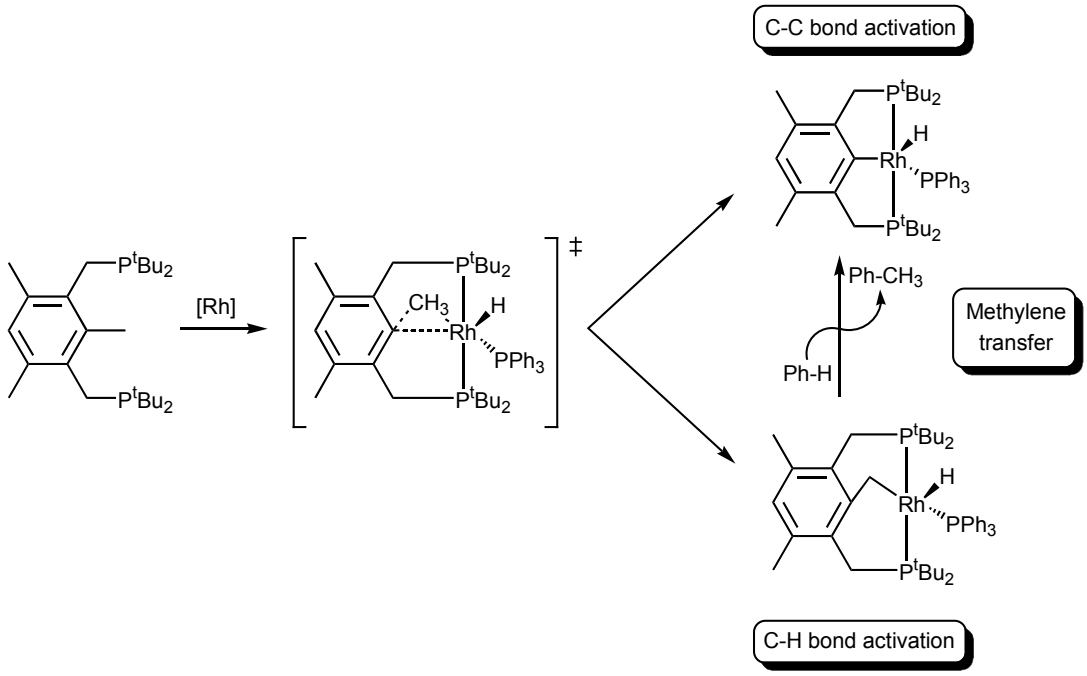

Scheme 9. Competitive C-H and C-C activation processes in $PC(CH_3)P$ pincer ligands.

[Rh] = $[RhH(PPh_3)_4]$

[51] (a) van der Boom, M. E.; Liou, S.-Y.; Ben-David, Y.; Gozin, M.; Milstein, D. *J. Am. Chem. Soc.* **1998**, *120*, 13 415. (b) Rybtquinski, B.; Vigalok, A.; Ben-David, Y.; Milstein, D. *J. Am. Chem. Soc.* **1996**, *118*, 12406. (c) Liou, S.-Y.; Gozin, M.; Milstein, D. *J. Am. Chem. Soc.* **1995**, *117*, 9774; (d) Rybtquinski, B.; Milstein, D. *J. Am. Chem. Soc.* **1999**, *121*, 4528. (e) Sundermann, A.; Uzan, O.; Milstein, D.; Martin, J. M. J. *J. Am. Chem.* Soc. **2000**, *122*, 7095.

[52] Liou, S.-Y.; Gozin, M.; Milstein, D. *J. Chem. Soc. Chem. Commun.* **1995**, 1965.

[53] (a) Gozin, M.; Aizenberg, M.; Liou, S.-Y.; Weisman, A.; Ben-David, Y.; Milstein, D. *Nature* **1994**, *370*, 42. (b) Cohen, R.; van der Boom, M. E.; Shimon, L. J. W.; Rozenberg, H.; Milstein, D. *J. Am. Chem. Soc.* **2000**, *122*, 7723.

These two competitive processes depend not only on the metal center employed, but also on the characteristics of the metal precursor (for example, whether it is an anionic or a neutral precursor), on the ligand and on the reaction conditions. Using neutral rhodium and iridium precursors and PCP pincer ligands, for example, the C-C bond activation is thermodinamically favorable regardless of the reaction conditions; however, the kinetic balance between C-C and C-H bond cleavage is significantly influenced by the nature of the donor groups E: C-C bond activation becomes kinetically more favorable with an increasing electron density on the metal center[51b,54]. The use of cationic rhodium precursors, on the other hand, shows a remarkable solvent effect on C-H vs. C-C bond activation processes[51d]. In weakly coordinating solvents (THF), C-C bond activation was observed, whereas in coordinating solvents (acetonitrile) C-H bond activation occurred. The C-H bond activation product can be converted to the C-C bond activacted complex, but this process is reversible. Thus, the solvent can provide a convenient tool in directing the bond activation process. The size of the alkyl substituents at the C_{ipso} carbon atom also plays an important role: if this group is a methyl group, both activations (C-H and C-C) can take place, but if a bigger substituent is used (ethyl), only the C-C bond activation product is observed[51a]. The dependence on the transition metal can be seen when the metal center was changed from rhodium or iridium to ruthenium or platinum: in the latter cases, the activation barrrier for C-C bond activation is apparently too high and the benzylic complex resulting from C-H bond activation is the exclusive product[55]. The addition of HCl induces the formation of the Pt-C_{aryl} bond, which corresponds to the net transfer of a methylene group of the ligand to HCl. Similar product discrimination has been obtained in the methoxy-functionalized pincer ligand PC(OMe)P with different metal precursors. Palladation results in the selective formation of six-membered metallacycles by the activation of the O-CH_3 bond, whereas rhodium(I) insertion occurred exclusively into the O-Caryl bond (Scheme 10)[56].

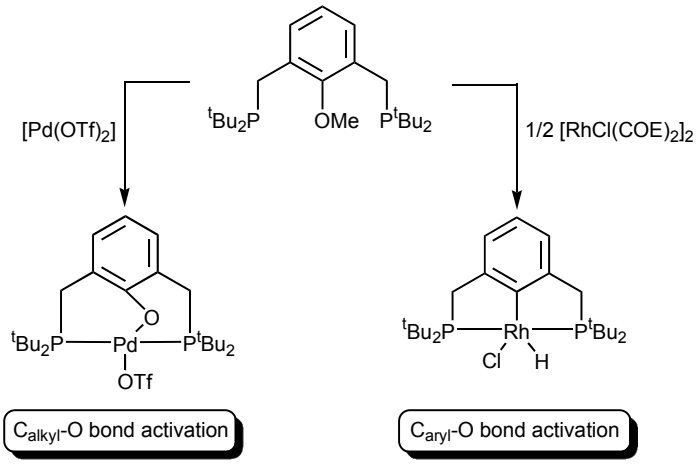

Scheme 10. Metal triggered preferences in C-O bond activation in PC(OCH_3)P pincer ligands.

[54] Rybtquinski, B.; Milstein, D. *Angew. Chem., Int. Ed. Engl.* **1999**, *38*, 871.

[55] (a) van der Boom, M. E.; Kraatz, H.-B.; Hassner, L.; Ben-David, Y.; Milstein, D. *Organometallics* **1999**, *18*, 3873.

[56] (a) van der Boom, M. E.; Liou, S.-Y.; Ben-David, Y.; Shimon, L. J. W.; Milstein, D. *J. Am. Chem. Soc.* **1998**, *120*, 6531. (b) van der Boom, M. E.; Liou, S.-Y.; Ben-David, Y.; Vigalok, A.; Milstein, D. *Angew. Chem. Int. Ed.* **1997**, *36*, 625.

2.5.4 Supramolecular Chemistry

The applications of pincer complexes in supramolecular chemistry have been developed mostly by the group of van Koten[3a]. The stability of square-planar palladium and platinum pincer complexes, along with the presence of a potentially free coordination site *trans* to the M-C bond and the possibility of functionalizing the complexes by aryl substitution has been used to prepare a bimetallic Pd_2-CN synthon and Pd_3 complexes with SCS pincer ligands, which were used for noncovalent metallodendrimer synthesis by controlled self-assembly (Scheme 11)[57].

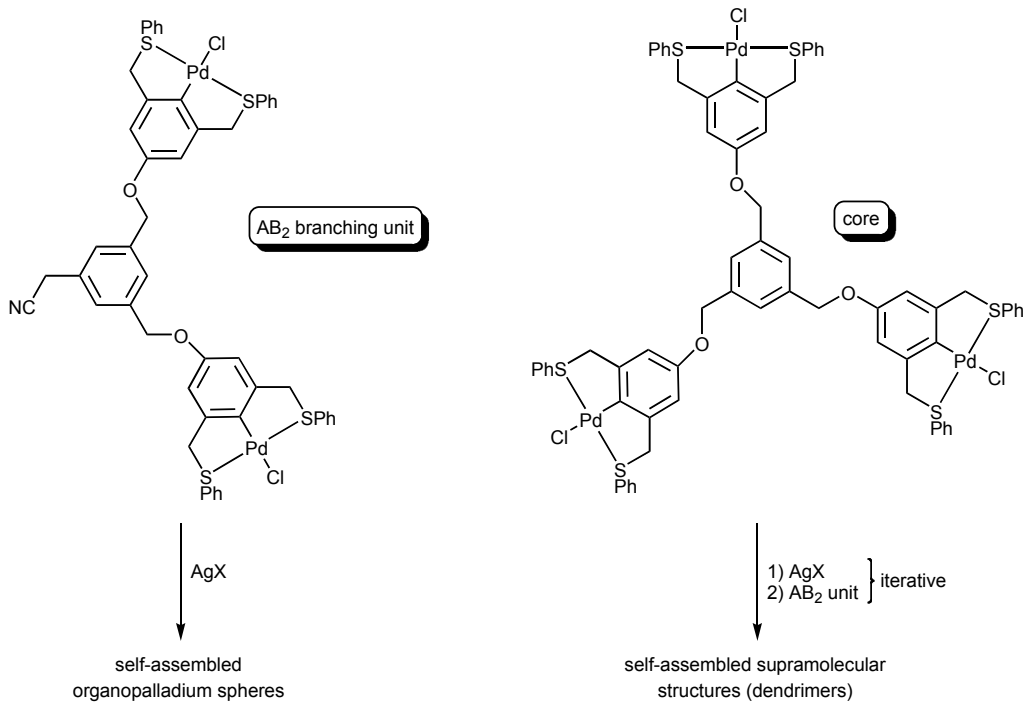

Scheme 11. Functionalized palladium SCS pincer complexes for the infinite (left) and finite (right) self-assembly of supramolecular structures

Palladium SCS pincer complexes bound to different crown ethers or calixarene substituents have been employed to prepare receptors for nitrile and pyridine guests (Scheme 12). Modification of the ring size and of the ring-closing molecule enable the differentiation between guanine and adenine, and therefore the specific detection of all DNA nucleobases[58].

---

[57] (a) Huck, W. T. S.; van Veggel, F. C. J. M.; Reinhoudt, D. N. *Angew. Chem. Int. Ed. Engl.* **1996**, *35*, 1213. (b) Huck, W. T. S.; Hulst, R.; Timmerman, P.; van Veggel, F. C. J. M.; Reinhoudt, D. N. *Angew. Chem. Int. Ed.* **1997**, *36*, 1006. (c) Huck, W. T. S.; van Veggel, F. C. J. M.; Reinhoudt, D. N. *New J. Chem.* **1998**, *22*, 165. (d) Huck, W. T. S.; Snellink-Ruél, B.; van Veggel, F. C. J. M.; Reinhoudt, D. N. *Organometallics* **1997**, *16*, 4287.

[58] (a) Kickham, J. E.; Loeb, S. J.; Murphy, S. L. *J. Am. Chem. Soc.* **1993**, *115*, 7031; (b) Kickham, J. E.; Loeb, S. J.; Murphy, S. L. *Chem. Eur. J.* **1997**, *3*, 1203.

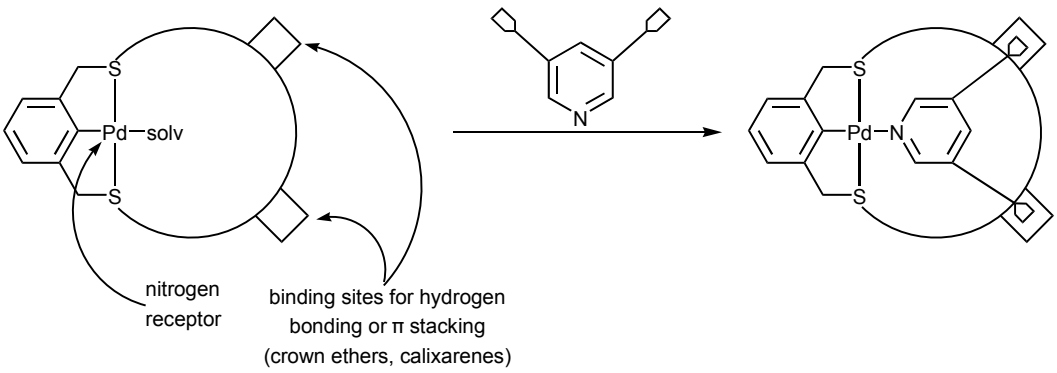

Scheme 12. Palladium SCS pincer complexes functionalized with secondary recognition sites for substrate discrimination

3 Results and Discussion

3.1 Ligands

3.1.1 Introduction

Although pincer ligands and their complexes with different transition metals have been known in the chemical literature for more than 30 years, it was only recently that they established themselves as a class of powerful compounds in organometallic chemistry. A wide array of pincer ligands, with different architectures and properties, and with applications that range from catalysis to supramolecular chemistry, is accessible through several synthetic methods, and some of them are even commercially available[59]. In the case of the PNP and PCP ligands, the first synthetic methods go back to the late 1970s[2a,f]. The synthesis of both PNP and PCP ligands with a methylene spacer between the aromatic backbone and the phosphine donors is possible in one step starting from 2,6-bis(bromomethyl)pyridine or 1,3-bis(bromomethyl)benzene, respectively (Scheme 13) upon treatment with phosphides ($Li^+PR_2^-$).

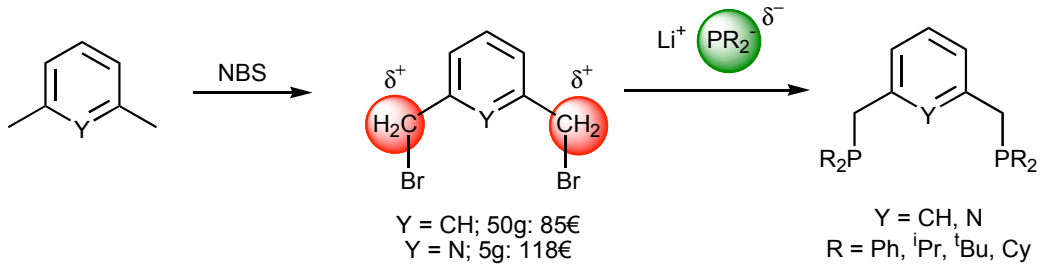

Scheme 13. Synthesis of methylene-bridged PNP and PCP pincer ligands

However, this synthesis has two major drawbacks: first, although both 2,6-bis(bromomethyl)pyridine and 1,3-bis(bromomethyl)benzene are commercially available, they are expensive. They can be prepared via a radical halogenation from 2,6-dimethylpyridine or 1,3-dimethylbenzene, but this adds one more step to the synthetic procedure. Second, the ligands result from the nucleophilic attack of the phosphine to the electrophilic carbon atoms of the methyl groups in the ortho positions of the aryl ring; thus, a nucleophilic phosphine is needed, which reduces the number of phosphines available to alkyl and aryl ones. The steric

[59] Strem Chemicals, Inc.

and electronic properties of the ligands can be modified (although with very little room for variations), but tuning the stereochemical properties turns out to be an extremely difficult task.

An improvement in the synthesis of PNP and PCP ligands is the use of a bridging other than a methylene group between the aryl backbone and the phosphines, a method reported independently by the research groups of Bedford[19a] and Jensen[19c] for the synthesis of several phosphinito PCP ligands. Through a polarity switch ("Umpolung"), the ligands can be prepared in one step by the electrophilic attack of a chlorophosphine on 1,3-dihydroxybenzene in the presence of a base to catch the released hydrochloric acid (Scheme 14). Interestingly, despite the possibility of using phosphines other than the common diphenyl-, diisopropyl- and ditertbutylchlorophosphine, there is only one example, reported by Shibasaki *et al.*[14a], where different phosphine substituents have been used.

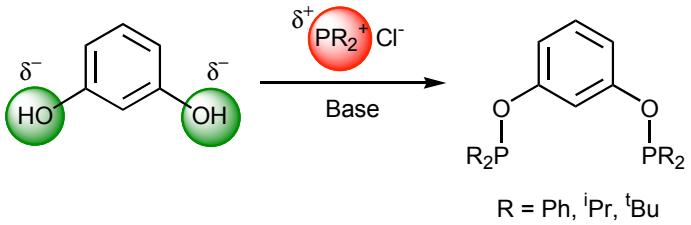

Scheme 14. Synthesis of oxygen-bridged phosphinito PCP pincer ligands

Nevertheless, only PCP ligands can be prepared by this method, since the synthesis of the analogous phosphinito PNP ligands is not possible due to the presence of a tautomeric species of 2,6-dihydroxypyridine. The keto-enol equilibrium is shifted towards the hydroxypyridinone **B**; therefore, the deprotonation and phosphorylation of the second oxygen atom cannot occur (Scheme 15).

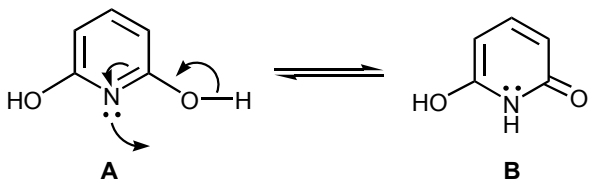

Scheme 15. Keto-enol tautomerism between 1,3-dihydroxypyridine and 6-hydroxypyridin-2-one

A third approach to PNP and PCP pincer ligands (and the one used in the course of this work) is possible by using an amino bridging between the aromatic backbone and the phosphine units; such a method was reported by Haupt and coworkers in 1987 for the synthesis

of *N*,*N*'-bis(diphenylphosphino)-2,6-diaminopyridine (PNP-Ph, **2a**)[60] and also involves the electrophilic attack of a chlorophosphine, this time to the nucleophilic amino groups of 2,6-diaminopyridine. This methodology can be extended to the preparation of PCP ligands by using 1,3-diaminobenzene instead of 2,6-diaminopyridine (Scheme 16). Compared to the PNP and PCP ligands with methylene bridgings, where a nucleophilic phosphide is necessary for the preparation of the ligands, a polarity switch (that is, changing the bridging to an amino group) makes the synthesis of both PNP and PCP ligands easier through the condensation of an aromatic diamine with an easier accessible electrophilic chlorophosphine. Both 2,6-diaminopyridine and 1,3-diaminobenzene are commercially available and cheap. Since different chlorophosphines can be used for the preparation of such ligands, the steric, electronic and stereochemical properties of the ligands can be easily modified by changing the phosphine building block.

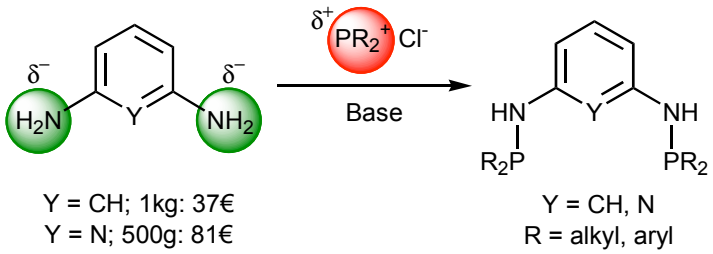

Scheme 16. Synthesis of amino-bridged PNP and PCP pincer ligands

3.1.2 Chlorophosphites

Synthesis

Chlorophosphines are building blocks for the synthesis of both PNP and PCP ligands; however, the number commercially available chlorophosphines is limited. Several N- and O-containing chlorophosphines (chlorophosphites) can be easily synthesized in one step from inexpensive, commercially available diols or aminoalcohols and PCl_3. Bidentate diols and aminoalcohols react with PCl_3 cleanly to give the desired chlorophosphites in high yields, whereas the reaction of monodentate alcohols (or amines) with PCl_3 gives a mixture of monosubstituted dichlorophosphites, disubstituted chlorophosphites and trisubstituted phosphites (or aminophosphines), as well as other byproducts resulting from P-P coupling reactions (Scheme 17).

[60] Schirmer, W.; Flörke, U.; Haupt, H.-J. *Z. anorg. allg. chem.* **1987**, *545*, 83.

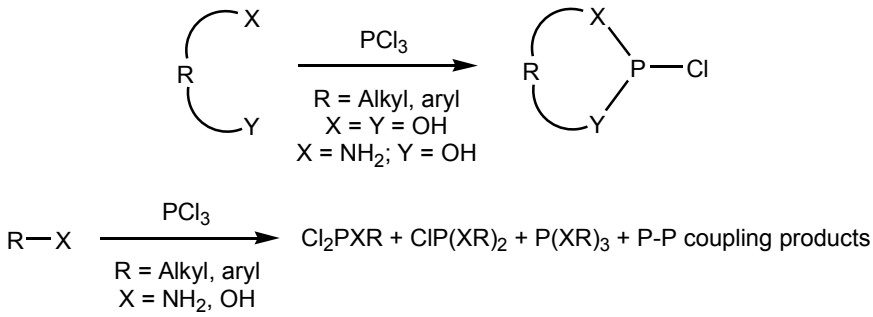

Scheme 17. Synthesis of chlorophosphites from diols and aminoalcohols

The general method for the synthesis of the chlorophosphites used in this work is depicted in Scheme 18 and consists of treating a diol or aminoalcohol with PCl_3 in the presence of a base. All the chlorophosphites are known in the literature and were prepared according to published procedures[61]. For the synthesis of **1d-f**, *N*-methylpyrrolidone was used in catalytic amounts as a base (1-10 mol%). Hydrochloric acid was released and the reaction was carried out in neat PCl_3 at 75-80ºC for three hours. The chlorophosphites could be isolated in good yields (70-80%) by removing the excess of PCl_3 under vacuum followed by bulb to bulb distillation. In the case of **1a**, **1c** and **1g**, stoichiometric amounts of base (triethylamine or *N*-methylmorpholine) were used, the reaction was typically carried out in an inert solvent (THF or toluene) at room temperature overnight, and the isolation of the chlorophosphites was easily achieved through filtration of the ammonium salt and removal of the solvent under vacuum. It was possible to prepare 2,2'-biphenylylenephosphochloridite (**1b**) using either a catalytic or a stoichiometric amount of base.

[61] (a) **1a**: Lucas, H. J.; Mitchell, F. W., Jr.; Scully, C. N. *J. Am. Chem. Soc.* **1950**, *72*, 5491. (b) **1b**: Lot, O.; Suisse, I.; Mortreux, A.; Agbossou, F. *J. Mol. Cat. A* **2000**, *164*, 125. (c) **1c**: Ini, S.; Oliver, A. G.; Tilley, T. D.; Bergman, R. G. *Organometallics* **2001**, *20*, 3839. (d) **1d** and **1e**: Kadyrov, R.; Heller, D.; Selke, R. *Tetrahedron: Asymmetry* **1998**, *9*, 329. (e) **1f**: Park, H.; RajanBabu, T. V. *J. Am. Chem. Soc.* **2002**, *124*, 734. (f) **1g**: Oka, N.; Wada, T.; Saigo, K. *J. Am. Chem. Soc.* **2003**, *125*, 8307.

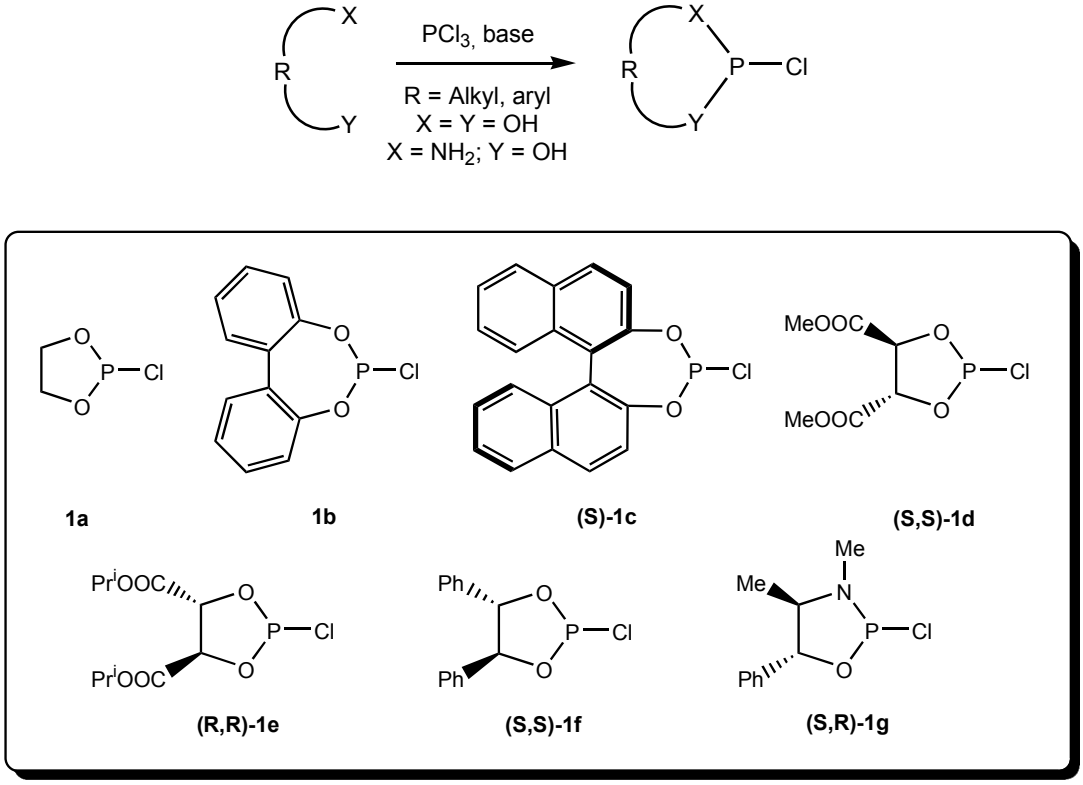

Scheme 18. Synthesis of the chlorophosphites **1a-g**

Characterization

All these compounds are colorless to pale yellow oils or solids and not extremely air sensitive, but hydrolyse easily in contact with moisture and are best stored under inert atmosphere. They were identified by ^{1}H and $^{31}P\{^{1}H\}$ NMR spectroscopy. The chlorophosphites **1a-g** exhibit a single resonance in the $^{31}P\{^{1}H\}$ NMR spectrum in the range between 169.0 and 181.1 ppm, consistent with a strong deshielding of the phosphorus atom (Table 2).

Table 2. Employed base, yields and characteristic $^{31}P\{^1H\}$ NMR resonances for the phosphites **1a-g**[a]

Phosphine	Base (mol%)	Yield (%)	$^{31}P\{^1H\}$ (δ, [ppm], 20ºC)
1a	Et_3N (250)	69	169.0
1b	Et_3N / NMP (250 / 1)	79 / 81	181.1
1c	Et_3N (220)	89	179.8
1d	NMP (10)	82	176.3
1e	NMP (10)	75	176.4
1f	NMP (10)	72	174.6
1g	N-Methylmorpholine (300)	92	172.7

[a] NMP: N-methylpyrrolidone

3.1.3 PNP Ligands

Synthesis

One of the goals of this work was to prepare new PNP and PCP ligands with different electronic, steric and stereochemical properties starting from cheap starting materials by a convergent synthetic method, that is, by the modular assembly of different building blocks. Only the PNP ligand with phenyl substituents at the phosphine groups had been reported in the literature so far[60], and the first step was to prepare analogous ligands with other commercially available chlorophosphines, *i.e.* the bulkier chlorodiisopropylphosphine and chloroditertbutylphosphine. Due to the different shifts of the free chlorophosphines and of the aminophosphine moieties in the PNP ligands, the course of the reaction could be easily monitored by $^{31}P\{^1H\}$ NMR spectroscopy.

The synthesis of PNP-Ph (**2a**) was straightforward and could be achieved by adding two equivalents of chlorodiphenylphosphine to a cooled mixture of one equivalent of 2,6-diaminopyridine and two equivalents of triethylamine in toluene and by heating the mixture at 80ºC for sixteen hours. Filtration of the formed ammonium salt, evaporation of the solvent under vacuum and recrystallization from toluene:*n*-hexane (1:1) gave **2a** in 86% yield as a white solid (Scheme 19).

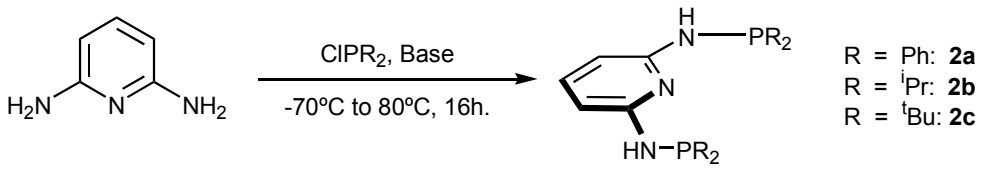

Scheme 19. Synthesis of the PNP pincer ligands **2a-c**

However, when the same conditions were applied to the synthesis of PNP-^{i}Pr (**2b**) and PNP-^{t}Bu (**2c**), no reaction took place. For **2b**, the PNP ligand could be obtained in some cases by refluxing the reaction mixture for sixteen hours. For **2c**, no reaction was observed even after refluxing the reaction mixture for 24 hours. In the cases where the reaction did not work, only unreacted chlorophosphines (and no decomposition products) were observed by $^{31}P\{^{1}H\}$ NMR spectroscopy. The use of a stronger base, *n*-BuLi, was also unsuccessful. That the condensation of 2,6-diaminopyridine with chlorodiisopropylphosphine and chloroditertbutylphosphine is more difficult than that of 2,6-diaminopyridine with chlorodiphenylphosphine can be attributed to the more basic, electron donating character of the alkyl phosphines. It was a combination of triethylamine and *n*-BuLi that proved reactive enough for the formation of the desired products to occur. *n*-BuLi in inert solvents and in diethyl ether is known to have a tetrameric structure (**A**), while in THF and in other coordinating solvents it is a mixture of both tetramer **A** and dimer **B**[62] (Scheme 20). Since *n*-BuLi is known to form 1:1 and 1:2 adducts with triethylamine[63], the role of this base might be to cleave the tetramer in order to make it more reactive. Such a combination of bases has been used to improve yields in several polymerization studies, for example[64].

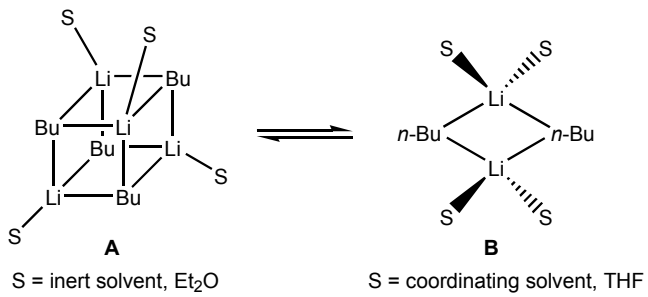

Scheme 20. The structure of n-BuLi in inert (left) and coordinating solvents (right)

Thus, for the preparation of **2b** and **2c**, two equivalents of the corresponding chlorophosphine were added to a cooled mixture of one equivalent of 2,6-diaminopyridine and two equivalents of triethylamine in toluene, followed by further cooling to -70ºC and addition of two equivalents of a *n*-BuLi solution. The mixture was then stirred at 80ºC for sixteen hours, filtered, and the solvent was removed under vacuum. Finally, both ligands were purified by recrystallization from toluene:*n*-hexane (1:1) (Scheme 19).

Following the procedure for the PNP ligands with phenyl, ^{i}propyl and ^{t}butyl substituents at

---

[62] Keresztes, I.; Williard, P. G. *J. Am. Chem. Soc.* **2000**, *122*, 10228. (b) Qu, B.; Collum, D. B. *J. Am. Chem. Soc.* **2006**, *128*, 9355.

[63] Zgonnik, V. N.; Sergutin, V. M.; Kalnin'sh, K. K.; Lyubimova, G. V.; Nikolaev, N. I. *Russ. Chem. Bull.* **1977**, *26(4)*, 709.

[64] (a) Welch, F. J. *J. Am. Chem. Soc.* **1960**, *82*, 6000. (b) Sanderson, R. D.; Costa, G.; Summers, G. J.; Summers, C. A. *Polymer* **1999**, *40*, 5429.

the phosphine groups, the preparation of other PNP ligands derived from the non commercially available chlorophosphites described in the previous section was carried out analogously. Phosphites are more electron withdrawing than phosphines; thus, the synthesis of the ligands **2d-j** proceeded in a similar way as that for PNP-Ph (**2a**): addition of two equivalents of the corresponding chlorophosphite to a suspension of one equivalent of 2,6-diaminopyridine and two equivalents of triethylamine in toluene at 0ºC followed by heating the reaction mixture at 80ºC for sixteen hours gave, after filtration and removal of the solvent under vacuum, the PNP ligands **2d-e** and **2g-j** as colorless/white to yellow oils or solids in moderate to good yields (52-95%) (Scheme 21). All the ligands prepared this way were pure enough (>97%) for their further use and required no purification steps.

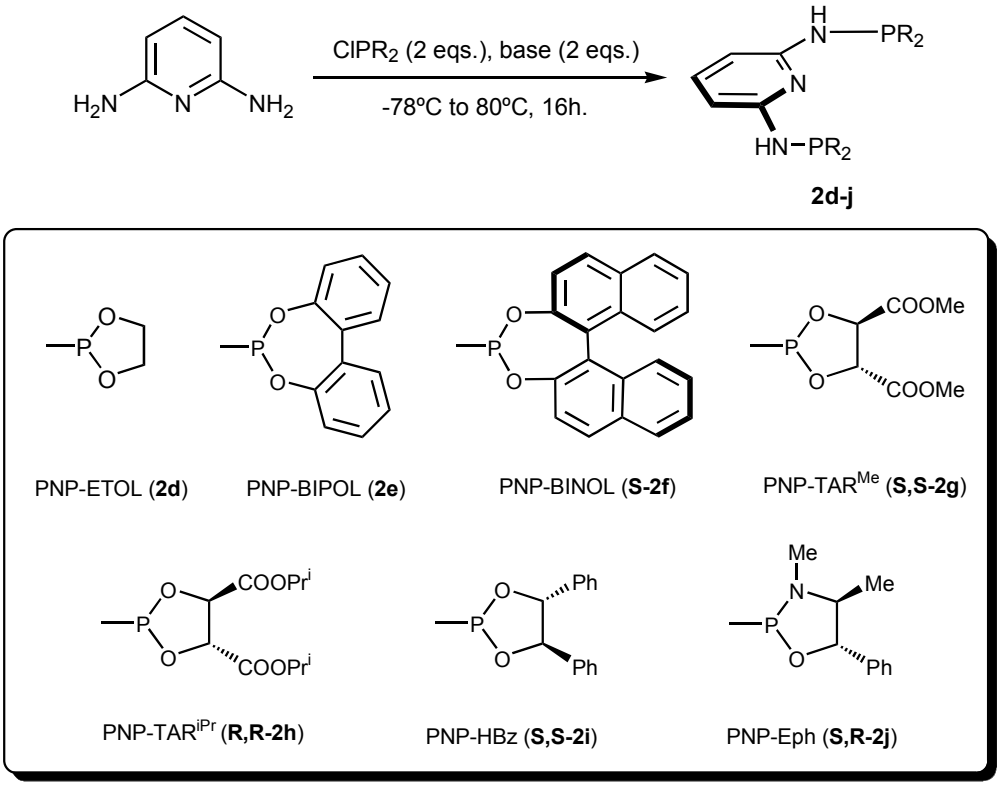

Scheme 21. Synthesis of the PNP ligands **2d-j**

Only in the case of PNP-BINOL (**2f**) a different synthetic approach was used: when triethylamine was used as a base, two peaks at 152.6 and 145.9 ppm in the $^{31}P\{^{1}H\}$ NMR spectrum were observed. At first it was thought that these two peaks corresponded to two different isomers of the PNP ligand, due to the chiral nature of the phosphine substituents; as it was realized laterm the peak at 145.9 ppm corresponded to **1c**, while the product showing the signal at 152.6 ppm could not be identified. However, a publication by Osborn and coworkers describing the synthesis of a similar pincer ligand reported only a single resonance for the

phosphines in the $^{31}P\{^1H\}$ NMR spectrum[65]. Thus, the reaction conditions were changed: using a different solvent (THF), a different base (*n*-BuLi) and lower temperatures (-78ºC for the addition of the base and room temperature for the reaction), only one resonance at 146.0 ppm in the $^{31}P\{^1H\}$ NMR spectrum was observed. After filtration and evaporation of the solvent under vacuum, **2f** was obtained in 94% yield as a white solid without any further purification steps. It is important to note that, unlike in the case of the PNP ligands with phosphine substituents (**2a-c**), where the reaction is not so sensitive towards air and/or moisture, (for example, **2a** can also be prepared under air using off the bench toluene with no decrease in the yield or in the purity of the product compared to when the reaction is carried out under argon with dry toluene), the synthesis of **2d-j** must be carried out under an inert atmosphere and using dry solvents. Otherwise, different by-products are obtained, which cannot be separated from the main product by common methods such as column chromatography due to the sensitive nature of the ligands. The sensitivity of the PNP ligands towards air and moisture can be described as follows:

air and moisture sensitivity

← PNP-Phosphite > PNP-^{t}Bu ≈ PNP-^{i}Pr > PNP-Ph

Characterization

The ligands **2a-j** were characterized by ^1H, $^{31}P\{^1H\}$ and $^{13}C\{^1H\}$ NMR spectroscopy. The formation of the PNP ligands can be confirmed, of course, by $^{31}P\{^1H\}$ spectroscopy, as well as by the shift differences in the signals of the pyridine and of the N*H* protons in the ^1H NMR spectra. While in 2,6-diaminopyridine the pyridine protons py^4 appear at 6.98 ppm, in the phosphorylated ligands they give rise to a triplet in the range between 7.54 and 7.11 ppm with coupling constants $^3J_{HH}$ of 7.5 to 8.0 Hz, whereas the pyridine protons py^{3,5} show a double doublet between 6.53 and 6.42 ppm (doublet at 5.60 ppm in 2,6-diaminopyridine) with coupling constants $^3J_{HH}$ of 7.5 to 8.0 Hz and $^4J_{PH}$ of 1.6 to 2.5 Hz. It has to be noted that in some cases the signals of the pyridine protons could not be detected independently due to the presence of other aromatic protons in the molecule. In the case of the N*H* protons, which appear as a broad singulet at 4.22 ppm in 2,6-diaminopyridine, in the PNP ligands they appear in the range between 4.29 and 6.54 ppm and give rise to broad singulets or doublets with coupling constants $^2J_{HP}$ between 7.8 and 11.2 Hz (Table 3).

[65] Sablong, R.; Newton, C.; Dierkes, P.; Osborn, J. A. *Tetrahedron Lett.* **1996**, *37*, 4933.

Table 3. Selected ^{1}H NMR resonances for the PNP ligands **2a-j**.

Ligand	^{1}H NMR (δ, [ppm], 20ºC)				
	py^{4} (1H)	py^{3,5} (2H)	$^{3}J_{HH}$ (Hz)	N*H* (1H)	$^{2}J_{HP}$ (Hz)[b]
2a	7.35	6.53	7.9	5.39	-
2b	7.23	6.42	7.9	4.29	11.2
2c	7.25	6.48	7.6	4.64	11.2
2d	7.28	6.29	7.9	5.70	-
2e	7-49 - 7.15[a]	5.89	7.8	4.32	-
2f	7.54 - 7.29[a]	6.06	7.9	5.72	8.2
2g	7.30	6.28	7.9	6.45	-
2h	7.28	6.26	7.9	6.54	-
2i	7.38 - 7.11[a]	6.43	7.9	6.05	8.2
2j	7.37 - 7.15[a]	7.37 - 7.15[a]	8.0	5.86	7.8

[a]Signal overlaps with other aromatic signals. [b]When no coupling costant is given, the signal appeared as a singulet.

In the ^{13}C{^{1}H} NMR spectra, the pyridine signals of the ligands do not vary too much when compared to those in 2,6-diaminopyridine: the py^{2,6} carbon atoms appear as a doublet between 153.8 and 162.2 ppm (158.5 in 2,6-diaminopyridine) with coupling constants $^{2}J_{CP}$ of 20.2 Hz for the phosphine PNP ligands (**2a-c**) and between 14.9 and 17.3 Hz for the phosphite PNP ligands (**2d-j**). The py^{3,5} carbon atoms give rise to a singulet[66] in the range between 138.7 and 140.2 ppm (138.0 ppm in 2,6-diaminopyridine), while the py^{4} carbon atoms give rise to a doublet between 98.1 and 101.9 ppm (95.0 ppm in 2,6-diaminopyridine) with coupling constants $^{4}J_{CP}$ of 18.4 Hz for the ligands **2a-c** and between 10.1 Hz and 12.3 Hz for the ligands **2d-j** (Table 4). As for the ^{31}P{^{1}H} NMR spectra, the signals of the ligands are in all cases shifted to the high field when compared to those of the corresponding chlorophosphines (or chlorophosphites); for the ligands **2a-c**, their ^{31}P{^{1}H} NMR signals appear between 28.0 (**2a**) and 60.2 ppm (**2c**). This is somewhat surprising, since one would expect the alkyl phosphine PNP ligands **2b** and **2c** to show resonances shifted to the high field when compared to the signal of **2a**, due to the electron donating properties of the ^{i}propyl and ^{t}butyl substituents. However, the +I effect of alkyl substituents is known to be very small, while the phenyl group can induce a higher electron density at the phosporus atom thanks to a +M effect. In the case of the ligands **2d-j**, with electron withdrawing phosphites, their signals appear in the range between 119.0 and 147.5 ppm, consistent with a stonger deshielding of the phosphorus atom (Table 4).

[66] Only in the case of **2a** a carbon-phosphorus coupling with $^{3}J_{CP}$ = 12.1 Hz was observed.

Table 4. Selected $^{13}C\{^1H\}$ and $^{31}P\{^1H\}$ NMR resonances for the ligands **2a-j.**

Ligand	$^{13}C\{^1H\}$ NMR (δ, [ppm], 20ºC)			$^{31}P\{^1H\}$ NMR
	$py^{2,6}$	$py^{3,5}$	py^4	(δ, [ppm], 20ºC)
2a	157.6	139.9	99.2	28.0
2b	159.5	139.1	98.1	49.0
2c	155.1	138.7	98.2	60.2
2d	157.0	139.6	100.8	129.9
2e	154.2	140.0	101.5	147.5
2f	162.2	139.7	100.6	146.1
2g	153.8	139.7	101.9	142.9
2h	154.1	139.6	101.5	142.7
2i	157.6	140.2	100.7	130.0
2j	157.0	140.1	99.7	119.0

In our research group, several other PNP ligands have also been prepared: for example, the amino bridgings can be alkylated to circumvent the possible problems derived from the acidity of the NH protons (**A**, Figure 14)[67]. Furthermore, a different aromatic backbone, such as 2,6-diamino-4-phenyl-1,3,5-triazine, can be used to prepare PNP pincer ligands (**B**)[68]. Until now, however, these alternative PNP ligands have only been synthesized with phenyl substituents at the phosphines, and the preparation of ligands with different substituents has proven to be more difficult than expected.

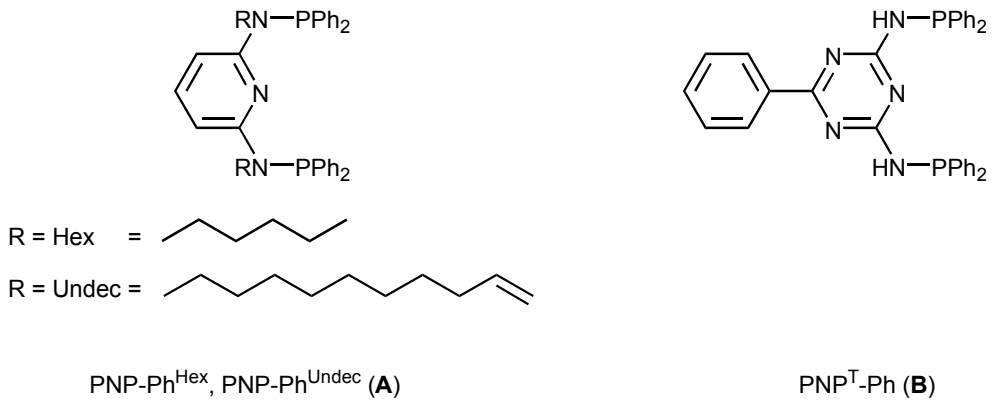

Figure 14. *N*-alkylated amino-bridged (**A**) and triazine-based (**B**) PNP pincer ligands

[67] Pollak, M. Diploma Thesis, Vienna University of Technology, 2006.

[68] Wiedermann, J. Ph. D. Thesis, Vienna University of Technology, unpublished.

3.1.4 PCP Ligands

Synthesis

One of the advantages of the modular synthesis of aminophosphine based pincer ligands is that both neutral PNP as well as anionic PCP ligands can be easily obtained just by changing the diamine precursor. The synthesis of PCP-Ph (**3a**) and PCP-^{i}Pr (**3b**) can be achieved under the same conditions than those described for the preparation of PNP-Ph (**2a**): the addition of two equivalents of the corresponding chlorophosphine to a suspension of one equivalent of 1,3-diaminobenzene and two equivalents of triethylamine in toluene followed by heating the reaction mixture at 80ºC for sixteen hours, filtration of the resulting ammonium salt and evaporation of the solvent under vacuum gave ligands **3a** and **3b** as white solids in good yields (84 and 79%, respectively) (Scheme 22).

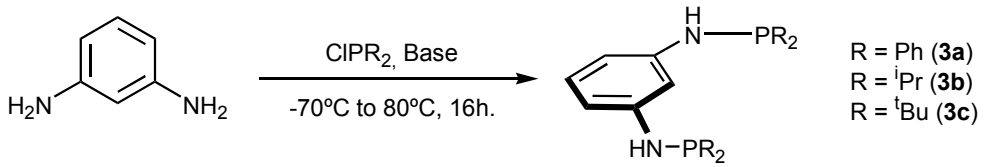

Scheme 22. Synthesis of the PCP pincer ligands **3a-c**

In the case of PCP-^{t}Bu (**3c**), a combination of triethylamine and *n*-BuLi had to be used; following the same synthetic procedure as that for PNP-^{i}Pr (**2b**) and PNP-^{t}Bu (**2c**), **3c** could be isolated as a white solid in an excellent yield (96%).

Compared to the PNP ligands, where a combination of bases was needed for the preparation of both alkyl phosphine ligands **2b** and **2c**, the only case in the synthesis of the PCP ligands where such a combination was necessary was when a very bulky, basic phosphine such as di-tert-butylchloriphosphine was used (ligand **3c**). The reason for this cannot be the pK_a data of the aromatic diamines; 2,6-diaminopyridine has pK_a values of 2.16 and 2.90 for each of the amino groups[69], respectively, while 1,3-diaminobenzene has a pK_a value of 2.50 for both amino groups[70]. However, when looking at the intermediate formed by the deprotonation of one amino group (Scheme 23), an important difference between both diamines can be recognized: while in the case of 1,3-diaminobenzene only the resonant structure **A** is more stable than the others, for 2,6-diaminopyridine the resonances **A** and **D** are more stable due to the negative

[69] Moghimi, A.; Alizadeh, R.; Shokrollahi, A.; Aghabozorg, H.; Shamsipur, M.; Shockravi, A. *Inorg. Chem.* **2003**, *42*, 1616.

[70] David R. Lide, ed., CRC Handbook of Chemistry and Physics 2006 - 2007, 87th ed., Taylor and Francis, Boca Raton, FL, **2007**.

charge at the more electronegative nitrogen atom; thus, for 2,6-diaminopyridine, the negative charge is distributed between the nitrogen atoms of the deprotonated amine and of the pyridine ring, making an electrophilic attack of the phosphine more difficult. While this is not relevant when the reaction is performed with chlorodiphenylphosphine, it is when using bulkier, more basic phosphines.

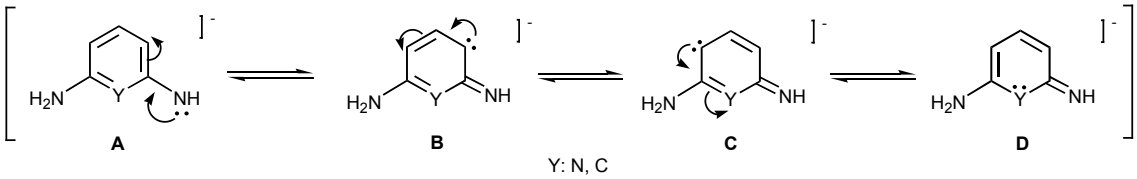

Scheme 23. Resonance structures for a deprotonated aromatic *ortho,ortho*-diamine

The synthesis of PCP pincer ligands substituted at the central aromatic moiety is also possible: two such ligands were prepared starting from the commercially available diamines 5-(trifluoromethyl)-1,3-benzenediamine and 3,5-diamino-4-chloroisobutylbenzoate (Scheme 24). Their synthesis is analogous to that of **3a**[71], with the only difference that THF was used instead of toluene; **3d** and **3e** were obtained as a colourless oil and a white solid in 94 and 82% yield, respectively.

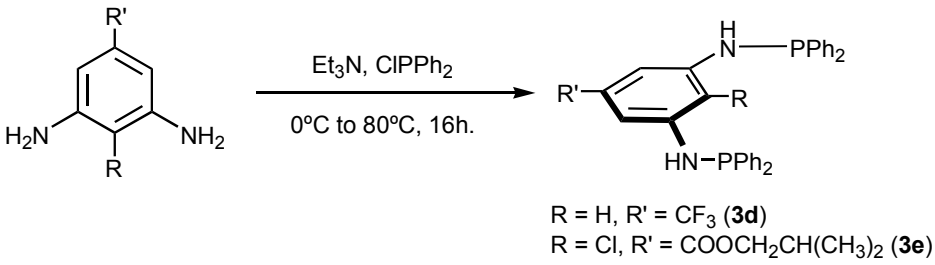

Scheme 24. Synthesis of the PCP pincer ligands **3d-e**

Characterization

The PCP ligands **3a-e** were characterized by ^{1}H, $^{31}P\{^{1}H\}$ and $^{13}C\{^{1}H\}$ NMR spectroscopy[72] and, like in the case of the PNP ligands, their formation can be monitored by $^{31}P\{^{1}H\}$ spectroscopy. In the ^{1}H NMR spectra, the Ph^{4} protons give rise to a triplet between 6.89 and 6.99 ppm, while the $Ph^{3,5}$ protons appear as a doublet between 6.36 and 7.61 ppm. The

[71] For **3d**, no heating was necessary, for **3e** the reaction was performed at 50ºC.

[72] For comparison: 1,3-diaminobenzene: ^{1}H NMR (δ, $CDCl_3$, 20°C): 3.53 (NH_2), 5.94 (H^{ipso}), 6.08 ($Ph^{3,5}$), 6.91 (Ph^{4}). $^{13}C\{^{1}H\}$ NMR (δ, $CDCl_3$, 20°C): 102.0 (Ph^{ipso}), 106.0 ($Ph^{3,5}$), 130.2 (Ph^{4}), 147.5 ($Ph^{2,6}$).

coupling constants $^{3}J_{HH}$ lie between 7.9 and 8.0 Hz. The Ph^{ipso} protons give rise to a triplet in the range between 6.64 and 7.61 ppm with small coupling constants $^{4}J_{HH}$ between 2.1 and 2.3 Hz. The N*H* protons appear as doublets between 3.63 and 5.10 ppm with coupling constants $^{2}J_{HP}$ between 7.3 and 11.0 Hz depending on the ligand backbone and the phosphine substituent (Table 5).

Table 5. Selected ^{1}H NMR resonances for the ligands **3a-e**.

Ligand	^{1}H NMR (δ, [ppm], 20ºC)					
	Ph^{4} (1H)	$Ph^{3,5}$ (2H)	$^{3}J_{HH}$ (Hz)	Ph^{ipso} (1H)	N*H* (2H)	$^{2}J_{HP}$ (Hz)
3a	6.99	6.50	8.0	6.72	4.39	8.2
3b	6.92	6.37	8.0	6.64	3.63	10.5
3c	6.89	6.36	7.9	6.73	3.96	11.0
3d	-	6.76	-	6.88	4.56	8.2
3e	-	7.61 - 7.36	-	-	5.10	7.3

[a]Signal overlaps with other aromatic signals.

In the $^{13}C\{^{1}H\}$ NMR spectra, the signals of the benzene ring do not vary much when compared to those of 1,3-diaminobenzene: the $Ph^{2,6}$ carbon atoms give rise to a doublet in the range between 143.4 and 150.1 ppm with coupling constants $^{2}J_{CP}$ between 16.5 and 19.6 Hz. The Ph^{4} carbon atoms appear around 130.0 ppm, the $Ph^{3,5}$ carbon atoms show a doublet in the range between 105.5 and 107.3 ppm with coupling constants $^{3}J_{CP}$ of about 13.0 Hz and the Ph^{ipso} carbon atoms give rise to a triplet between 103.2 and 106.4 ppm with coupling constants $^{3}J_{CP}$ between 4.4 and 13.4 Hz. As for the $^{31}P\{^{1}H\}$ NMR spectra, all the ligands show a single resonance between 28.6 and 59.3 ppm. Similarly to the PNP pincer ligands **2a-j**, the signals of the PCP ligands **3a-e** appear shifted to the upfield when compared to those of the chlorophosphines or chlorophosphites (Table 6).

Table 6. Selected $^{13}C\{^{1}H\}$ and $^{31}P\{^{1}H\}$ NMR resonances for the ligands **3a-e**.

Ligand	$^{13}C\{^{1}H\}$ NMR (δ, [ppm], 20ºC)				$^{31}P\{^{1}H\}$ NMR
	$Ph^{2,6}$	Ph^{4}	$Ph^{3,5}$	Ph^{ipso}	(δ, [ppm], 20ºC)
3a	147.7	130.1	107.3	103.3	28.6
3b	149.6	129.5	106.5	103.4	48.9
3c	150.1	129.6	106.5	103.5	59.3
3d	148.2	130.3	105.5	103.7	27.0
3e	143.4	130.3	107.2	106.4	30.6

Finally, it has to be noted that the preparation of PCP ligands with P-O bond containing substituents at the phosphorus atoms is possible and has also been investigated in our research group[73].

3.1.5 PN Ligands

Synthesis

The synthetic approach used to prepare tridentate PNP and PCP pincer complexes can also be applied to the synthesis of bidentate PN ligands, and several such ligands were synthesized with two different aromatic backbones. In the first case, several “one-armed” versions of the PNP ligands can prepared by using 2-aminopyridine instead of 2,6-diaminopyridine. Alternatively, phosphite PN ligands with an oxygen bridging between the aromatic backbone and the phosphine group can be prepared using 2-hydroxyquinoline as precursor. While the synthesis of oxygen-bridged PNP pincer ligands is not possible due to the presence of a keto-enol equilibrium (Scheme 15), such a tautomerism is not possible in the case of 2-hydroxyquinoline and the hydroxy group can be easily deprotonated and phosphorylated.

The PN ligands **4a-d** and **5a-b** featuring different phosphine substituents were all synthesized using the same method: one equivalent of the corresponding chlorophosphine was added at 0ºC to a solution of equimolar amounts of 2-aminopyridine or 2-hydroxyquinoline and triethylamine in toluene, followed by heating the reaction mixture at 80ºC for three hours. After filtration of the formed ammonium salts and evaporation of the solvent under vacuum, the ligands **4a-d** and **5a-b** were obtained in moderate to good yields (66-95%) as white/yellow solids or oils (Scheme 25). All the ligands are air stable, but decompose in the presence of water. Since these ligands are bidentate and only one condensation step is required for their synthesis, the reaction times were shorter (three hours) than those needed for the preparation of the tridentate PNP pincer ligands **2a-j** (sixteen hours).

[73] Bocokic, V. Diploma Thesis, Vienna University of Technology, **2006**.

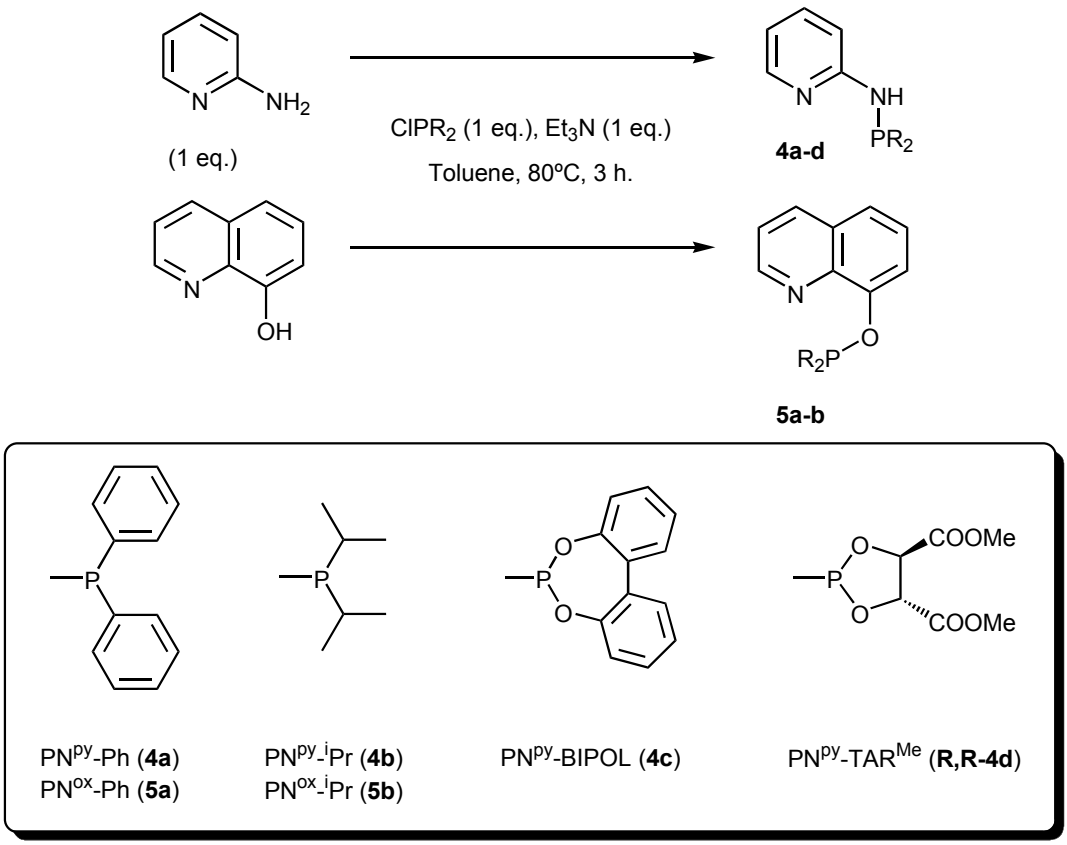

Scheme 25. Synthesis of the PN ligands **4a-d** and **5a-b**

Characterization

The ligands **4a-d** and **5a-b** were characterized by ^{1}H, $^{31}P\{^{1}H\}$ and $^{13}C\{^{1}H\}$ NMR spectroscopy. Like in the case of the PNP and PCP pincer ligands, their formation can be monitored by $^{31}P\{^{1}H\}$ NMR spectroscopy.

Table 7. Selected ^{1}H NMR resonances for the PN ligands **4a-d**.

Ligand	^{1}H NMR (δ, [ppm], 20ºC)				
	py^{6} (1H)	py^{4} (1H)	py^{3} (1H)	py^{5} (1H)	N*H* (1H)
4a	7.93	7.36-7.33[a]	7.06	6.64	5.93
4b	8.00	7.42	7.08	6.61	4.94
4c	8.12	7.54-7.47[a]	6.84-6.79[a]	6.84-6.79[a]	6.38
4d	8.14	7.48	6.80	6.70	6.60

[a]Signal overlaps with other aromatic signals.

In the ^{1}H NMR spectra of the pyridine-based ligands **4a-d** (Table 7), the py[6] hydrogen atoms appear as doublets between 7.93 and 8.14 ppm with coupling constants $^{3}J_{HH}$ between 3.9 and 5.0 Hz. The other hydrogen atoms of the central pyridine ring give rise to signals at higher fields between 6.61 and 7.54 ppm, while the N*H* protons appear as singulets or doublets between 4.94 and 6.60 ppm, with coupling constants $^{2}J_{HP}$ between 8.4 and 10.5 Hz. In the case of the quinoline-based ligands **5a-b**, the hydrogen atoms in the ortho and para positions to the nitrogen atom in the aromatic ring appear as double doublets between 8.96 and 8.92 ppm and between 8.13 and 8.07 ppm, respectively. The coupling constants $^{3}J_{HH}$ and $^{4}J_{HH}$ lie between 4.0 and 8.2 Hz and between 1.5 and 1.8 Hz, respectively. The other protons in the aromatic backbone give rise to signals between 7.87 and 7.26 ppm. The ^{13}C{^{1}H} NMR spectra of the ligands **4a-d** and **5a-b** bear no unusual features and the signals appear within the expected ranges. All the ligands show a single resonance in the ^{31}P{^{1}H} NMR spectra (Table 8): this signal lies at 27.5 and 50.1 ppm for the phosphine ligands **4a** and **4b** and at 147.3 and 142.6 ppm for the phosphite ligands **4c** and **4d**. In the case of the phosphite ligands **5a-b**, in which the phosphorus atom is bound to an electron withdrawing oxygen atom, their ^{31}P{^{1}H} NMR signals are shifted to the low field and appear at 118.4 and 158.2 ppm, respectively.

Table 8. ^{31}P{^{1}H} NMR resonances for the PN ligands **4a-d** and **5a-b**.

Ligand	^{31}P{^{1}H} NMR (δ, [ppm], 20ºC)
4a	27.5
4b	50.1
4c	147.3
4d	142.6
5a	118.4
5b	158.2

3.1.6 NPN Ligands

Synthesis

The concept of aminophosphine-based PNP ligands can be modified to prepare NPN pincer ligands. Several such ligands based on oxazolines and transition metal complexes thereof have been reported in the literature[74]. Ligand **6** was prepared according to a published

[74] (a) Braunstein, P.; Naud, F.; Dedieu, A.; Rohmer, M.-M.; DeCian, A.; Rettig, S. *Organometallics* **2001**, *20*, 2966. (b) Braunstein, P.; Naud, F.; Pfalz, A.; Rettig, S. J. *Organometallics* **2000**, *19*, 2676.

procedure[75] by adding one equivalent dichlorophenylphosphine to a cooled solution of four equivalents of 2-aminopyridine in THF. In this case, the excess of 2-aminopyridine acts as the base required for the trapping of the released hydrochloric acid. The reaction mixture was stirred for three hours at room temperature and, after the ammonium salt was filtered and the solvent removed under vacuum, **6** was obtained in 91% yield as an air stable white solid (Scheme 26). In contrast to the PNP ligands **2a-j**, which coordinate to the metal center in a meridional way, ligand **6** can only coordinate in a facial way, because the central phosphorus atom needs to adopt a tetrahedral geometry and the pyridine rings are planar.

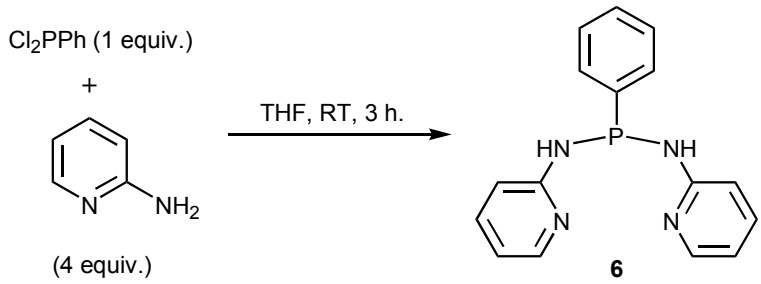

Scheme 26. Synthesis of NPN^{py} (**6**)

Characterization

Ligand **6** was identified by ^{1}H, ^{31}P{^{1}H} and ^{13}C{^{1}H} NMR spectroscopy. In the ^{1}H NMR spectrum, the aromatic protons appear between 8.01 and 7.07 ppm, while the N*H* hydrogen atoms of the amino bridging give rise to a triplet at 6.58 ppm with coupling constant $^{2}J_{PH}$ = 6.1 Hz. In the ^{13}C{^{1}H} NMR spectrum, the signals appear within the expected ranges, and in the ^{31}P{^{1}H} NMR spectrum ligand **6** shows a single resonance at 45.5 ppm.

[75] Lindner, E.; Rauleder, H.; Hilller, W. *Z. Naturforsch.* **1983**, *38b*, 417.

3.2 Iron Complexes

3.2.1 Introduction

Despite the fact that they have been known in the chemical literature for a long time, the chemistry of pincer complexes has only been developed for a few transition metals, and iron is not among these. One could think of several reasons to explain this, one of them being that the chemistry of iron is not an easy one. In the first place, iron complexes are usually air- and moisture sensitive and, in the case of iron(II) complexes, prone to oxidation to iron(III). Furthermore, many iron complexes are paramagnetic, which makes their characterization difficult with NMR spectroscopy. Besides, most of the pincer ligands reported so far are of the ECE type, which means that the metalation of the ligand must proceed by either a C-H or a C-C bond activation process, something that iron is very unlikely to do, in contrast to other transition metals like palladium or iridium. Thus, the chemistry of iron pincer complexes is rather new and remains relatively unexplored.

In the late 1990s, Brookhart[76a] and Gibson[76b] independently reported the synthesis of a series of iron bis(imino) pyridine complexes (**A**, Figure 15), which are excellent catalysts for the polymerization of ethylene. Using these NNN pincer ligands, Chirik and coworkers have prepared several iron alkyl- bis(dinitrogen)- and carbonyl complexes[77], which can be used in olefin and alkyne hydrogenation[77a], hydrosilation[77a] and polymerization[77b] reactions. Recently they have reported examples of α,ϖ-diene cyclizations that are unique to iron[78]. Interestingly, theoretical and mechanistic investigations have shown that, in these complexes, it is the ligand and not the iron center that is reduced, a feature that seems to be unique for this class of ligands[79] (Scheme 27).

---

[76] (a) Small, B. L.; Brookhart, M.; Bennett, A. M. A. *J. Am. Chem. Soc.* **1998**, *120*, 4049. (b) Britovsek, G. J. P.; Bruce, M.; Gibson, V. C.; Kimberley, B. S.; Maddox, P. J.; Mastroianni, S.; McTavish, S. J.; Redshaw, C.; Solan, G. A.; Strömberg, S.; White, A. J. P.; Williams, D. J. *J. Am. Chem. Soc.* **1999**, *121*, 8728.

[77] (a) Bart, S. C.; Lobkovsky, E.; Chirik, P. J. *J. Am. Chem. Soc.* **2004**, *126*, 13794. (b) Bouwkamp, M. W.; Lobkovsky, E.; Chirik, P. J. *J. Am. Chem. Soc.* **2005**, *127*, 9660. (c) Bouwkamp, M. W.; Lobkovsky, E.; Chirik, P. J. *Inorg. Chem.* **2006**, *45*, 2. (d) Bart, S. C.; Lobkovsky, E.; Bill, E.; Chirik, P. J. *J. Am. Chem. Soc.* **2006**, *128*, 5302. (e) Archer, A. M.; Bouwkamp, M. W.; Cortez, M.-P.; Lobkovsky, E.; Chirik, P. J. *Organometallics* **2006**, *25*, 4269.

[78] Bouwkamp, M. W.; Bowman, A. C.; Lobkovsky, E.; Chirik, P. J. *J. Am. Chem. Soc.* **2006**, *128*, 13340.

[79] Bart, S. C.; Chlopek, K.; Bill, E.; Bouwkamp, M. W.; Lobkovsy, E.; Neese, F.; Wieghardt, K.; Chirik, P. J. *J. Am. Chem. Soc.* **2006**, *128*, 13901.

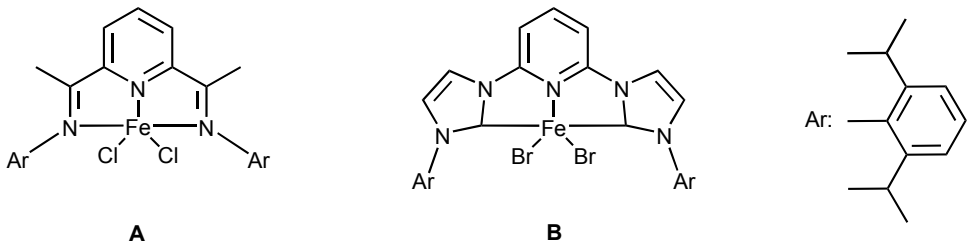

Figure 15. Iron NNN and CNC pincer complexes

Iron(II)-dibromo pincer complexes have also been prepared using CNC pincer ligands featuring N-heterocyclic carbenes as two-electron donor groups[80a] (**B**, Figure 15); in these complexes, the metal center can be reduced to the oxidation state zero to give iron(0) bis(dinitrogen) and carbonyl complexes[80b].

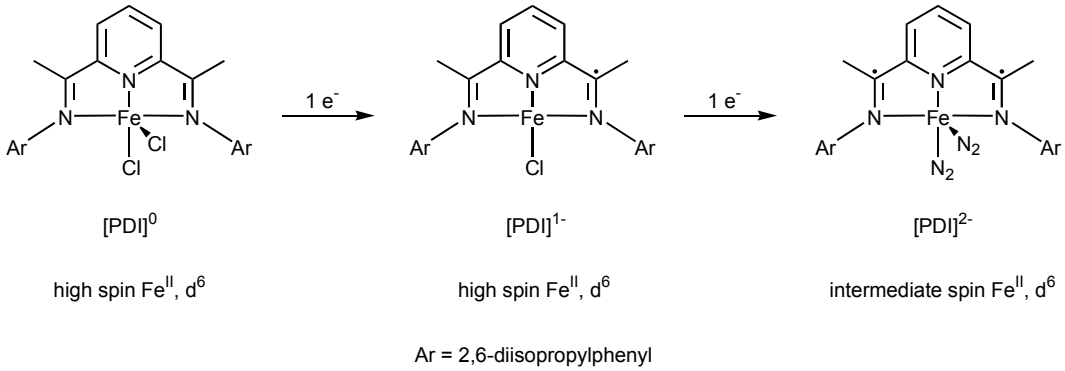

Scheme 27. Electronic structure of bis(imino) pyridine iron complexes

Finally, Milstein and coworkers have prepared iron PNP pincer complexes in which a methylene group is used as spacer between the pyridine ring and the phosphines[81] (**A**, Figure 16), while Chirik et al. have reported some reductive chemistry with these iron complexes[82] (**B**).

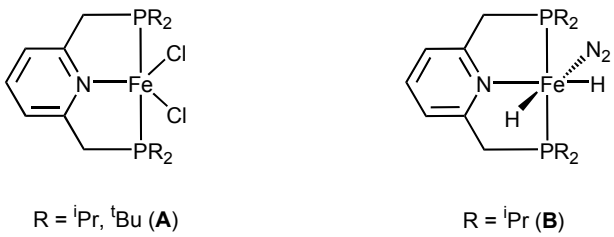

Figure 16. Iron PNP pincer complexes

---

[80] (a) Danopoulos, A. A.; Tsoureas, N.; Wright, J. A.; Light, M. E. *Organometallics* **2004**, *23*, 166. (b) Danopoulos, A. A.; Wright, J. A.; Motherwell, W. B. *Chem. Commun.* **2005**, *6*, 784.

[81] Zhang, J.; Gandelman, M.; Herrman, D.; Leitus, G.; Shimon, L. J. W.; Ben-David, Y.; Milstein, D. *Inorg. Chim. Acta* **2006**, *359*, 1955.

[82] Trovitch, R. J.; Lobkovsky, E.; Chirik, P. J. *Inorg. Chem.* **2006**, *45*, 7252.

3.2.2 Precursors

Iron is a widely utilized metal in certain areas of inorganic chemistry, such as coordination chemistry, physical inorganic chemistry and bioinorganic chemistry; however, its use in organometallic chemistry, when compared to other transition metals, is rather limited. Despite the fact that some progress has been made in the recent years in the catalytic applications of iron, mostly in polymerization reactions, the methodologies employed usually involve the use of a simple iron salt in combination with an organic molecule which acts as cocatalyst. Therefore, the use of defined complexes with a determined stoichiometry and structure is more the exception than the rule when it comes to describe the applications of iron compounds in organic synthesis. We were interested in investigating the possibility of preparing defined iron complexes with the PNP ligands, and in exploring their activity as catalysts in several organic coupling reactions. This objective required the use of different metal precursors other than iron(II) or iron(III) halide salts.

The first one of these precursors was the complex hexaaquoiron(II) tetrafluoroborate[83], which is an air stable pale green solid that can be easily prepared in very good yields and in large quantities from metallic iron powder and tetrafluoroboric acid (Scheme 28). The advantage of this compound is that all the water molecules are substitutionally labile and can be displaced by ligands and by stronger coordinating solvents, such as acetonitrile or THF to give diamagnetic octahedral complexes. However, the ligands need to be water stable, since up to six equivalents of water are set free for each equivalent of the iron precursor.

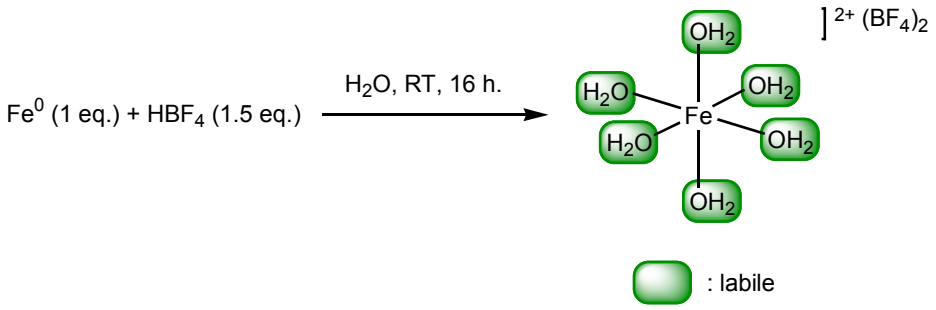

Scheme 28. Synthesis of $[Fe(H_2O)_6](BF_4)$

Another iron(II) complex used as precursor was the tetracarbonyl dibromide complex $Fe(CO)_4Br_2$,[84] which can also be prepared in good yields and in large quantities by oxidative addition of bromine to iron pentacarbonyl (Scheme 29). This complex is moderately sensitive towards air and moisture, but decomposes relatively fast when exposed to light; therefore, it needs to be stored in the dark, preferably under inert atmosphere.

---

[83] Kirchner, K. Ph. D. Thesis, Vienna University of Technology, **1987**.

[84] Hales, L. A. W.; Roger, I. J. *J. Chem. Soc. (A)* **1967**, *8*, 1389.

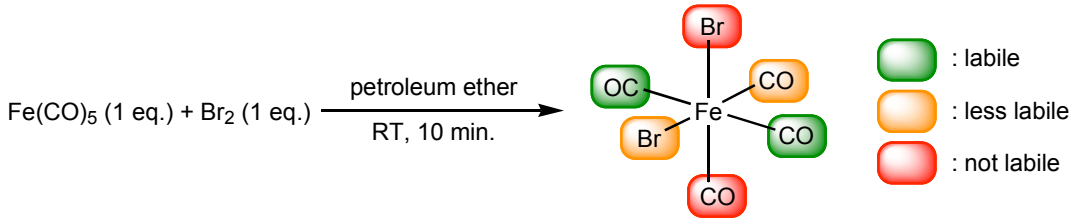

Scheme 29. Synthesis of $Fe(CO)_4Br_2$

Unlike in the case of the hexaaquoiron(II) tetrafluoroborate complex, the groups attached to the iron center in $Fe(CO)_4Br_2$ have different labilities, which can be described as follows:

lability in $Fe(CO)_4Br_2$

$\longleftarrow$

CO(1) > CO(2) > CO(3) ≈ Br(1)

Two of the carbonyl groups (presumably those in the trans positions to each other) are very labile, the first one being slightly more labile than the second one, and they can be easily displaced in the presence of better coordinating ligands (such as phosphines) and even in coordinating solvents. Despite the similar lability, thermodinamic and spectroscopic data seem to suggest that two different mechanisms are involved in the displacement of these carbonyl groups[85]. For the first carbonyl ligand, a reductive elimination-oxidative addition pathway has been proposed: dissociation of molecular bromine from $Fe(CO)_4Br_2$ takes place to yield $Fe(CO)_4$ as a reactive intermediate. This then reacts with any given reagent Y (Y: phosphine, arsine, stibine) to yield $FeY(CO)_4$ which reacts with Br_2 to form $FeY(CO)Br_2$ under the release of carbon monoxide gas:

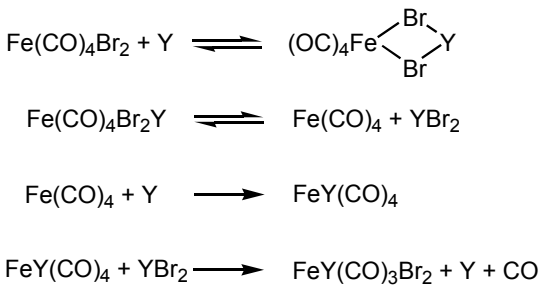

[85] Cohen, I. A.; Basolo, F. *J. Inorg. Nucl. Chem.* **1966**, *28*, 511.

The reaction mechanism for the substitution of the second carbonyl group is postulated as a S_N^1 dissociation process followed by a rapid reaction with Y:

$$FeY(CO)_3Br_2 \xrightarrow[k]{-CO} FeY(CO)_2Br_2 \xrightarrow[fast]{+Y} FeY_2(CO)_2Br_2$$

As for further substitution reactions, the third carbonyl group and one of the halide atoms are similarly labile; thus, it is possible to obtain mixtures of both neutral and cationic complexes if a tridentate ligand is used. However, it should be possible to shift the reaction towards the displacement of a bromine by using a halide scavenger such as sodium tetraphenylborate or ammonium hexafluorophosphate, for example. The remaining two ligands, a bromine and a carbonyl group, are much more difficult to remove and their substitution requires harsher conditions.

Finally, anhydrous $FeCl_2$ and $Fe(py)_4Cl_2$[86] (py: pyridine) were also used as precursors. While anhydrous $FeCl_2$ is air and moisture sensitive and must be stored under inert atmosphere, $Fe(py)_4Cl_2$, which can be easily prepared by the reaction of $FeCl_2{\cdot}4H_2O$ and pyridine and can be seen as a "$FeCl_2$" fragment stabilized by four labile pyridine ligands, is air stable and can be used instead of anhydrous $FeCl_2$. For example, an iron(II) bis(imino)pyridine complex has been recently prepared using $Fe(py)_4Cl_2$ as the metal precursor by ligand metathesis[87] (Scheme 30).

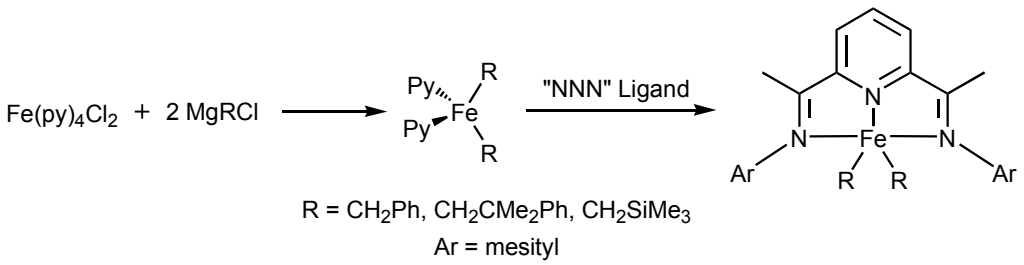

Scheme 30. Synthesis of alkylated bis(imino) pyridine complexes from $Fe(py)_4Cl_2$

[86] Baudisch, O; Hartung, W. H. *Inorg. Synth.* **1939**, *1*, 184.
[87] Cámpora, J.; Naz, A. M.; Palma, P.; Álvarez, E.; Reyes, M. L. *Organometallics* **2005**, *24*, 4878.

3.2.3 Iron(II) PNP Complexes from $[Fe(H_2O)_6](BF_4)_2$

Iron(II) Tris(acetonitrile) PNP Complexes

Synthesis

Octahedral iron(II) complexes of the formula $[Fe(PNP)(CH_3CN)_3](BF_4)_2$ (**7a-f**) were obtained by reacting equimolar amounts of $Fe(H_2O)_6(BF_4)_2$ and the corresponding PNP ligands **2a-b** and **2d-g** in acetonitrile at room temperature for two hours (Scheme 31). Upon addition of the ligand to a solution of $Fe(H_2O)_6(BF_4)_2$ in acetonitrile, the colour of the solution immediately changed from colourless to deep orange. The displacement of the water molecules is fast; three of them are substituted by a PNP ligand, which coordinates in a meridional mode occupying three of the four positions in the octahedral plane, while the remaining basal position and the two apical positions are occupied by N-coordinated acetonitrile molecules. After precipitation and washing with diethyl ether or petroleum ether, the complexes **7a-f** were isolated in good to excellent yields (72-97%) as orange solids. Only when PNP-BINOL (**2f**) was used as the ligand was the yield poorer (36%). In some cases, the formation of paramagnetic impurities, which induce a broadening of the peaks in the ^1H NMR spectra, thus making the characterization of the complexes more difficult, could be observed. They could be, however, easily removed by flashing the complexes through a plug of neutral aluminum oxide using acetonitrile as the eluent. As shown in Scheme 31, six different complexes, featuring ligands with diverse steric, electronic and stereochemical properties were prepared. However, when **2c** and **2i-j** were used, the reaction mixture turned green and intractable materials were obtained. For **2c**, this may be due to the sterically demanding *tert*-butyl phosphines, but the reason why **2i-j** did not react similarly to the other PNP ligands remains unknown.

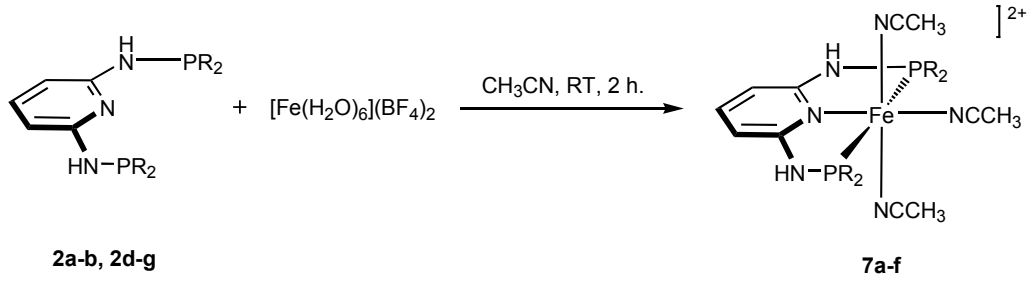

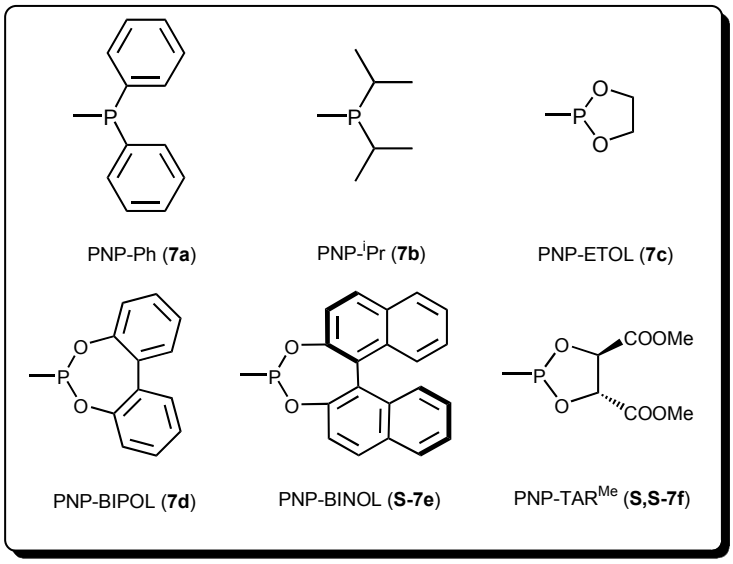

Scheme 31. Synthesis of the iron(II) tris(acetonitrile) PNP complexes **7a-f**

Interestingly, the presence of relatively large amounts of water in the reaction mixture (six equivalents H_2O are set free in the course of the reaction per equivalent iron(II) precursor used) does not seem to affect the formation of the complexes, despite the fact that the ligands, especially the phosphoramidite ones, are moisture sensitive, and hydrolisis of the P-N and/or the P-O bonds might occur. The complexes **7a-f** decompose slowly in air, presumably due to oxidation of the iron(II) center to iron(III). These complexes are soluble in almost all common organic solvents, such as acetonitrile or acetone, but insoluble in chlorinated solvents.

It has to be noted that, when the reaction between $[Fe(H_2O)_6](BF_4)_2$ and PNP-Ph (**2a**) was carried out in neat water for two hours at room temperature, a white solid precipitated from the reaction mixture. After decanting the excess of water and drying the remaining solid under vacuum, infrared analysis of the product revealed the presence of coordinated water within its structure (ν= 3500cm^{-1}). It was impossible to characterize this product by NMR spectroscopy because a deep purple solution formed immediately when the white solid was put in contact with any solvent other than water. The white solid itself also turns purple after being exposed to air for several hours. When one of these deep purple solutions was dried, NMR spectra indicated the formation of complex **8c** (see below). A plausible explanation is that the trisaquo

intermediate complex **A** is formed in the first place, and that two molecules of this complex rearrange in solution to form the more stable complex **8c** with concomitant release of one equivalent of $[Fe(H_2O)_6](BF_4)_2$ (Scheme 32).

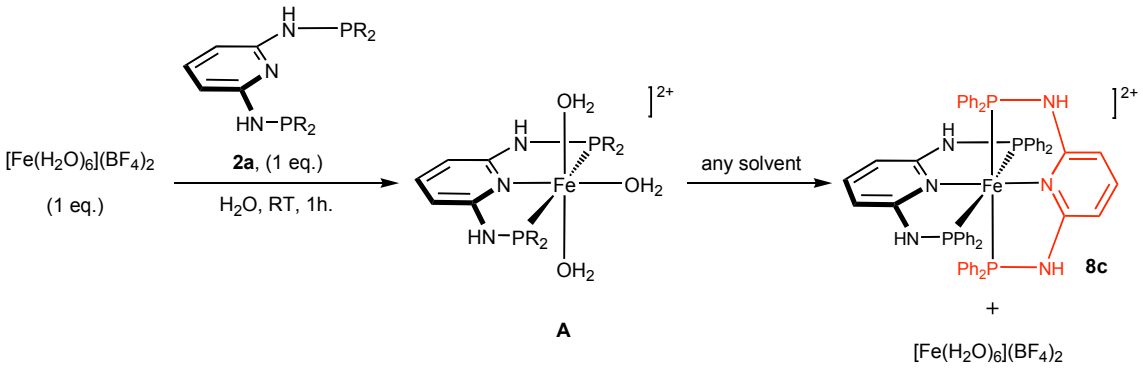

Scheme 32. Formation of **8c** via the tris(aquo) complex **A**

Characterization

The tris(acetonitrile) complexes **7a-f** were characterized by ^{1}H, ^{31}P{^{1}H} and ^{13}C{^{1}H} NMR spectroscopy. They all display a diamagnetic behavior in solution, probably due to their octahedral geometry. As an example, the ^{1}H NMR spectrum of **7f** is depicted in Figure 17. Some characteristic ^{1}H and ^{31}P{^{1}H} resonances of the complexes **7a-f** are summarized in Table 9.

Table 9. Selected ^{1}H and ^{31}P{^{1}H} NMR resonances of the iron tris(acetonitrile) complexes **7a-f**

Complex	^{1}H (δ, [ppm], 20ºC)			^{31}P{^{1}H} (δ, [ppm], 20ºC)
	N*H* (2H)	py^4 (1H)	py^{3,5} (2H)	
7a	8.36	7.91-7.62[a]	6.64	103.9
7b	7.30	7.16	6.30	115.1
7c	8.14	7.36	6.22	183.6
7d	8.89	7.23	6.52	186.7
7e	8.35-8.02[a]	7.48-7.27[a]	5.97-5.80[a]	189.9
7f	8.17	7.57	6.64	193.8

[a]Signal overlaps with other aromatic signals.

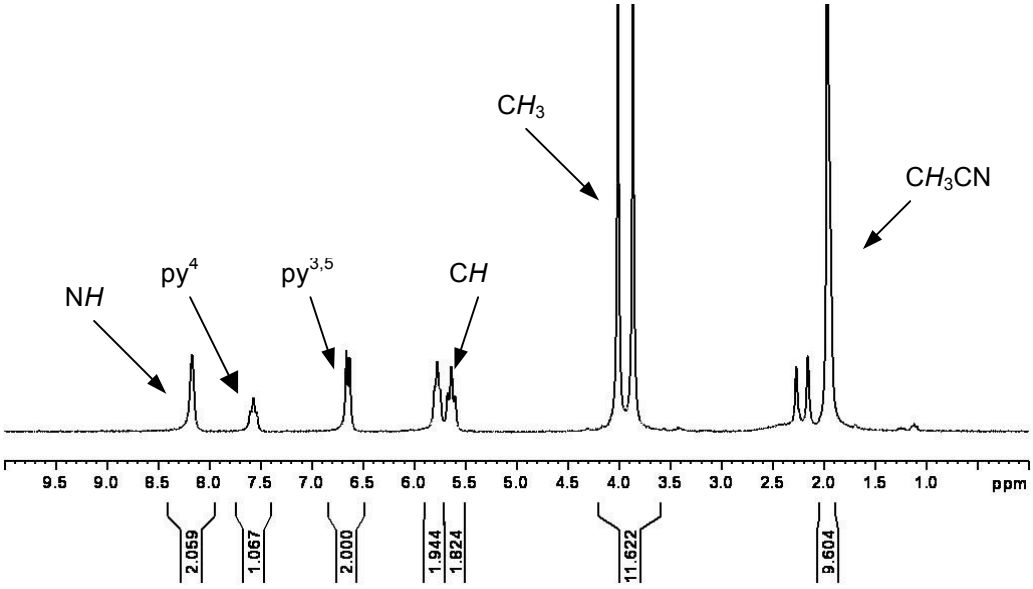

Figure 17. ^{1}H NMR spectrum of [Fe(PNP-^{Me}TAR)(CH_3CN)$_3$](BF_4)$_2$ (**7f**)

In the ^{1}H NMR spectra, the signals of the N*H* protons appear shifted to the low field when compared to those of the free ligands; this indicates an increased acidity of these protons due to the formation of strong hydrogen bonds with the fluorine atoms of the counterion molecules. They give rise to broadened singulets between 7.30 and 8.89 ppm. The signals of the pyridine protons are only slightly shifted to the high or to the low field; the py^{4} signals appear as triplets between 7.16 and 7.91 ppm and the py^{3,5} signals give rise to doublets in the range between 5.97 and 6.64 ppm. The coupling constant $^{3}J_{HH}$ lies between 7.6 and 8.2 Hz. The methyl groups of the coordinated acetonitrile molecules appear as singulets between 1.13 and 3.28 ppm. In the ^{13}C{^{1}H} NMR spectra, the signals of the pyridine ring appear shifted to the high field in respect to the signals of the ligands: the quaternary py^{2,6} carbon atoms give rise to triplets between 158.2 and 164.1 ppm with coupling constants $^{2}J_{CP}$ between 8.1 and 13.2 Hz, while the py^{4} and py^{3,5} carbon atoms appear between 140.6 and 146.1 and between 95.7 and 103.0 ppm, respectively.

As for the ^{31}P{^{1}H} NMR spectra, all the complexes show a single resonance, indicating a tridentate coordination of the PNP ligand and the equivalence of both phosphorus atoms. This signal is shifted to the low field due to coordination of the phosphines to the iron center and appears at 103.9 ppm for **7a**, at 115.1 ppm for **7b** and between 183.6 and 193.8 ppm in the case of the phosphoramidite complexes **7c-f**.

Additionally, the structures of the complexes **7a**, **7b**, **7d** and **7f** were determined by X-ray crystallography. For all these compounds, suitable crystals were grown by slow diffusion of diethyl ether into a saturated solution of the complexes in acetonitrile. Structural views of **7a**, **7b** and **7f** are depicted in Figures 18-20; a structural view of **7d** is depicted in Figure 25 for comparison with the crystal structure of **10** (Figure 26).

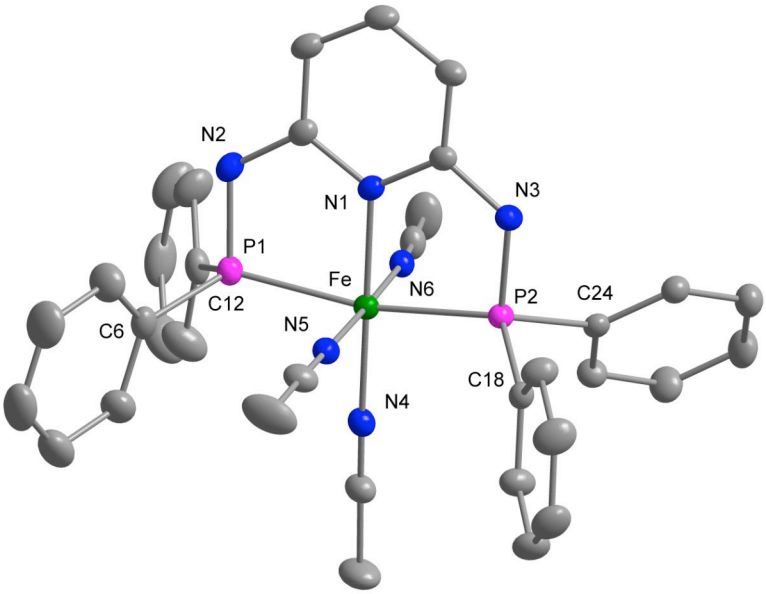

Figure 18. Structural view of $[Fe(PNP\text{-}Ph)(CH_3CN)_3](BF_4)_2$ (**7a**) showing 30% thermal ellipsoids (hydrogen atoms, counterions and crystallization solvent omitted for clarity). Selected bond lengths (Å) and angles (º): Fe-P(1) 2.2338(9), Fe-P(2) 2.2775(8), Fe-N(1) 1.977(2), Fe-N(4) 1.934(3), Fe-N(5) 1.902(2), Fe-N(6) 1.920(2), P(1)-N(2) 1.677(3), P(2)-N(3) 1.684(2), P(1)-Fe-P(2) 166.76(3), N(5)-Fe-N(6) 177.42(10).

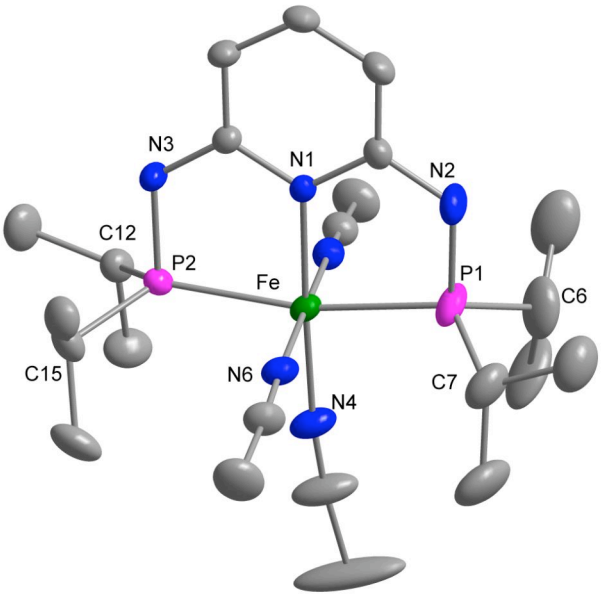

Figure 19. Structural view of $[Fe(PNP\text{-}^{i}Pr)(CH_3CN)_3](BF_4)_2$ (**7b**) showing 30% thermal ellipsoids (hydrogen atoms and counterions omitted for clarity). Selected bond lengths (Å) and angles (º):Fe-P(1) 2.258(1), Fe-P(2) 2.268(1), Fe-N(1) 1.988(2), Fe-N(4) 1.932(2), Fe-N(5) 1.926(3), Fe-N(6) 1.914(2), P(1)-N(2) 1.693(3), P(2)-N(3) 1.699(3), P(1)-Fe-P(2) 167.23(4), N(5)-Fe-N(6) 175.44(10).

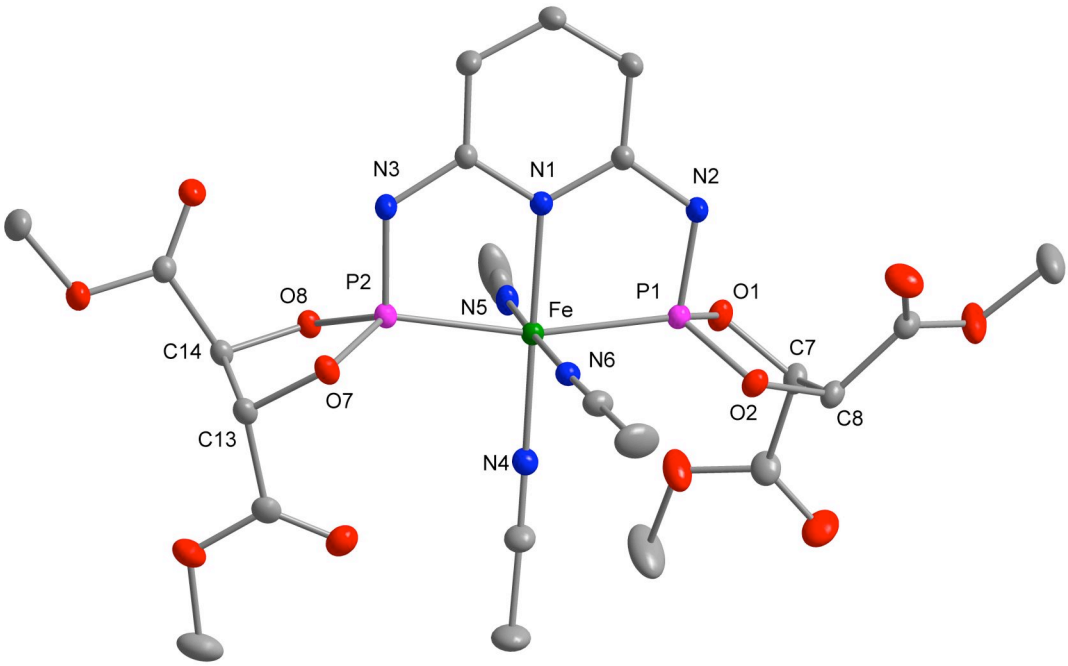

Figure 20. Structural view of $[Fe(PNP\text{-}^{Me}TAR)(CH_3CN)_3](BF_4)_2$ (**7f**) showing 30% thermal ellipsoids (hydrogen atoms and counterions omitted for clarity). Selected bond lengths (Å) and angles (º): Fe-P(1) 2.1916(4), Fe-P(2) 2.2134(4), Fe-N(1) 1.976(2), Fe-N(4) 1.930(2), Fe-N(5) 1.919(2), Fe-N(6) 1.930(2), P(1)-N(2) 1.661(2), P(2)-N(3) 1.673(2), P(1)-Fe-P(2) 166.74(2), N(5)-Fe-N(6) 174.47(6).

The iron(II) center in these complexes adopts a distorted octahedral geometry, with the PNP ligands coordinating in a tridentate meridional mode occupying three of the four positions in the octahedral plane. The remaining position in the octahedral plane and the two apical positions are occupied by *N*-coordinated acetonitrile molecules. The Fe-N(1) bond lengths are almost identical: 1.977(2) Å in **7a**, 1.988(2) Å in **7b** and 1.976(2) Å in **7f**. The Fe-P distances are longest for **7b** (mean value: 2.263 Å), which contains alkyl substituted phosphines in the PNP ligand. These distances are slightly shorter for the phenyl bearing complex **7a** ($\Delta d \approx 0.03$ Å, mean value: 2.230 Å) and around 0.1 Å shorter for the P-O bond containing phosphoramidite complex **7f** (mean value: 2.202 Å). The Fe-N distances of the nitriles *trans* to the pyridine nitrogen atom are typically longer than the ones *cis* to the PNP moiety. Moreover, the Fe-N bond lengths for the nitriles in the apical positions are also different: the Fe-N(5) distances are usually between 0.1 and 0.2 Å shorter than the Fe-N(6) distances (e.g. in **7f**, the Fe-N(5) and Fe-N(6) bond lengths are 1.919(2) and 1.930(2) Å, respectively). The aminophosphine nitrogen atoms are good hydrogen bond donors, with counterions as well as suitable solvent molecules being anchored by this hydrogen bonding. Finally, the deviation from the planarity of the octahedral plane defined by the pyridine nitrogen atom, the two phosphorus atoms and the nitrogen atom of one acetonitrile molecule can be observed best along the P(1)-Fe-P(2) axis: while the N(1)-Fe-N(4) angle is close to 180º in all complexes, the P(1)-Fe-P(2) angle is smaller and lies between 166.74º (**7f**) and 167.27º (**7b**).

Lability of the Acetonitrile Ligands

Synthesis

The acetonitrile ligands in the complexes **7a-f** are labile and can be readily replaced by other nitrogen donor ligands; this substitution chemistry was exemplarily investigated with **7a** as a model complex. When one equivalent of a monodentate ligand (pyridine) was added to a solution of **7a** in nitromethane and the reaction mixture was stirred for five hours, no displacement of the acetonitrile molecules was observed (Scheme 33); this can be attributed to the similar coordinating properties of acetonitrile and pyridine.

Nevertheless, when chelating nitrogen donor ligands were used, the reaction proceeded smoothly and the substitution products could be easily isolated. Thus, the treatment of one equivalent of **7a** with one equivalent of 2, 2'-bipyridine (bipy) or 2, 2':6', 2''-terpyridine (terpy) in nitromethane at room temperature for two hours resulted in the formation of the complexes **8a** and **8b**, respectively (Scheme 33). The solution immediately changed its colour from orange to deep red upon addition of the chelating nitrogen donor ligand and, after evaporating the solvent under vacuum and washing the residue twice with diethyl ether, **8a** and **8b** were obtained in excellent yields (95 and 83%, respectively) as air stable deep red solids.

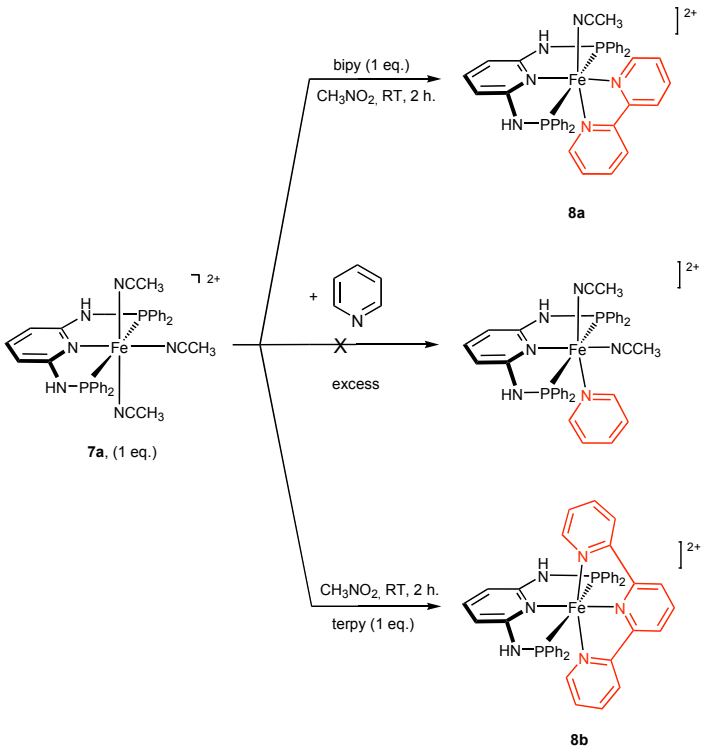

Scheme 33. Reaction of **7a** with pyridine, 2, 2'-bipyridine (bipy) and 2, 2':6', 2''-terpyridine (terpy)

The acetonitrile molecules can be also substituted by a second molecule of the PNP ligand: when one equivalent of PNP-Ph (**2a**) was added to a solution of **7a** in nitromethane, the solution immediately turned purple. Upon removal of the solvent under vaccum and washing the residue with diethyl ether, an air stable purple solid was obtained in 88% yield, which was identified as the bis-PNP complex $[Fe(PNP\text{-}Ph)_2](BF_4)_2$ (**8c**). Alternatively, this complex can also be prepared directly in 90% yield by the reaction of one equivalent of $[Fe(H_2O)_6](BF_4)$ with two equivalents of PNP-Ph (**2a**) in THF for two hours at room temperature (Scheme 34).

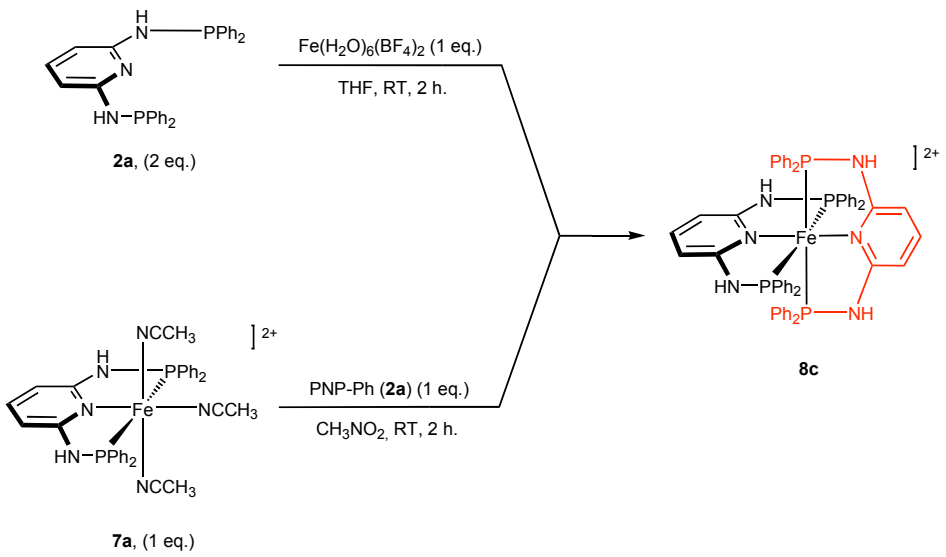

Scheme 34. Synthesis of $[Fe(PNP\text{-}Ph)_2](BF_4)_2$ (**8c**)

Other substitution attempts, such as the reaction of equimolar amounts of **7a** and sodium acetylacetonate in nitromethane for two hours did not result in the formation of the desired monocationic complex $[Fe(PNP\text{-}Ph)(acac)(CH_3CN)](BF_4)$; instead, the more stable bis-PNP complex **8c** was obtained.

Similarly, the attempt to synthesize mixed, bis-PNP complexes failed; when **7a** was treated with one equivalent of PNP-^{i}Pr (**2b**) or PNP-BIPOL (**2e**) under the same reaction conditions than those used for the preparation of **8c**, only the starting materials were recovered from the reaction mixture. The preparation of different bis-PNP complexes by reacting two equivalents of other PNP ligands (such as **2b** and **2e**) with one equivalent $[Fe(H_2O)_6](BF_4)_2$ in nitromethane at room temperature for two hours was also unsuccessful. The presence of bulkier groups at the phosphines is probably the cause for the absence of reaction.

It is also possible to substitute just one of the acetonitrile molecules by using carbon monoxide: when CO was bubbled into a solution of **7a** or **7b** in acetone for ten minutes and the reaction mixture was stirred at room temperature for sixteen hours, the mono carbonyl

complexes *cis*-[Fe(PNP-Ph)(CO)(CH_3CN)$_2$]$^{2+}$ (**9a**) and *cis*-[Fe(PNP-*i*Pr)(CO)(CH_3CN)$_2$]$^{2+}$ (**9b**) were obtained upon workup as air stable yellow solids in 88 and 93% isolated yields, respectively (Scheme 35). Like the tris(acetonitrile) complexes **7a** and **7b**, **9a** and **9b** are soluble in most common organic solvents, but not in chlorinated ones. Interestingly, there was no evidence for the formation of the dicarbonyl complexes [Fe(PNP)(CO)$_2$(CH_3CN)]$^{2+}$. This substitution reaction works smoothly with the iron complexes containing the phosphine substituted PNP ligands **2a** and **2b**; however, with [Fe(PNP-BIPOL)(CH_3CN)$_3$]$^{2+}$ (**7d**), where the PNP ligand contains the stronger π-accepting BIPOL units, no reaction took place.

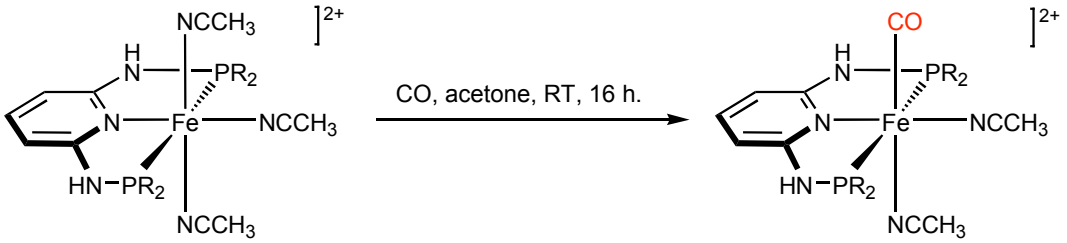

R: Ph **(7a)**
R: iPr **(7b)**

R: Ph **(9a)**
R: iPr **(9b)**

Scheme 35. Reaction of **7a** and **7b** with carbon monoxide

A counterion exchange from the weakly coordinating BF_4^- to the non-coordinating anion $BArF^-$ (BArF: tetrakis[(3,5-trifluoromethyl)phenyl]borate) was performed in the case of **9b** in order to study the influence of the counterion on the catalytic activity of the complexes **9a**, **9b** and **9b'** in the coupling of aromatic aldehydes with ethyl diazoacetate (see below). The reaction was performed by adding two equivalents of NaBArF to a suspension ofone equivalent of **9b** in methylene chloride and stirring the reaction mixture at room temperature for two hours. During this time a yellow solution and a white precipitate ($NaBF_4$) were formed. After filtering the reaction mixture and removing the solvent from the filtrate under vacuum, complex **9b'** was obtained as an air stable yellow solid in 88% yield (Scheme 36).

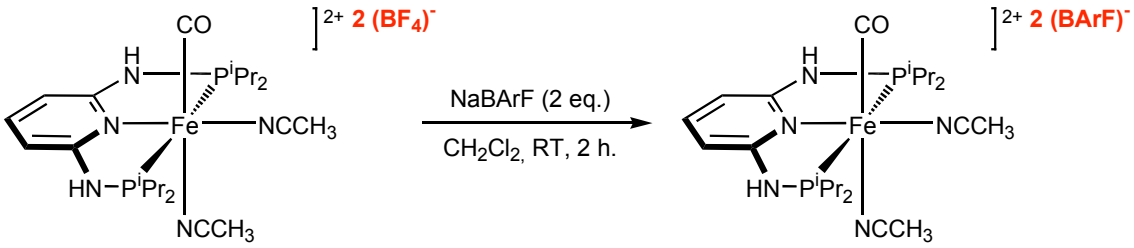

9b (1 eq.)

9b'

Scheme 36. Counterion exchange from **9b** to **9b'**

Characterization

The complexes **8a-c** and **9a**, **9b** and **9b'** were all characterized by ^{1}H, $^{31}P\{^{1}H\}$ and $^{13}C\{^{1}H\}$ NMR spectroscopy. Some selected resonances of these complexes are shown in Table 10.

Table 10. Selected ^{1}H and $^{31}P\{^{1}H\}$ NMR resonances of the complexes **8a-c**, **9a**, **9b** and **9b'**

Complex	^{1}H (δ, [ppm], 20ºC)			$^{31}P\{^{1}H\}$ (δ, [ppm], 20ºC)
	N*H* (2H)	py^{4} (1H)	py^{3,5} (2H)	
8a	8.56	7.72-7.53[a]	6.49	101.8
8b	8.15	7.19-7.16[a]	6.89-6.83[a]	100.3
8c	7.25-6.48[a]	7.95	7.25-6.48[a]	92.0
9a	9.21	7.99-7.84[a]	6.70	95.9
9b	6.90	7.39	6.34	114.7
9b'	5.68	7.33	6.30	114.5

[a]Signal overlaps with other aromatic signals.

In the case of the complexes **8a-c** and **9a**, the signals of the N*H* protons appear as broad singulets between 6.48 and 9.21 ppm in the ^{1}H NMR spectra. In the case of **9b'**, these resonances appear at 5.68 ppm, most likely due to the sterical hinderance of the BArF anion, which hampers the formation of hydrogen bonds between the counterion and the N*H* protons. When compared to the related tris(acetonitrile) complexes **7a** and **7b**, the signals of the py^{4} hydrogen atoms are shifted to the high field in the complexes **8a-c**, where two or more of the acetonitrile molecules have been substituted by a nitrogen donor ligand, and to the low field in the case of the complexes **9a**, **9b** and **9b'**, where one acetonitrile molecule has been displaced by an electron withdrawing carbonyl group. The py^{3,5} signals show almost no shift at all in comparison to the signals in the tris(acetonitrile) complexes **7a** and **7b**. In the $^{13}C\{^{1}H\}$ NMR spectra, the carbonyl groups in **9a**, **9b** and **9b'** appear as triplets between 212.4 and 219.9 ppm with coupling constants $^{2}J_{CP}$ between 25.9 and 27.0 Hz. The py^{2,6} signals appear between 163.3 and 161.1 ppm, while the py^{4} and py^{3,5} carbon atoms give rise to signals between 143.6 and 141.5 and between 100.6 and 103.2 ppm, respectively.

In the $^{31}P\{^{1}H\}$ NMR spectra, the signals of the substituted complexes **8a-c**, **9a**, **9b** and **9b'** appear shifted to the high field when compared to the signals of the related tris(acetonitrile) complexes. In all cases a single resonance was observed, indicating the equivalence of both phosphines. The complexes **8a-c** give rise to singulets between 92.0 and 101.8 ppm, while the signals of the carbonyl complexes **9a**, **9b** and **9b'** appear at 95.9, 114.7 and 114.5 ppm, respectively.

Due to the presence of carbonyl groups, the complexes **9a** and **9b** were also characterized by IR-spectroscopy. The CO stretquing bands appear at 2021 and 1995 cm^{-1} for **9a** and **9b**, respectively, indicating that the carbonyl group is not bound very strongly to the iron center. The π interaction is weaker in the case of **9a** than in **9b** (for comparison, free CO appears at 2143 cm^{-1}).

The structures of the complexes **8a-c** and **9b** were also determined by X-ray crystallography. Crystals of **8a-c** and of **9b** were obtained by slow diffusion of diethyl ether into saturated solutions of the complexes in nitromethane and acetone, respectively. Structural views of **8a-c** and of **9b** are depicted in Figures 21-24.

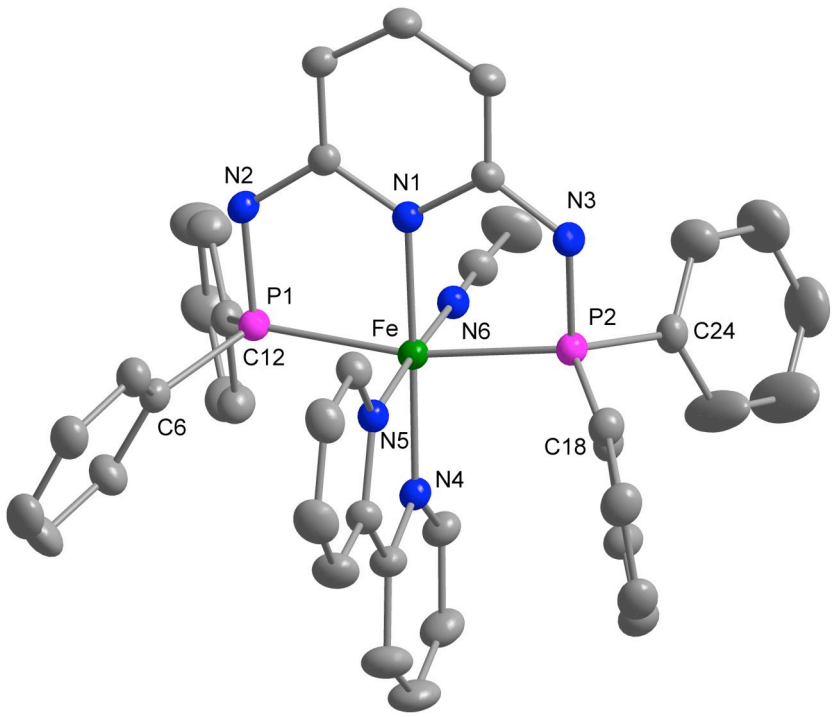

Figure 21. Structural view of $[Fe(PNP\text{-}Ph)(bipy)(CH_3CN)](BF_4)_2$ (**8a**) showing 20% thermal ellipsoids (hydrogen atoms, crystallization solvent and counterions omitted for clarity). Selected bond lengths (Å) and angles (º): Fe-P(1) 2.2323(8), Fe-P(2) 2.2274(8), Fe-N(1) 1.978(2), Fe-N(4) 1.958(2), Fe-N(5) 1.960(2), Fe-N(6) 1.908(2), P(1)-N(2) 1.6881(19), P(2)-N(3) 1.683(2), P(1)-Fe-P(2) 167.60(3), N(1)-Fe-N(4) 175.61(8).

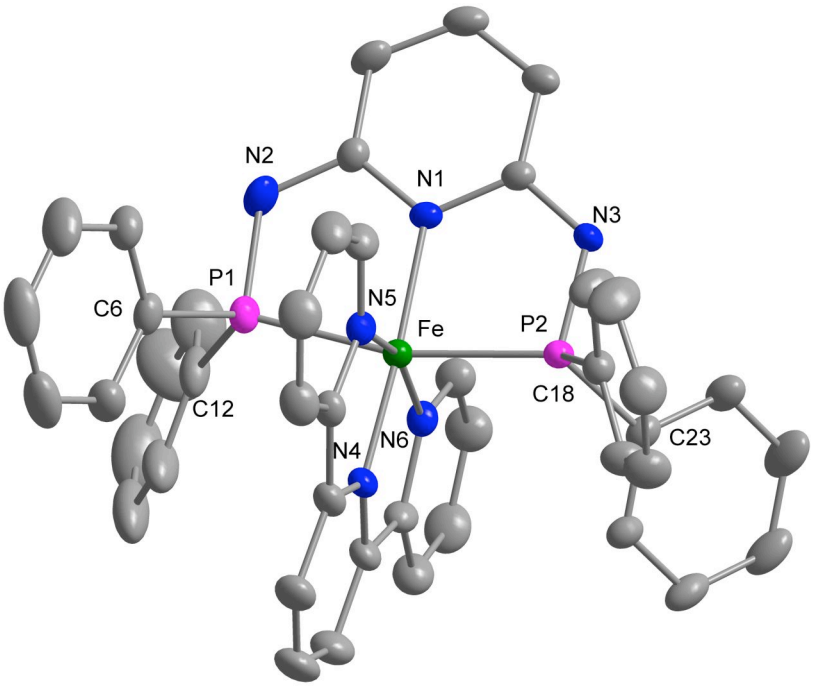

Figure 22. Structural view of [Fe(PNP-Ph)(terpy)]$(BF_4)_2$ (**8b**) showing 30% thermal ellipsoids (hydrogen atoms, crystallization solvent and counterions omitted for clarity). Selected bond lengths (Å) and angles (º): Fe-P(1) 2.2361(9), Fe-P(2) 2.2401(9), Fe-N(1) 1.989(2), Fe-N(4) 1.878(3), Fe-N(5) 1.968(3), Fe-N(6) 1.967(3), P(1)-N(2) 1.676(3), P(2)-N(3) 1.689(3), P(1)-Fe-P(2) 165.97(4), N(1)-Fe-N(4) 176.53(11).

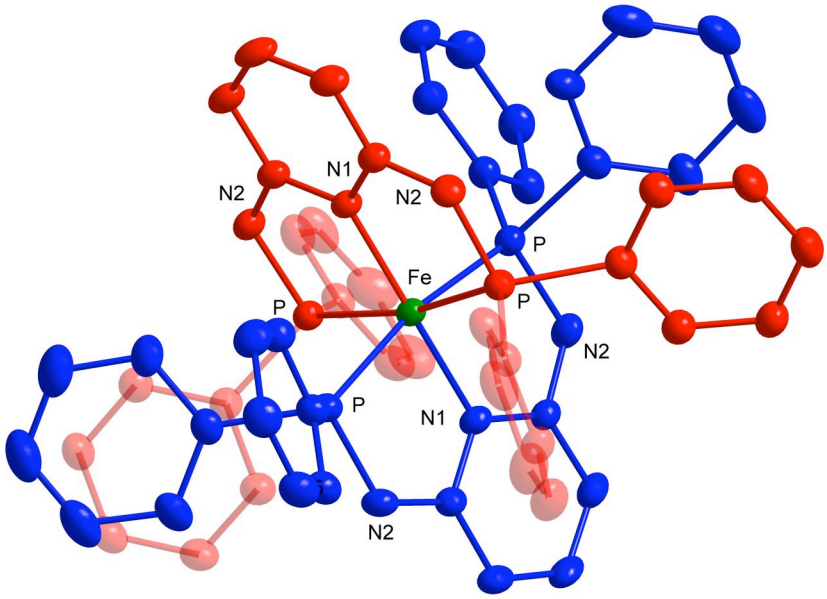

Figure 23. Structural view of [Fe(PNP-Ph)$_2$]$(BF_4)_2$ (**8c**) showing 20% thermal ellipsoids (hydrogen atoms, crystallization solvent and counterions omitted for clarity). Selected bond lengths (Å) and angles (º): Fe-P 2.2595(9), Fe-N 1.967(3), P-Fe-P 168.92(5), N-Fe-N 180.0(0).

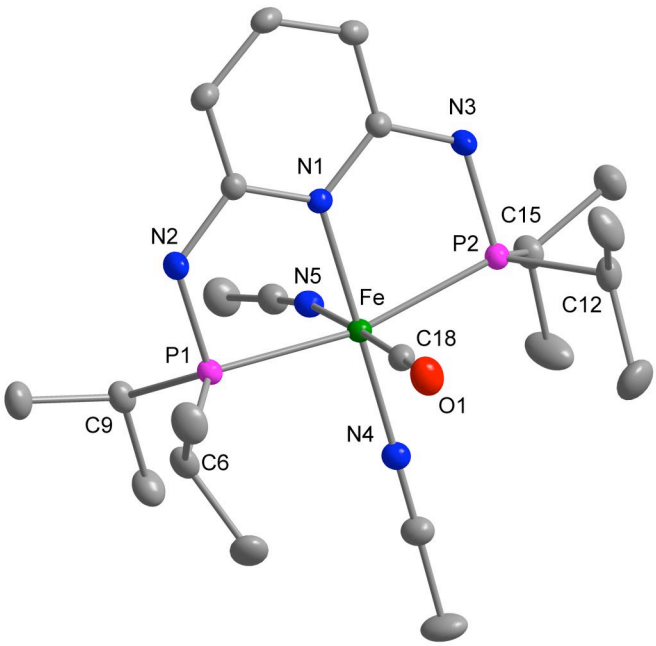

Figure 24. Structural view of cis-[Fe(PNP-^{i}Pr)(CO)$(CH_3CN)_2$]$(BF_4)_2$ (**9b**) showing 50% thermal ellipsoids (hydrogen atoms, crystallization solvent and counterions omitted for clarity). Selected bond lengths (Å) and angles (º): Fe-C(18) 1.7635(16), Fe-P(1) 2.2670(4), Fe-P(2) 2.2674(5), Fe-N(1) 1.9785(13), Fe-N(4) 1.9286(14), Fe-N(5) 1.9786(14), P(1)-N(2) 1.6902(14), P(2)-N(3) 1.6936(14), P(1)-C(6) 1.8458(16), P(1)-C(9) 1.8428(16), P(2)-C(12) 1.8411(17), P(2)-C(15) 1.8404(16), O(1)-C(18) 1.141(2), P(1)-Fe-P(2) 167.59(2), N(1)-Fe-N(4) 177.77(7).

All the complexes display a distorted octahedral geometry around the iron center with the PNP ligands coordinated in a tridentate meridional mode. The Fe-N(1) and Fe-P distances are very similar for all complexes. In the case of **8a**, the bipyridine ligand occupies one apical position and one position in the octahedral plane, while the acetonitrile molecule occupies the remaining apical position. The Fe-N bond length for the acetonitrile group (Fe-N(6)) has a value of 1.908(2) Å; all the other Fe-N bond lengths in the molecule are about 0.06 Å shorter. In **8b** and **8c**, all the three acetonitrile molecules have been displaced; in **8b**, the distance between the iron center and the terpyridine nitrogen atom N(4) in the *trans* position to the central pyridine ring has a value of 1.878(3) Å. The remaining Fe-N bond lengths are about 0.1 Å longer. **8c** shows a very high degree of symmetry; the mean values for the Fe-P and Fe-N bond lengths are 2.2595(9) and 1.967(3) Å, respectively. In the case of **9b**, the carbonyl group is situated in one of the apical positions, *trans* to an acetonitrile ligand. Carbon monoxide is a good π-acceptor and acetonitrile is a better π-donor than the nitrogen atom of the pyridine ring; therefore, as expected, the substitution of an acetonitrile molecule with a CO ligand takes place at one of the apical positions rather than at the acetonitrile ligand *trans* to the pyridine ring. The Fe-C(18) distance is 1.7635(16) Å, and the Fe-N bond of the nitrile *trans* to the pyridine nitrogen of the PNP ligand is slightly longer than the one *cis* to the PNP moiety (Fe-N(4) 1.9286(14) Å

and Fe-N(5) 1.9786(14) Å). Like in the tris(acetonitrile) complexes **7a-f**, a certain degree of distortion in the octahedral plane can be observed around the iron center also in the substituted complexes: the N(1)-Fe-N(4) angles are close to 180º in all cases, while the values of the P(1)-Fe-P(2) angles are always below 170º and range from 165.97(4)º (**8b**) to 168.92(5)º (**8c**).

Reduction attempts

Attempts to obtain zerovalent iron complexes of the type $[Fe(PNP)(CH_3CN)_2]$ (**A**, Scheme 37) by reacting $[Fe(PNP\text{-}BIPOL)(CH_3CN)_3)](BF_4)_2$ (**7d**) with an excess of 3% NaHg failed. In fact, treatment of **7d** with an excess NaHg in acetonitrile resulted in the immediate evolution of gas (H_2). After the hydrogen evolution had ceased (~15 minutes) and the insoluble materials had been filtered, removal of the solvent under vacuum and washing of the remaining residue with diethyl ether afforded the deprotonated monocationic tris(acetonitrile) complex $[Fe(PNP\text{-}BIPOL)(CH_3CN)_3]BF_4$ (**10**) as a brown solid in 76% yield. This complex could also be obtained in 81% yield if, during the purification process of **7d**, this was chromatographed on basic alumina using acetonitrile as the eluent. It has to be noted that the same effect (hydrogen evolution) was observed when **7a** was treated with an excess 3% NaHg; however, only decomposition products were isolated from the reaction mixture. The electron withdrawing phosphite substituents in **7d** presumably make the deprotonation of the N*H* groups easier. Thus, unlike for other iron(II) complexes reported in the literature containing methylene bridged PNP ligands, in which their reduction to iron(0) species is possible[82], the reduction of the tris(acetonitrile) complexes **7a-f** is apparently hampered by the acidity of the N*H* protons of the amino linkages of the PNP ligands.

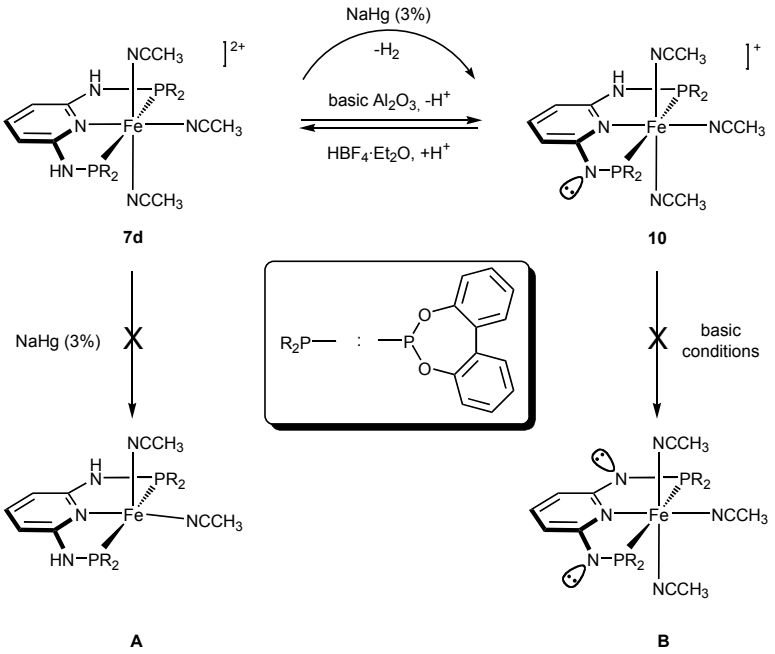

Scheme 37. Deprotonation of one aminophosphine N*H* group in 7d to give 10

The deprotonation of **10** is reversible and the addition of one equivalent of $HBF_4{\cdot}Et_2O$ to a solution of **10** in CD_3CN cleanly yielded the starting complex **7d** quantitatively (Scheme 37), as monitored by ^1H and $^{31}P\{^1H\}$ NMR spectroscopy. Finally, all attempts to deprotonate the second N*H* group in **10** under basic conditions (3% NaHg, *n*-BuLi, LDA) were unsuccessful, and in all cases only the starting complex **7d** was recovered. There was no indication for the formation of the bis-deprotonated neutral iron(II) complex $[Fe(PNP\text{-}BIPOL)(CH_3CN)_3]$ (**B**).

Complex **10** was characterized by ^1H, $^{31}P\{^1H\}$ and $^{13}C\{^1H\}$ NMR spectroscopy; however, the ^1H NMR spectrum was not very informative and displayed broad and featureless resonances, even at -70ºC in THF-d^8, which may be attributed to a fast proton exchange between the two *N*-sites. The $^{31}P\{^1H\}$ NMR spectrum showed a single resonance shifted to the low field when compared to that observed for **7d** (**7d**: 186.7 ppm, **10**: 194.4 ppm). This is not surprising considering that the presence of a negative charge split between both aminophosphine nitrogen atoms deshields the phosphorus atoms. As for the $^{13}C\{^1H\}$ NMR spectrum of **10**, the signals of the pyridine ring appear at 158.9 ppm ($py^{2,6}$), 149.0 ppm (py^4) and 101.7 ppm ($py^{3,5}$).

The complexes **7d** and **10** were also characterized by X-ray crystallography; crystals were obtained in both cases by slow diffusion of diethyl ether into a saturated acetonitrile solution of the corresponding complex. Structural views of **7d** and **10** are depicted in Figures 25 and 26.

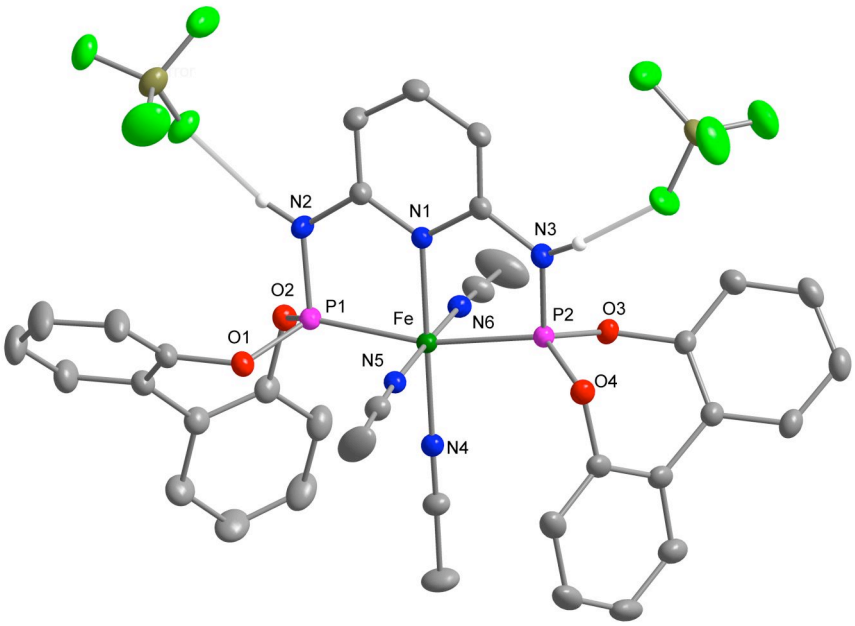

Figure 25. Structural view of $[Fe(PNP\text{-}BIPOL)(CH_3CN)_3](BF_4)_2$ (**7d**) showing 30% thermal ellipsoids (hydrogen atoms, counterions and crystallization solvent omitted for clarity). Selected bond lengths (Å) and angles (º): Fe-P(1) 2.1895(5), Fe-P(2) 2.1881(5), Fe-N(1) 1.975(2), Fe-N(4) 1.931(2), Fe-N(5) 1.917(2), Fe-N(6) 1.913(2), P(1)-N(2) 1.658(2), P(2)-N(3) 1.653(2), N(2)-C(1) 1.387(2), N(3)-C(5) 1.389(2), P(1)-Fe-P(2) 165.62(2), N(4)-Fe-N(1) 178.32(10).

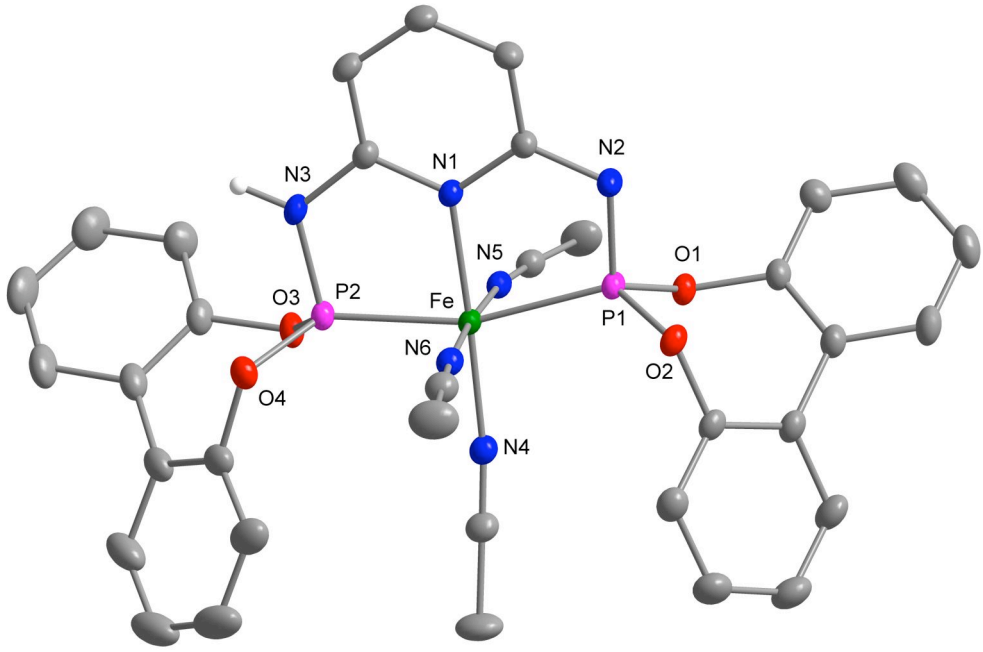

Figure 26. Structural view of [Fe(PNP-BIPOL)(CH_3CN)$_3$](BF_4) (**10**) showing 40% thermal ellipsoids (hydrogen atoms, counterion and crystallization solvent omitted for clarity). Selected bond lengths (Å) and angles (º): Fe-P(1) 2.2114(4), Fe-P(2) 2.1736(4), Fe-N(1) 1.982(1), Fe-N(4) 1.931(1), Fe-N(5) 1.910(1), Fe-N(6) 1.927(1), P(1)-N(2) 1.614(1), P(2)-N(3) 1.656(1), N(2)-C(1) 1.362(2), N(3)-C(5) 1.392(2), P(1)-Fe-P(2) 163.30(2), N(1)-Fe-N(4) 175.72(5).

The iron center shows a distorted octahedral geometry in both complexes, with the values for the bond lengths and angles of **7d** in line with those observed for the other tris(acetonitrile) complexes; however, in the case of **10**, the bond lengths involving the deprotonated nitrogen N(2) are significantly shorter than their hydrogen-bearing counterparts (e.g. the P(1)-N(2) distance is 1.658(2) Å in **7d** and 1.614(1) Å in **10**). The usual deviation fom the planarity of the octahedral plane is also slightly bigger in the case of **10** than in **7d**: the P(1)-Fe-P(2) angle has a value of 165.62(2)º in **7d** and of 163.30(2)º in **10**, and the N(1)-Fe-N(4) angle is 178.32(10)º in **7d** and 175.72(5)º in **10**.

3.2.4 Iron(II) PNP Complexes from $Fe(CO)_4Br_2$

Synthesis

An iron(II) dicarbonyl PNP complex could be obtained by reacting equimolar amounts of $Fe(CO)_4Br_2$ and PNP-Ph (**2a**) in the presence of one equivalent of $NaBPh_4$. The iron precursor was added to a solution of the ligand and $NaBPh_4$ in methylene chloride at room temperature. Gas evolution (CO) could be observed immediately; once the bubbling in the reaction mixture

subsided (~30 minutes), the solvent was removed under vacuum and the remaining residue was washed twice with diethyl ether and dried to give [Fe(PNP-Ph)$(CO)_2$Br]Br (**11**) as an orange solid in 82% yield (Scheme 38). As stated in the beginning of this chapter (Scheme 29), two of the four cabonyl groups in $Fe(CO)_4Br_2$ are very labile, and the third coordination site required for the coordination of the PNP ligand can be made available by shifting the reaction towards the displacement of a bromine atom through the addition of the halide scavenger $NaBPh_4$.

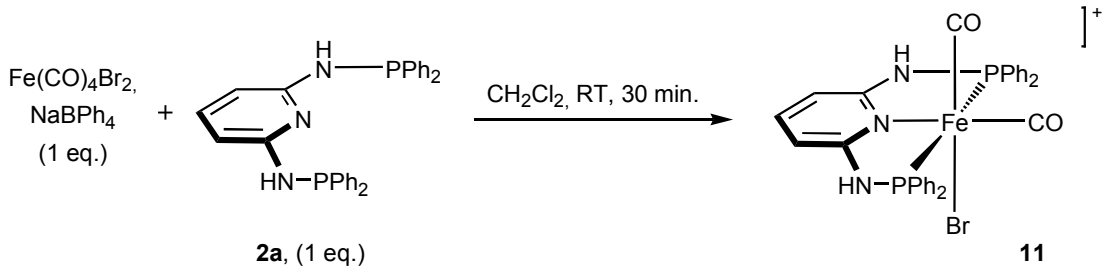

Scheme 38. Synthesis of [Fe(PNP-Ph)$(CO)_2$Br]Br (**11**)

Characterization

Complex **11** was characterized by ^{1}H, ^{31}P{^{1}H} and ^{13}C{^{1}H} NMR spectroscopy. In the ^{1}H NMR spectrum, it gives rise to signals at 7.90 ppm (N*H*), 7.47 (py^4) and 6.58 (py^{3,5}). The $^3J_{HH}$ coupling constant of the pyridine protons is 7.9 Hz. In the ^{13}C{^{1}H} NMR spectrum, the CO groups appear as triplets at 209.8 and 206.5 ppm with coupling constants $^2J_{CP}$ of 20.2 and 23.1 Hz, respectively. The appearance of two different signals for the carbonyl groups indicates that they are *cis* to one another. The py^{2,6} carbon atom gives rise to a triplet at 159.3 ppm with a coupling constant $^2J_{CP}$ of 8.7 Hz, while the py^4 and py^{3,5} signals appear as singulets at 142.4 and 102.7 ppm. As for the ^{31}P{^{1}H} NMR spectrum, complex **11** displays a single resonance at 100.5 ppm. It has to be noted that when the reaction was performed with PNP-^{i}Pr (**2b**) or PNP-^{t}Bu (**2c**) under the same reaction conditions, no clean reaction took place and several products, revealed by the appearance of different resonances in the ^{31}P{^{1}H} NMR spectra, were formed. Thus, this reaction was not further investigated.

3.2.5 Iron(II) PNP Complexes from $FeCl_2$ and $Fe(py)_4Cl_2$

Synthesis

All the iron(II) complexes described in the previous chapters are hexacoordinated, octahedral, diamagnetic complexes. It is, however, possible to prepare neutral, pentacoordinated, square-pyramidal paramagnetic complexes by the reaction of $FeCl_2$ or $Fe(py)_4Cl_2$ with the PNP ligands (Scheme 39). The synthesis of such complexes was only successful when ligands with very bulky substituents at the phosphines were used, such as PNP-^{i}Pr (**2b**) and PNP-^{t}Bu (**2c**). When PNP-Ph (**2a**) or the phosphoramidite PNP ligands **2d-j** were used, the products obtained were not paramagnetic, ruling out the possibility of the formation of pentacoordinated species. Tentatively, it could be assumed that some kind of dimeric species with μ–coordinated chlorine atoms might be formed; however, since no crystal structure of these products could be obtained, this is all purely speculative.

It has to be noted, however, that there is only one precedent for the preparation of iron(II) PNP pincer complexes, reported in the year 2006[81]. The PNP ligands in these complexes possess a methylene group as bridging between the pyridine ring and the phosphines, and their synthesis was only possible when bulky groups (i.e. ^{i}Pr, ^{t}Bu) were used as substituents at the phosphines (see Figure 16). Thus, it seems that the formation of stable, pentacoordinated dichloro iron(II) PNP complexes requires the use of sterically demanding ligands.

The complexes **12a** and **12b** were synthesized by reacting equimolar amounts of $FeCl_2$ or $Fe(py)_4Cl_2$ and PNP-^{i}Pr (**2a**) or PNP-^{t}Bu (**2b**), respectively. The reaction was carried out at room temperature for sixteen hours in THF. The use of either one of the two iron precursors had no influence on the reaction time or on its yield; however, $Fe(py)_4Cl_2$ is air stable and easier to handle. Yellow solutions were obtained in both cases, which were dried under vacuum and the remaining residues were washed twice with diethyl ether and dried to give **12a** and **12b** as yellow solids in very good yields (84-90%). Both complexes are relatively air stable in the solid state, but they decompose fast in solution to produce black oils when exposed to air. They are soluble in several organic solvents, such as acetone, nitromethane and acetonitrile, but unsoluble in chlorinated solvents.

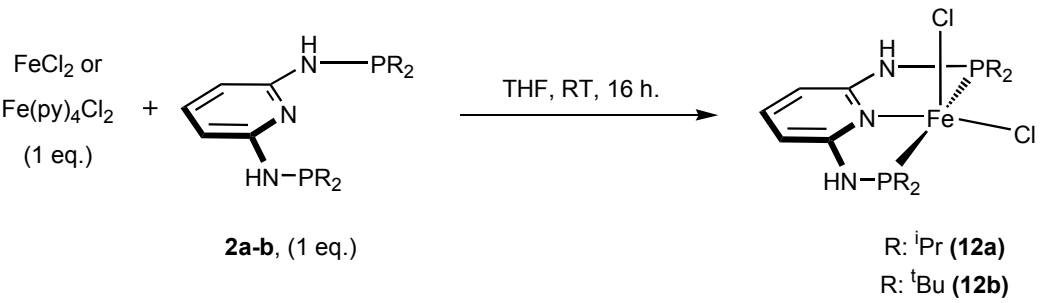

Scheme 39. Synthesis of the pentacoordinated iron(II) dichloro PNP complexes **12a** and **12b**

Characterization

The complexes **12a-b** are paramagnetic and display contact-shifted ^{1}H NMR spectra with relatively narrow line widths at room temperature. The signals can, however, be integrated and assigned to the different protons of the molecule. The ^{1}H NMR spectrum of **12a** is depicted in Figure 27. Due to their paramagnetic nature, no ^{31}P{^{1}H} and ^{13}C{^{1}H} NMR spectra could be obtained. Some characteristic ^{1}H NMR data for both complexes are summarized in Table 11.

Table 11. Selected ^{1}H NMR resonances of the complexes **12a** and **12b**

Complex	^{1}H (δ, [ppm], 20ºC)		
	N*H* (2H)	py^{3,5} (2H)	py^{4} (1H)
12a	75.30	47.49	21.26
12b	64.68	51.57	20.18

Due to the paramagnetic nature of the complexes and to the uncommon shifts at which the signals appear in the ^{1}H NMR spectra, the signals of the N*H* protons and of the py^{3,5} protons could not be differentiated at first. However, when two equivalents D_2O were added to a solution of one equivalent **12a** in acetone-d^{6}, the signal at 75.30 ppm disappeared. With this experiment, this signal can be assigned to the aminophosphine N*H* protons, because their higher acidity makes them more prone to undergo a hydrogen-deuterium exchange than the py^{3,5} protons. All the signals appear as broad singulets; the N*H* hydrogen atoms appear at around 70 ppm, the py^{3,5} at around 50 ppm and the py^{4} at around -20 ppm. The *iso*propyl and *tert*butyl substituents at the phosphines appear at 140.35 (4H, C*H*), 13.13 (12H, CH_3) and 7.00 (12H, CH_3) and at 17.46 ppm (36H, CH_3), respectively. Although NMR spectra of paramagnetic iron(II) pincer complexes have been reported before in the literature[76,77], these are the first examples of ^{1}H NMR spectra of paramagnetic iron(II) PNP pincer complexes described so far.

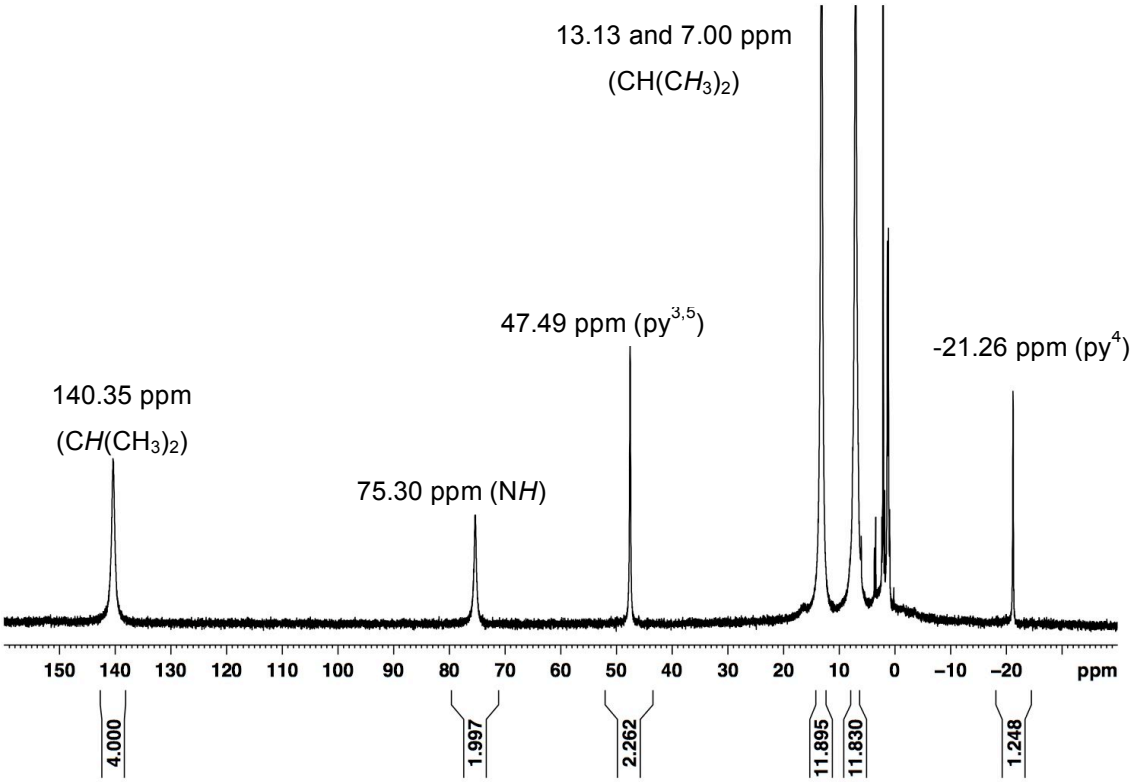

Figure 27. ^{1}H NMR spectrum of **12a**

Complex **12a** was also characterized by X-ray crystallography; crystals suitable for X-ray analysis were obtained by slow diffusion of diethyl ether into a saturated solution of **12a** in methanol. A structural view of **12a** is depicted in Figure 28.

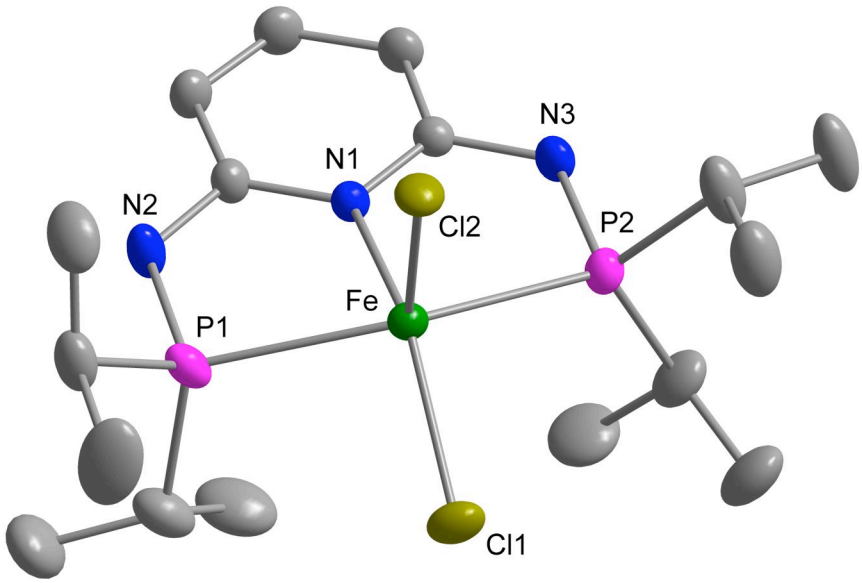

Figure 28. Structural view of [Fe(PNP-^{i}Pr)(Cl)$_2$] (**12a**) showing 30% thermal ellipsoids (hydrogen atoms and crystallization solvent omitted for clarity). Selected bond lengths (Å) and angles (º): Fe-N(1) 2.250(2), Fe-Cl(1) 2.3708(7), Fe-Cl(2) 2.3040(6), Fe-P(1) 2.4631(7), Fe-P(2) 2.4844(7), P(1)-N(2) 1.686(2), P(1)-C(6) 1.877(3), P(1)-C(9) 1.819(3), P(2)-N(3) 1.691(2), P(2)-C(12) 1.832(3), P(2)-C(15) 1.845(3); P(1)-Fe-P(2) 146.56(3), N(1)-Fe-Cl(1) 146.13(6), Cl(2)-Fe-N(1) 106.24(5), Cl(2)-Fe-P(1) 105.19(3), Cl(2)-Fe-P(2) 100.48(3), Cl(2)-Fe-Cl(1) 107.60(3), N(1)-Fe-P(1) 75.95(5), N(1)-Fe-P(2) 76.55(5), Cl(1)-Fe-P(1) 93.75(3), Cl(1)-Fe-P(2) 98.60(3).

The coordination geometry around the iron center is distorted square pyramidal with the iron atom lying 0.615(1) Å out of the basal plane (defined by N(1)-P(1)-P(2)-Cl(1)) in the direction of the apical atom Cl(2) with a r.m.s aplanarity of 0.056 Å. This feature is similar to that reported for analogous, iron(II), five-coordinate complexes[76a,81,88]. The bond distance Fe-P(1) (2.4631(7) Å) is slightly shorter than that of Fe-P(2) (2.4844(7) Å). The Fe-Cl(1) (basal) bond length is longer at 2.371(1) Å, as is the distance to the apical chlorine (Fe-Cl(2) 2.304(1) Å). In comparison to the octahedral, hexacoordinated, tris(acetonitrile) complex [Fe(PNP-^{i}Pr)(CH$_3$CN)$_3$](BF$_4$)$_2$ (**7b**), the Fe-N(1) and Fe-P bond lengths are about 0.25 Å and about 0.20 Å longer in **12a** than in **7b**, respectively.

It is possible to abstract both chlorine atoms from **12a** in a coordinating solvent and turn it from a pentacoordinated complex into a hexacoordinated one: when **12a** was treated with one equivalent of AgBF$_4$ in acetonitrile for one hour, an orange solution and a white solid (AgCl) were obtained. After filtering the solution and drying the filtrate, the remaining orange solid was identified by ^{1}H and ^{31}P{^{1}H} NMR spectroscopy as the diamagnetic complex [Fe(PNP-

[88] (a) O'Reilly, R. K.; Gibson, V. C.; White, A. J. P.; Williams, D. J. *Polyhedron* **2004**, *23*, 2921. (b) Britovsek, C. J. P.; Gibson, V. C.; Mastroianni, S.; Oakes, D. C. H.; Redshaw, C.; Solan, G. A.; White, A. J. P.; Williams, D. J. *Eur. J. Inorg. Chem.* **2001**, 431.

^{i}Pr)(CH$_3$CN)$_3$](BF$_4$)$_2$ (**7b**). The yield of this reaction was less than 50% and unreacted complex **12a** was also recovered. This indicates that the abstraction of both chlorines is more favored than the abstraction of just one chlorine atom. Thus, when two equivalents AgBF$_4$ were used, complex **7b** was obtained in 86% yield (Scheme 40).

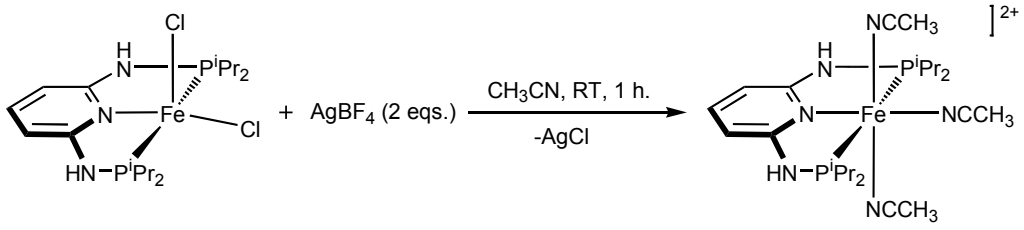

12a, (1 eq.) **7b**

Scheme 40. Formation of **7b** by abstraction of both chlorines of **12a** in acetonitrile

Surprisingly, this is in contrast with the results reported by Milstein and coworkers with a similar, methylene bridged, PNP pincer complex (**A**, Figure 29), where only one of the chlorines could be substituted with THF and, regardless of the amount of silver salt used and of the reaction conditions, the second chlorine could not be abstracted[81].

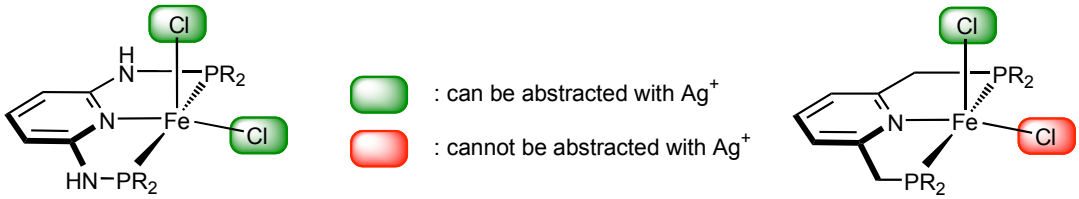

R: ^{i}Pr **(12a)**
R: ^{t}Bu **(12b)**

A

Figure 29. Lability of the chlorides in amino- and methylene bridged iron(II) PNP complexes

3.2.6 Iron(II) PN complexes

Synthesis

While [Fe(H$_2$O)$_6$](BF$_4$)$_2$ is an excellent precursor for the synthesis of hexacoordinated, iron(II) PNP complexes, the high lability of all the six water molecules makes it impossible to substitute just two of them by a bidentate PN ligand, even in coordinating solvents such as acetonitrile. When equimolar amounts of PN^{py}-Ph (**4a**) and [Fe(H$_2$O)$_6$](BF$_4$) were reacted in acetonitrile at room temperature for two hours, [Fe(PN^{py}-Ph)$_2$(CH$_3$CN)$_2$](BF$_4$)$_2$ (**13**) was obtained in 37% yield, and not [Fe(PN^{py}-Ph)(CH$_3$CN)$_4$](BF$_4$)$_2$. Moreover, the ^{31}P{^{1}H} NMR spectrum of the

product revealed the presence of a mixture of different isomers of **13** (**A**-**C**, Figure 30). Isomers **A** and **C** give rise to two doublets at 119.0 and 113.6 ppm with a coupling constant $^2J_{PP}$ = 53.3 Hz, while isomer **B**, in which the phosphines of the two PN ligands are equivalent, shows a singulet at 110.8 ppm. Complex **13 A-C** could be obtained as an air stable purple solid in 89% yield by reacting $[Fe(H_2O)_6](BF_4)_2$ and **4a** in a 1:2 molar ratio in acetonitrile at room temperature for two hours.

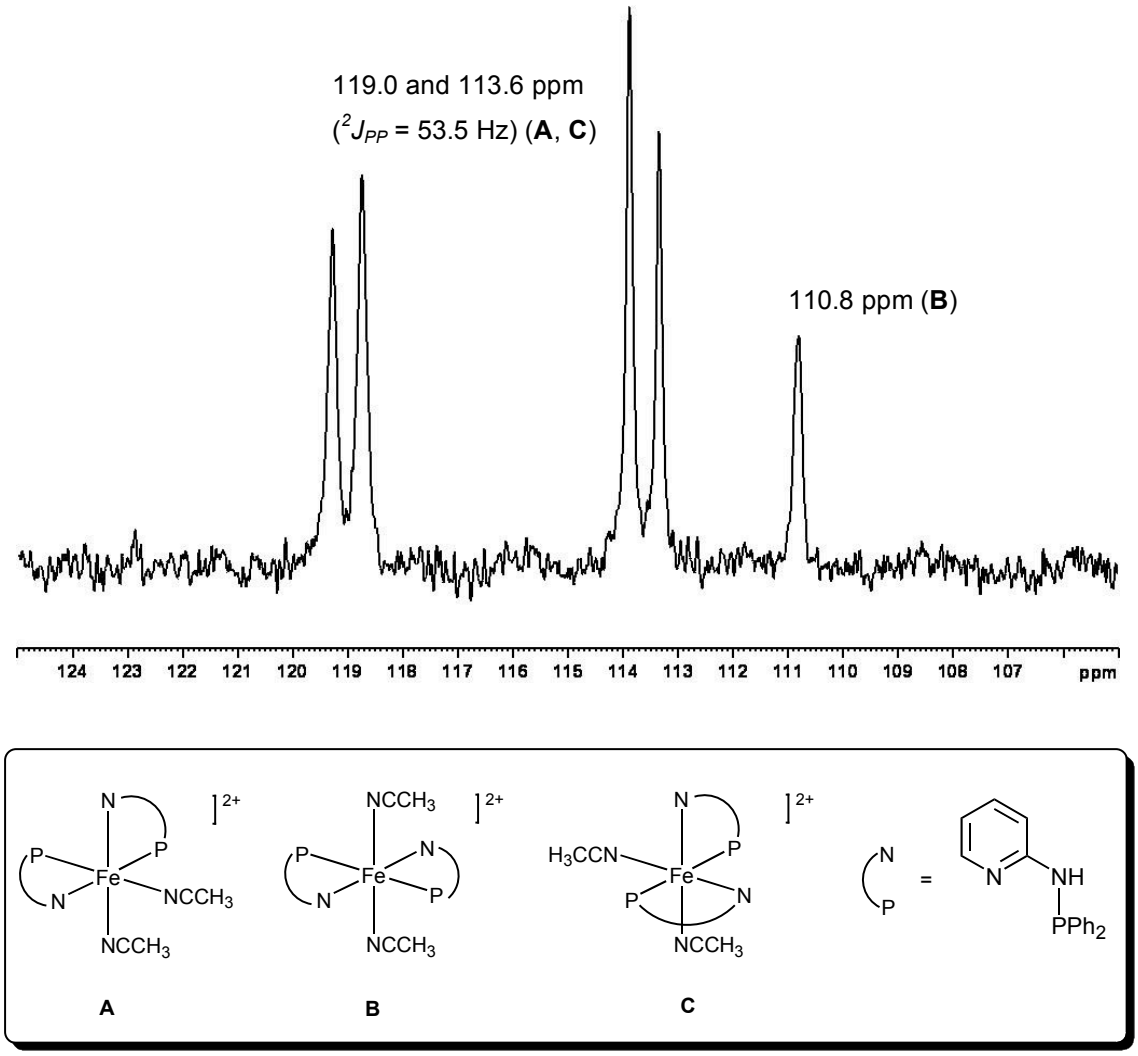

Figure 30. $^{31}P\{^1H\}$ NMR spectrum of the reaction between $[Fe(H_2O)_6](BF_4)_2$ and **4a**, indicating the presence of the isomers **A**-**C** of **13**

On the other hand, the high lability of only two of the substituents (carbonyl groups) attached to the iron center in $Fe(CO)_4Br_2$ makes it a more suitable precursor for the synthesis of iron(II) PN complexes than $[Fe(H_2O)_6](BF_4)_2$. When equimolar amounts of $Fe(CO)_4Br_2$ and the ligands **4a-c** and **5a** were mixed in toluene at room temperature, gas evolution (CO) immediately took place. After CO evolution was complete (~30 min.), the solvent was decanted from the solid residue and this was washed twice with diethyl ether and dried under vacuum to

give the neutral complexes **14a-c** and **15** as reddish-brown solids in moderate to good yields (58-81%) (Scheme 41).

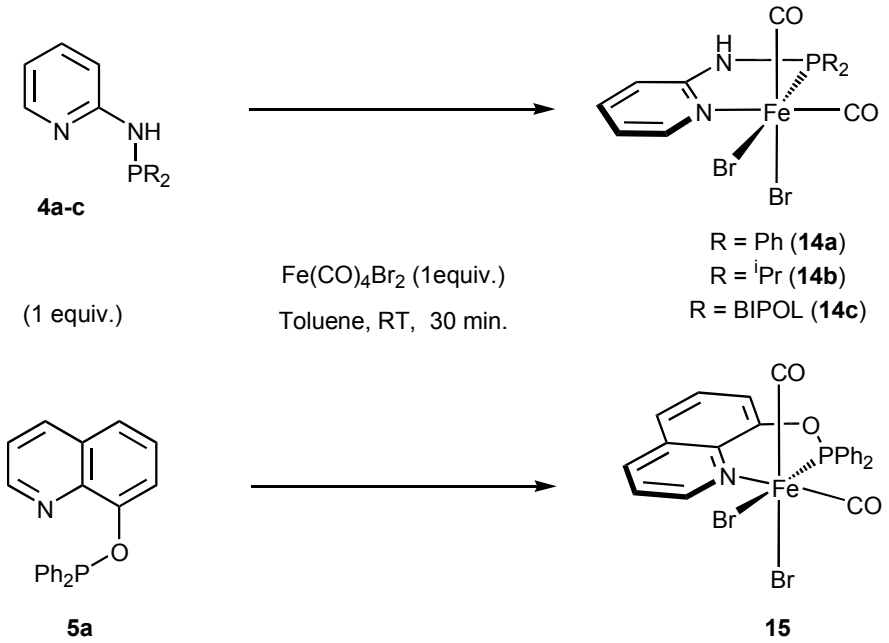

Scheme 41. Synthesis of the complexes **14a-c** and **15**

Characterization

The complexes **13**, **14a-c** and **15** were characterized by ^{1}H, $^{31}P\{^{1}H\}$ and $^{13}C\{^{1}H\}$ NMR spectroscopy. In the ^{1}H NMR spectrum of **13 A-C**, the signals of the methyl groups of the acetonitrile ligands appear at 2.17 and 1.87 ppm for isomers **A** and **C** and at 2.08 ppm for isomer **B**, in which both acetonitrile molecules are equivalent. In its $^{13}C\{^{1}H\}$ NMR spectrum, the signals of the pyridine ring of the isomers **A** and **C** appear shifted to the low field in comparison to those of the isomer **B**: the carbon atoms of the pyridine ring of isomers **A** and **C** give resonances at 163.9, 152.6, 140.9, 118.1 and 111.7 ppm, while the signals of isomer **B** appear at 162.7, 150.1, 139.3, 117.2 and 111.6 ppm. The methyl groups of the acetonitrile ligands give rise to signals at 3.1 and 2.5 ppm for isomers **A** and **C** and at 2.7 ppm for isomer **B**. The $^{31}P\{^{1}H\}$ NMR spectrum of **13** shows two doublets at 119.0 and 113.6 ppm with a coupling constant $^{2}J_{PP}$ of 53.5 Hz (isomers **A** and **C**) and one singulet at 110.8 ppm for isomer **B**[89]. The characterization data make it impossible to assign the doublets in the $^{31}P\{^{1}H\}$ NMR spectrum to either isomer **A** or isomer **C**.

In the ^{1}H NMR spectra of the complexes **14a-c** and **15**, the signals of the protons in the *ortho* position to the pyridine nitrogen atom are shifted to the low field when compared to those

[89] For comparison, analogous ruthenium(II) complexes featuring two PN ligands show a $^{2}J_{PP}$ coupling constant of 36.6 Hz for the isomers **A** and **C**. Yang, H.; Lugan, N.; Mathieu, R. *C. R. Acad. Sci. Paris* **1999**, 251.

in the free ligands; they appear as singulets between 9.45 and 9.40 ppm for **14a-c** and at 10.57 ppm for **15** (c.f., 8.96 ppm in **5a**). The signals of the other aromatic hydrogen atoms appear within the same range than those in the free ligands **4a-c** and **5a**. In the ^{13}C NMR spectra, the carbonyl groups give rise to doublets between 214.0 and 209.2 ppm with coupling constants $^{2}J_{CP}$ between 34.0 and 24.0 Hz. As for the $^{31}P\{^{1}H\}$ NMR spectra, the complexes **14a-c** and **15** show a single resonance at 123.1 ppm (**14a**), 153.1 ppm (**14b**), 207.0 ppm (**14c**) and 172.3 ppm (**15**). Complexes **14a** and **14c** were also characterized by IR spectroscopy: the spectra show the two carbonyl stretquing bands at 1997 and 2048 cm^{-1} (**14a**) and at 2035 and 2065 cm^{-1} (**14c**). These data indicate that the carbonyl groups are bound more strongly to the iron center in **14a** than in **14c**, which contains the π-accepting ligand PN^{py}-BIPOL.

Furthermore, complex **15** was also characterized by X-ray crystallography; suitable crystals were grown by slow diffusion of diethyl ether into a saturated solution of **15** in acetone. A structural view of **15** is depicted in Figure 31 .

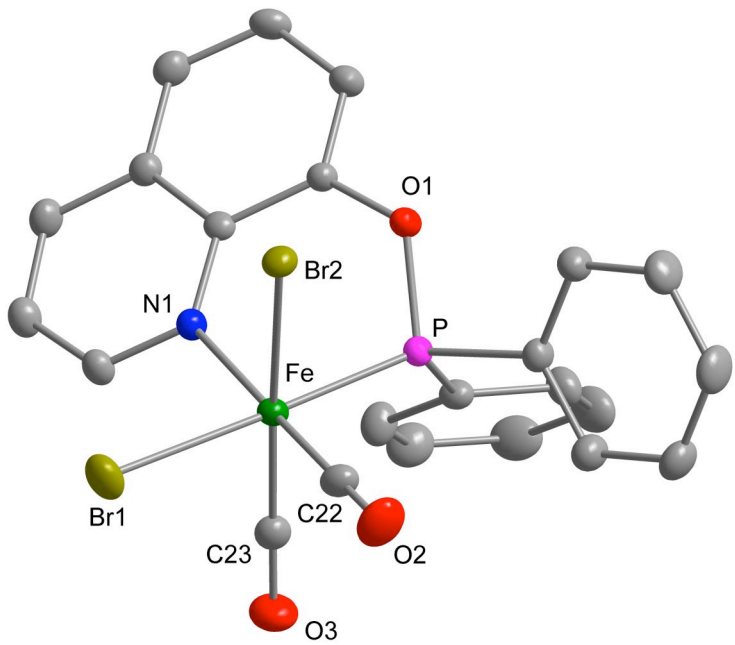

Figure 31. Structural view of $[Fe(PN^{py}\text{-}Ph)(CO)_2(Br)_2]$ (**15**) showing 40% thermal ellipsoids (hydrogen atoms omitted for clarity). Selected bond lengths (Å) and angles (º): Fe-C(22) 1.786(3), Fe-C(23) 1.786(4), Fe-P 2.1666 (8), Fe-N 2.076 (2), P-O(1) 1.625(1), Fe-Br(1) 2.5099(5), Fe-Br(2) 2.4461(6), N-Fe-C(22) 176.11(13), C(23)-Fe-Br(2) 172.5(2).

Complex **15** shows a distorted octahedral geometry with the nitrogen atom of the quinoline ring, the phosphorus atom, a carbonyl group and a bromine in the octahedral plane and with the second carbonyl group and bromine located *trans* to each other in the apical positions. Neither the quinoline ring nor the oxygen bridging are coplanar with the octahedral plane. In the *trans* positions to the pyridine nitrogen atom and the phosphorus atom are a

carbonyl ligand and a bromine atom, respectively, and the carbonyls are *cis* to each other. The P-O bond distance is 1.625(1) Å, which is about 0.05 Å shorter than the P-N bond lengths in the aminophosphine PNP complexes (e.g. in **7a**, the P(1)-N(2) distance is 1.677(3) Å). The Fe-N distance is similar to that in the iron(II) complexes bearing PNP ligands (**7a**: Fe-N(1) 1.977(2) Å; **15**: Fe-N 2.076 Å). The Fe-Br bond length is about 0.05 Å longer for the bromine in the *trans* position to the phosphorus atom than for the bromine in the apical position (Fe-Br(1) 2.5099(5) Å, Fe-Br(2) 2.4461(6) Å). The deviation from the planarity in the octahedral plane can be observed along the N-Fe-C(22) and C(23)-Fe-Br(2) axis: the bond angles are 176.11(13) and 172.5(2)º, respectively.

3.2.7 Iron(II) NPN Complexes

Synthesis

When equimolar amounts of $[Fe(H_2O)_6](BF_4)_2$ and NPN^{py} (**6**) were reacted at room temperature in acetonitrile for two hours, the complex $[Fe(NPN^{py})_2](BF_4)_2$ (**16**) was obtained in 35% yield instead of the expected complex of the formula $[Fe(NPN^{py})(CH_3CN)_3](BF_4)_2$. Thus, it seems that the formation of an iron bis-NPN complex is favored when compared to the formation of a tris(acetonitrile) NPN complex. Complex **16** (with chlorine counterions instead of tetrafluoroborate) was also obtained even when $FeCl_2$ was used as the metal precursor and the reaction was carried out in THF instead of acetonitrile. The yield of the reaction could be improved up to 86% by reacting $[Fe(H_2O)_6](BF_4)_2$ and NPN^{py} (**6**) in a 1:2 molar ratio under otherwise the same reaction conditions (Scheme 42). Complex **16** is an air stable deep red solid.

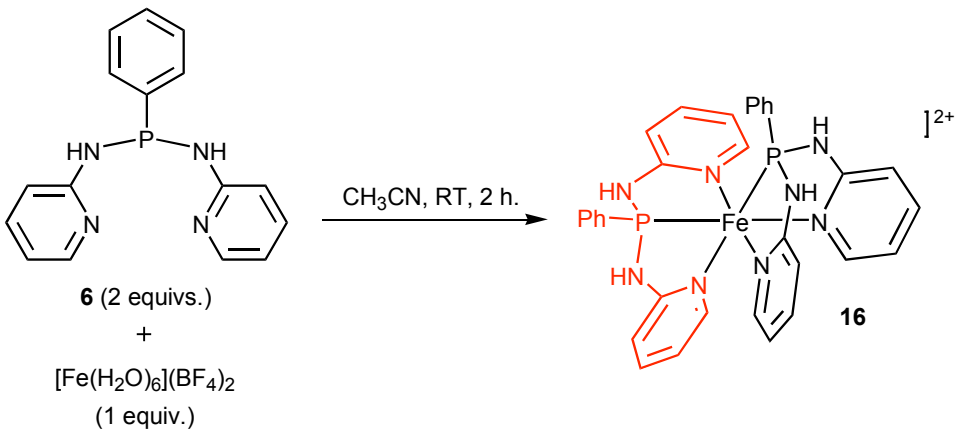

Scheme 42. Synthesis of complex **16**

Characterization

Complex **16** was characterized by ^{1}H, $^{31}P\{^{1}H\}$ and $^{13}C\{^{1}H\}$ NMR spectroscopy. In the ^{1}H NMR spectrum, the py[6] signals are shifted to the low field as a singulet at 8.25 ppm (**6**: 8.00 ppm), and the N*H* protons give rise to a multiplet at 6.30 ppm. All the other aromatic hydrogen atoms appear between 7.50 and 6.46 ppm. The $^{13}C\{^{1}H\}$ NMR spectrum bears no unusual features; the signals of the pyridine and phenyl rings are only shifted slightly to the low field compared to those of the free ligands. In the $^{31}P\{^{1}H\}$ NMR spectrum, complex **16** shows a single resonance at 164.5 ppm, consistent with a deshielding of the phosphorus atoms due to coordination to the metal center.

Alternatively, complex **16** was also characterized by X-ray crystallography; suitable crystals were obtained by slow diffusion of diethyl ether into a saturated solution of **16** in acetonitrile. A structural view of **16** is depicted in Figure 32.

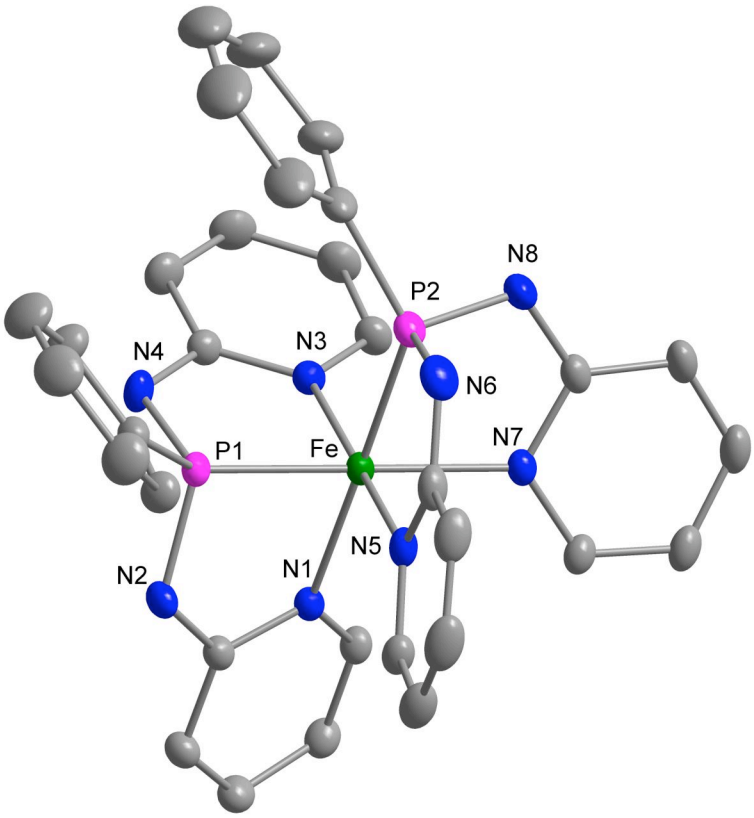

Figure 32. Structural view of $[Fe(NPN^{py})_2](BF_4)_2$ (**16**) showing 20% thermal ellipsoids (hydrogen atoms omitted for clarity). Selected bond lengths (Å) and angles (º): Fe-N(1) 2.073(3), Fe-N(3) 2.007(3), Fe-N(5) 2.003(3), Fe-N(7) 2.080(3), Fe-P(1) 2.1209(10), Fe-P(2) 2.1137(11), N(1)-Fe-P(2) 178.99(9), N(7)-Fe-P(1) 178.90(8), N(3)-Fe-N(5) 173.55(12).

Complex **16** shows a distorted octahedral geometry around the metal center. In contrast to the iron PNP complexes (and more concretely to the bis-PNP complex **8c**), in which the ligands coordinate in a meridional mode to the iron center, in **16** both NPN ligands are coordinated to the metal center in a facial mode. All the Fe-N and Fe-P bond distances are very similar (Fe-N 2.040 Å (mean value), Fe-P 2.1173 Å (mean value)). The N(1)-Fe-P(2), N(7)-Fe-P(1) and N(3)-Fe-N(5) bond angles have values of 178.99(9), 178.90(8) and 173.55(12)º, respectively, deviating from the octahedral geometry around the metal center.

3.2.8 Iron (II) catalyzed coupling of aromatic aldehydes with EDA

Transition metal complexes that can act as catalysts in organic reactions are an essential tool for chemists. The current requirements for clean, fast, efficient and selective processes have increased the demand for such metal-based reaction promoters, especially the ones that can be applied in catalytic amounts and/or that are recyclable. However, many of these catalysts are based on heavy and/or rare metals, which constitutes a major drawback for large-scale applications due to their toxicity and expensive prices. In contrast, iron is the most abundant metal on Earth, and one of the most inexpensive and environmentally friendly metals. Surprisingly, until recently, iron was underrepresented in the field of catalysis when compared to other transition metals. Nevertheless, the last few years have seen an increase in the interest in iron-catalyzed reactions, and some very efficient processes able to compete with other metal-catalyzed ones have emerged, also in the field of asymmetric catalysis[90]. The most spectacular example for the use of iron compounds in catalysis is the polymerization of ethylene catalyzed by the Brookhart-Gibson pyridine-diimine catalysts, which show a very high activity coupled with a remarkable selectivity and make them far better catalysts than other compounds based on more expensive transition metals[76,91]. Other applications include the use of $FeCl_3$ and $Fe(acac)_3$ in the cross-coupling reactions of Grignard reagents with aryl, heteroaryl and alkyl chlorides, tosylates and triflates, developed among others by Fürstner and co-workers[92].

---

[90] For a comprehensive review on iron-catalyzed reactions in organic synthesis, see: Bolm, C.; Legros, J.; Le Paih, J.; Zani, L. *Chem. Rev.* **2004**, *104*, 6217 and references therein.

[91] (a) Small, B. C.; Brookhart, M. *J. Am. Chem. Soc.* **1998**, *120*, 7143. (b) Small, B. C.; Brookhart, M. *Macromolecules* **1999**, *32*, 2120. (c) Smit, T. M.; Tomov, A. K.; Gibson, V. C.; White, A. J. P.; Williams, D. J. *Inorg. Chem.* **2004**, *43*, 6511. (d) Tellmann, K. P.; Gibson, V. C.; White, A. J. P.; Williams, D. J. *Organometallics* **2005**, *24*, 280. (e) Gibson, V. C.; Long, N. J.; Oxford, P. J.; White, A. J. P.; Williams, D. J. *Organometallics* **2006**, *25*, 1932. (f) Britovsek, G. J. P.; Gibson, V. C.; Hoarau, O. D.; Spitzmesser, S. K.; White, A. J. P.; Williams, D. J. *Inorg. Chem.* **2003**, *42*, 3454.

[92] For a review, see: (a) Fürstner, A.; Leitner, A.; Méndez, M.; Krause, H. *J. Am. Chem. Soc.* **2002**, *124*, 13856 and references therein. See also: (b) Scheiper, B.; Bonnekessel, M.; Krause, H.; Fürstner, A. *J. Org. Chem.* **2004**, *69*, 3943. (c) Fürstner, A.; Martín, R.; Majima, K. J. Am. Chem. Soc. **2005**, 127, 12236. (d) Seidel, G.; Leurich, D.; Fürstner, A. *J. Org. Chem.* **2004**, *69*, 3950.

As a Lewis acid, iron is also capable of mediating Lewis acid-catalyzed processes. One of such reactions is the coupling of ethyl diazoacetate (EDA) with aromatic aldehydes, which can, depending on the mechanism of the reaction, give either 3-hydroxy-2-arylacrylic acid ethyl esters (3-hydroxacrylates, **A**,
Scheme 43) or 3-oxo-3-arylpropanoic acids (β-ketoesters, **B**). It has to be noted that, while β-ketoesters can be easily synthesized by a wide variety of methods, 3-hydroxyacrylates are more difficult to prepare and only one synthetic procedure can be found in the literature in which their preparation can be carried out in five steps via acidic hydrolysis of oxazinones[93].

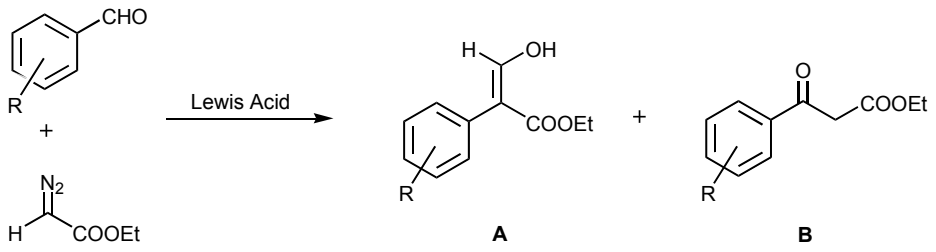

Scheme 43. Lewis acid catalyzed reaction between aromatic aldehydes and EDA

The reaction of aromatic aldehydes with EDA catalyzed by simple Lewis acids, such as BF_3, $ZnCl_2$, $AlCl_3$, $GeCl_2$ and $SnCl_4$, gives mainly b-ketoesters as the products[94]. Using $ZnCl_2$ as the catalyst in combination with chlorotrimethylsilane, it is possible to switch the regioselectivity of the reaction towards the formation of 3-hydroxyacrylates[95]. However, substantial amounts of β-ketoesters are typically formed (up to a 60:40 ratio), and the reaction only takes place satisfactorily when it is carried out at low temperatures and when EDA is added slowly over a period of 6-7 hours. Recently, Hossain and co-workers have found that the cyclopentadienyl dicarbonyl iron complex $[FeCp(CO)_2(THF)]BF_4$ is an active catalyst for the coupling of aromatic aldehydes with EDA to afford 3-hydroxyacrylates as the main products[96a]. Similar results were obtained by the same authors with the Brönsted acid $HBF_4{\cdot}Et_2O$ as the catalyst[97]. This methodology has been applied to the synthesis of a Naproxen precursor, a highly valued anti-inflammatory drug[96b]. Moreover, salicylaldehydes can also be coupled with EDA to prepare

---

[93] Beccalli, E. M.; La Rosa, C.; Marchesini, A. *J. Org. Chem.* **1984**, *49*, 4287.

[94] (a) Holmquist, C. R.; Roskamp, E. J. *J. Org. Chem.* **1989**, *54*, 3258. (b) Holmquist, C. R.; Roskamp, E. J. *Tetrahedron Lett.* **1992**, *33*, 1131. (c) Padwa, A.; Hornbuckle, S. F.; Zhang, Z.; Zhi, L. *J. Org. Chem.* **1990**, *55*, 5297. (d) Sudrik, S. G.; Balaji, B. S.; Singh, A. P.; Mitra, R. B.; Sonawane, H. R. *Synlett* **1996**, 369. (e) Nomura, K.; Iida, T.; Hori, K.; Yoshii, E. *J. Org. Chem.* **1994**, *59*, 488.

[95] Kanemasa, S.; Kanai, T.; Araki, T.; Wada, E. *Tetrahedron Lett.* **1999**, *40*, 5055.

[96] (a) Mahmood, S. J.; Hossain, M. M. *J. Org. Chem.* **1998**, *63*, 3333. (b) Mahmood, S. J.; Brennan, C.; Hossain, M. M. *Synthesis* **2002**, 1807.

[97] Dudley, M. E.; Morshed, Md. Monzur, Brennan, C. L.; Islam, M. S.; Ahmad, M. S.; Atuu, M.-R.; Branstetter, B.; Hossain, M. M. *J. Org. Chem.* **2004**, *69*, 7599.

benzofuranes, which can be used as building blocks in the synthesis of several biologically active compounds[98] (Scheme 44).

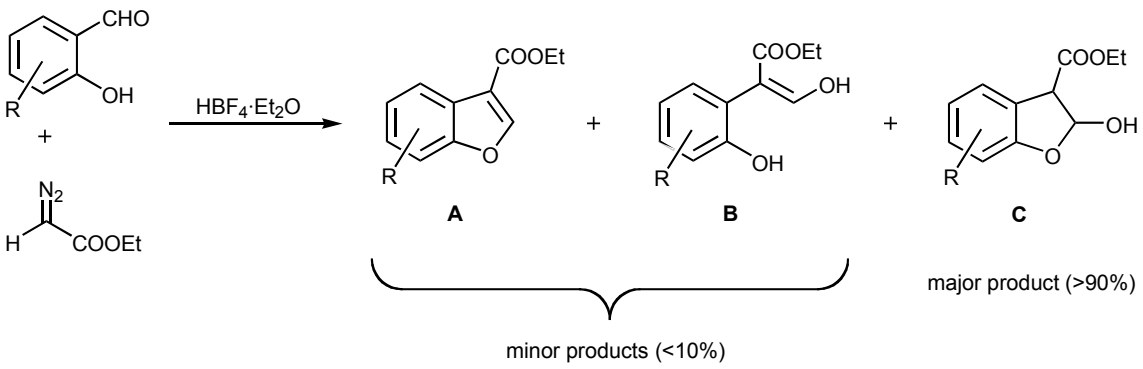

Scheme 44. Synthesis of benzofuranes from salicylaldehydes and EDA catalyzed by $HBF_4 \cdot Et_2O$

The reaction of aromatic aldehydes with EDA catalyzed by $[FeCp(CO)_2(THF)]BF_4$ presents the same drawbacks than those observed when $ZnCl_2$ and chlorotrimethylsilane were used as catalysts: a diluted solution of the diazo compound has to be added dropwise over a long period of time (typically seven hours for 1.2 mmol EDA) and reaction temperatures between 0 and -78ºC are necessary. Furthermore, mixtures of β-ketoesters and 3-hydroxyacrylates are obtained. We were therefore interested in investigating whether the iron(II) PNP complexes described above could be used as catalysts in this reaction with a higher chemoselectivity under milder reaction conditions.

In the first place, a solvent screening using p-anisaldehyde as the model substrate and **7b** as the catalyst was made optimize the solvent for the reaction (Table 12).

Table 12. Optimization of the reaction solvent in the coupling of EDA with aromatic aldehydes catalyzed by **7b**[a]

Entry	Solvent	yield (%) **A**	yield (%) **B**
1	CH3CN	0	0
2	CH2Cl2	42	2
3	CH3NO2	66	3
4	1,4-dioxane	45	9

[a]Reaction conditions: 1 equiv. anisaldehyde, 1 equiv. EDA, 10 mol% **7b**, RT, reaction time 16 h.; yields represent isolated yields.

[98] Dudley, M. E.; Morshed, M. M.; Hossain, M. M. *Synthesis* **2006**, *10*, 1711.

In the course of the catalytic reaction, one or both reactants must somehow coordinate to the iron(II) center by displacing one or more of the acetonitrile coligands in **7b**; thus, acetonitrile (entry 1) is an unsuitable solvent because it blocks the necessary coordination site(s). The yields obtained when methylene chloride or 1,4-dioxane (entries 2 and 4) were used as the solvents are similar but low; this can be attributed to the low solubility of the complex **7b** in these solvents. Nitromethane (entry 3), which is a non coordinating solvent and one in which the catalyst is highly soluble, turned out to be the best solvent to carry out the catalytic reaction. From Table 12 it can also be seen that the complex **7b** ia a chemoselective catalyst, since the main product was in all cases the 3-hydroxyacrylate and only very small amounts of β-ketoester were obtained. Furthermore, EDA was added at once and the reaction was carried out at room temperature, and therefore at higher reaction rates.

A survey of the catalyst activity was carried out next with several iron(II) PNP complexes to determine the most suitable complex for the reaction (Table 13); for comparison, the yields obtained with $[FeCp(CO)_2(THF)]BF_4$[96a] (**A**) as well as with *N*-alkylated[67] (**B**) and triazine-based[68] (**C**) PNP complexes are given in Table 13. The structures of the different complexes used as catalysts are depicted in Figure 33. Three different *para*-substituted aromatic aldehydes, possessing no functional groups as well as electron withdrawing and electron donating groups were used as model substrates.

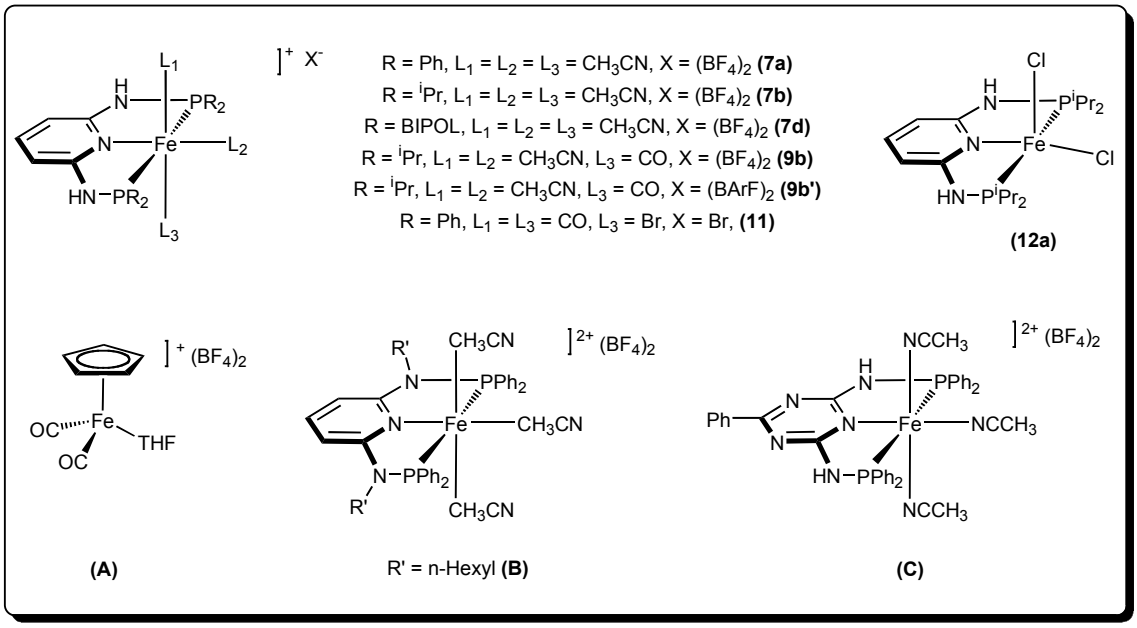

Figure 33. Catalysts employed in the coupling of EDA with aromatic aldehydes catalyzed by iron(II) complexes

Table 13. Optimization of the catalyst in the coupling of EDA with aromatic aldehydes catalyzed by iron(II) complexes[a].

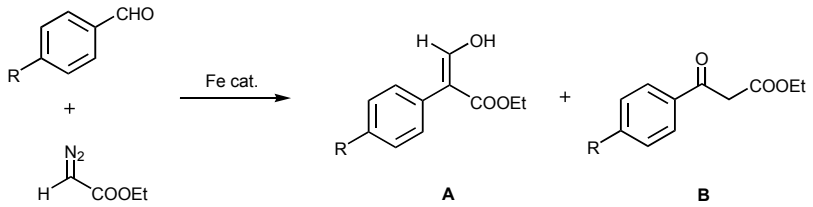

Entry	R	Catalyst	yield (%) A	yield (%) B
1	OMe	**7a**	22	2
2	OMe	**7b**	66	3
3	OMe	**7d**	53	3
4	OMe	**A**[b]	60	20
5	OMe	**B**[c]	49	3
6	OMe	**C**[c]	44	5
7	OMe	**9b**	84	4
8	OMe	**9b'**	80	4
9	OMe	**11**	0	0
10	OMe	**11** + AgSbF6 (1 equiv.)	13	3
11	OMe	**12a** + AgSbF6 (1 equiv.)	26	3
12	OMe	**12a** + AgSbF6 (2 equivs.)	37	3
13	H	**7b**	72	11
14	H	**9b**	91	4
15	H	**B**[c]	60	10
16	H	**C**[d]	56	12
17	F	**7b**	86	14
18	F	**9b**	88	4
19	F	**C**[d]	63	11

[a]Reaction conditions: 1 equiv. anisaldehyde, 1 equiv. EDA, 10 mol% catalyst, CH_3NO_2 as the solvent, RT, reaction time 16 h.; yields represent isolated yields. [b]1.2 equivs. aldehyde, 1 equiv. EDA, 0ºC, 10 mol% catalyst, CH_2Cl_2 as the solvent, overall reaction time 16 h.; isolated yields (ref. [96a]). [c]Ref. [67]. [d]Ref. [68].

The first important feature that can be extracted from the results summarized in Table 13 is the high chemoselectivity displayed by the iron(II) PNP complexes in the coupling of aromatic aldehydes with EDA compared to $[FeCp(CO)_2(THF)]BF_4$ (**A**). For the three different substrates, the most effective catalyst was found to be $[Fe(PNP\text{-}^{i}Pr)(CO)(CH_3CN)_2](BF_4)_2$ (**9b**) (entries 7, 14 and 18), bearing both strongly electron donating and bulky *iso*propyl substituents. The isolated yields are in all cases over 80%, with the 3-hydroxyacrylates being the major products and the β-ketoesters as by-products in less than 5% isolated yield. The tris(acetonitrile) complexes **7a** (entry 1), **7b** (entries 2, 13 and 17), **7d** (entry 3), **B** (entries 5 and

15) and **C** (entries 6, 16 and 19) were all less efficient catalysts than **9b**, probably because the presence of a carbonyl group in **9b** renders the iron center more Lewis acidic. Likewise, the complexes [Fe(PNP-Ph)$(CO)_2$Br]BPh_4 (**11**) (entries 9 and 10) and [Fe(PNP-^{i}Pr)Cl_2] (**12a**) (entries 11 and 12) both in the presence and in the absence of $AgSbF_6$ as halide scavenger turned out to be rather inefficient as catalysts, most likely due to decomposition of the complexes, since the reactions were carried out in a non coordinating solvent.

Changing the counterion in **9b** from the weakly coordinating BF_4^- to the non coordinating anion tetrakis(3,5-bis(trifluoromethyl)phenyl)borate ($BArF^-$) (entry 8) led to a similar yield when p-anisaldehyde was used as the substrate (**9b**: 84%, **9b'**: 80%). Thus, the nature of the counterion does apparently not affect the coupling reaction, contrarily to what has been frequently observed for Lewis acid catalyzed processes[99].

Since this reaction is known to be catalyzed by Lewis acids such as HBF_4[97], and the aminophosphine N*H* protons in the iron(II) PNP complexes are known to be acidic, there could be some doubts about the real nature of the catalyst. HBF_4 could be released in the course of the reaction, being an additional or even the only source of the catalytically active species. However, when the *N*-alkylated iron(II) PNP complex **B**, which lacks acidic N*H* hydrogen atoms, was used as the catalyst, the isolated yield was even higher than the one obtained with the hydrogen containing analogous complex **7a**. Thus, the influence of HBF_4 on the yields of the catalytic reaction can be ruled out. Nevertheless, the yield obtained when using complex **B**, which bears phenyl substituents at the phosphorus atoms, was still significantly lower than the yield obtained when the ^{iso}propyl phosphine containing complex **7b** was used as the catalyst.

The effect of the catalyst loading on the reaction rate was then investigated using the same reaction conditions, two different substrates and two different catalysts' loadings (10 mol% and 1 mol%) (Figure 34). The reaction proceeds well when 10 mol% **9b** is used, showing a conversion of 95 and 83% for p-fluorobenzaldehyde and p-anisaldehyde, respectively. However, the conversion decreases to 60 and 50% when the catalyst loading is decreased to 1 mol%. Catalyst decomposition might play a role in these observations.

---

[99] Kündig, E. P.; Saudan, C. M.; Bernardinelli, G. *Angew. Chem.Int. Ed.* **1999**, *38*, 1219.

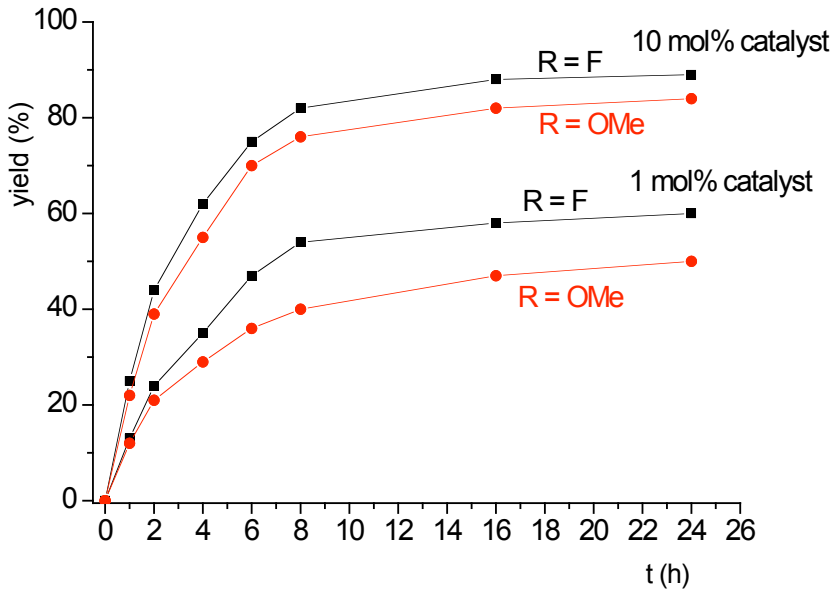

Figure 34. Plot of yield vs. time for the formation of 3-hydroxyacrylates from p-fluorobenzaldehyde and p-anisaldehyde with EDA using 10 and 1 mol% of [Fe(PNP-^{i}Pr)(CO)(CH_3CN)$_2$](BF_4)$_2$ (**9b**), respectively.

To investigate the scope and limitations of the iron(II) PNP system, complex **9b** was used as catalyst with a range of different aromatic aldehydes (Table 14). Experimentally, EDA and the aldehyde were added at once in a 1:1 ratio to a stirred solution of 10 mol% **9b** in nitromethane. The reaction was then stirred for sixteen hours at room temperature, and the isolation of the products was achieved by flash chromatography (silica gel, CH_2Cl_2). The catalytic effect of the iron complexes was confirmed by running the standard reaction, i.e., p-anisaldehyde and EDA, without catalyst. As expected, no product was formed and only starting materials were recovered from the reaction mixture.

Table 14. Yields of the coupling of EDA with various aromatic aldehydes catalyzed by **9b**[a].

Entry	aldehyde	3-hydroxyacrylate	yield (%)	β-ketoester	yield (%)
1	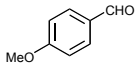	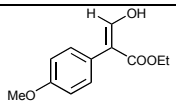	84	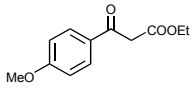	4
2	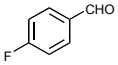	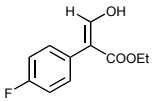	88	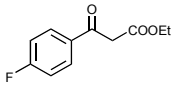	5
3	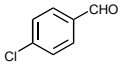	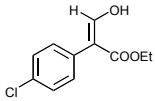	86	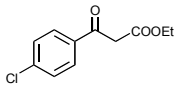	5
4	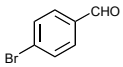	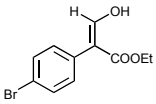	86	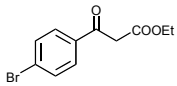	5
5	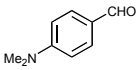	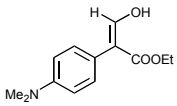	58	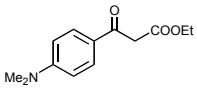	3
6	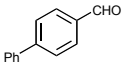	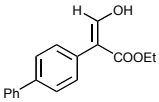	83	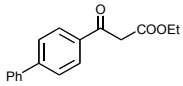	5
7		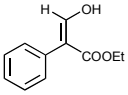	91	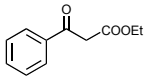	4
8		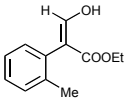	78	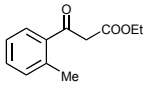	3
9		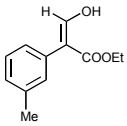	89	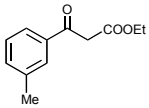	5
10	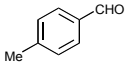	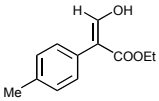	84	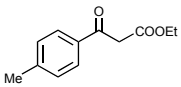	5
11	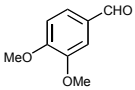	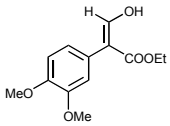	74	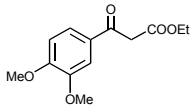	0
12	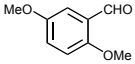	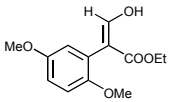	80	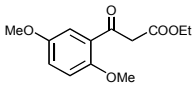	5
13	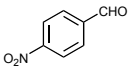	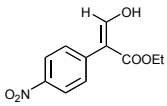	64	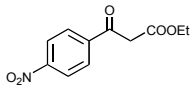	4
14	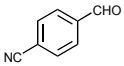	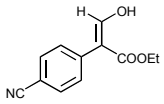	58	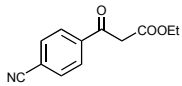	21

15	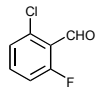	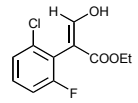	31	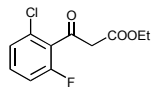	29
16	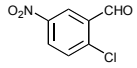	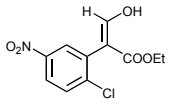	34	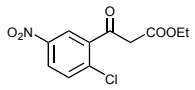	8

[a]Reaction conditions: 1 equiv. anisaldehyde, 1 equiv. EDA, 10 mol% **9b**, CH_3NO_2 as the solvent, RT, reaction time 16 h.; yields represent isolated yields.

In all cases but two, 3-hydroxyacrylates, as isolated from the reaction mixture, were formed selectively, and the formation of β-ketoesters was <5%. The formation of epoxides was not observed in any of these reactions. This is in contrast to the results observed in the reactions catalyzed by $[FeCp(CO)_2(THF)]BF_4$ (**A**), where mixtures of 3-hydroxyacrylates and β-ketoesters were obtained. For example, the reaction of benzaldehyde and EDA with 10 mol% **A** affords a 58:25% mixture of 3-hydroxy-2-phenylacrylic acid ethyl ester and 3-oxo-3-phenylpropionic acid ethyl ester. The same reaction performed with **9b** yields almost exclusively 3-hydroxy-2-phenylacrylic acid ethyl ester in 91% yield (entry 7). Even in the case of the two worst results (entries 14 and 15), the acrylate:ketoester ratio lies in the range of that observed when **A** was used as the catalyst. In all the other cases, complex **9b** surpasses even the best compounds known to catalyze this reaction in terms of yield, chemoselectivity, scope and ease of the reaction.

A mechanistic proposal for the coupling of aromatic aldehydes with EDA catalyzed by **9b** is presented in Scheme 45. This mechanism has been supported by theoretical investigations based on DFT/B3LYP calculations (Figure 35). Since CO exhibits a much stronger *trans* effect (and *trans* influence) than pyridine, the acetonitrile ligand trans to CO is much more labile than the one trans to the pyridine ring of the PNP ligand. This might account for the higher reactivity of **9b** compared to **7b**. Accordingly, the substitution of this acetonitrile ligand by an aldehyde molecule (which is present in a large excess under the catalytic conditions) may afford $[Fe(PNP\text{-}^{i}Pr)(CO)(CH_3CN)(\kappa^1(O)\text{-aldehyde})]^{2+}$ (**A**). The nucleophilic attack of EDA to the coordinated aldehyde via a S_N^2-type mechanism would yield, via transition state TS_{AB}, intermediate **B**. In the course of this step N_2 is liberated. The preferential [1,2]-migration of the aryl substituent over a hydride migration would lead to intermediate **C**, featuring a $\kappa^1(O)$-coordinated aldehyde ester molecule. This would be displaced by an incoming unreacted aldehyde molecule and then tautomerize to yield the corresponding thermodinamically more stable 3-hydroxyacrylate. Thus, the catalytic process can be seen as an equilibrium reaction in which the product must be displaced by fresh aldehyde, which can coordinate better to the iron center. In the beginning of the reaction, there is enough aldehyde present to displace the product; however, when conversions of around 80% are achieved, there is very little aldehyde left to free the products. Taking this into consideration, it is logical then

that the catalytic reaction stops at around 90% conversion (Figure 34) and that the yields never reach 100%.

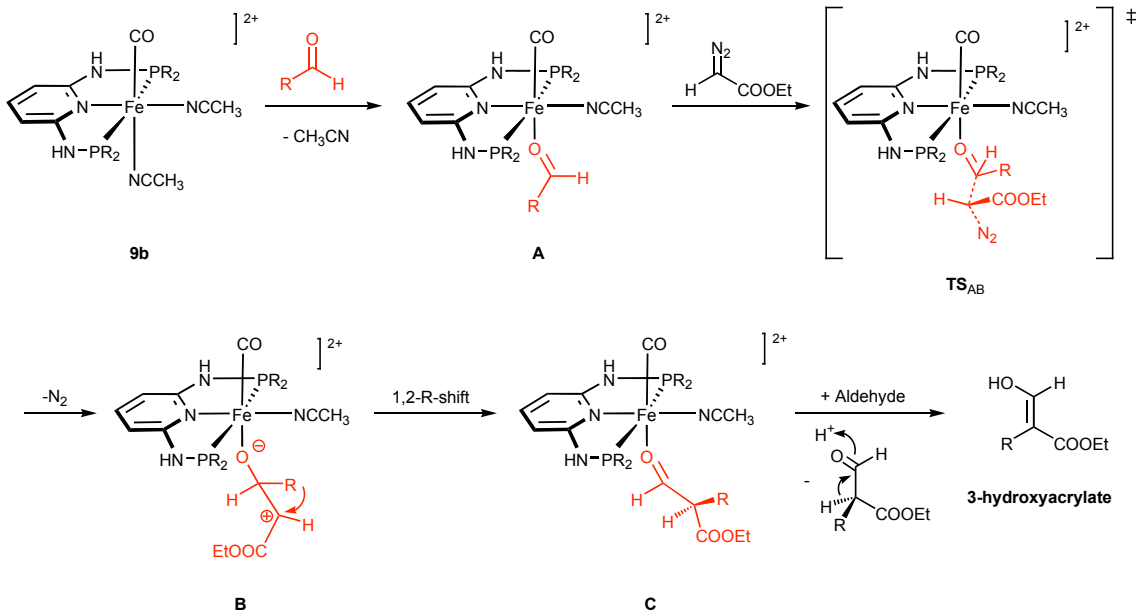

Scheme 45. Proposed mechanism for the coupling of EDA with aromatic aldehydes catalyzed by **9b**.

The theoretical investigations show that the nucleophilic attack of EDA to compound **A** to form transition state TS_{AB} is endothermic but requires only 4.1 Kcal/mol. In it, it can be clearly appreciated how the N_2 molecule is starting to detach from the diazo compound (the CH-N bond length is 1.40 Å) and how the bond between the carbon atom of the aldehyde molecule and the CH group of EDA is being formed (the CO-CH bond length is 1.76 Å). The coupling of the aldehyde molecule and EDA with concomitant release of N_2 from TS_{AB} to **B** is exothermic (ΔE = -8.3 Kcal/mol), which means that the formation of **B** from **A** is also exothermic (ΔE = -4.2 Kcal/mol). It has to be noted that in **B** the carbonyl group of the ester moiety is bent towards the carbocation, with a C^+-O distance of 1.85 Å. The formation of the transition state TS_{BC} from **B** requires only 1.7 Kcal/mol, and the aryl migration is so energetically favored that 64.4 Kcal/mol are liberated in the step from TS_{BC} to **C**. Thus, the whole process is exergonic (ΔE = -66.9 Kcal/mol), and the energies required to form the corresponding transition states are verly low.

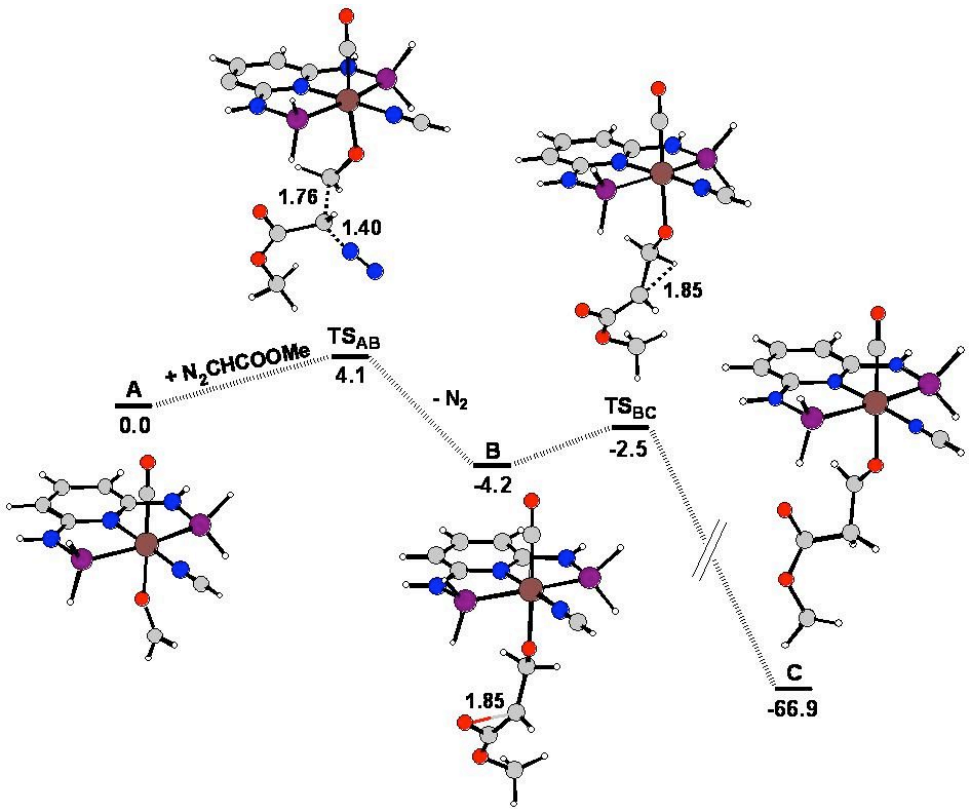

Figure 35. Energy profile for the coupling of EDA with aromatic aldehydes catalyzed by **9b**

In principle, an alternative pathway could proceed via the formation of the epoxide ethyl-3-arylglycidate from complex **B** with subsequent rearrangement (epoxide opening) to the corresponding enol ester (Scheme 46), since it is known that transition metal complexes are able to convert epoxides to ketones and aldehydes[100]. If this mechanism was possible, **9b** should be able to form 3-hydroxy-2-phenylacrylic acid ethyl ester from ethyl-3-phenylglycidate; however, when the epoxide was stirred with 10 mol% **9b** in nitromethane for 16 hours, no reaction was observed (Scheme 46). Thus, this alternative mechanism was dismissed.

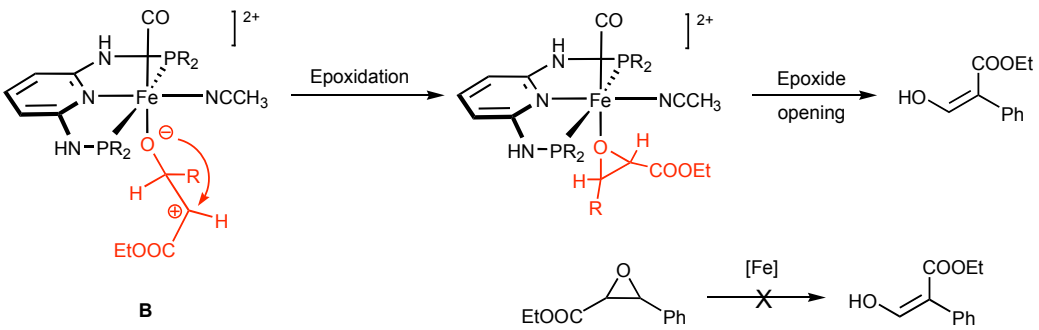

Scheme 46. Alternative mechanism for the formation of 3-hydroxyacrylates from aromatic aldehydes and EDA catalyzed by **9b**

[100] (a) Maruoka, K.; Nagahara, S.; Ooi, T.; Yamamoto, H. *Tetrahedron Lett.* **1989**, *30*, 5607. (b) Miyashita, A.; Shimada, T.; Sugawara, A.; Nohira, H. *Chem. Lett.* **1986**, 1323.

A mechanism where both EDA and the aldehyde are coordinated to the iron center, as proposed by Kanemasa et al.[95], seems to be less likely since the theoretical investigations indicate that the energy required for the formation of the corresponding transition state lies around 19 Kcal/mol, which is almost five times bigger than the energy required for the formation of TS_{AB} described in Figure 35. Likewise, the intermediacy of carbenes is also a possibility. However, since **9b** does not react with EDA in the absence of aldehydes and there is no indication whatsoever pointing to the formation of an iron carbene, this alternative can also be ruled out.

3.2.9 Summary

Iron(II) PNP complexes could be prepared starting from three different metal precursors: when $[Fe(H2O)_6](BF_4)_2$ and the PNP ligands were reacted in equimolar quantities, octahedral, diamagnetic, iron(II) tris(acetonitrile) PNP complexes were obtained. The acetonitrile ligands in these complexes are labile and can be substituted by bidentate or tridentate nitrogen donor ligands and by another equivalent of a PNP ligand. Alternatively, the Lewis acidity of the iron center in these complexes can be increased by substituting one of the acetonitrile molecules by a carbon monoxide ligand. The synthesis of zerovalent iron complexes was not possible due to the acidity of the N*H* protons of the amino bridgings of the PNP ligands, which are deprotonated easily, thus hampering the reduction of the metal center from iron(II) to iron(0). An octahedral, diamagnetic dicarbonyl iron(II) PNP complex could also be obtained from PNP-Ph (**11**) and $Fe(CO)_4Br_2$; due to the similar lability of one of the carbonyl groups and one of the bromines in the precursor complex, a halide scavenger was needed in order to shift the reaction towards the abstraction of bromine. Paramagnetic, pentacoordinated iron(II) PNP complexes were also prepared from $FeCl_2$ and $Fe(py)_4Cl_2$; the two chlorine atoms in these complexes can be abstracted in the presence of a silver salt and, in a coordinating solvent, be converted into hexacoodinated, diamagnetic iron(II) PNP complexes. Several iron(II) complexes of the formula $[Fe(PN)(CO)_2Br_2]$ were obtained by reacting pyridine- and quinoline-based PN ligands with $Fe(CO)_2Br_2$; while this precursor requires the addition of a halide scavenger to form defined complexes with the tridentate PNP ligands, the higher lability of two carbonyl groups in $Fe(CO)_4Br_2$ makes it a perfect precursor for the formation of the complexes **14a-c** and **15**. An iron(II) bis-NPN complex (**16**), in which the ligand is coordinated to the metal center not in a meridional mode but in a facial one, could be prepared by the reaction of $[Fe(H_2O)_6](BF_4)_2$ and NPN^{py} (**6**) in a 1:2 molar ratio.

The catalytic activity of several iron(II) PNP complexes was tested in the coupling of EDA with aromatic aldehydes; the best catalysts in terms of efficiency and chemoselectivity turned out to be the bis(acetonitrile) carbonyl complexes **9a**, **9b** and **9b'**. In contrast to other compounds known to mediate this reaction, the iron(II) PNP complexes catalyze the selective

formation of 3-hydroxyacrylates in high yields with the formation of traces of the corresponding β-ketoesters. Besides, the reaction conditions are moderate, and the slow addition of the reagents at low temperatures over several hours is not required.

3.3 Nickel, Palladium and Platinum complexes

3.3.1 Introduction

While there are few examples of iron pincer complexes, the number of nickel, palladium and platinum pincer complexes described in the literature is huge, and it is very likely that there exists a pincer complex with one of these transition metals for each class of pincer ligands reported so far. In fact, the first transition metal pincer complexes were nickel, palladium and platinum compounds[2]. Moreover, the discovery of their many applications in catalytic processes has made their study one of the major research fields in modern organometallic chemistry[3].

Nickel pincer complexes have been prepared with a wide variety of both neutral and anionic ENE and ECE (E: neutral, two-electron donor group) pincer ligands[2a,3]; some examples of nickel pincer complexes are shown in Figure 36[101]. An interesting class of nickel pincer complexes of the PNP type has been reported by Ozerov et al. (**C**, Figure 36); in these complexes, the nitrogen atom is not part of an aromatic ring and must be deprotonated prior to metalation[101c]. Nickel complexes bearing pincer ligands have been used in several catalytic reactions, such as the Kharasch reaction[33], the coupling of nitriles with aldehydes[102] or polymerization and P-C bond forming reactions[103], and they have also been reported to promote C-H, C-C and C-O bond activation processes in solution[104].

---

[101] (a) **A**: van de Kuil, L. A.; Veldhuizen, Y. S. J.; Grove, D. M.; Zwikker, J. W.; Jenneskens, L. W.; Drenth, W.; Smeets, W. J. J.; Spek, A. L.; van Koten, G. *Recl. Trav. Chim. Pays-Bas* **1994**, *113*, 267. (b) **B**: Cámpora, J.; Palma, P.; del Río, D.; Conejo, M. M.; Álvarez, E *Organometallics* **2004**, *23*, 5653. (c) **C**: Ozerov, O. V.; Guo, C.; Fan, L.; Foxman, B. M. *Organometallics* **2004**, *23*, 5573.

[102] Fan, L.; Ozerov, O. V. *Chem. Commun.* **2005**, 4450.

[103] Clarke, M. L.; Guy, O. A.; Pringle, P. G.; Turley, E. *Dalton Trans.* **2003**, *23*, 4393.

[104] van der Boom, M. E.; Liou, S.-Y.; Shimon, L. J. W.; Ben-David, Y.; Milstein, D. *Inorg. Chim. Acta* **2004**, *357*, 4015.

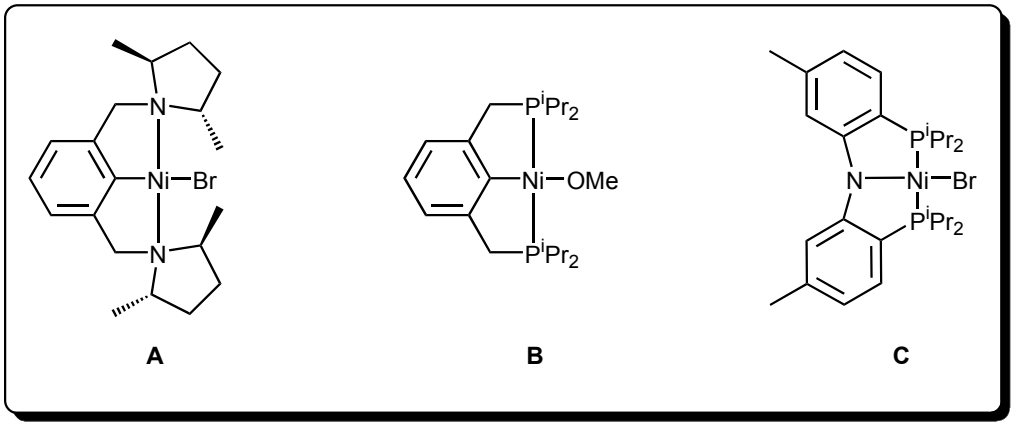

Figure 36. Some examples of nickel pincer complexes

Following the discovery by Brookhart and co-workers that nickel α-diimine complexes are able to catalyze the dimerization and oligomerization of ethylene[105], several nickel complexes containing bidentate PN ligands were also reported to catalyze this reaction. Most of the research in this area has been performed by the group of Braunstein et al.; this group has reported the preparation of several nickel PN complexes[106] (**A-C**, Figure 37), including chiral ones[107], with mediocre to excellent catalytic activities.

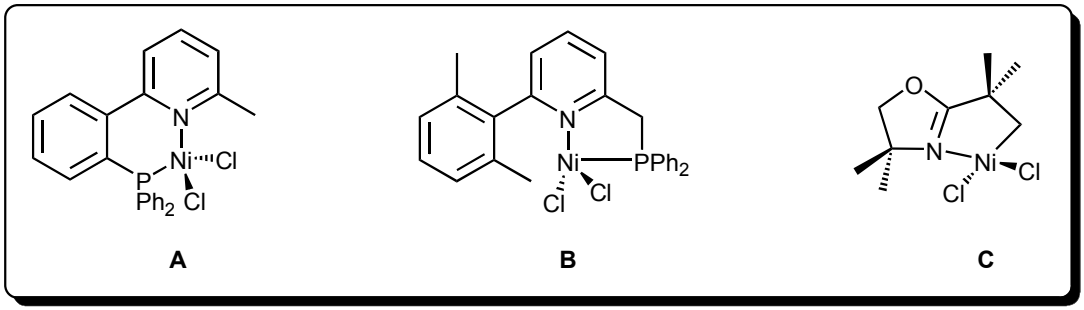

Figure 37. Some examples of nickel PN complexes

By far the biggest number of examples of pincer complexes are palladium ones[3]; they have been prepared by different metalation procedures with pincer ligands featuring a wide variety of backbones and donor groups, and several chiral palladium pincer complexes have

---

[105] (a) Ittel, S. D.; Johnsson, L.K.; Brookhart, M. *Chem. Rev.* **2000**, *100*, 1169 and references therein. (b) Johnsson, L. K.; Killian, C. M.; Brookhart, M. *J. Am. Chem. Soc.* **1995**, *117*, 6414.

[106] (a) For a review, see: Speiser, F.; Braunstein, P.; Saussine, L. *Acc. Chem. Res.* **2005**, *38*, 784 and references therein. (b) Speiser, F.; Braunstein, P.; Saussine, L. *Organometallics* **2004**, *23*, 2625. (c) Speiser, F.; Braunstein, P.; Saussine, L. *Organometallics* **2004**, *23*, 2633.

[107] Speiser, F.; Braunstein, P.; Saussine, L.; Welter, R. *Organometallics* **2004**, *23*, 2613.

also been reported (Figure 38[108]). For example, a new class of achiral[109a] and chiral[109b] palladium NCN pincer complexes has been prepared via a self assembly reaction pathway (Scheme 47). They are known to catalyze a big number of reactions, including C-C bond forming reactions (Suzuki[19], Heck[19,20] and Sonogashira[110] couplings), cyclopropanation reactions[111], aldol reactions[23] and Michael addition reactions[109b]. Additionally, they have also been reported to promote C-C, C-H and C-C bond activation processes[3a].

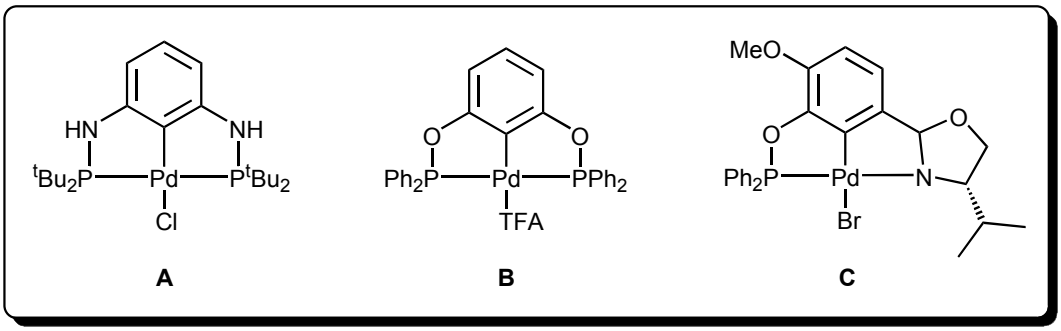

Figure 38. Some examples of palladium pincer complexes

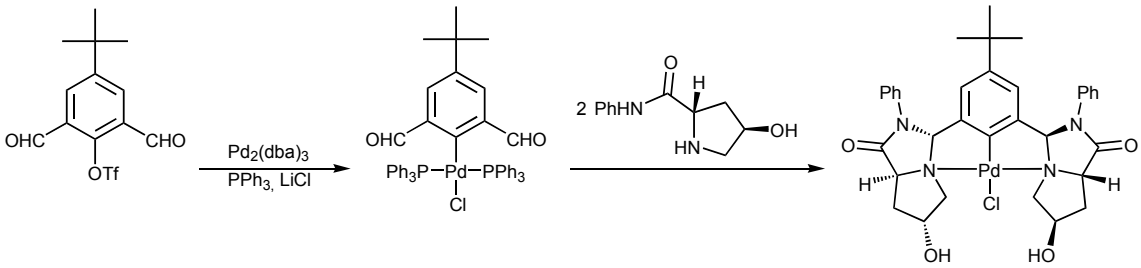

Scheme 47. Synthesis of a palladium pincer complex via a self-assembly reaction pathway

In contrast to nickel, there are not many examples of palladium complexes containing bidentate PN ligands[112]. However, when the pyridine ring of a PN ligand is substituted by a benzene ring, it is possible to obtain dimeric palladium complexes. These so-called

---

[108] (a) **A**: Benito-Garagorri, D.; Becker, E.; Wiedermann, J.; Lackner, W.; Pollak, M.; Mereiter, K.; Kisala, J.; Kirchner, K. *Organometallics* **2006**, *25*, 1900. (b) **B**: Solin, N.; Kjellgren, J.; Szabó, K. J. *J. Am. Chem. Soc.* **2004**, 126, 7026. (c) **C**: Motoyama, Y.; Shimozono, K.; Nishiyama, H. *Inorg. Chim. Acta* **2006**, 359, 1725.

[109] (a) Takenaka, K.; Minakawa, M.; Uozumi, Y. *J. Am. Chem. Soc.* **2005**, *127*, 12273. (b) Takenaka, K.; Uozumi, Y. *Org. Lett.* **2004**, *6*, 1833.

[110] Mas-Marza, E.; Segarra, A. M.; Claver, C.; Peris, E.; Fernández, E. *Tetrahedron Lett.* **2003**, *44*, 6595.

[111] Denmark, S. E.; Stavenger, R. A.; Faucher, A. M.; Edwards, J. P. *J. Org. Chem.* **1997**, *62*, 3375.

[112] See, for example: (a) Seidel, W.; Scholer, H. *Z. Chem.* **1967**, *11*, 441. (b) Aucott, S. M.; Slawin, A. M. Z.; Woolins, J. D. *J. Chem. Soc. Dalton Trans.* **2000**, 2559 and references therein. (c) Arena, C. G.; Drommi, D.; Faraone, F. *Tetrahedron: Asymmetry* **2000**, *11*, 4753.

palladacycles (Figure 39[113]) are extremely effective catalysts in several C-C and C-heteroatom bond forming reactions, and they are even capable of coupling relatively unreactive substrates, such as aryl chlorides[114].

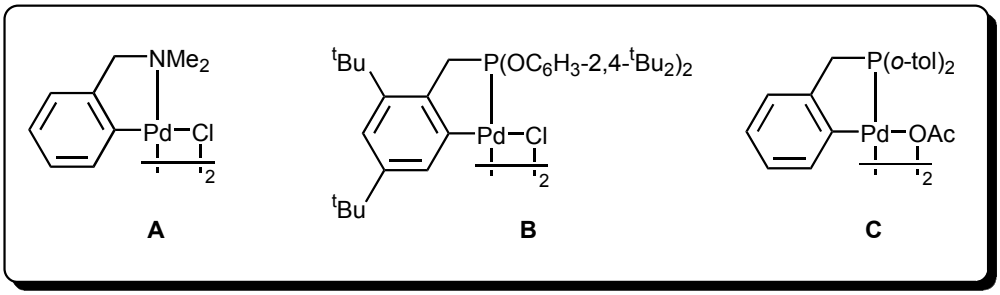

Figure 39. Palladacyclic palladium complexes

Platinum pincer complexes have also been prepared with different kinds of pincer ligands, both of the ENE and ECE type[3] (Figure 40[115]), and they have been employed in various catalytic processes (aldol[116] and polymerization reactions[117], intramolecular hydroamination of alkenes[118] and diene cycloisomerizations[119], for example). Platinum pincer complexes are also known to promote C-H, C-C and C-O bond activation processes[3a,120], and self assembled platinum pincer complexes structures have also been used in macromolecular chemistry as sensors in the crystalline phase[46b] or for the synthesis of dendrimers[121].

---

[113] (a) **A**: Albisson, D. A.; Bedford, R. B.; Scully, P. N. *Tetrahedron Lett.* **1998**, *39*, 9793. (b) **B**: Böhm, V. P. W.; Herrmann, W. A. *Chem. Eur. J.* **2000**, *6*, 1017. (c) **C**: Beller, M.; Fischer, H.; Herrmann, W. A.; Öfele, K.; Brossmer, C. *Angew. Chem. Int. Ed.* **1995**, *34*, 1844.

[114] For a review, see: Bedford, R. B.; Cazin, C. S. J.; Holder, D. *Coord. Chem. Rev.* **2004**, *248*, 2283 and references therein.

[115] (a) **A**: Grove, D. M.; van Koten, G.; Ubbels, G.; Henk, J. C.; Spek, A. L. *J. Am. Chem. Soc.* **1982**, *104*, 4285. (b) **B**: Hahn, C.; Morvillo, P.; Herdtweck, E.; Vitagliano, A. *Organometallics* **2002**, *21*, 1807. (c) **C**: Poverenov, E.; Gandelman, M.; Shimon, L. J. W.; Rozenberg, H.; Ben-David, Y.; Milstein, D. *Chem. Eur. J.* **2004**, *10*, 4673.

[116] Gorla, F.; Togni, A.; Venanzi, L. M.; Albinati, A.; Lianza, F. *Organometallics* **1994**, *13*, 1607.

[117] Cucciolito, M. E.; D'Amora, A.; Vitagliano, A. *Organometallics* **2005**, *24*, 3359.

[118] Michael, F. E.; Cochran, B. M. *J. Am. Chem. Soc.* **2006**, *128*, 4246.

[119] Kerber, W. D.; Koh, J. H.; Gagne, M. R. *Org. Lett.* **2004**, *6*, 3013.

[120] (a) Ortiz, J. V.; Havlas, Z.; Hoffmann, R. *Helv. Chim. Acta* **1984**, *67*, 1. (b) Grove, D. M.; van Koten, G.; Ubbels, H. J. C. *Organometallics* **1982**, *1*, 1366.

[121] (a) Davies, P. J.; Grove, D. M.; van Koten, G. *Organometallics* **1997**, *16*, 800. (b) Albrecht, M.; Gossage, R. A.; Spek, A. L.; van Koten, G. *Chem. Commun.* **1998**, 1003.

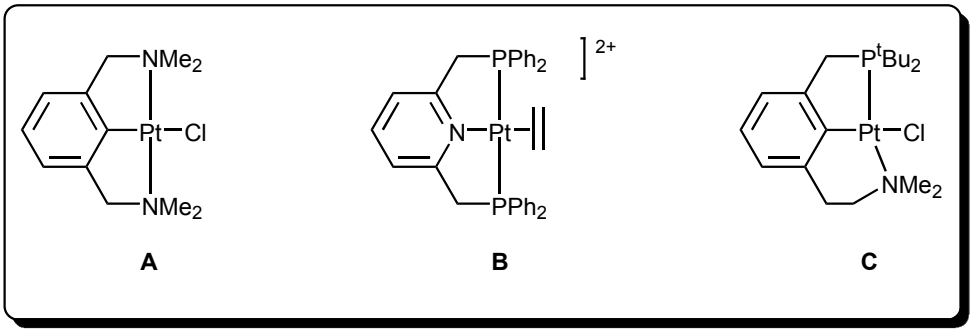

Figure 40. Some examples of platinum pincer complexes

3.3.2 Nickel Complexes

Tetracoordinated Nickel(II) PNP Complexes

Synthesis

The preparation of the complex [Ni(PNP-Ph)Cl]Cl was first described by Haupt and coworkers in 1987 by the reaction of $NiCl_2{\cdot}6H_20$ and PNP-Ph in a mixture of boiling ethanol and acetone[60]; however, a recrystallization step was required in order to obtain the pure product and the yield was moderate (54%). In the course of this work, the synthesis of cationic, tetracoordinated nickel(II) complexes with the aryl and alkyl PNP ligands **2a-c** could be improved by reacting equimolar amounts of NiX_2(DME) (X: Cl, Br) and the corresponding ligand in methylene chloride at room temperature for 16 hours (Scheme 48). Upon removal of the solvent under vacuum and washing with diethyl ether, the chloride and bromide complexes **17a-c** and **17a'-c'** were obtained as orange to orange-brown solids in good yields (72-94%). Both the chloride and bromide complexes are air stable in the solid state and in solution, and they can be stored for one year in the solid state without any signs of decomposition. Even in solvents that are known to cleave the aminophosphine bond of the free ligand, such as dimethyl sulfoxide or dimethyl formamide, no degradation of the compounds was observed. As for the differences between the chloride and bromide complexes, their reactivity and stability are identical, and there is no indication whatsoever pointing to any difference in their chemical behavior. The use of the 1,2-dimethoxyethane adducts as precursors was preferred to that of inorganic nickel(II) halide salts due to the lability of the DME group, which made it possible to perform the reaction at room temperature, and the choice of methylene chloride over ethanol as the solvent for the reaction is preferable to avoid the possible decomposition of the ligands due to solvolysis of the P-N bonds. In the course of the reaction, the three sites for the coordination of the PNP ligand are provided by the removal of the 1,2-dimethoxyethane group and one of the

halide atoms, which is detached from the nickel center and acts as the counterion in the nickel complexes.

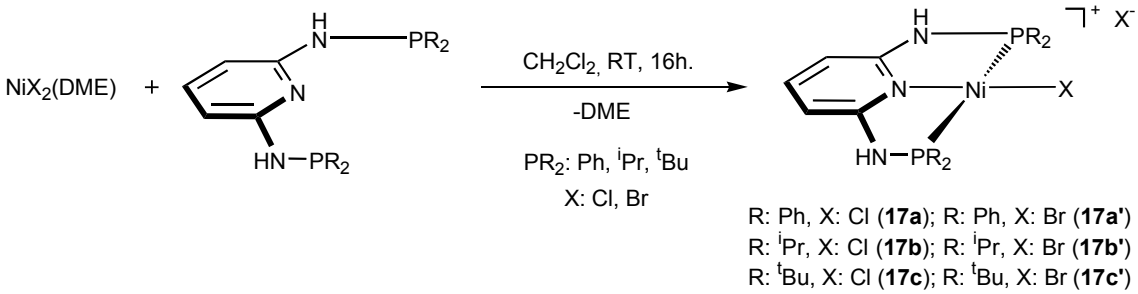

Scheme 48. Synthesis of nickel(II) phosphine PNP complexes **17a-c** and **17a'-c'**

Characterization

Nickel(II) compounds can display both diamagnetic or paramagnetic NMR behavior; all the nickel PNP complexes are diamagnetic (indicating a square planar geometry of the complexes in solution) and were characterized by ^{1}H, ^{31}P{^{1}H} and ^{13}C{^{1}H} NMR spectroscopy. Due to the limited solubility of the complexes in other deuterated solvents, the NMR were recorded in CD_3OD. Some characteristic ^{1}H and ^{31}P{^{1}H} NMR resonances are given in Table 15.

Table 15. Selected ^{1}H and ^{31}P{^{1}H} NMR resonances for the nickel(II) PNP complexes **17a-c** and **17a'-c'**.

Complex	^{1}H (δ, [ppm], 20ºC)			^{31}P{^{1}H} (δ, [ppm], 20ºC)
	py^{4} (1H)	py^{3,5} (2H)	N*H* (2H)	
17a	7.17-7.11[a]	6.00	3.18	60.7
17a'	7.89-7.48[a]	6.41	3.30	66.1
17b	7.51	6.26	3.30	97.8
17b'	7.54	6.32	3.30	100.6
17c	7.14	6.01	3.15	99.8
17c'	7.51	6.36	3.30	103.7

[a]Signal overlaps with other aromatic signals.

In the ^{1}H NMR spectra, the signals of the pyridine ring appear between 7.89 and 7.11 ppm (triplet, $^{3}J_{HH}$ = 8.0 Hz, py^{4}) and between 6.00 and 6.41 ppm (doublet, $^{3}J_{HH}$ = 8.0 Hz, py^{3,5}),

which is in the same range as the signals of the ligands **2a-c**. The signals of the N*H* protons, however, are shifted to the high field when compared to those in the free ligands (4.29-5.39 ppm), and give rise to broad singulets between 3.15 and 3.30 ppm. The $^{13}C\{^{1}H\}$ NMR spectra bear no unusual features, with the signals in the expected ranges. As for the $^{31}P\{^{1}H\}$ NMR spectra, they show only one sharp resonance, indicating that both aminophosphine "arms" of the ligand are equivalent and bound to the nickel center. The signals of the complexes are shifted towards the low field, which is consistent with a deshielding of the phosphorus atom due to coordination, and appear at 60.7 ppm (**17a**) and 66.1 ppm (**17a'**) and between 97.8 and 103.7 ppm (**17b-c** and **17b'-c'**).

Additionally, the structures of [Ni(PNP-Ph)Br]Br (**17a'**) and [Ni(PNP^{t}Bu)Br]Br (**17c'**) were determined by X-ray crystallography. Structural views of **17a'** and **17c'** are shown in Figures 41 and 42, along with selected bond lengths and angles. Crystals of both compounds were obtained by slow diffusion of diethyl ether into a saturated methanol solution of the corresponding complex.

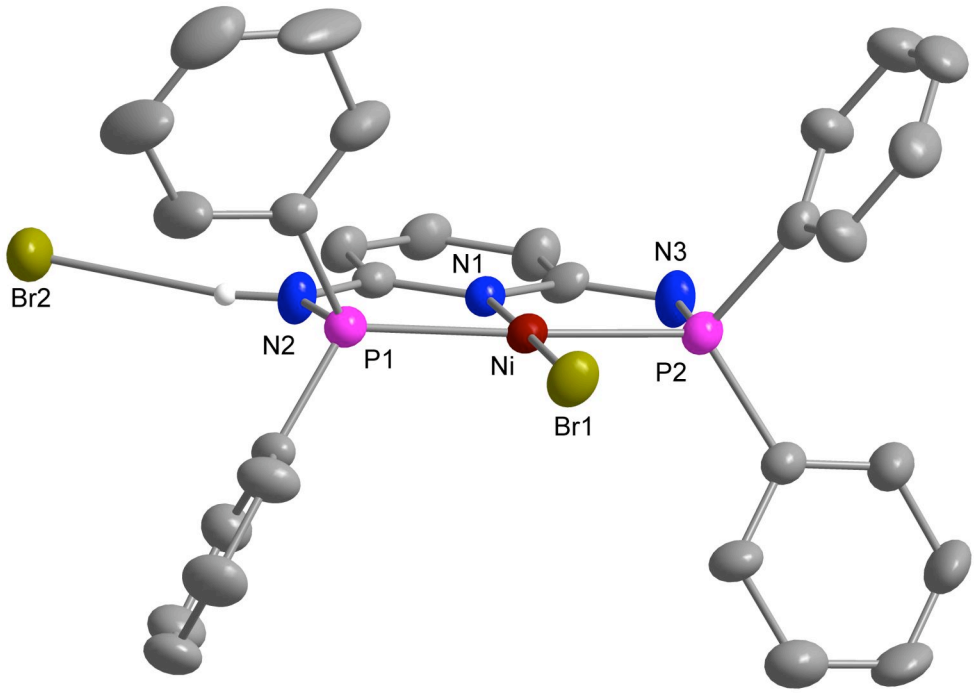

Figure 41. Structural view of [Ni(PNP-Ph)Br]Br (**17a'**) showing 30% thermal ellipsoids (Hydrogen atoms omitted for clarity). Selected bond lengths (Å) and angles (º): Ni-P(1) 2.1796(13), Ni-P(2) 2.1872(13), Ni-N(1) 1.884(3), Ni-Br(1) 2.2827(7), P(1)-N(2) 1.678(4), P(2)-N(3) 1.687(4), P(1)-Ni-P(2) 171.71(5), N(1)-Ni-Br(1) 178.54(11).

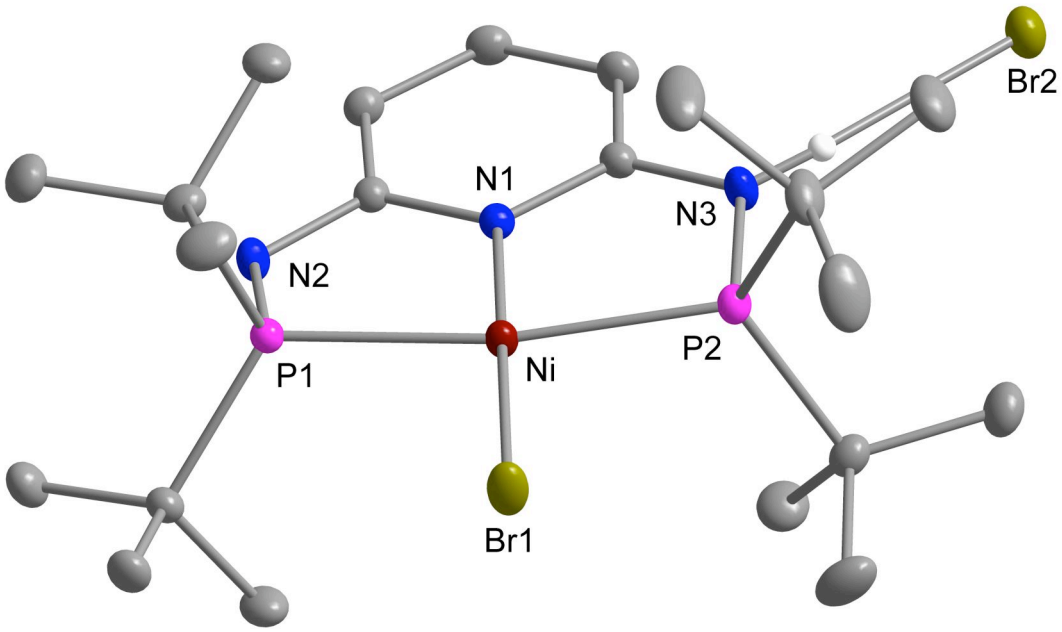

Figure 42. Structural view of [Ni(PNP-^{t}Bu)Br]Br (**17c'**) showing 50% thermal ellipsoids (Hydrogen atoms omitted for clarity). Selected bond lengths (Å) and angles (º): Ni-P(1) 2.2067(4), Ni-P(2) 2.2062(4), Ni-N(1) 1.894(1), Ni-Br(1) 2.2987(2), P(1)-N(2) 1.6930(11), P(2)-N(3) 1.6943(12), P(1)-Ni-P(2) 169.73(2), N(1)-Ni-Br(1) 177.98(3).

The bromide counterion in both complexes is located between the central pyridine ring and the phosphines, forming strong hydrogen bonds with the amino hydrogen atoms. In both compounds, the nickel(II) center adopts a distorted square-planar geometry defined by the two phosporus atoms, the pyridine nitrogen atom from the PNP ligand and the coordinated bromine atom. The Ni-P bond lengths are Ni-P(1) 2.1976(13) and Ni-P(2) 2.1872 Å for **17a'** and Ni-P(1) 2.2067(4) and Ni-P(2) 2.2062 Å for **17c'**. These bond lengths are consistent with a trans P-Ni-P arrangement, determined by the meridional coordination mode of the PNP ligands. The Ni-Br distance is similar in both complexes, 2.2827(7) Å in **17a'** and 2.2987(2) Å in **17c'**. For comparison, the complex [Ni(PNP-Ph)Cl]Cl, described by Haupt and co-workers[60], shows a Ni-Cl distance of 2.133(3) Å (Δd = 0.150 Å), which may in part be attributed to the smaller size of chlorine. The phenyl and ^{tert}butyl phosphine substituents are oriented into different sides of the plane defined by the two phosphorus atoms, the pyridine nitrogen atom and the nickel center and, in the case of **17a'**, the phenyl rings are almost perpendicular to each other. The distortion

of the square-planar geometry in the two complexes, attributed to packing effects, can be seen more clearly in Figure 43, showing a structural view of **17c'** without the phosphine substituents.

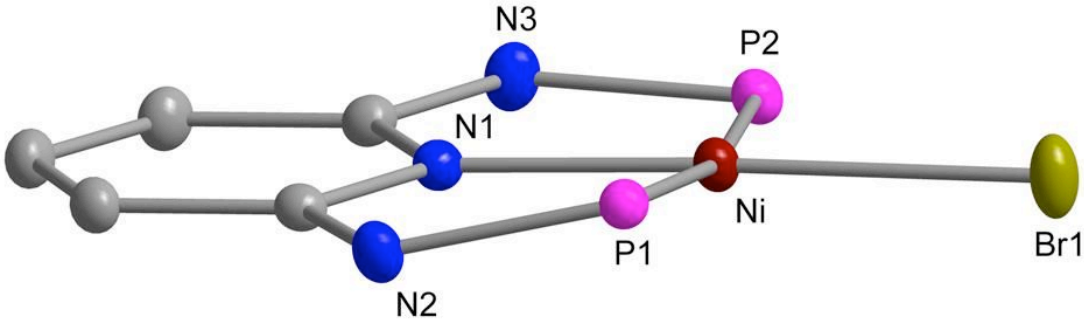

Figure 43. Structural view (50% thermal ellipsoids) of the distorted square-planar arrangement around the nickel center in [Ni(PNP-^{t}Bu)Br]Br (**17c'**).

The N(1)-Ni-Br(1) angles are close to 180º in both complexes, 178.54(11)º for **17a'** and 177.98(3)º in the case of **17c'**, while the P(1)-Ni-P(2) angles show a significant deviation from the planarity with values of 171.71(5) in **17a'** and 169.73(2) in **17c'**. This is most evident in the case of **17c'**, in which P(1) deviates from the meridional main plane by about 0.3 Å.

Pentacoordinated Nickel(II) PNP Complexes

Synthesis

When the phosphoramidite PNP ligand BIPOL-PNP (**2e**) was treated with equimolar amounts of $NiBr_2$(DME) under the same reaction conditions as those for the alkyl and aryl complexes **17a'-c'**, there was no evidence for the formation of the cationic, tetracoordinated square-planar complex [Ni(PNP-BIPOL)Br]Br. Instead, unreacted nickel precursor remained in the reaction vessel and an orange solution was obtained. Upon workup (filtration, evaporation of the solvent, washing with diethyl ether and drying under vacuum), the orange solid was identified as the neutral pentacoordinated complex [Ni(PNP-BIPOL){κ1(P)-R_2P=O}Br] (PR_2: BIPOL) **18a** in 35% yield, in which a PNP ligand, a bromine atom and an anionic phosphinite ligand BIPOL-P=O$^-$ are coordinated to the nickel(II) center (Scheme 49).

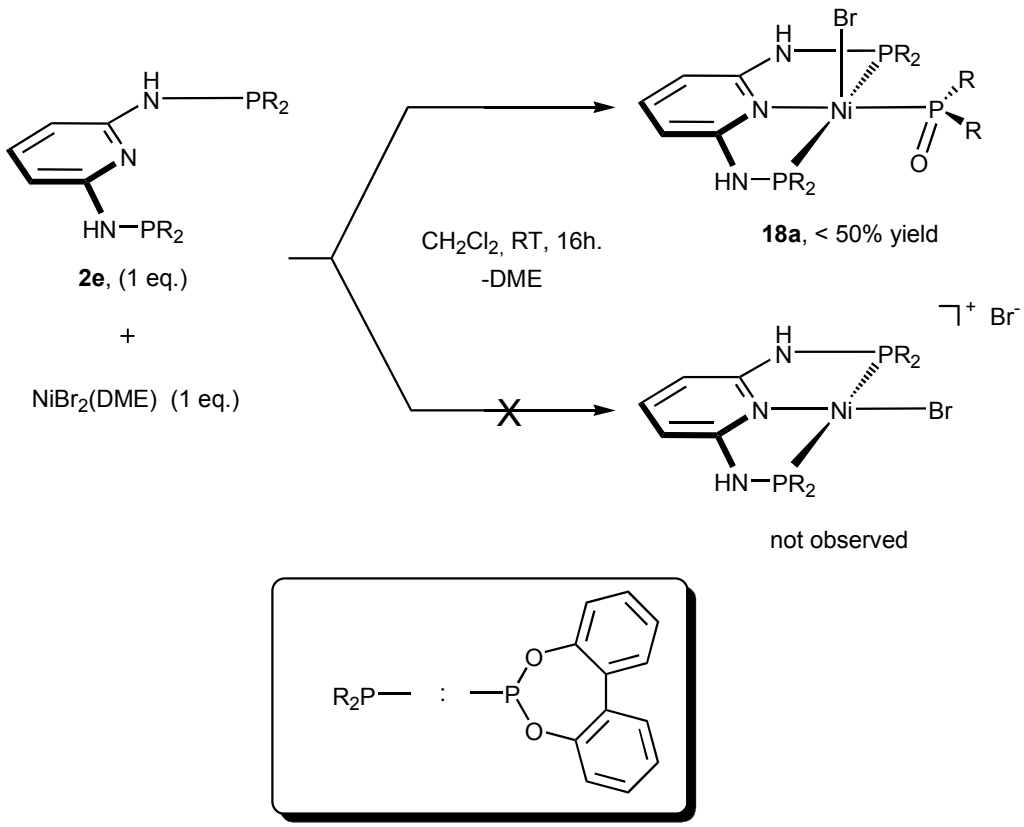

Scheme 49. Formation of the pentacoordinated neutral nickel(II) PNP complex [Ni(PNP-BIPOL){κ1(P)-R_2P=O}Br] (**18a**) instead of the expected tetracoordinated cationic complex [Ni(PNP-BIPOL)Br]Br

The low yield of this reaction must be attributed to the use of equimolar amounts of nickel precursor and ligand; in order to form the anionic phosphinite ligand, at least one of the P-N bonds of one PNP ligand has to be cleaved, leaving less intact ligand to react with the nickel precursor. Thus, an excess of ligand **2e** was used: it was found that, when 1.5 equivalents ligand were used per equivalent nickel precursor, the yield could be improved up to 89%. When more than 1.5 equivalents of **2e** were used, unreacted ligand was detected in the reaction mixture. Other metal precursors, such as anhydrous $NiBr_2$, are insoluble in methylene chloride and did not improve the reaction rate. However, when the reaction was performed with $NiBr_2$ in the presence of one equivalent of DMSO or DMF, the insoluble nickel salt dissolved immediately and the colour of the solution changed from colorless to bright orange, indicating the formation of **18a**. DMSO (or DMF) did not participate in the reaction as oxygen-transfer reagent (see mechanism in Scheme 52) but merely increased the solubility of the nickel salt. Under these conditions, the reaction time could be reduced to only one hour.

Although the synthesis of square planar nickel(II) PNP complexes with phosphoramidite PNP ligands failed and seems to be limited to the alkyl and aryl substituted phosphine ligands

2a-c, which lack P-O bonds, the selective decomposition of a P-N bond to give a κ^1-(P)-coordinated phosphinite ligand could be used to prepare several pentacoordinated nickel(II) complexes featuring both achiral and chiral PNP ligands (Scheme 50). Experimentally, one equiv. DMSO was added to a mixture of one equiv. $NiBr_2$ and 1.5 equiv. ligand in CH_2Cl_2, whereupon the colour of the solution immediately changed to bright orange. After stirring for one hour at room temperature, the solvent was removed under vacuum and the remaining orange oils were precipitated and washed several times with diethyl ether.

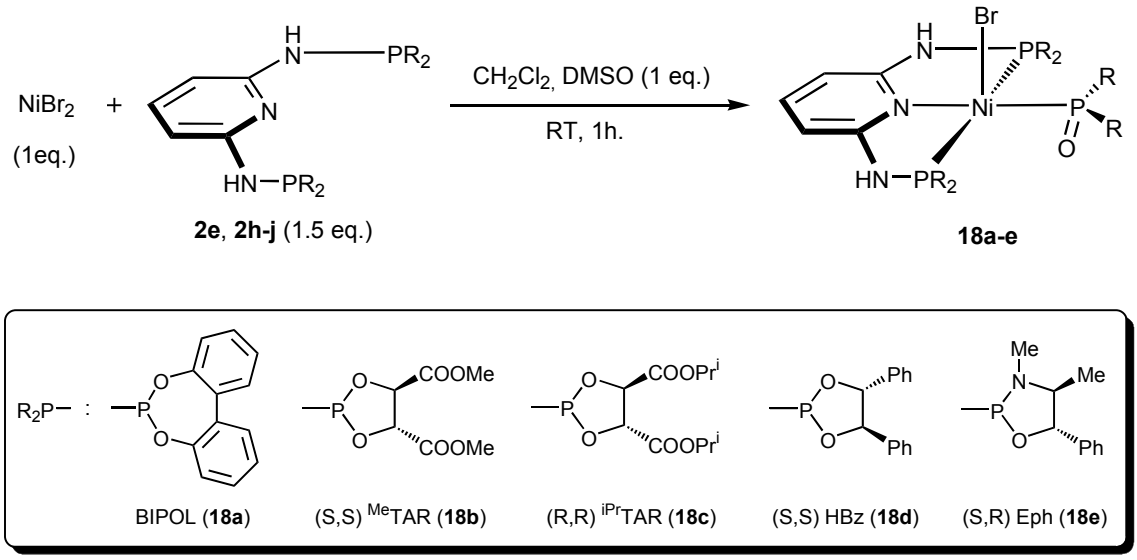

Scheme 50. Synthesis of the neutral pentacoordinated nickel(II) PNP complexes **18a-e**

Characterization

The complexes **18a-e** were obtained as orange, air stable solids in moderate to good yields (55-89%), and were characterized by ^{1}H, ^{31}P{^{1}H} and ^{13}C{^{1}H} NMR spectroscopy; some characteristic ^{1}H and ^{31}P{^{1}H} resonances are given in Tables 16 and 17.

Table 16. Selected ^{1}H NMR resonances for the pentacoordinated PNP complexes **18a-e**.

Complex	^{1}H (δ, [ppm], 20ºC)				
	py^4 (1H)	py^{3,5} (2H)	$^3J_{HH}$ [Hz]	N*H* (2H)	$^2J_{HP}$ [Hz]
18a	6.70	6.36	7.3	5.80	8.0
18b	7.44	6.40	8.0	5.83	8.3
18c	7.42	6.41	7.8	5.81	8.2
18d	7.29-7.00[a]	7.29-7.00[a]	n.d.	5.70	8.0
18e	7.40-7.02[a]	7.40-7.02[a]	n.d.	5.60	[b]

[a]Signal overlaps with other aromatic signals. [b]Broad singulet, no coupling constant detected.

Table 17. $^{31}P\{^1H\}$ NMR resonances for the pentacoordinated PNP complexes **18a-e**.

Complex	$^{31}P\{^1H\}$ (δ, [ppm], 20ºC)		
	PNP (d)	κ^1-R_2P=O (t)	$^2J_{PP}$ [Hz]
18a	147.7	86.6	98.6
18b	146.2	85.3	104.2
18c	146.1	85.5	100.8
18d	143.4	87.8	107.2
18e	116.8	74.5	114.1

The ^1H NMR spectra show signals that are very similar to those of the free ligands, with a slight downfield shift of the signals of the pyridine ring. The py^4 signals appear as triplets between 7.40 and 6.70 ppm while the py^{3,5} protons show doublets between 7.02 and 6.41 ppm. The coupling constants $^3J_{HH}$ lie between 7.3 and 8.0 Hz. In the case of the N*H* protons, their signals appear as doublets in the range between 5.60 and 5.83 ppm with coupling constants $^2J_{HP}$ between 8.0 and 8.3 Hz and are either not shifted or display a small shift to the high field compared to the signals of the free ligands. Only when 2,2'-biphenyl was the substituent at the phosphines was a shift to the low field observed (free ligand: 4.32 ppm, **18a**: 5.80 ppm). The $^{13}C\{^1H\}$ NMR spectra show no special features; the signals of the complexes are shifted only slightly to the low field.

Most diagnostic, however, are the $^{31}P\{^1H\}$ NMR spectra of the complexes: they show an A_2X pattern with a doublet in the range between 116.8 and 147.7 ppm, assignable to the intact PNP ligand, and a triplet in the range between 74.5 and 87.8 ppm, assignable to the κ^1-(P)-coordinated phosphinite ligand $R_2P{=}O^-$. The $^2J_{PP}$ coupling constants range from 98.6 to 114.1 Hz.

Furthermore, crystals suitable for X-ray crystallography were obtained from **18d** by slow diffusion of diethyl ether into a concentrated solution of **18d** in methanol; the exact ligand arrangement around the metal center could thus be determined. A crystal structure of **18d** is given in Figure 44 along with selected bond lengths and angles.

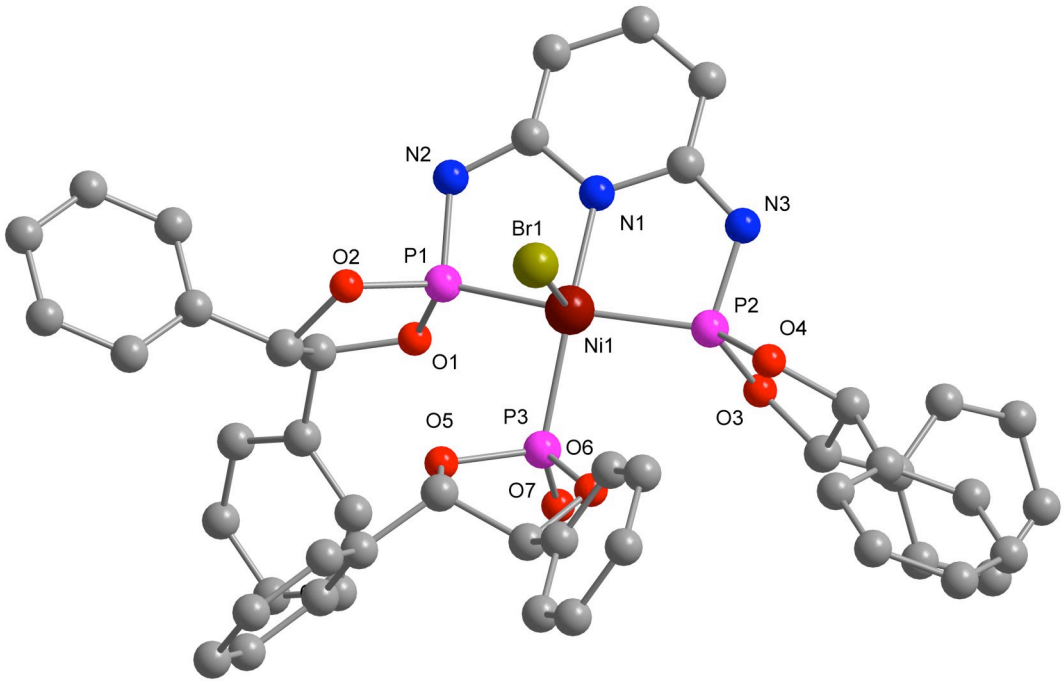

Figure 44. Structural view of [Ni(PNP-HBz){k1(P)-HBBz-P=O}Br] (**18d**) (second independent nickel complex, hydrogen atoms and crystallization solvent omitted for clarity). Selected bond lengths (Å) and angles (º): Ni(1)-N(1) 1.913(8), Ni(1)-P(1) 2.144(3), Ni(1)-P(2) 2.114(3), Ni(1)-P(3) 2.132(6), Ni(1)-Br(1) 2.535(4), P(1)-N(2) 1.630(10), P(2)-N(3) 1.630 (10), N(1)-Ni(1)-P(3) 163.6(4), Br(1)-Ni(1)-N(1) 97.1(4), Br(1)-Ni(1)-P(1) 98.7(2), Br(1)-Ni(1)-P(2) 101.8(2), Br(1)-Ni(1)-P(3) 99.2(2).

The nickel center exhibits a square-pyramidal coordination geometry with the bromine in the apical position. The PNP ligand is coordinated in the typical meridional κ^3-(P,N,P) fashion, and the hydrobenzoine-phosphinite ligand clearly coordinates to the nickel atom through the lone pair at the phosphorus atom rather than through the oxygen lone pairs. The Ni-P distances are similar for the three phosphorus atoms (Ni(1)-P(1) 2.144(3), Ni(1)-P(2) 2.114(3) and Ni(1)-P(3) 2.132(6) Å) and their values are close to those observed in the related tetracoordinated, square planar complexes. The square-pyramidal geometry of the complex, with the nickel atom located above the plane defined by the pyridine nitrogen atom and the three phosphorus atoms, is depicted in Figure 45.

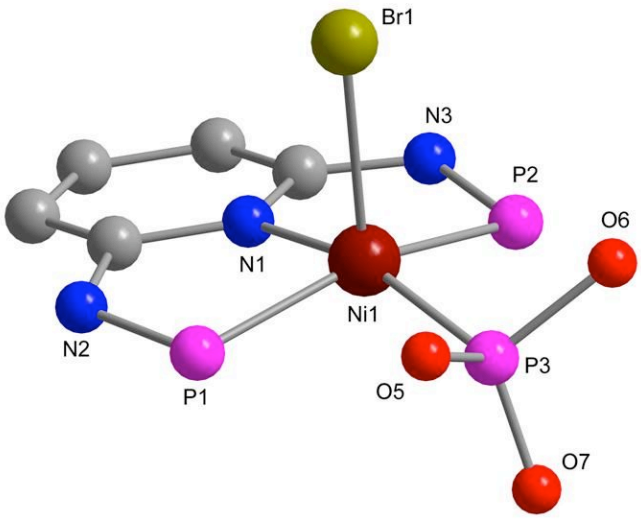

Figure 45. Structural view of **18d** showing the coordination geometry around the nickel center.

Noticeably, nickel pentacoordination is rare in organometallic chemistry and only about 9% of all complexes adopt this coordination number of which about half belong to the trigonal-bipyramidal and the rest to the square-pyramidal type (Cambridge Structural Database, CSD, version 5.27, release 2006). Only one compound was found in this database with a square-pyramidal Ni(PNP)(P)Br coordination (**A**, Figure 46); however, the bromine atom is located in the basal and the nitrogen atom in the apical position[122]. Another example with a coordination related to that of **18d** is dibromo{bis[2-(diphenyl-phosphanyl)ethyl]amine}nickel(II)[123] (**B**), with a basal Ni-Br bond of 2.33 Å and an apical Ni-Br bond of 2.70 Å. For comparison, the basal Ni(1)-P(3) bond length in **18d** has a value of 2.132(6) Å and the apical Ni(1)-Br(1) bond measures 2.54 Å on average for the two independent complexes.

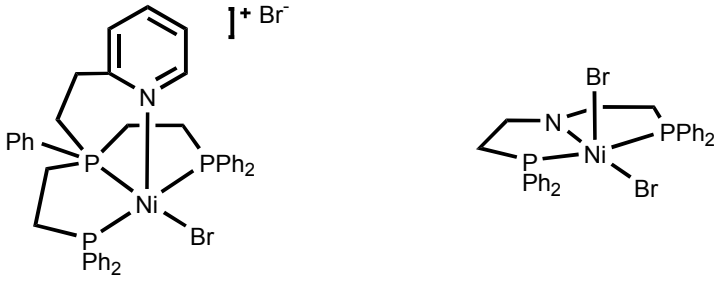

A **B**

Figure 46. Two examples of pentacoordinated nickel(II) complexes

[122] Hessler, A.; Ficher, J.; Kucken, S.; Stelzer, O. *Chem. Ber.* **1994**, *127*, 481.

[123] Orioli, P. L.; Ghilardi, C. A. *J. Chem. Soc. A* **1970**, 1511.

Mechanistic Investigations

In order to achieve some insight into the mechanism of the formation of the neutral pentacoordinated nickel(II) complexes **18a-e**, the reaction between $NiBr_2$(DME) and PNP-BIPOL (**2e**) was monitored via ^{1}H and ^{31}P{^{1}H} NMR spectroscopy with varying amounts of the ligand (ranging from 0.8 to 4.0 equivalents) in CD_2Cl_2. Spectra were measured regularly every hour and, in the hope to be able to detect some reaction intermediates, no DMSO or DMF was added to the NMR tubes so that the reaction would proceed more slowly. Surprisingly, in all cases there was no evidence for the formation of any phosphorus-containing species as a result of ligand decomposition. In fact, when $NiBr_2$(DME) was treated with 0.8 equivalents of PNP-BIPOL (**2e**), complex **18a** was formed cleanly after 16 hours but the conversion was not quantitative and substantial amounts of the unreacted nickel precursor remained in the NMR tube. If $NiBr_2$(DME) was reacted with 1.5 equivalents of **2e**, complete consumption of both ligand and metal precursor took place, while with an excess of ligand (>1.5 equivalents), $NiBr_2$(DME) was completely consumed to afford **18a** but unreacted PNP ligand was still present in solution. Moreover, the formation of an intermediate species could be detected in the ^{31}P{^{1}H} NMR spectrum in all cases regardless of the metal precursor:ligand ratio used. This intermediate species exibits, like the final complex, an A_2X pattern with a doublet centered at 145.7 ppm and a triplet centered at 122.4 ppm ($^2J_{PP}$ = 109.8 Hz). The formation of this intermediate is relatively fast; it could be first detected within five hours after the reaction was started and isomerized slowly but quantitatively at room temperature within sixteen hours to afford the final product **18a**, which shows a doublet centered at 145.8 ppm and a triplet centered at 95.4 ppm ($^2J_{PP}$ = 104.2 Hz). The pattern in the ^{31}P{^{1}H} NMR spectrum is consistent with a square-pyramidal pentacoordinated species (**A**, Scheme 51) in which, in contrast to the final product **18a** (**B**), the phosphinite ligand is coordinated to the nickel(II) center in the apical position with the bromine atom located in a basal position. The ^{31}P{^{1}H} NMR spectra of a mixture of **A** and **B** as well as that of the final product **B** are shown in Figure 47.

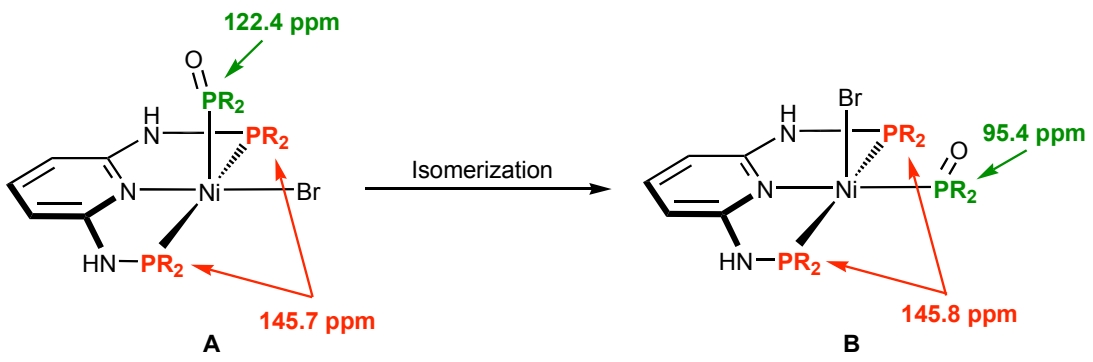

Scheme 51. Phosphite-bromine isomerization in the pentacoordinated nickel(II) PNP complexes **18a-e**. The ^{31}P{^{1}H} NMR shifts are those of **18a**.

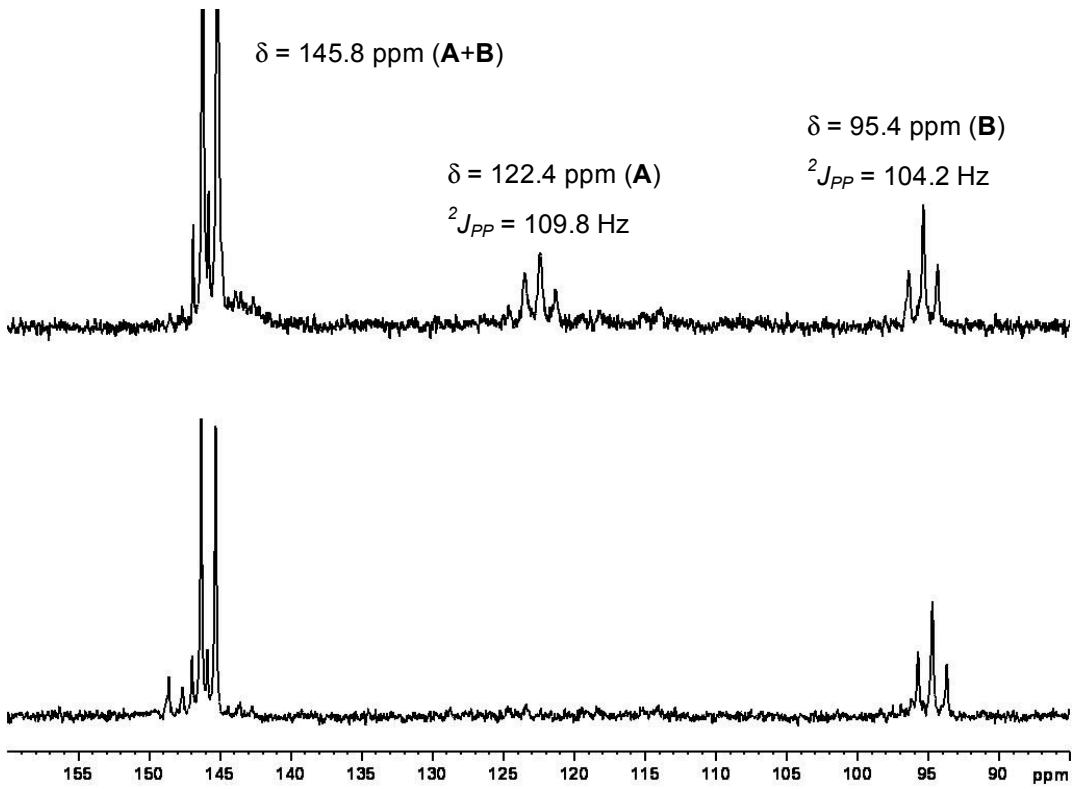

Figure 47. $^{31}P\{^{1}H\}$ spectra of the the reaction between PNP-BIPOL (**2e**) and $NiBr_2$ (a) reaction time: two hours and (b) reaction time: sixteen hours, indicating the formation of the isomer **A** which transforms into isomer **B**.

Another important piece of information about the mechanism was provided by a white solid that formed in all the NMR experiments: upon filtration and dissolution in CD_3CN, this compound was inequivocally identified as 2,6-diaminopyridinium bromide. Its ^{1}H NMR spectrum[124] is in agreement with literature data for this compound[125] as well as with data from an authentic sample prepared in our laboratory by reacting one equivalent of 2,6-diaminopyridine with 1.2 equivalents of trifluoroacetic acid. The protonation occurs preferentially at the pyridine nitrogen atom, according to the pK_a data (2.16 and 2.90 for the NH_2 protonation and 7.22 for the protonation at the pyridine nitrogen atom[126]).

Finally, although the synthesis of cationic tetracoordinated nickel(II) complexes with phosphoramidite PNP ligands failed, it is possible to prepare such compounds with other metals of the same group, such as palladium(II) and platinum(II). The complex [Pd(PNP-BIPOL)Cl]Cl,

---

[124] ^{1}H NMR (δ, CD_3CN, 20°C): 13.4(bs, 1H, N*H*), 7.46 (t, $^{3}J_{HH}$ = 7.5 Hz, 1H, py^{4}), 7.20 (bs, 4H, NH_2), 5.92 (d, $^{3}J_{HH}$ = 7.5 Hz, 2H, $py^{3,5}$).

[125] Liu, S.-H.; Chen, J.-D.; Liou, L.-S.; Wang, J.-C. *Inorg. Chem.* **2001**, *40*, 6499.

[126] Moghimi, A.; Alizadeh, R.; Shokrollahi, A.; Aghabozorg, H.; Shamsipur, M.; Shockravi, A. *Inorg. Chem.* **2003**, *42*, 1616.

prepared by reacting equimolar amounts of $Pd(COD)Cl_2$ and BIPOL-PNP (See section 3.3.3 below), is a perfectly air stable yellow solid. However, due to its lower solubility in common organic solvents, several attempts were made to obtain crystals suitable for X-ray crystallography by slow solvent evaporation of a concentrated DMF solution of the complex under air at room temperature for up to 10 days. In all cases, small amounts of pale-yellow crystals were obtained, which were identified as the square planar palladium chloride complex [Pd{κ^2(P,N)-NH_2-PN-BIPOL}{κ^1(P)-BIPOL-P=O}Cl] (**24**)[127]. If the cleavage of one aminophosphine bond in the case of palladium(II) phosphoramidite PNP complexes can take place, it would be logical to think that such a process might also be involved at a much faster rate in the formation of the complexes **18a-e** (**B**, Figure 48).

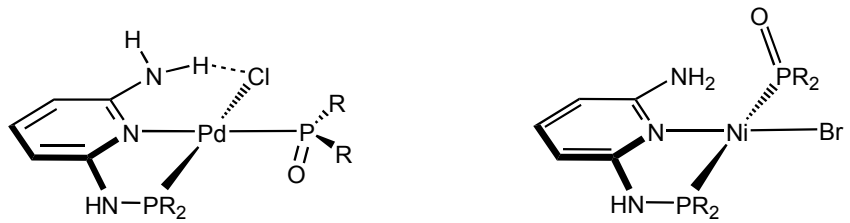

24, hydrolysis product of [Pd(PNP-BIPOL)Cl]Cl DMF, RT, 10 d.

B, possible intermediate in the formation of **18a-e**?

Figure 48. P-N bond cleavage in phosphoramidite palladium (left) and nickel (right) PNP complexes

A proposed plausible mechanism for the formation of the neutral pentacoordinated nickel(II) complexes **18a-e**, supported by the observed stoichiometry and by the findings described above is depicted in Scheme 52.

[127] A structural view of the complex as well as selected bond lengths and angles is shown in Figure 56. See Section 3.3.3 for more information about the chemistry of palladium with pincer complexes.

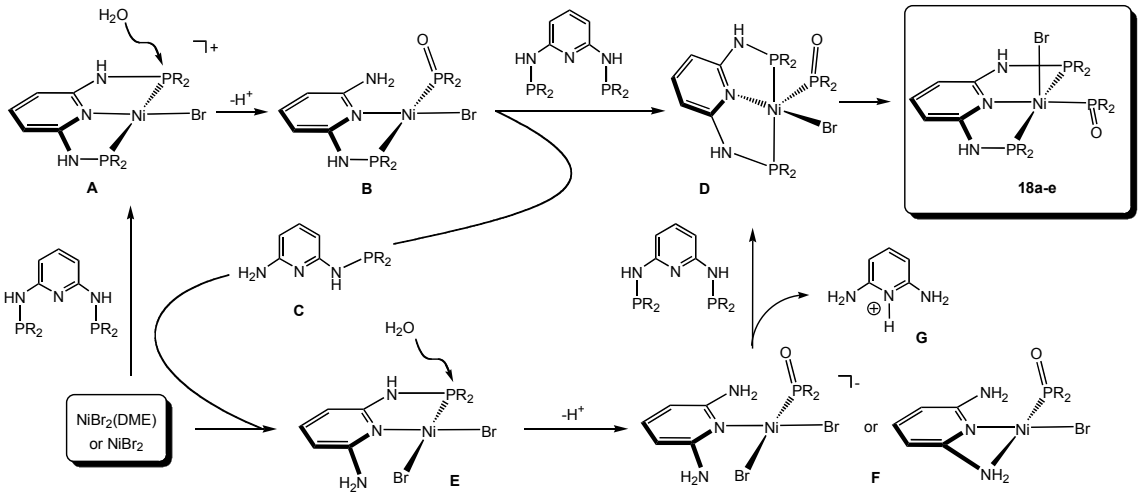

Scheme 52. Proposed mechanism for the formation of the pentacoordinated nickel(II) PNP complexes **18a-e**

The reaction may be initiated by the formation of the cationic square-planar $[Ni(PNP)Br]^+$ complex **A**. The nucleophilic attack of water at one of the two electrophilic phosphorus atoms of the coordinated PNP ligand would lead to a P-N bond cleavage, affording **B**, which has a similar structure as that observed for the palladium complex **24**. This compound would react readily with a free PNP molecule to give **D**, which isomerizes to the final complex. Thereby the monophosphorilated 2,6-diaminopyridine ligand **C** would be released and could in turn react with $NiBr_2$(DME) to give complex **E**, adopting either a square-planar or a tetrahedral geometry. The latter would react again with water to give **F**. The 2,6-diaminopyridine ligand would then be replaced by a free tridentate PNP ligand to yield **D** with concomitant release of 2,6-diaminopyridine in the form of its pyridinium cation **G**. Although this mechanism is tentative, it is supported by the direct observation of the intermediates **D** and **G** as well as by the identification of a tetracoordinated palladium(II) complex (**24**) with structural features very similar to those of **B**.

In theory, another possible mechanism for the formation of the complexes **18a-e** consistent with the observed stoichiometry and with the experimental results is depicted in Scheme 53. Two molecules of the square-planar complex **A** could form a dimeric species **B** bridged by an intact PNP ligand; complex **B** would also show a doublet and a triplet in the $^{31}P\{^1H\}$ NMR spectrum. The nucleophilic attack of water at the electrophilic phosphorus atoms would lead to the formation of the complexes **18a-e** with concomitant release of the 2,6-diaminopyridinium cation. At this moment, there is not enough experimental data to support either one of the two mechanisms.

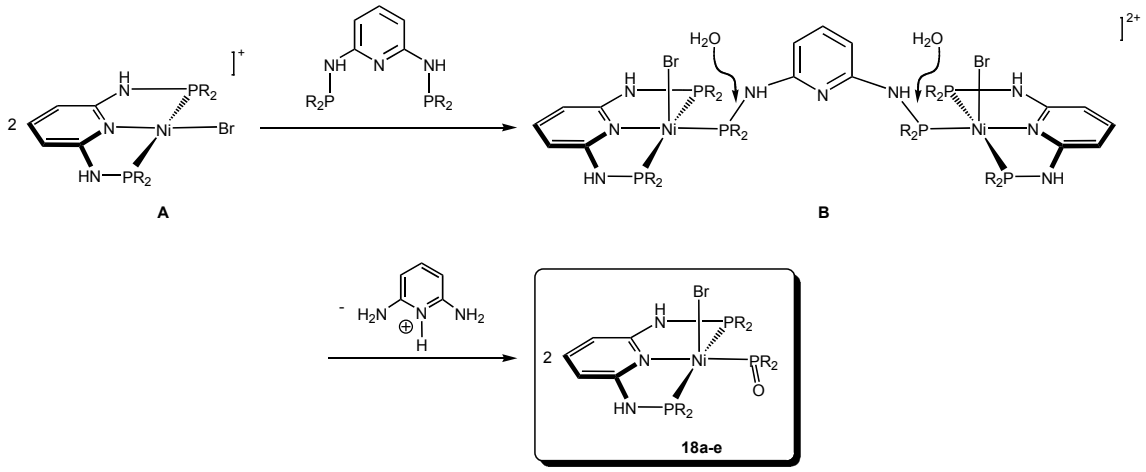

Scheme 53. Alternative mechanism for the formation of the pentacoordinated nickel(II) PNP complexes **18a-e**

Over the course of the reaction, both phosphoramidite P-N bonds of one PNP ligand are selectively cleaved to afford two molecules of an anionic phosphinite ligand $R_2P{=}O^-$. There are only a few mononuclear complexes with a single $R_2P{=}O^-$ ligand reported in the literature, including [RuCp{=C(CH_2Ph)-NHPh}(PPh_2NHPh){κ^1(P)-$Ph_2P{=}O$}][128], [Pt(PPh_3)(Ph)-(NC-9-anthracenyl){κ^1(P)-$Ph_2P{=}O$}][129] and $HNEt_3$-[$W(CO)_5$){κ^1(P)-$Ph_2P{=}O$}][130]. However, all these complexes contain the anionic diphenylphosphinito ligand $Ph_2P{=}O^-$, and none of them has nickel as its metal center. Furthermore, in these cases, the diphenylphosphinito ligand is found in conjunction with the corresponding phosphinous acid PPh_2OH to form Ph_2P-O-H···O=PPh_2 moieties with very strong and almost symmetric hydrogen bonds. In the case of the phosphinite ligand containing complexes **18a-e**, no indication could be obtained for the formation of the related phosphinous acids. The stability of the phosphoramidite PNP ligands **2e** and **2g-j** was also investigated; these ligands are perfectly stable in CH_2Cl_2 and only decompose slowly in DMSO or DMF. In the case of PNP-BIPOL (**2e**), about 50% decomposition was observed at room temperature after sixteen hours leading to the formation of several intractable materials giving rise to signals in the range between 6.0 and 20.0 ppm in the $^{31}P\{^1H\}$ NMR spectrum. That the decomposition of **2e** proceeds slowly in neat DMSO suggests that traces of water and not DMSO are responsible for the cleavage of the phosphoramidite P-N bond, especially when considering that DMSO is present only stoichiometrically in the reaction mixture. For comparison, BIPOL-P(OH)=O, a possible decomposition product, gives rise to a signal at 5.71

---

[128] Pavlik, S.; Mereiter, K.; Puchberger, M.; Kirchner, K. *Organometallics* **2005**, *24*, 3561.

[129] Beck, W.; Keubler, M.; Leidl. E.; Nagel, U.; Schaal, M.; Cenini, S.; del Butttero, P.; Licandro, E.; Maiorana, S.; Villa, A. C. *J. Chem. Soc., Chem. Commun.* **1981**, 446.

[130] Zeiher, C.; Hilller, W.; Lorenz, I.-P. *Chem. Ber.* **1985**, *118*, 3127.

ppm[131]. Finally, it has to be noted that the sensitivity of a P^{III}-N bond towards acid- or base-catalyzed hydrolysis during complexation reactions is not new and has been reported in the literature[132].

Nickel PCP Complexes

Synthesis

For the synthesis of neutral tetracoordinated nickel(II) complexes of the type [Ni(PCP)Cl] (**19a-c**), direct metalation was chosen as complexation method. The precursor used was a nickel(II) halide salt, $NiCl_2{\cdot}6H_2O$. Since the formation of the Ni-C bond requires elevated temperatures, it was not necessary to use precursors with labile leaving groups (such as NiX_2(DME), X: Cl, Br); the creation of free coordination sites is easier as the reaction temperature increases. The hydrated nickel salt was used because both the ligands and the complexes did not show any sign of decomposition under the reaction conditions, even considering that six equivalents of water are released per each equivalent nickel salt. The resulting complexes are to some extent air sensitive, and the complexation had to be carried out under an inert atmosphere of argon; otherwise, an unidentified green paramagnetic product was formed as by-product. Hydrochloric acid is released in the course of the reaction; however, its presence did not seem to affect the stability of neither the ligands or the complexes, and no decomposition due to HCl was observed. Tentatively, it can be assumed that, after the metalation of the central benzene ring takes place and HCl is released, it goes into the gas phase and does not affect the formed complex. Thus, equimolar amounts of $NiCl_2{\cdot}6H_2O$ and the PCP ligands **3a-c** were allowed to react for sixteen hours under argon in refluxing ethanol (Scheme 54). The solvent was then decanted from the formed orange precipitates, and these were washed twice with pentane and dried under vacuum. The complexes were isolated in good yields (72-90%) as orange solids. The phenyl complex **19a** is only soluble in apolar solvents (such as benzene), whereas the alkyl complexes **19b-c** are soluble in common organic solvents.

---

[131] Kuchen, W.; Mahler, H. F. *Phosphorus Sulfur* **1980**, *8*, 139.

[132] (a) Fei, Z.; Biricik, N.; Zhao, D.; Scopelliti, R.; Dyson, P. *Inorg. Chem.* **2004**, *43*, 2228. (b) Priya, S.; Balakrishna, M. S.; Mague, J. T.; Mobin, S. M. *Inorg. Chem.* **2003**, *42*, 1272. (c) Burrows, A. D.; Mahon, M. F.; Palmer, M. T.; Varrone, M. *Inorg. Chem.* **2002**, *41*, 1695. (d) Balakrishna, M. S.; Krishnamurthy, S. S. *Ind. J. Chem.* **1991**, *30A*, 536. (e) Newton, M. G.; King, R. B.; Chang, M.; Gimeno, J. *J. Am. Chem. Soc.* **1978**, *100*, 1632. (f) Geicke, J.; Lorenz, I. P.; Murschel, P.; Polborn, K. *Z. Naturforsch.* **1997**, *52B*, 593.

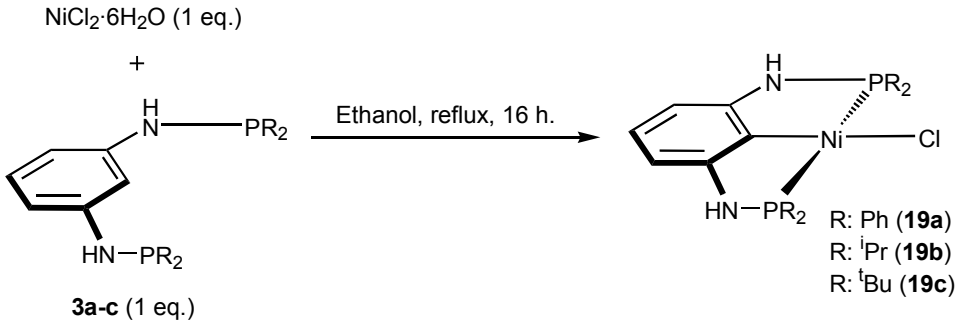

Scheme 54. Synthesis of the nickel(II) phosphine PCP complexes **19a-c**

Characterization

The complexes **19a-c** were characterized by ^{1}H, $^{31}P\{^{1}H\}$ and $^{13}C\{^{1}H\}$ NMR spectroscopy; some characteristic ^{1}H and $^{31}P\{^{1}H\}$ NMR resonances are given in Table 18.

Table 18. Selected ^{1}H and $^{31}P\{^{1}H\}$ NMR resonances for the nickel PCP complexes **19a-c**.

Complex	^{1}H (δ, [ppm], 20ºC)			$^{31}P\{^{1}H\}$ (δ, [ppm], 20ºC)
	Ph^{4} (1H)	$Ph^{3,5}$ (2H)	N*H* (2H)	
19a	6.90	6.39	8.08	77.8
19b	6.61	5.94	3.95	110.8
19c	6.67	5.95	4.12	113.5

In the ^{1}H NMR spectra, apart from the disappearance of the H^{ipso} signal due to complexation, the only remarkable feature is a shift to the high field of the signals of the aromatic benzene ring protons compared to those of the free ligand: the Ph^{4} signals appear between 6.61 and 6.90 ppm and the $Ph^{3,5}$ signals between 5.94 and 6.39 ppm. In the case of the N*H* protons, the signals are shifted to the low field and appear at 8.08 ppm for **19a**, at 3.95 ppm for **19b** and at 4.12 ppm for **19c**. In the $^{13}C\{^{1}H\}$ NMR spectra, the C^{ipso} signals appear shifted about 25.0 ppm to the low field between 127.1 and 128.5 ppm; this shift can be attributed to the direct coordination of the C^{ipso} carbon atom to the electron poor nickel center. While the $Ph^{2,6}$ and Ph^{4} signals are also shifted to the low field, this shift is bigger for the former ($\Delta\delta \approx 10.0$ ppm) than for the latter ($\Delta\delta \approx 3.0$ ppm). The $Ph^{2,6}$ carbon atoms give signals in the range between 159.2 and 160.7 ppm and the Ph^{4} signals appear between 130.7 and 134.6 ppm. The signals of the $Ph^{3,5}$ carbon atoms show a small shift to the high field compared to the free ligands and appear between 101.1 and 103.0 ppm. In order to explain these shift

deviations, the metalation can be seen as an electrophilic substitution at the *ipso* position of the central benzene ring; it seems logical, therefore, that the loss of electron density at the C^{ipso} position can be shared with the *ortho* ($Ph^{2,6}$) and *para* (Ph^{4}) positions, which are favored electronically by mesomeric effects. The contrary can be observed for the *meta* ($Ph^{3,5}$) positions. A comparison between the $^{13}C\{^{1}H\}$ NMR resonances of the free ligands **3a-c** and of the complexes **19a-c** is shown in Table 19.

Table 19. Selected $^{13}C\{^{1}H\}$ NMR resonances for the ligands **3a-c** and the nickel PCP complexes **19a-c**.

Compound	$^{13}C\{^{1}H\}$ (δ, [ppm], 20ºC)			
	$Ph^{2,6}$	Ph^{4}	Ph^{ipso}	$Ph^{3,5}$
3a	147.7	130.1	103.3	107.3
19a	159.2	130.7	128.5	103.0
3b	149.6	129.5	103.4	106.5
19b	160.7	131.1	127.3	101.1
3c	150.1	129.6	103.5	106.5
19c	160.1	134.6	127.1	103.0

In the case of the $^{31}P\{^{1}H\}$ NMR spectra, the complexes give rise to a sharp singulet at 77.8 ppm (**19a**), 110.8 ppm (**19b**) and 113.5 ppm (**19c**). These signals are strongly shifted to the low field in respect to the signals of the free ligands, indicating a strong deshielding of the phosphorus atom due to complexation. Besides, the existence of a single resonance indicates that both phosphorus atoms are equivalent and coordinated to the nickel center.

The structures of **19a** and **19c** were also determined by X-ray crystallography; crystals were obtained by slow solvent evaporation from a concentrated solution of **19a** in benzene and by slow diffusion of diethyl ether into a concentrated solution of **19c** in ethanol. Structural views of **19a** and **19c** are depicted in Figures 49 and 50.

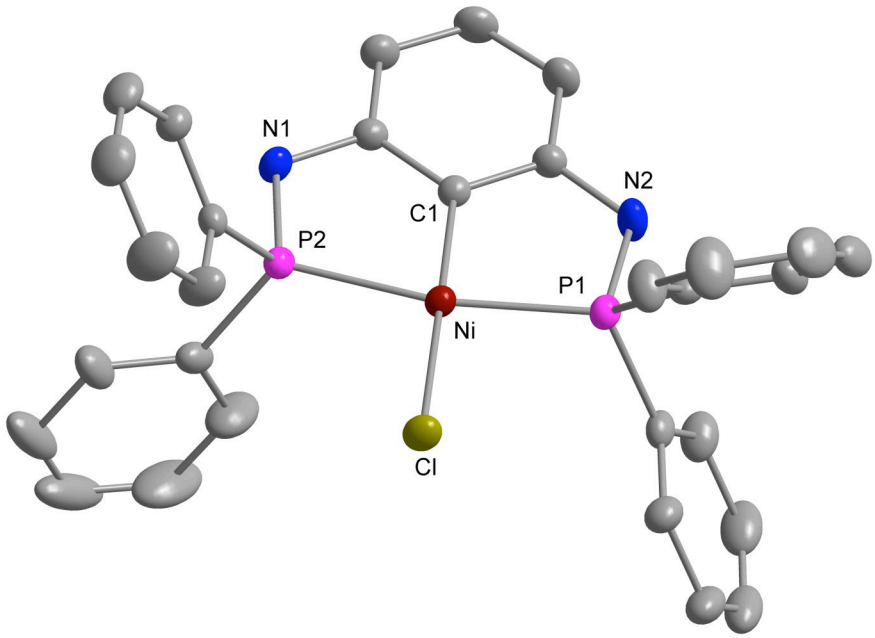

Figure 49. Structural view of [Ni(PCP-Ph)Cl] (**19a**) showing 20% thermal ellipsoids (hydrogen atoms and crystallization solvent omitted for clarity). Selected bond lengths (Å) and angles (º): Ni-C(1) 1.894(3), Ni-P(1) 2.1774(8), Ni-P(2) 2.1768(8), Ni-Cl 2.2137(8), P(1)-N(2) 1.670(2), P(2)-N(1), 1.664(2), P(1)-Ni-P(2) 167.32(3), C(1)-Ni-Cl 178.28(8), C(1)-Ni-P(1) 83.59(8), C(1)-Ni-P(2) 83.73(8), Cl-Ni-P(1) 95.91(3), Cl-Ni-P(2) 96.75(3).

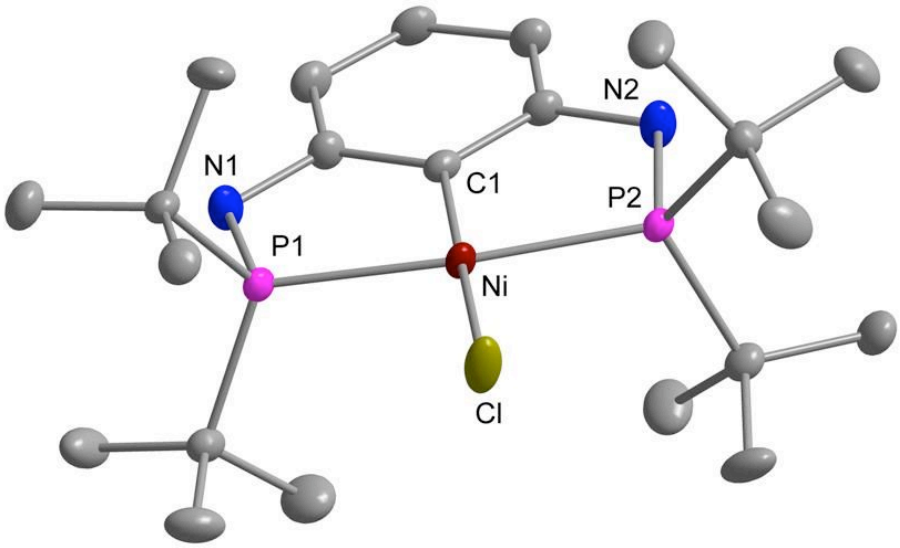

Figure 50. Structural view of [Ni(PCP-^{t}Bu)Cl] (**19c**) showing 60% thermal ellipsoids (hydrogen atoms and crystallization solvent omitted for clarity). Selected bond lengths (Å) and angles (º): Ni-C(1) 1.912(2), Ni-P(1) 2.213(1), Ni-P(2) 2.201(1), Ni-Cl 2.232(1), P(1)-N(1) 1.690(2), P(2)-N(2), 1.692(2), P(1)-Ni-P(2) 166.82(3), C(1)-Ni-Cl 178.07(7), C(1)-Ni-P(1) 84.00(1), C(1)-Ni-P(2) 83.50(1), Cl-Ni-P(1) 96.46(2), Cl-Ni-P(2) 96.15(2).

Like in the cationic tetracoordinated PNP complexes **18a-c**, the nickel center adopts a distorted square-planar geometry with the PCP ligands coordinated to the metal in a tridentate meridional mode. The phosphine substituents are also oriented to different sides of the plane defined by the two phosphorus atoms, C(1) and the nickel center. The Ni-C(1) distances in the PCP complexes could be expected to be somewhat shorter than the Ni-N(1) distances in the related PNP complexes due to the presence of the (supposedly) stronger Ni-C bond; however, the Ni-C(1) bond lengths are 1.894(3) and 1.912(2) Å in **19a** and **19c**, whereas the Ni(1)-N(1) distances in **18a'** and **18c'** are 1.884(3) and 1.894(1) Å, respectively. The C(1)-Ni-Cl angle is 178.28(8)º for **19a** and 178.07(7)º for **19c**, which is close to 180º, while the P(1)-Ni-P(2) angles are 167.32(3) and 166.82(3)º; these values account for the observed distorted square-planar geometry.

Several attempts were also made to obtain the analogous [Ni(PCP)Cl] complexes with phosphoramidite PCP ligands; however, when PCP-BIPOL (**2e**) was reacted in equimolar amounts with $NiCl_2{\cdot}6H_2O$ under the same reaction conditions as those for **19a-c**, the desired product could not be isolated. Instead, intractable decomposition products were detected. Given the fact that the analogous phosphoramidite PNP ligands did not yield the desired cationic tetracoordinated [Ni(PNP)Br]Br complexes under milder conditions, it is not surprising that the reaction between PCP-BIPOL and $NiCl_2{\cdot}6H_2O$ did not afford the corresponding tetracoordinated neutral PCP complex. Since the C-H bond activation process necessary for the metalation of the PCP ligands requires high energies, lower temperatures resulted in no reaction and only starting materials were recovered. The addition of one equivalent of an external base, triethylamine, which can act as a hydrochloric acid captor thus shifting the equilibrium towards the formation of the products, was also unsuccessful: decomposition of the ligand took place. Thus, this reaction was no further investigated.

It has to be noted, however, that the preparation of palladium(II) PCP complexes with P-O containing ligands is indeed possible and has been the object of a more detailed study in our research group[73].

In theory, another synthetic strategy for the preparation of nickel(II) PCP complexes is the oxidative addition of a C^{Ar}-Cl bond in the ipso position of the benzene ring to a nickel(0) precursor. The reaction of PCP^{Cl}-Ph (**3e**) with different nickel(0) complexes, such as $Ni(COD)_2$ or $Ni[P(OEt)_3]_4$ in refluxing toluene for sixteen hours was unsuccessful and only starting materials were recovered (Scheme 55). A reason for this might be the high energy required for the oxidative insertion of nickel into the C^{Ar}-Cl bond; the use of other halides (Br or I) would lower the energy barrier and could favor the oxidative addition. However, since the only commercially available precursor for the preparation of **3e** contains a chlorine, this reaction was no further investigated. This oxidative addition pathway was successful, however, for the preparation of palladium(II) PCP complexes (see below).

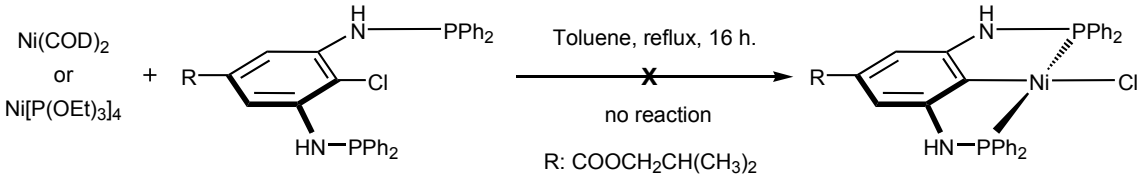

Scheme 55. Failed synthesis of nickel(II) PCP complexes by oxidative addition

Nickel PN complexes

Synthesis

Tetracoordinated nickel complexes of the formula $[Ni(PN^{py})Cl_2]$ were prepared by reacting equimolar amounts of $NiCl_2$(DME) and of the ligands **4a-b** in methylene chloride. The reaction mixture was stirred for two hours at room temperature, and after evaporating the solvent and washing the remaining residues twice with diethyl ether, the complexes **20a-b** were obtained as air stable deep red solids in 86 and 92% yield, respectively (Scheme 56).

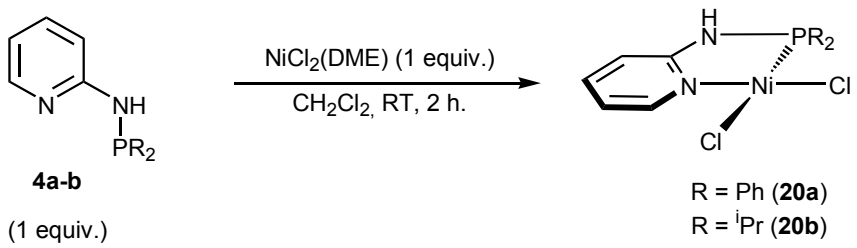

Scheme 56. Synthesis of the complexes **20a-b**

Characterization

Contrarily to the nickel PNP complexes **17a-c**, which are diamagnetic, the complexes **20a-b** are paramagnetic, giving rise to very broad signals in the ^1H and to no signal at all in the $^{31}P\{^1H\}$ NMR spectra. Therefore, these complexes should display a tetrahedral geometry in solution. This observation is in agreement with the findings reported by Braunstein et al. with similar nickel PN complexes[106b].

Nevertheless, complex **20b** could be characterized by X-ray crystallography; suitable crystals were obtained by slow diffusion of diethyl ether into a saturated solution of **20b** in acetone. A structural view of **20b** is shown in Figure 51.

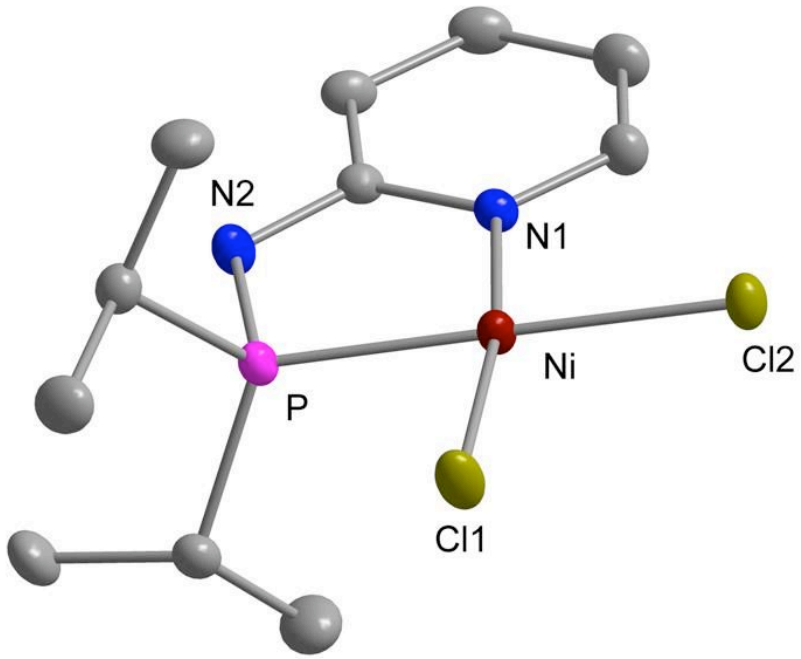

Figure 51. Structural view of [Ni(PN^{py}-^{i}Pr)Cl$_2$] (**20b**) showing 40% thermal ellipsoids (hydrogen atoms and crystallization solvent omitted for clarity). Selected bond lengths (Å) and angles (º): P-N(2) 1.6839(11), Ni-N(1) 1.9259(10), Ni-P 2.1209(4), Ni-Cl(1) 2.2710(4), Ni-Cl(2) 2.2359(3), P-Ni-Cl(2) 177.509 (14), N(1)-Ni-Cl(1) 170.75(3).

The nickel(II) center in **20b** shows a distorted square planar geometry; this result is surprising in view of the paramagnetic nature of this complex in solution, but such a difference between the geometry in solution and in the solid state has been reported previously for a similar nickel PN complex[106b]. The Ni-Cl bond distance is about 0.05 Å shorter for the chlorine in the *trans* position to the pyridine nitrogen atom than that for the chlorine *trans* to the phosphorus atom. The Ni-P bond length is slightly shorter than that observed in the complexes **17a-c** featuring tridentate PNP pincer ligands (e.g. in **17a**, the Ni-P(1) bond distance is 2.1872(13) Å, while in **20b** this distance has a value of 2.1209(4) Å). The Ni-N(1) bond length is slightly longer in **20b** than in the PNP complexes **17a** and **17c** (**17a**: Ni-N(1) 1.884(3) Å, **20b**: Ni-N(1) 1.9259(10) Å). The deviation of the planarity in this complex can be seen best along the N(1)-Ni-Cl(1) axis, with a bond angle of 170.73(3)º; the P-Ni-Cl(2) angle is 177.509(14)º.

Mechanistic Investigations

Due to the apparently different geometries of the complexes **20a-b** in the solid state and in solution, theoretical investigations based on DFT/B3LYP calculations were performed to determine the energy barriers between the tetrahedral and square planar geometries of the complexes **20a-b**. The calculations were performed both for methyl (Figure 52) and phenyl (Figure 53) substituents at the phosphorus atom in the gas phase and in two different solvents, methylene chloride and acetone. From the energy profiles depicted in Figures 52 and 53, it can be appreciated that the tetrahedral geometry is the energetically favored one for the nickel PN complexes **20a-b**. In the gas phase, the isomerization from **A** (tetrahedral) to **B** (square planar) requires around 14 Kcal/mol both with methyl and phenyl substituents, but the energy barrier is lowered when the solvent is taken into account in the calculations. In acetone, the energy required for the isomerization is around 10 Kcal/mol for both complexes, while in methylene chloride it is 10.1 Kcal/mol for the methyl substituted complex and 13.4 Kcal/mol for the phenyl substituted one. Thus, since the tetrahedral geometry is energetically favored, the paramagnetic behavior in solution of the complexes **20a-b** can be explained. However, the energy required for these complexes to adopt a square planar geometry is not very high, and it is thinkable that such a geometry might be favored in the solid state due to packing effects.

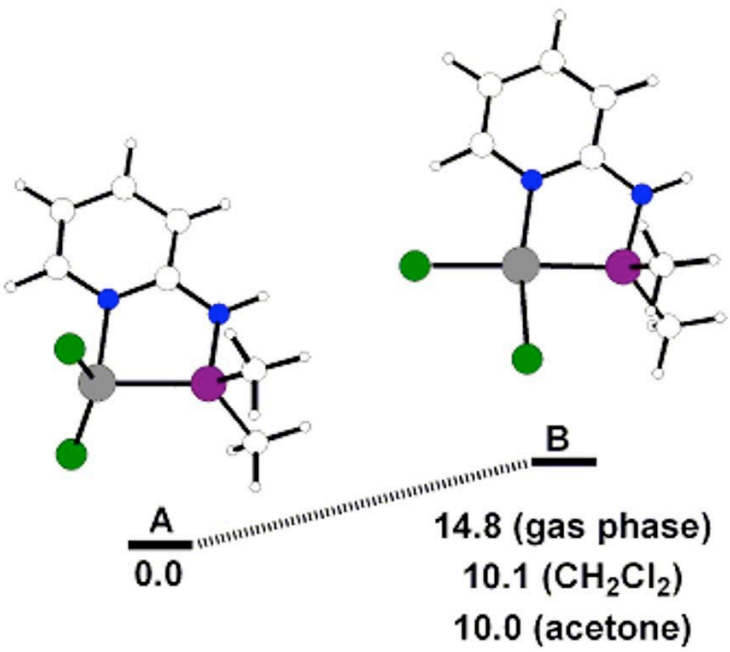

Figure 52. Energy profile for the isomerization of a methyl substituted nickel PN complex from a tetrahedral (**A**) to a square planar geometry (**B**) in the gas phase and in solution.

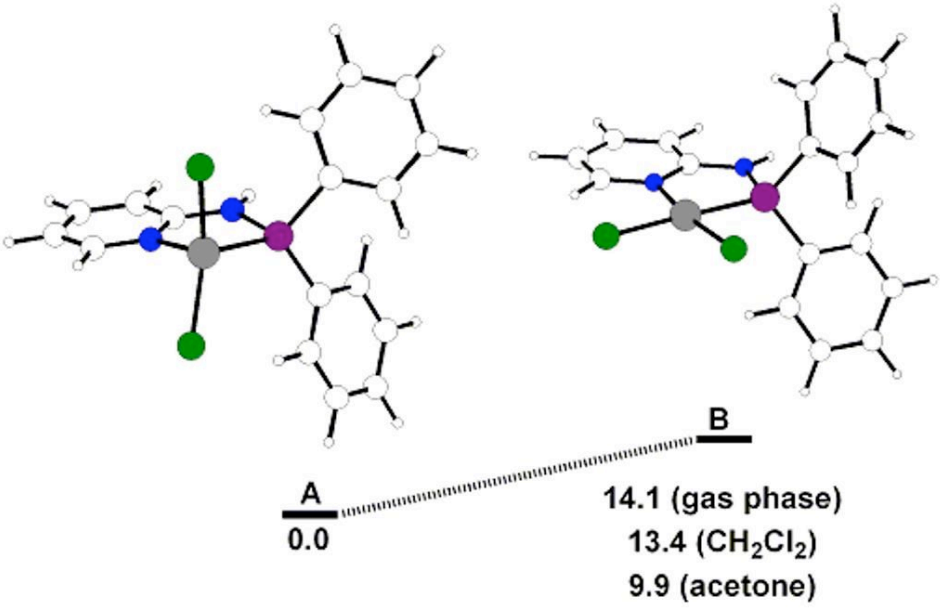

Figure 53. Energy profile for the isomerization of the phenyl substituted nickel PN complex **20a** from a tetrahedral (**A**) to a square planar geometry (**B**) in the gas phase and in solution.

3.3.3 Palladium and platinum complexes

Palladium and platinum PNP Complexes

Synthesis

Like in the case of the nickel(II) PNP complexes with alkyl and aryl phosphines, the choice of a suitable metal precursor proved to be important for the synthesis of the palladium(II) PNP complexes. A metal salt, such as palladium(II) chloride, turned out to be a poor precursor: in order to obtain the desired products, the reaction had to be carried out in boiling acetonitrile to form the real metal precursor, $[Pd(CH_3CN)_2Cl_2]$, prior to the complexation reaction. However, this complex is air- and moisture sensitive and needs to be prepared *in situ*; for this reason, $[Pd(COD)Cl_2]$ (COD: 1,5-cyclooctadiene) was used instead. The formation of the palladium complexes starting from this precursor proceeds faster than that of the analogous nickel(II) complexes and can be achieved by reacting equimolar amounts of $[Pd(COD)Cl_2]$ and the PNP ligand in methylene chloride at room temperature for two hours. After evaporating the solvent and washing the remaining solids twice with diethyl ether, the complexes **21a-c** were obtained in very good yields (81-98%) as air and moisture stable yellow solids (Scheme 57). With the

ligands **2d-h**, the obtained palladium complexes turned out to be hardly soluble in common organic solvents, which made their characterization difficult. Nevertheless, when the reaction was performed under the same reaction conditions using acetonitrile instead of methylene chloride as the solvent in the presence of one equivalent of KCF_3SO_3 as a halide scavenger, the counterion exchange proceeded smoothly and the triflate complexes **21e-h** were obtained in good yields (76-92%) upon filtration of the remaining KCl salt, evaporation of the solvent, washing the residues with diethyl ether and drying the products under vacuum. The complexes **21d-h** are yellow, air and moisture stable solids which are soluble in all common organic solvents. The platinum(II) PNP complexes were obtained analogously, using $[Pt(COD)Br_2]$ as precursor and no halide scavenger in the case of the alkyl and aryl ligands **2a-c** and one equivalent of KCF_3SO_3 for solubility reasons in the case of the phosphoramidite ligands **2e** and **2g**. The reaction conditions remained the same: methylene chloride or acetonitrile were used as the solvents and the reactions were completed at room temperature within two hours (Scheme 57). The complexes were obtained as air- and moisture stable off-white solids in excellent yields (85-94%). It has to be noted that, while the reaction of the phosphoramidite PNP ligands **2d-h** with nickel precursors resulted in the formation of unusual pentacoordinated neutral complexes (see section 3.3.2), the reaction of these ligands with palladium and platinum precursors cleanly afforded the expected cationic tetracoordinated complexes **21d-h** and **22d-e**. No indication for the formation of other products was observed in any case.

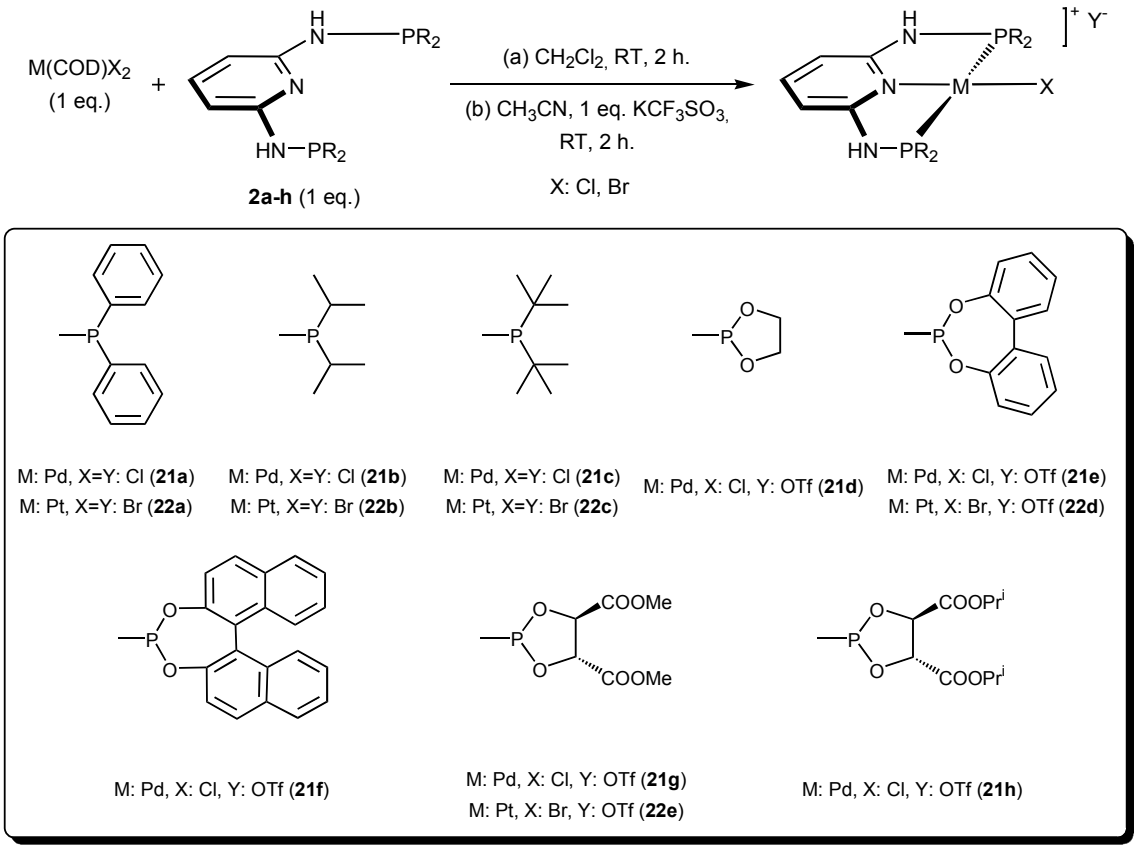

Scheme 57. Synthesis of the palladium and platinum PNP complexes **21a-h** and **22a-e**

A palladium η^1-allyl PNP complex was prepared from $[Pd(allyl)Cl]_2$ and PNP-Ph (**2a**). One equivalent of the dimeric precursor was treated with two equivalents of $AgBF_4$ for fifteen minutes in acetonitrile to form the complex $[Pd(allyl)(CH_3CN)_2](BF_4)$. The AgCl precipitate was filtered off and two equivalents **2a** were added to the colorless solution, whereupon it turned yellow. The reaction mixture was then stirred for further fifteen minutes, the solvent was evaporated and the remaining residue was washed twice with diethyl ether and dried under vacuum to give complex **23** as an air stable yellow solid in an excellent yield (97%) (Scheme 58).

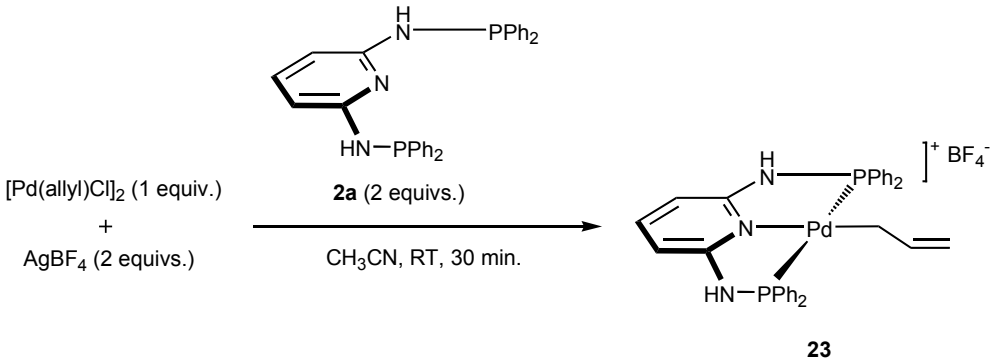

Scheme 58. Synthesis of the complex **23**

Characterization

The complexes **21a-h** and **22a-e** were characterized by ^1H, $^{31}P\{^1H\}$ and $^{13}C\{^1H\}$ NMR spectroscopy; characteristic ^1H NMR resonances of the palladium and platinum complexes are collected in Tables 20 and 21, respectively.

Table 20. Selected ^1H NMR resonances for the palladium PNP complexes **21a-h**

Complex	^1H (δ, [ppm], 20ºC)			
	N*H* (2H)	py^4 (1H)	py^{3,5} (2H)	$^3J_{HH}$ [Hz]
21a	10.47	8.00-7.28[a]	6.84	8.0
21b	9.44	7.20	6.81	7.6
21c	9.43	7.16	6.95	7.5
21d	6.20	7.54	6.03	8.2
21e	8.97	7.83	6.67	8.2
21f	8.10-7.91[a]	7.54-7.31[a]	7.12	7.9
21g	8.44	7.83	6.81	8.2
21h	8.42	7.53	6.79	8.2

[a]Signal overlaps with other aromatic protons.

Table 21. Selected ^{1}H NMR resonances for the platinum PNP complexes **22a-e**.

Complex	^{1}H (δ, [ppm], 20ºC)				
	N*H* (2H)	$^{1}J_{HPPt(sat)}$ [Hz]	py^{4} (1H)	py^{3,5} (2H)	$^{3}J_{HH}$ [Hz]
22a	10.54	26.8	7.05	5.61	xx
22b	9.43	30.4	7.16	6.95	8.0
22c	9.21	33.6	7.42	6.95	7.8
22d	9.52	26.0	7.71	6.68	8.2
22e	8.93	29.2	7.77	6.86	8.2

The signals of the pyridine ring and of the N*H* protons show a shift to the low field compared to those of the free ligands; this shift difference is biggest in the case of the amino bridging protons, which appear as broad singulets between 8.42 and 10.47 ppm in the case of the palladium complexes **21a-h**. The increase in the acidity of these protons due to the formation of strong hydrogen bonds with the counterion is most likely responsible for this shift. In the platinum complexes **22a-e**, they give rise to singulets between 8.93 and 10.54 ppm; the coupling constants $^{1}J_{HPt(sat)}$ are in the range from 26.0 to 33.6 Hz. The py^{4} signals appear as triplets between 7.16 and 7.83 ppm in the palladium complexes and between 7.05 and 7.77 ppm in the platinum complexes, while the py^{3,5} signals give rise to doublets between 6.03 and 7.12 ppm in the palladium complexes and between 5.61 and 6.95 ppm in the platinum complexes. The coupling constants $^{3}J_{HH}$ range between 7.5 and 8.2 Hz and between 7.8 and 8.2 Hz, respectively. In the ^{13}C{^{1}H} NMR spectra, the signals of the pyridine ring are also shifted slightly to the low field; the py^{2,6} signals appear at around 160 ppm, the py^{4} at around 140 ppm and the py^{3,5} at around 100 ppm both for the palladium and platinum complexes.

Finally, the ^{31}P{^{1}H} NMR spectra of the palladium complexes show a single resonance at 69.9 ppm for **21a**, 108.4 ppm for **21b**, 115.7 ppm for **21c** and between 123.8 and 130.2 ppm for the phosphite complexes **21d-h**, in which the phosphorus atom is bound to strongly electron withdrawing oxygen atoms (Table 22). The appearance of a single resonance indicates the equivalence of both phosphorus atoms, revealing that both phosphines are bound to the metal center. A shift to the low field due to coordination to the metal was observed in all cases.

Table 22. Selected $^{31}P\{^1H\}$ NMR resonances for the palladium and platinum PNP complexes **21a-h** and **22a-e**.

Complex	$^{31}P\{^1H\}$ (δ, [ppm], 20ºC)	$^1J_{PPt(sat)}$ [Hz]
21a	69.9	
21b	108.4	
21c	115.7	
21d	123.8	
21e	124.6	
21f	124.1	
21g	130.2	
21h	129.7	
22a	65.5	2686
22b	100.4	2556
22c	103.9	2534
22d	123.4	4190
22e	131.6	4286

The signals of the platinum complexes in the $^{31}P\{^1H\}$ NMR spectra are also shifted to the low field, and they appear as singulets between 65.5 and 131.6 ppm with $^1J_{PPt(sat)}$ coupling constants in the range between 2534 and 2556 Hz for the phosphine complexes and between 4190 and 4286 Hz for the phosphoramidite complexes (Table 22).

Complex **23** was characterized by ^1H, $^{31}P\{^1H\}$ and $^{13}C\{^1H\}$ NMR spectroscopy. In the ^1H NMR spectrum, the pyridine signals appear at 6.99 (triplet, py^4) and 6.54 ppm (doublet, py^{3,5}) with a coupling constant $^3J_{HH}$ = 8.0 Hz. The N*H* protons give rise to a singulet at 7.90 ppm, and the η^1-coordinated allyl group gives signals at 5.55 (C*H*), 4.29 (=C*H*), 4.19(=C*H*) and 2.66 ppm (CH_2). In the $^{13}C\{^1H\}$ NMR spectrum, the allyl group gives rise to signals at 141.2 (*C*H), 109.6 (=*C*H) and 17.6 ppm (*C*H_2); the signals of the pyridine carbon atoms show almost no shift difference when compared to those of the free ligands. Complex **23** shows a single resonance at 69.1 ppm in the $^{31}P\{^1H\}$ NMR spectrum, indicating that both phosphine groups are equivalent and coordinated to the palladium center. Thus, the P,N,P coordination of the ligand **2a** to the metal center and the formation of a η^1-allyl complex is favored in respect to the formation of a η^3-allyl complex, in which the ligand **2a** would coordinate in a P,N mode to the palladium atom. This observation is in agreement with those reported for similar, methylene-bridged palladium PNP pincer complexes[133].

[133] Barloy, L.; Ramdeehul, S.; Osborn, J. A.; Carlotti, C.; Taulelle, F.; De Cian, A.; Fischer, J. *Eur. J. Inorg. Chem.* **2000**, 2523.

Complexes **21c** and **21e** were also characterized by X-ray crystallography; suitable crystals were obtained by slow diffusion of diethyl ether into saturated solutions of **21c** in methylene chloride and of **21e** in acetonitrile, respectively. Structural views of both complexes are depicted in Figures 54 and 55.

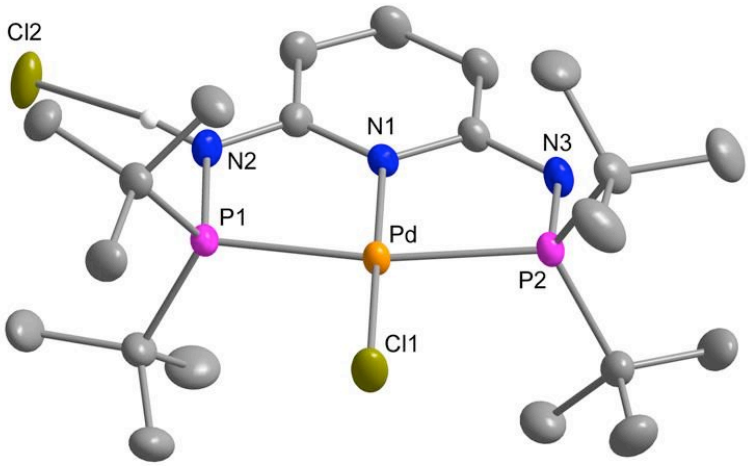

Figure 54. Structural view of [Pd(PNP-^{t}Bu)Cl]Cl (**21c**) showing 40% thermal ellipsoids (hydrogen atoms, counterion and crystallization solvent omitted for clarity). Selected bond lengths (Å) and angles (º): Pd-P(1) 2.2987(5), Pd-P(2) 2.2985(5), Pd-N(1) 2.015(2), Pd-Cl(1) 2.3002(6), P(1)-N(2) 1.702(2), P(2)-N(3) 1.693(2), P(1)-Pd-P(2) 166.54(2), N(1)-Pd-Cl(1) 179.88(6).

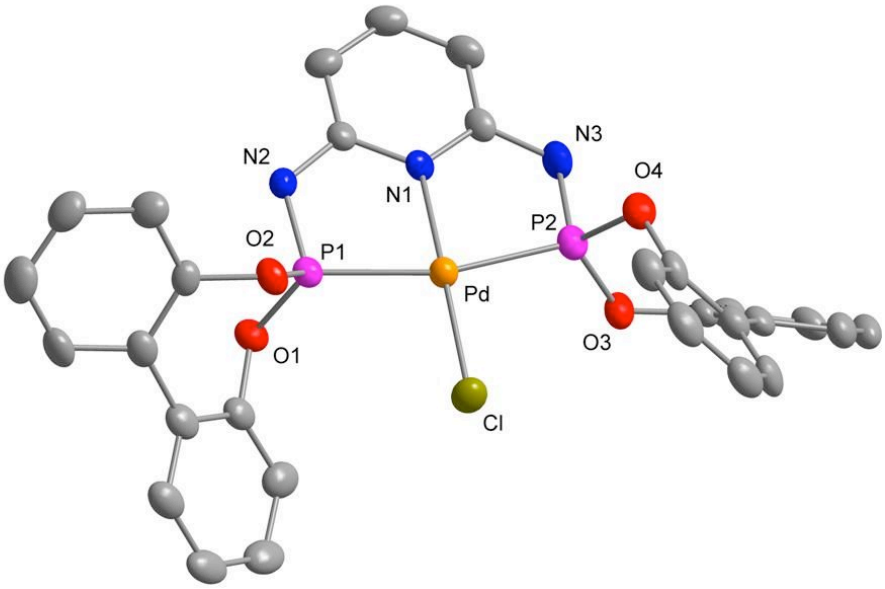

Figure 55. Structural view of [Pd(PNP-BIPOL)Cl]OTf (**21e**) showing 70% thermal ellipsoids (hydrogen atoms, counterion and crystallization solvent omitted for clarity). Selected bond lengths (Å) and angles (º): Pd-P(1) 2.251(2), Pd-P(2) 2.252(2), Pd-N(1) 2.028(4), Pd-Cl(1) 2.271(2), P(1)-N(2) 1.653(4), P(2)-N(3) 1.645(4), P(1)-Pd-P(2) 165.27(5), N(1)-Pd-Cl(1) 178.98(11).

Both complexes display a distorted square-planar geometry around the metal center defined by the two phosphorus atoms, the pyridine nitrogen atom from the PNP ligand and the coordinated chlorine atom. The Pd-P bond lengths, which are about 0.05 Å shorter for the oxygen bearing complex **21e**, are consistent with a trans P-Pd-P arrangement, determined by the meridional coordination mode of the PNP ligands. These distances are, however, about 0.1 Å longer for the palladium complexes than for the related nickel complexes: for comparison, the Ni-P bond lengths are Ni-P(1) 2.2067(4) and Ni-P(2) 2.2062(4) Å in [Ni(PNP-tBu)Br]Br (**17c**) and the Pd-P distances are Pd-P(1) 2.2987(5) and Pd-P(2) 2.2985(5) Å in **21c**. The N(1)-Pd-Cl(1) angles are similar and almost 180º in both complexes, 179.88(6)º in **21c** and 178.98(11)º in **21e**, while the P(1)-Pd-P(2) angles show a significant deviation from the planarity, with values of 166.54(2)º for **21c** and 165.27(5)º for **21e**. This deviation is also bigger than that observed for the nickel complexes (i.e the P(1)-Ni-P(2) angle in [Ni(PNP-tBu)Br]Br (**17c**) has a value of 169.73(2)º).

Like in the case of the nickel(II) PNP complexes, the palladium and platinum alkyl and aryl complexes **21a-c** and **22a-c** are perfectly stable and can be stored up to one year under air without showing any signs of decomposition. The phosphoramidite complexes **21d-h** and **22d-e**, however, are air stable as solids but slowly decompose in solutions when traces of water are present. Several attempts to crystalize the otherwise poorly soluble chloride complex **22e'** over long periods of time (up to ten days) by evaporation of the solvent of a saturated dimethyl formamide solution of **22e'** repeatedly resulted in the formation of small pale yellow crystals, which were identified as the hydrolized product [Pd{κ^2(P,N)-NH_2-PN-BIPOL}{κ^1(P)-BIPOL-P=O}Cl] (**24**) (Scheme 59).

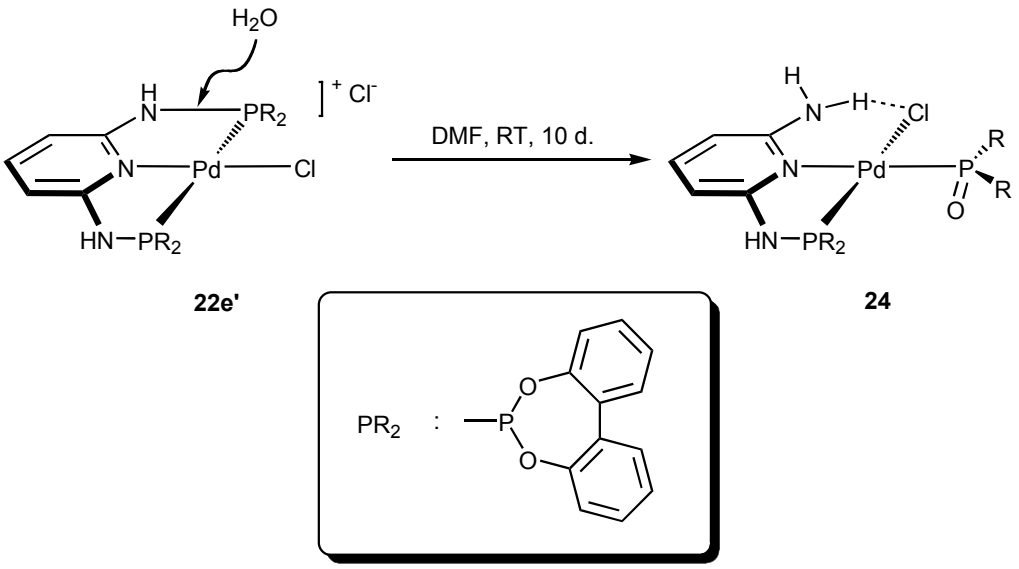

Scheme 59. Water triggered P-N bond cleavage in complex **22e**

During the reaction from **22e** to **24**, the P-N bond of one of the phosphoramidite moieties of the PNP ligand breaks and the phosphine is oxidized (presumably by water) to give an anionic phosphinite ligand BIPOL-P=O$^-$. The PNP ligand is decomposed to a bidentate ligand and the complex changes from cationic to neutral. The entire process takes place while the ligand is still coordinated to the metal center. A structural view of **24** is shown in Figure 56.

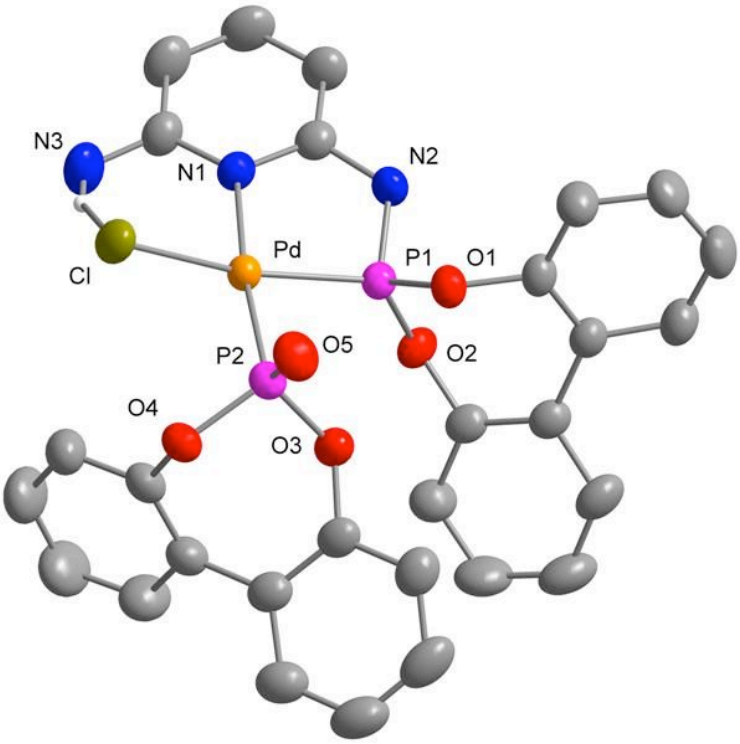

Figure 56. Structural view of [Pd{κ^2(P,N)-NH_2-PN-BIPOL}{κ^1(P)-BIPOL-P=O}Cl] (**24**) showing 70% thermal ellipsoids (hydrogen atoms and crystallization solvent omitted for clarity). Selected bond lengths (Å) and angles (º): Pd-N(1) 2.171(2), Pd-P(1) 2.1787(5), Pd-P(2) 2.2276(6), Pd-Cl 2.3505(5), P(1)-Pd-P(2) 91.78(2), Cl-Pd-P(2) 86.76(2), N(1)-Pd-P(2) 173.51(5), Cl-Pd-P(1) 165.39 (2).

In this molecule, the palladium center also adopts a distorted square-planar geometry, this time defined by the two phosphorus atoms, the central pyridine nitrogen atom of the PNP ligand and the chlorine atom. The $PdNP_2Cl$ coordination deviates significantly from the planarity most likely due to short intramolcular contact between C(28) and Cl (Figure 56). Moreover, there is a stabilizing short intramolcular bond N(3)-H···Cl with a N···Cl distance of 3.15 Å.

Palladium and platinum PCP complexes

Synthesis

Analogously to the nickel PCP complexes, several palladium and platinum PCP complexes were synthesized by direct metalation of the PCP ligands **3a-d** using $M(COD)X_2$ (M: Pd, Pt, X: Cl, Br) and $Pd(TFA)_2$ (TFA: trifluoroacetate) as the metal precursors (Scheme 60). In the case of the palladium chloride complexes **25a-d**, equimolar amounts of $Pd(COD)Cl_2$ and of the corresponding ligand were refluxed in toluene for five hours. High temperatures (110ºC) were required fot the C-H activation at the *ipso* carbon atom. In contrast to the preparation of the related nickel PCP complexes, no inert atmosphere was required since the complexes are air stable and the formation of byproducts was not observed. It has to be noted also that, like for the nickel PCP complexes, the release of hydrochloric acid during the reaction does not affect the complexes. The complexes **25a-d** precipitate from the reaction mixture and, after decanting the solution, washing the solids twice with diethyl ether and drying under vacuum, they were obtained as yellow solids in excellent yields (83-96%). The phenyl substituted complex **25a**, bearing no substituents at the benzene backbone, is only soluble in very polar solvents (DMSO, DMF), which makes its characterization difficult; however, when a substituent is introduced at the *para* position of the benzene ring (i.e. a trifluoromethyl group (**25d**) or an alkyl ester (**27**), see below), the solubility improves dramatically. The alkyl substituted complexes **25b-c**, on the other hand, are soluble in all common organic solvents.

The formation of the trifluoroacetate complexes **26a-c** proceeds under much milder conditions (lower reaction temperatures and shorter reaction times), probably because the release of one trifluoroacetate molcule in the course of the reaction, which can act as a base, facilitates the deprotonation of the *ipso* position of the central benzene ring. Again, no inert atmosphere was required and the release of trifluoroacetic acid did not have any influence on the formation or on the stability of the complexes. Thus, one equiv. of the corresponding ligand and one equiv. of $Pd(TFA)_2$ were reacted in THF at room temperature for three hours. The solvent and the released trifluoroacetic acid were then removed, the remaining solids washed twice with diethyl ether and the products dried under vacuum. The complexes **26a-c** were obtained as air stable brown solids in good yields (78-91%).

When equimolar amounts of $Pt(COD)Br_2$ and the corresponding ligand were reacted in refluxing toluene, only traces of the complexes **28a-c** were observed. This is not surprising, since the synthesis of analogous platinum PCP complexes containing a methylene moiety between the central benzene ring and the phosphines requires the addition of an external

base[134]. Thus, when one equiv. of $Pt(COD)Br_2$ and one equiv. of the ligands **3a-c** were reacted in toluene at 110ºC for sixteen hours in the presence of one equiv. of triethylamine, the formation of the complexes proceeded smoothly. After the reaction, the mixture was filtered while still hot to separate the unsoluble ammonium salt, and the solvent was removed under vacuum. Upon washing twice with diethyl ether and drying, the complexes **28a-c** were obtained in good yields (79-93%) as air stable off-white solids (Scheme 60).

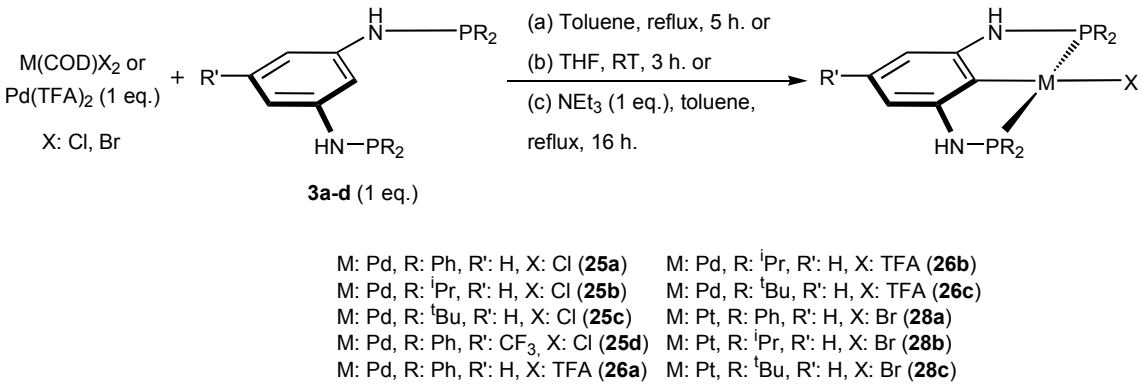

Scheme 60. Synthesis of the palladium and platinum PCP complexes **25a-d**, **26a-c** and **28a-c**

Another method for the synthesis of PCP pincer complexes is the oxidative addition of the C^{Ar}-Cl bond in the *ipso* position of the benzene ring in ligand **3e** to a metal precursor in a low oxidation state. Although this synthetic approach did not work with nickel, it was possible to prepare palladium(II) PCP pincer complexes starting from the palladium(0) precursor $Pd_2(dba)_3$ (dba: dibenzylideneacetone) and the ligand **3e** (Scheme 61). In theory, such a ligand would also be suitable for the synthesis of PCP pincer complexes via a transmetalation procedure with *n*-BuLi or LDA and further treatment with a suitable metal precursor, but such a method was abandoned due to the acidity of the N*H* protons of the amino bridging and to the problems derived from competition reactions between the deprotonation of the N*H* group and the Li-Cl exchange. The synthesis of the complex **27** was performed by reacting one equiv. of $Pd_2(dba)_3$ and two equivs. of the ligand **3e** in toluene at 80ºC for twelve hours. The reaction mixture changed its color from deep purple (dissolved metal precursor) to yellow. After the solvent was removed under vacuum, the remaining residue was washed twice with pentane and dried to give **27** as an air stable yellow solid in 90% yield. Due to the presence of the COO-^{i}Bu substituent in the *para* position of the benzene ring, **27** shows a very high solubility in most organic solvents, including methylene chloride and diethyl ether. It has to be noted that, while the oxidative addition of the ligand **3e** to nickel(0) precursors was unsuccessful even at very high temperatures, the reaction of this ligand with $Pd_2(dba)_3$ proceeds at a relatively mild

[134] Fischer, S.; Wendt, O. F. *Acta Cryst.* **2004**, *E60*, m69.

temperature (80ºC). Additionally, given the fact that the reported yields for complexes prepared by oxidative addition are in the range between 20 and 40%, the synthesis of **27** proceeds very smoothly in a very high yield (90%). The formation of palladium black, which can be a problem in the preparation of palladium complexes by oxidative addition, was not observed in this case. Finally, the synthesis of palladium(II) PCP pincer complexes with achiral and chiral P-O bond containing phosphoramidite ligands both *via* direct metalation and oxidative addition is possible, and has been studied in our research group[73].

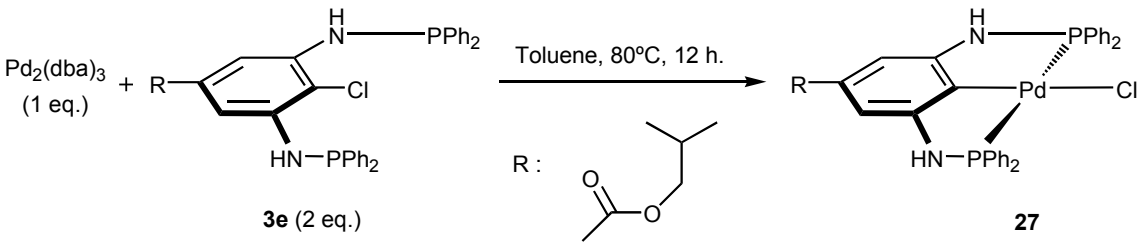

Scheme 61. Synthesis of the palladium PCP complex **27** by oxidative addition

Characterization

All the complexes were characterized by ^{1}H, $^{31}P\{^{1}H\}$ and $^{13}C\{^{1}H\}$ NMR spectroscopy; the characteristic ^{1}H NMR resonances for the palladium and platinum PCP complexes are shown in Tables 23 and 24, respectively.

Table 23. Selected ^{1}H resonances for the palladium PCP complexes **25a-d**, **26a-c** and **27**

Complex	^{1}H (δ, [ppm], 20ºC)			
	py^{4} (1H)	py^{3,5} (2H)	$^{3}J_{HH}$ [Hz]	N*H* (2H)
25a	6.77	6.23	7.8	8.00
25b	6.76	6.14	7.7	3.91
25c	6.73	6.12	7.8	4.18
25d	-	6.57	[b]	5.12
26a	6.86	6.26	7.9	4.67
26b	6.76	6.11	7.9	3.91
26c	6.73	6.13	7.9	4.18
27	-	7.87-7.43[a]	[b]	5.25

[a]Signal overlaps with other aromatic protons. [b]Singulet.

Table 24. Selected ^{1}H resonances for the platinum PCP complexes **28a-c**

Complex	^{1}H (δ, [ppm], 20ºC)				
	py^4 (1H)	py^{3,5} (2H)	$^3J_{HH}$ [Hz]	N*H* (2H)	$^1J_{HPt(sat)}$ [Hz]
28a	6.89	6.37	8.0	5.35	38.8
28b	6.77	6.18	7.7	4.35	37.9
28c	6.86	6.16	7.9	4.47	38.2

In the palladium complexes **25a-d**, **26a-c** and **27**, the N*H* protons of the amino bridging give rise to singulets between 3.91 and 8.00 ppm, slightly shifted to the low field when compared to the signals of the free ligands, and only in the case of **25a**, which was measured in a very polar solvent capable of interacting with these protons (DMSO), was this shift bigger. In the case of the platinum complexes **28a-c**, the N*H* protons appear as singulets, also shifted to the low field between 4.35 and 5.35 ppm with platinum satellites ($^1J_{HPt(sat)}$ in the range between 75.8 and 76.4 Hz). The small shift in the signals of the N*H* protons is in contrast to that observed for the analogous palladium and platinum PNP complexes, in which it is much bigger (Δδ(N*H*, PNP) ≈ 5.0 ppm; Δδ(N*H*, PCP) ≈ 0.7 ppm). This may be attributed to the different ionic nature of the complexes: while the PNP complexes are cationic and the counterion can build strong hydrogen bonds to the N*H* protons, thus making them much more acidic, the PCP complexes are neutral and have no counterion with which these protons can interact with. Furthermore, in the pyridine-based PNP complexes, there may exist a certain degree of delocalization of the N*H* protons between the amino spacers and the nitrogen atom of the pyridine ring, whereas this is not possible in the case of the PCP complexes, where benzene poses as the aromatic backbone of the molcule. In the complexes of both metals, the py^4 protons give rise to triplets between 6.73 and 6.89 ppm and the py^{3,5} protons appear as doublets between 6.11 and 6.57 ppm. The coupling constants $^3J_{HH}$ lie between 7.7 and 8.0 Hz.

Like in the case of the nickel PCP complexes, in the palladium and platinum complexes the signals of the C^{ipso} and Ph^{2,6} carbon atoms appear shifted to the low field in the ^{13}C{^{1}H} NMR spectra: this effect may be attributed to the formation of the M-C^{ipso} bond, which withdraws electron density from the benzene ring. Compared to the free ligands, the C^{ipso} signals are shifted about 25.0 ppm to the low field and appear between 117.0 and 129.8 ppm. It has to be noted that this signal could not be detected for the complexes **25d**, **27** and **28a**, probably because it is overlapped by the signals of the phenyl substituents at the phosphorus atoms, which appear in the same range as the C^{ipso} signals. The Ph^{2,6} carbon atoms give rise to signals between 160.7 and 151.3 ppm shifted between 3.0 and 12.0 ppm to the low field compared to the signals of the free ligands, while the Ph^4 signals appear between 124.0 and 134.6 ppm with smaller shifts of about 3.0 to 5.0 ppm. The Ph^{3,5} signals, on the other hand, are shifted about 4.0 ppm to the high field and appear between 100.9 and 104.0 ppm. A comparison between the signals of the free ligands and those of the palladium and platinum PCP complexes **25a-d**, **26a-c**, **27** and **28a-c** is shown in Table 25.

Table 25. Selected $^{13}C\{^1H\}$ NMR resonances for the palladium and platinum PCP complexes and comparison with the signals of the free ligands

Compound	$^{13}C\{^1H\}$ (δ, [ppm], 20ºC)			
	$Ph^{2,6}$	Ph^4	Ph^{ipso}	$Ph^{3,5}$
3a	147.7	130.1	103.3	107.3
25a	156.9	131.4	129.2	103.2
26a	156.0	128.2	128.8	103.5
28a	153.7	127.2	[a]	103.0
3d	148.2	130.3	103.7	105.5
25d	151.3	133.8	[a]	100.9
3e	143.4	130.3	106.4	107.2
27	155.7	130.4	[a]	104.0
3b	149.6	129.5	103.4	106.5
25b	157.3	127.0	124.0	101.9
26b	157.7	124.0	127.3	102.1
28b	155.2	125.2	128.5	101.6
3c	150.1	129.6	103.5	106.5
25c	157.9	126.7	117.0	101.4
26c	158.0	126.7	129.8	101.4
28c	155.7	134.6	126.6	101.1

[a]Not detected.

All the complexes display a single resonance in the $^{31}P\{^1H\}$ NMR spectra, indicating the equivalence of both phosphorus atoms; this is consistent with the formation of the PCP complexes with the ligand coordinating in a meridional mode. Due to complexation and deshielding of the phosphorus atoms, the signals are in all cases shifted to the low field compared to the signals of the free ligands (Table 26). The palladium phenyl PCP complexes give singulets at 76.9 (**25a**), 81.4 (**25d**), 82.1 (**26a**) and 80.5 ppm (**27**), while the alkyl complexes **25b-c** and **26b-c** display singulet resonances between 114.3 and 120.4 ppm. In the case of the phenyl PCP complexes substituted at the central benzene ring (**25d** and **27**), the shift to the low field is slightly bigger than that for the unsubstituted complexes. The coligand attached to the metal center seems to have little or no influence on the NMR shift of the complexes. The platinum complexes give, like their PNP analogues, rise to singulets at 76.1 (**28a**), 106.6 (**28b**) and 109.5 ppm (**28c**) showing satellites with coupling constannts $^1J_{PPt(sat)}$ in the range between 3112 and 3208 Hz; this constant is bigger than the one observed in the PNP complexes **22a-c** ($\Delta J \approx 300$ Hz).

Table 26. Selected $^{31}P\{^{1}H\}$ NMR resonances for the palladium and platinum PCP complexes

Complex	$^{31}P\{^{1}H\}$ (δ, [ppm], 20ºC)	$^{1}J_{PPt(sat)}$ [Hz]
25a	76.9	
25b	114.3	
25c	120.4	
25d	81.4	
26a	82.1	
26b	114.5	
26c	120.4	
27	80.5	
28a	76.1	3208
28b	106.6	3112
28c	109.5	3736

The crystal structures of the complexes **25a**, **25d, 26b** and **28a** were also determined by X-ray crystallography. Crystals of these compounds were obtained by slow evaporation of the solvent of a concentrated solution of **25a** in DMF, by slow diffusion of diethyl ether into a concentrated solution of **25d** in acetonitrile and by layering a concentrated solution of **26b** in methylene chloride with pentane. Crystals of **28a** were obtained in an NMR tube by slow evaporation of CD_2Cl_2. Structural views of these complexes are shown in Figures 57-60.

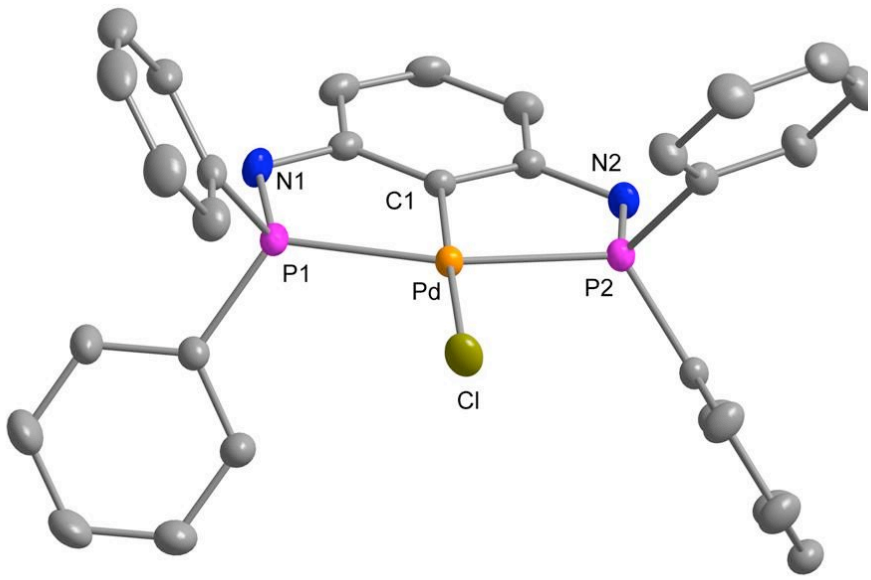

Figure 57. Structural view of [Pd(PCP-Ph)Cl]·2DMF (**25a**) showing 40% thermal ellipsoids (hydrogen atoms and crystallization solvent omitted for clarity). Selected bond lengths (Å) and angles (°): Pd-C(1) 2.002(2), Pd-P(1) 2.2748(4), Pd-P(2) 2.2851(5), Pd-Cl 2.3699(4), P(1)-N(1) 1.673(2), P(2)-N(2) 1.671(2), P(1)-Pd-P(2) 163.54(2), C(1)-Pd-P(1) 81.80(5), C(1)-Pd-P(2) 81.79(5), Cl-Pd-P(1) 96.97(2), Cl-Pd-P(2) 99.46(2); hydrogen bonds: N(1)···O(1S) 2.889(2), N(2)···O(2S) 2.833(3).

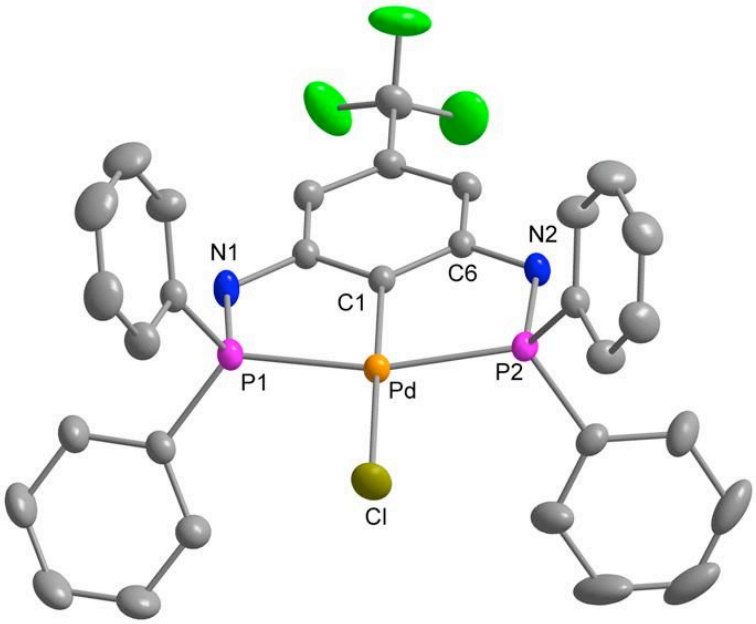

Figure 58. Structural view of [Pd(PCP-Ph^{F})Cl] (**25d**) showing 30% thermal ellipsoids (hydrogen atoms and crystallization solvent omitted for clarity). Selected bond lengths (Å) and angles (º): Pd-C(1) 2.000(2), Pd-P(1) 2.2768(3), Pd-P(2) 2.2831(3), Pd-Cl 2.3950(3), P(1)-N(1) 1.6770(10), P(2)-N(2) 1.6806(10), P(1)-Pd-P(2) 163.18(1), C(1)-Pd-Cl 177.11(3), C(1)-Pd-P(1) 81.63(3), C(1)-Pd-P(2) 81.97(3), Cl-Pd-P(1) 98.42(1), Cl-Pd-P(2) 98.16(1).

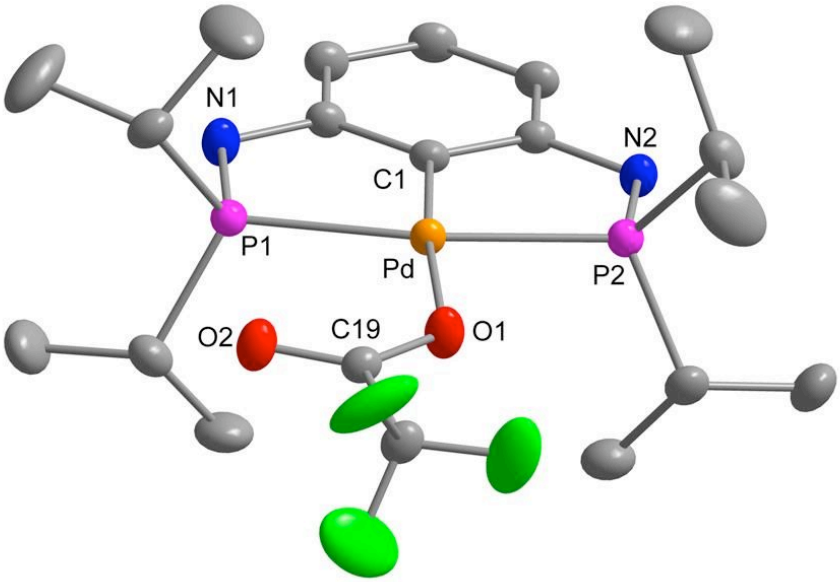

Figure 59. Structural view of [Pd(PCP-^{i}Pr)TFA] (**26b**) showing 40% thermal ellipsoids (hydrogen atoms and crystallization solvent omitted for clarity). Selected bond lengths (Å) and angles (º): Pd-C(1) 1.988(1), Pd-P(1) 2.2988(4), Pd-P(2) 2.2830(4), Pd-O(1) 2.131(1), P(1)-N(1) 1.685(1), P(2)-N(2) 1.676(1), P(1)-Pd-P(2) 164.45(2), C(1)-Pd-O(1) 173.35(6), C(1)-Pd-P(1) 82.34(5), C(1)-Pd-P(2) 82.30(5), O(1)-Pd-P(1) 103.40(3), O(1)-Pd-P(2) 91.79(3); donor interaction O(2)···P(1) 3.114(1).

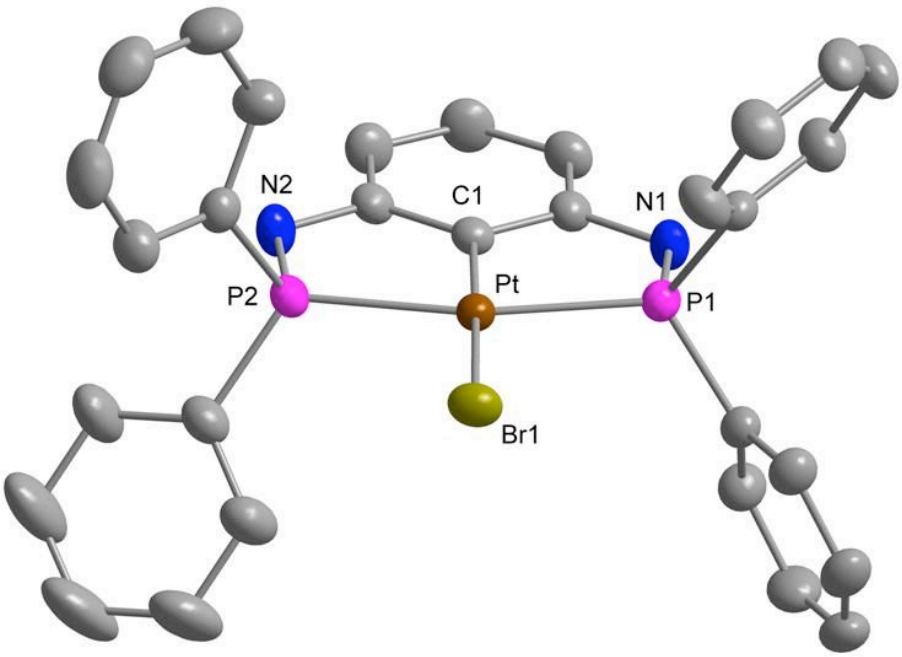

Figure 60. Structural view of [Pt(PCP-Ph)Cl] (**28a**) showing 60% thermal ellipsoids (hydrogen atoms, triethylamine and crystallization solvent omitted for clarity). Selected bond lengths (Å) and angles (º): Pt-C(1) 2.006(3), Pd-P(1) 2.2750(8), Pd-P(2) 2.2712(8), Pd-Br(1) 2.5100(4), P(1)-N(1) 1.672(3), P(2)-N(2) 1.666(3), P(1)-Pt-P(2) 164.33(3), C(1)-Pt-Br(1) 178.48(9), C(1)-Pt-P(1) 81.90(9), C(1)-Pt-P(2) 82.50(9), Br(1)-Pt-P(1) 99.31(2), Br(1)-Pt-P(2) 96.27(2); hydrogen bonds N(1)···Br(2) 3.429(3), N(2)···Br(2A) 3.451(3), N(3)···Br(2) 3.260(5).

All the complexes display a distorted square-planar conformation with the PCP ligands coordinated to the metal center in a tridentate meridional mode. The aminophosphine hydrogen atoms are in the solid state active hydrogen bond donors to suitable acceptor atoms (e.g. oxygen from DMF in **25a** and nitrogen from acetonitrile in **25d**). This is in contrast to the NMR measurements made in solution, where the high field shift of the N*H* bridging protons indicates the absence of such hydrogen bonds. In all complexes, the phosphine substituents are oriented to different sides of the plane defined by the two phosphorus atoms, C(1) and the metal center. The M-C(1) distances are very similar in all complexes, 2.002(2), 2.000(2), 1.988(1) and 2.006(3) Å for **25a**, **25d**, **26b** and **28a**, respectively. These distances are about 0.1 Å longer than the Ni-C(1) distances in the nickel PCP complexes **19a** (1.894(3) Å) and **19c** (1.912(2) Å) and almost 0.3 Å shorter than the Pd-N(1) bond lengths in the analogous PNP complexes (for comparison, the Pd-N(1) distance in [Pd(PNP-^{t}Bu)Cl]Cl (**21c**) is 2.2987(5) Å). This difference in the bond lengths of related PNP and PCP complexes was not observed for the nickel complexes, where the Ni-N and Ni-C distances were almost identical. The metal-coligand distances are about 2.30 Å in the case of the halide complexes **25a**, **25d** and **28a** and 0.2 Å shorter (2.131(1) Å) for the Pd-O(1) bond in **26b**. Most likely due to packing effects, all the complexes show a deviation from planarity: while the C(1)-M-X (M: Pd, Pt, X: Cl, Br, TFA)

angles are close to 180º, this deviation is evident along the P(1)-M-P(2) axis, with angle values of 163.54(2), 163.18(1), 164.45(2) and 164.33(3)º for **25a**, **25d**, **26b** and **28a**, respectively. This deviation is bigger than that observed both in the nickel PNP and PCP complexes and in the analogous palladium and platinum PNP complexes. The complex **26b** is stabilized in the solid state by a clear-cut intramolcular donor interaction between the TFA oxygen O(2) and the phosphorus atom P(1): the corresponding P(1)-O(2) distance of 3.114(1) Å is shorter than the distance limit of 3.35 Å given by Holmes (2004)[135]. This observation difffers from the measurements made for the related complex [Pd(PCP-BIPOL)TFA], where the P(1) atom is more polarized by one P-N and two P-O bonds and less prone to such interactions with the result that the TFA group points away from the phosphorus and adopts an orientation inclined to the PCP main plane.

Palladium PN complexes

Synthesis

Several neutral palladium complexes of the formula [Pd(PN)Cl_2] with the pyridine- and oxazoline-based PN ligands **4a-d** and **5a** were prepared. For the synthesis of the complexes **29a-d** and **30**, equimolar amounts of Pd(COD)Cl_2 and of the ligands **4a-d** and **5a** were stirred at room temperature for two hours. The yellow solutions were then evaporated to dryness and the resulting residues were washed twice with diethyl ether and dried under vacuum (Scheme 62). The complexes **29a-d** and **30** were obtained in good yields (74-88%) as air stable yellow solids.

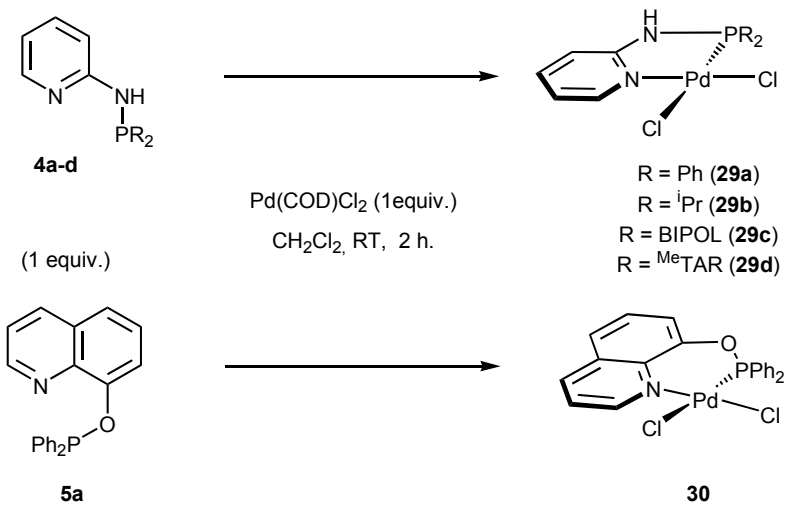

Scheme 62. Synthesis of the complexes **29a-d** and **30**

[135] Holmes, R. R. *Acc. Chem. Res.* **2004**, *37*, 746 and references therein.

Furthermore, several palladium allyl complexes were prepared with the PN ligands **4a-b**; depending on the reaction conditions, both η^3- as well as η^1-allyl complexes were obtained. When the ligands **4a-b** and the dimeric precursor $[Pd(allyl)Cl]_2$ were reacted in a 2:1 molar ratio in methylene chloride at room temperature for two hours, the complexes **31a-b** were obtained in moderate to good yields (68-83%) as air stable yellow solids upon removal of the solvent, washing the residues with diethyl ether and drying under vacuum (Scheme 63).

Alternatively, palladium η^3-allyl complexes were prepared by treating one equivalent of $[Pd(allyl)Cl]_2$ with two equivalents of $AgBF_4$ in acetonitrile. After stirring the reaction mixture for ten minutes, the white precipitate of AgCl was filtered under argon and two equivalents of the ligands **4a-b** were added to the colorless solution of $[Pd(allyl)(CH_3CN)_2](BF_4)_2$. The reaction mixture was then stirred for one hour at room temperature and the solvent was removed under vacuum, the residue washed with diethyl ether and dried to give the complexes **32a-b** as air stable off white solids in good yields (75-92%) (Scheme 63).

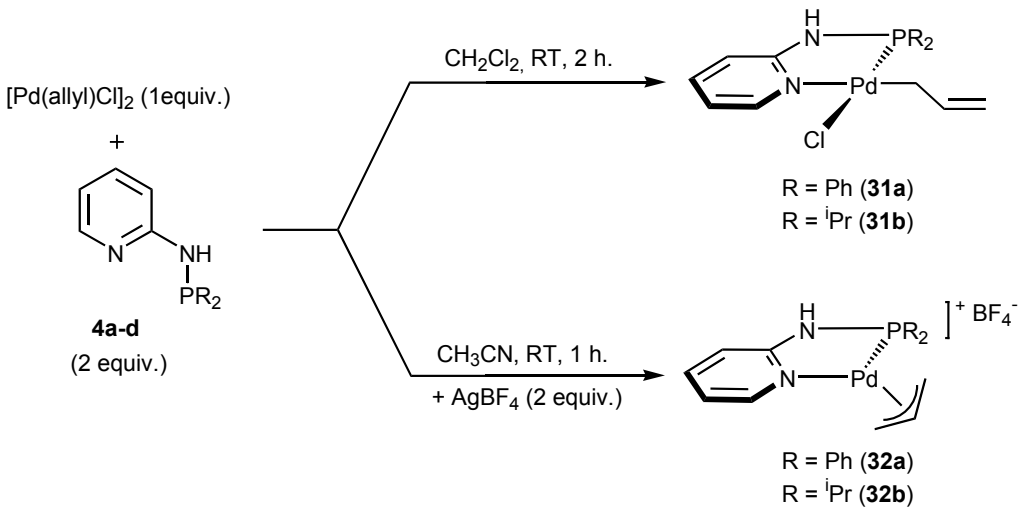

Scheme 63. Synthesis of the palladium η^1- and η^3 allyl complexes **31a-b** and **32a-b**

The complexes **29a-d**, **30**, **31a-b** and **32a-b** were characterized by ^1H, $^{31}P\{^1H\}$ and $^{13}C\{^1H\}$ NMR spectroscopy. In the ^1H NMR spectra of the complexes **29a-b**, the signals of the N*H* hydrogen atoms are strongly shifted to the low field when compared to those of the free ligands (**4a**: 5.93 ppm, **29a**: 10.11 ppm), while in the complexes **29c-d**, this shift difference is minimal ($\Delta\delta \approx 0.1$ ppm). In all the complexes the signal of the pyridine proton in the ortho position to the pyridine nitrogen atom is also shifted towards the low field, and gives rise to doublets between 8.83 and 9.17 ppm with coupling constants $^3J_{HH}$ between 5.2 and 6.2 Hz. The signals of the other hydrogen atoms show no shifts to the high or to the low field when compared to those of the free ligands **4a-d**. The $^{13}C\{^1H\}$ NMR spectra of the complexes **29a-d** show no special features, and the carbon atoms give rise to signals at similar shifts than those

of the free ligands. In the $^{31}P\{^1H\}$ NMR spectra, all the complexes show a single resonance between 79.5 (**29a**) and 125.7 ppm (**29b**) (Table 27). The signal of the proton in the ortho position to the nitrogen atom of the quinoline backbone in complex **30** is also shifted to the low field (**5a**: 8.96 ppm, **30**: 10.54 ppm) and gives rise to a doublet with a coupling constant $^3J_{HH}$ = 5.5 Hz. All the other signals appear within the expected ranges. In the $^{31}P\{^1H\}$ NMR spectrum, complex **30** gives rise to a single resonance at 115.7 ppm.

Table 27. Selected ^1H and $^{31}P\{^1H\}$ NMR resonances for the complexes **29a-d**

Complex	^1H (δ, [ppm], 20ºC)			$^{31}P\{^1H\}$ (δ, [ppm], 20ºC)
	N*H* (1H)	py^6 (1H)	$^3J_{HH}$ [Hz]	
29a	10.11	9.00	5.8	79.5
29b	8.90	8.83	5.2	125.7
29c	6.25	9.00	5.9	109.5
29d	6.27	9.17	6.2	118.5

In the neutral η^1-allyl complexes **31a-b**, the signals of the N*H* hydrogen atoms are strongly shifted to the low field compared to those of the free ligands; this shift is most likely due to the formation of hydrogen bonds between the N*H* proton and a chlorine atom attached to the palladium center of a neighboring molecule. These protons give rise to signals between 10.40 and 11.21 ppm. However, in the case of the cationic η^3-allyl complexes **32a-b**, the shift of the signals of these protons is smaller; they appear between 8.24 and 8.30 ppm. The py^6 signals for the complexes **31a-b** and **32a-b** are also shifted to the high field in respect to the signals of the free ligands; they give rise to singulets between 7.63 and 8.37 ppm. The hydrogen atom of the central carbon atom of the allyl groups gives rise to multiplets between 5.66 (**31b**) and 5.90 ppm (**31a** and **32a**); the signals of the other allylic protons appear as multiplets between 3.19 and 4.67 ppm in the case of the complexes **31a-b** and between 2.69 and 6.81 ppm in the complexes **32a-b**. In the $^{13}C\{^1H\}$ NMR spectra, the allyl groups appear at around 120 ppm (C*H*), 80 ppm (=CH_2) and 45 ppm (CH_2). All the complexes show a single resonance in the$^{31}P\{^1H\}$ NMR spectrum at 78.4 (**31a**), 115.3 (**31b**), 77.6 (**32a**) and 115.4 ppm (**32b**).

Table 28. Selected ^1H and $^{31}P\{^1H\}$ NMR resonances for the complexes **31a-b** and **32a-b**

Complex	^1H (δ, [ppm], 20ºC)			$^{31}P\{^1H\}$ (δ, [ppm], 20ºC)
	N*H* (1H)	py^6 (1H)	allyl C*H* (1H)	
31a	11.21	8.37	5.90	78.4
31b	10.40	8.23	5.66	115.3
32a	8.24	8.34	5.90	77.6
32b	8.30	7.63	5.70	115.4

Additionally, the complexes **30** and **32a-b** were characterized by X-ray crystallography. Suitable crystals were grown by slow diffusion of diethyl ether into saturated solutions of **30** and **32b** in methylene chloride and by slow evaporation of the solvent of a concentrated solution of **32a** in CD_2Cl_2. Structural views of **30**, **32a** and **32b** are depicted in Figures 61-63.

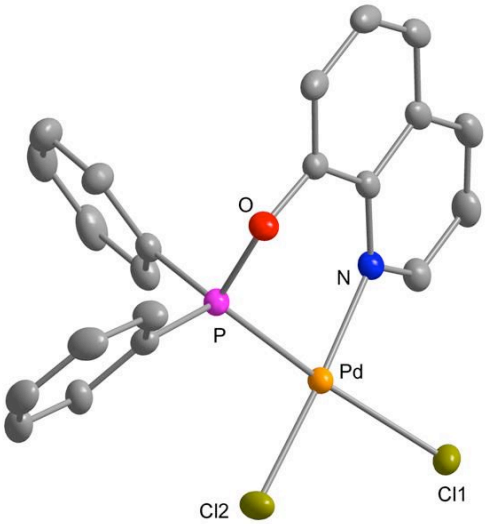

Figure 61. Structural view of [Pd(PN^{ox}-Ph)Cl_2] (**30**) showing 40% thermal ellipsoids (hydrogen atoms omitted for clarity). Selected bond lengths (Å) and angles (º): Pd-P 2.180(8), P-O 1.621(2), Pd-Cl(1) 2.3859(8), Pd-Cl(2) 2.2923(9), Pd-N 2.081(2), N-Pd-Cl(2) 176.37(7), P-Pd-Cl(1) 170.62(3).

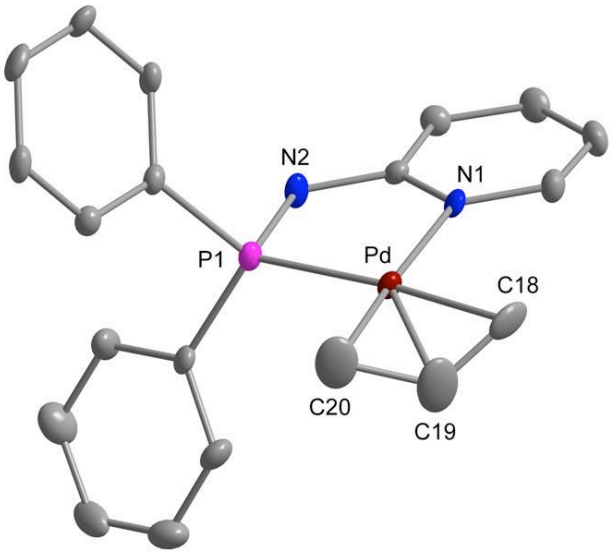

Figure 62. Structural view of [Pd(PN^{py}-Ph)(η^3-allyl)](BF_4) (**32a**) showing 50% thermal ellipsoids (hydrogen atoms and counterion omitted for clarity). Selected bond lengths (Å) and angles (º): Pd-N(1) 2.0876(14), Pd-P 2.2499(4), P-N(2) 1.6953(13), Pd-C(18) 2.1993(16), Pd-C(19) 2.160(2), Pd-C(20) 2.1115(19), N(1)-Pd-C(20) 173.34(7), P(1)-Pd-C(18) 170.89(5), N(1)-Pd-C(19) 137.50(18), C(18)-C(19)-C(20) 124.39.

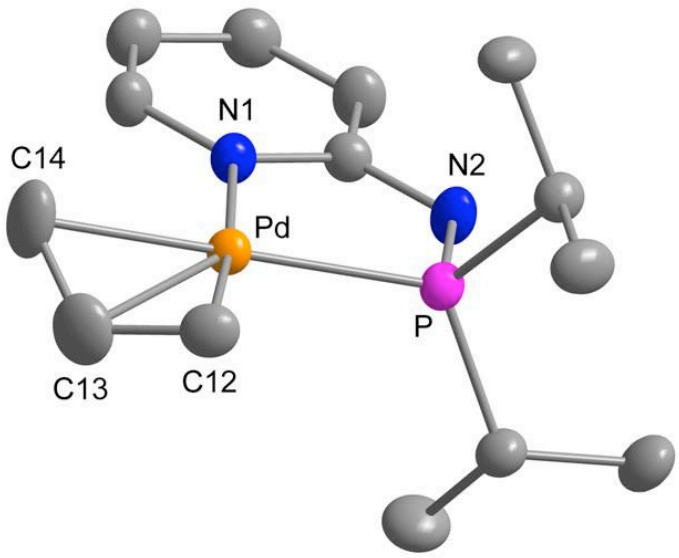

Figure 63. Structural view of [Pd(PN^{py}-^{i}Pr)(η^3-allyl)](BF_4) (**32b**) showing 60% thermal ellipsoids (hydrogen atoms and counterion omitted for clarity). Selected bond lengths (Å) and angles (º): Pd-N(1) 2.1098(19), Pd-P 2.2577(6), P-N(2) 1.694(2), Pd-C(12) 2.109(2), Pd-C(13) 2.168(3), Pd-C(14) 2.222(3), N(1)-Pd-C(12) 174.05(10), P(1)-Pd-C(14) 168.69(8), N(1)-Pd-C(13) 137.43(11), C(12)-C(13)-C(14) 121.57.

Complex **30** shows a distorted square planar geometry around the palladium center, with the aromatic quinoline backbone and the oxygen tether above this plane. The Pd-Cl bond length is slightly shorter for the chlorine atom in the trans position to the aromatic nitrogen atom than for the chlorine trans to the phosphorus atom (Pd-Cl(1) 2.3859(8) Å, Pd-Cl(2) 2.2923(9) Å). The Pd-N and Pd-P distances are similar to those observed in the complexes **21a-c**, which contain tridentate PNP ligands. Likewise, the deviation from the planarity in this complex can be seen along the P-Pd-Cl(1) axis, with an angle of 170.62(3)º; the N-Pd-Cl(2) bond angle has a value of 176.37(7)º.

The metal center in complexes **32a** and **32b** adopts also a distorted square planar geometry defined by the palladium, phosphorus and pyridine nitrogen atoms and by the lateral carbon atoms of the allyl groups. The Pd-P bond lengths are about 0.05 Å shorter in the complexes **32a-b** than in the PNP bearing complexes **21a-c** (**32a**: Pd-P 2.2499(4) Å, **21c**: Pd-P(2) 2.2985(5) Å), and the Pd-N bond distances are slightly longer in the allyl complexes than in the PNP complexes (**32a**: Pd-N 2.0876(14) Å, **21c**: Pd-N(1) 2.015(2) Å). The longer Pd-C(18) and Pd-C(14) bond lengths in complexes **32a** and **32b** compared to Pd-C(20) and Pd-C(12), respectively, reflect the larger trans influence of the phosphorus donor, and has been observed also in oxazoline-based palladium allyl complexes[136]. The distortion of the square planar

[136] (a) Braunstein, P.; Zhang, J.; Welter, R. *Dalton Trans.* **2003**, 507. (b) Zhang, J.; Braunstein, P.; Welter, R. *Inorg. Chem.* **2004**, *43*, 4172.

geometry can be appreciated along the N-Pd-C and P-Pd-C axis; the values of these bond angles are N(1)-Pd-C(20) 173.34(7) and P(1)-Pd-C(18) 170.89(5)º for **32a** and N(1)-Pd-C(12) 174.05(10) and P(1)-Pd-C(14) 168.69(8)º for **32b**. The allyl ligands make an angle of C(18)-C(19)-C(20) 124.39º in **32a** and C(12)-C(13)-C(14) 121.57º in **32b** with the plane containing the palladium, phosphorus and nitrogen atoms, which is also in agreement for related palladium η^3-allyl complexes containing other PN ligands[136].

Characterization

3.3.4 Palladium(II) catalyzed Suzuki Coupling

As stated in Section 2.5.1, pincer complexes have found numerous applications as homogeneous catalysts in various organic reactions, mostly due to their reactivity-to-stability properties. Palladium pincer complexes are among the most utilized transtition metal compounds as catalysts for several C-C and C-N bond forming reactions, such as the Suzuki-Miyaura coupling[19], the Heck reaction[19,20] or the Sonogashira coupling[110]. Among these, the cross coupling of organic halides with organoboron compounds (Suzuki-Miyaura coupling[137]) has become one of the most straightforward methods for C-C bond formation in organic synthesis. Its main advantage over other coupling reactions lies in the application of organoboron reagents as nucleophiles. These are generally thermally stable and inert towards air and moisture, non-toxic and can be handled more easily than other common reagents in coupling reactions: for example, the organostannanes used in Stille coupling reactions are highly toxic and air sensitive, just as the organomagnesium compounds used in the Grignard cross-coupling and the organoaluminum and organozinc reagents. However, organoboron compounds are not nucleophilic enough to react with electrophiles such as aryl and/or vinyl halides without additives and a transition metal catalyst. To increase their nucleophility the use of a base is required; the base coordinates to the boron atom, increasing the negative charge of the adjacent carbon atom, and facilitates its migration to an electrophilic centre. The presence of a metal center in the catalytic process is also necessary for the transmetalation step (see mechanism below), and besides palladium, nickel and platinum complexes are also known to catalyze the Suzuki coupling[138]. Nickel and platinum complexes are, however, less efficient catalysts.

A general view of the catalytic cycle of the Suzuki coupling of an aryl halide with phenylboronic acid is depicted in Scheme 64. Three are the key steps involved in this process:

---

[137] Miyaura, N.; Suzuki, A. *Chem. Rev.* **1995**, *95*, 2457.

[138] (a) Griffiths, C.; Leadbeater, N. E. *Tetrahedron Lett.* **2000**, *41*, 2487. (b) González-Bobes, F.; Fu, G. C. *J. Am. Chem. Soc.* **2006**, *128*, 5360.

the oxidative addition of the organic halide to the Pd(0) species, transmetalation, and the reductive elimination of the coupled product. Thus, the palladium center changes its oxidation from zero to two and back. The oxidative addition step is considered to be the rate determining step in the catalytic cycle. It is facilitated when the C-halide bond is electron poor and/or the palladium center is electron rich. The direct product of the oxidative addition is complex ***cis*-B**, which isomerizes immediately via different pathways to give ***trans*-B**. The reason for this isomerization is thought to be the strong *trans* effect of the phosphine ligands, which destabilise the bond between palladium and the *trans* standing substituents. Complex ***trans*-B** then undergoes a transmetalation process to give complex ***cis*-C** in which the halide is exchanged for the organic group attached to the boronic acid. ***Cis*-C** can then reductively eliminate the coupling product and regenerate the active species.

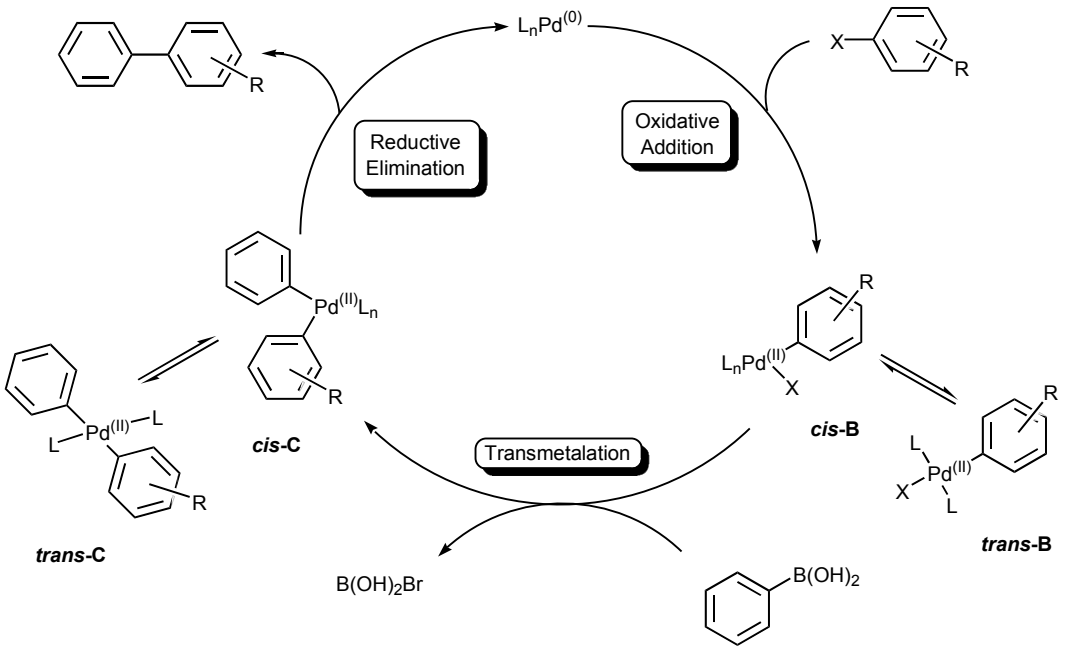

Scheme 64. General catalytic cycle for the palladium catalyzed Suzuki-Miyaura coupling

In the course of the catalytic cycle of the Suzuki reaction, it is generally assumed that the oxidation states of the palladium center switch from zero to two, both palladium species being stabilized by neutral electron donors, such as phosphines or *N*-heterocyclic carbenes. The catalytic activity of the different palladium complexes described in the literature does not depend, however, on the oxidation state of palladium in the precatalyst, and it is certain that the catalytically active species differs from the palladium compound used. Thus, the role of the coligands present in the reaction mixture in during the catalytic process is not to stabilize the palladium precursor, but to be labile enough to allow for the formation of the real catalytically active species and to create favorable electronic and steric conditions around the palladium center. Nevertheless, although the mechanism shown in Scheme 64 is generally accepted as a correct one, the question is how the palladium catalyst introduced in the reaction vessel is

converted into the active species. This is of course a very difficult task, because this process depends on the catalytic syste. In the case of palladium *N*-heterocyclic carbene[139] and pincer complexes[19b], however, some proposals have been made in the literature. In the case of the palladium pincer complexes, there is also some evidence that these are just favorable precursors for the formation of Pd(0) nanoparticles[24], which can act as the real catalysts, and the same proposal has been made to explain the activity of pincer complexes as catalysts in the Heck reaction[140].

Whatever the mechanism for the formation of the catalytically active species might be, since other palladium pincer complexes have been described in the literature to be effective catalysts in the Suzuki coupling, we were interested in investigating the activity of the palladium PNP and PCP complexes in this reaction. It is interesting to note that there are two different schools of thinking when it comes to define a catalyst, whatever the reaction it is it mediates, as a “good” one or as a “bad” one. For inorganic chemists, the issue of the catalyst amount is crucial: the aim is to synthesize molcules that can catalyze a reaction with as low catalyst loadings as possible without any activity loss. Organic chemists, on the other hand, prefer to focus on systems that are able to perform a reaction catalytically with as many different substrates as possible, even if this requires higher catalyst loadings. Although the primary concern when testing the palladium PNP and PCP complexes was to go as low as possible with the amount of catalyst used, we also focused on testing the complexes with different substrates; thus, the catalytic activity of the complexes was first tested under various conditions and catalyst loadings with three different aryl bromides as substrates: 4-bromoacetophenone (activated, easiest oxidative addition), 4-bromotoluene (“neutral”) and 4-bromoanisole (deactivated, hardest oxidative addition). Then, the most efficient catalyst was tested with other substrates.

Catalytic Activity of the Pd(II) PNP Complexes

For the PNP complexes, the model reaction along with the catalysts used as well as the optimized experimental conditions under which the reactions were performed are shown in Figure 64.

---

[139] Viciu, M.S.; Kelly, R. A., III; Stevens, E. D.; Naud, F.; Studer, M.; Nolan, S. P. *Org. Lett.* **2003**, *5*, 1479.

[140] Trzeciak, A. M.; Ziólkowski, J. *Coord. Chem. Rev.* **2006**, in press.

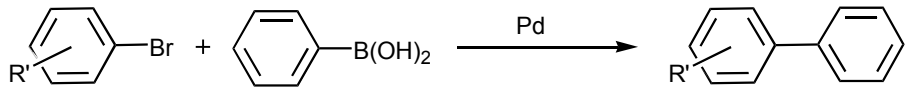

R' = $COCH_3$, CH_3, OCH_3

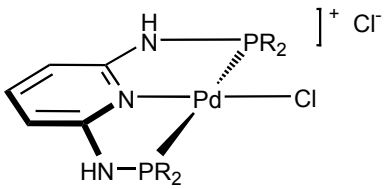

R = Ph: **21a**
R = ^{i}Pr: **21b**
R = ^{t}Bu: **21c**

Reaction time (h)	16
Temperature (ºC)	80
Solvent	1,4-Dioxane
Ar-Br (eqs.)	1.0
$PhB(OH)_2$ (eqs.)	1.5
Base (eqs.)	Cs_2CO_3 (2.0)

Figure 64. Optimized reaction conditions and catalysts used in the Suzuki-Miyaura coupling of phenylboronic acid with aryl bromides catalyzed by palladium PNP complexes

The yields of the catalytic reactions were determined by isolation of the final products by flash chromatography (silica gel, petroleum ether) and their characterization by ^{1}H NMR spectroscopy. The results of the catalytic reactions are summarized in Table 29.

Table 29. Yields of the Suzuki-Miyaura cross coupling of different aryl bromides with phenylboronic acid catalyzed by Pd(II) PNP complexes[a].

Entry	R'	Catalyst	Catalyst Loading (mol%)	Isolated Yield (%)[b]	TON[c]	TOF (h^{-1})[d]
1	4-CH_3	**21a**	2	91	46	3
2	4-CH_3	**21b**	2	90	45	3
3	4-CH_3	**21c**	2	60	30	2
4	4-CH_3	**21a**	2	65[e]	33	0.5
5	4-CH_3	**21a**	2	90	46	15
6	4-$COCH_3$	**21a**	2	98	49	3
7	4-$COCH_3$	**21a**	2	98[f]	49	16
8	4-$COCH_3$	**21a**	0.5	98	196	12
9	4-$COCH_3$	**21a**	0.05	97	1940	121
10	4-OCH_3	**21a**	2	98	49	3
11	4-OCH_3	**21b**	2	93	47	3
12	4-OCH_3	**21a**	2	96[f]	48	16
13	4-OCH_3	**21a**	0.5	95	190	12
14	4-OCH_3	**21a**	0.05	87	1740	109

[a]Unless stated otherwise, the experimental conditions are those described in Figure 64. [b]The isolated yield is the average of at least two experiments. [c]Defined as mol product per mol catalyst. [d]Defined as mol product per mol catalyst and reaction time. [e]The reaction was stirred at RT for 70 h. [f]The reaction was stirred for 3 h.

As can be seen from the results depicted in Table 29, both **21a** and **21b** exhibit similar activities as catalysts in the coupling of neutral (entries 1-2) and deactivated (entries 10-11) substrates. Due to the lower cost of chlorodiphenylphosphine, **21a** was the catalyst of choice for further experiments. In the case of **21c**, its lower activity (entry 3) may be attributed to the presence of the basic, sterically demanding *tert*butyl phosphines, which might impede the formation of the catalytically active Pd(0) species. The catalyst is also active at room temperature, but longer reaction times are needed to reach reasonable conversions and the yield obtained is not as high as when the reaction is performed at higher temperatures (entry 4). On the other hand, the reaction reaches its maximum conversion already after three hours at 80ºC (entries 7 and 12). The catalyst loading does needs not be as high as 2 mol%, and it can be lowered up to 0.05 mol% for activated and deactivated substrates with a minimal yield diminishment (entries 8, 9, 13 and 14); however, if the catalyst loading is lowered any further, the yields drop significantly and only traces of the product are recovered. **21a** was then used as a catalyst in the coupling of phenylboronic acid with other alkyl and aryl bromides; the results are summarized in Table 30.

Table 30. Yields of the Suzuki-Miyaura cross coupling of phenylboronic acid with various alkyl and aryl bromides catalyzed by **21a**[a].

Entry	Bromide	Isolated Yield (%)[c]	TON[d]	TOF (h^{-1})[e]
1	4-nitro-4-bromonitrobenzenebenzene	94	47	16
2	2,6-dimethylbromobenzene	66	33	11
3	2,6-dimethylbromobenzene	78[b]	39	13
4	1-bromo-2-ethylbenzene	83	42	3
5	1-bromododecane	0	0	0
6	1-bromododecane	93[b]	47	3
7	2-bromopyridine	94	47	16

[a]The reaction conditions are the same as the ones depicted in Figure 64 except the reaction time, which was 3 h.; the catalyst loading was 2 mol%. [b]The reaction was stirred for 16 h. [c]The isolated yield is the average of at least two experiments. [d]Defined as mol product per mol catalyst. [e]Defined as mol product per mol catalyst and reaction time.

The results show that **21a** can be used efficiently as a catalyst in the coupling of different alkyl and aryl bromides with phenylboronic acid. Substituted as well as sterically hindered aryl bromides can be coupled (entries 1-4), but also heterocycles and alkyl bromides, even if these bear β-hydrogen atoms (entries 5-7). In the case of sterically hindered and alkyl substrates, though, the reaction takes longer times in order to achieve reasonable yields (entries 3 and 6).

The Pd(II) PNP complexes **21a-c** can be used as catalysts in the Suzuki-Miyaura coupling, but their use is limited to aryl and alkyl bromides, since all attempts to apply them to

the coupling of aryl chlorides with phenylboronic acid failed. There is some evidence that pincer complexes are mere precatalysts to the catalytically active species, which is suggested to be some kind of Pd(0) species. Whatever the real active species may be, the stability imparted by the PNP ligands to the Pd(II) center might hamper its formation; this could explain why these complexes are not able to catalyze the coupling of aryl chlorides. It has to be noted, however, that palladium black is visible in the reaction vessel upon completion of the catalytic reaction. This could account for the low turnover numbers and turnover frequencies observed for the palladium(II) PNP complexes.

Catalytic activity of the Palladium(II) PCP Complexes

Some of the Pd(II) PCP complexes were tested as catalysts in the Suzuki coupling of aryl bromides with phenylboronic acid. Due to the large number of complexes prepared during this work, only representative ones were tested: for example, although both chloride and trifluoroacetate complexes were tested, only those with phenyl and *tert*butyl substituents, but not those with *iso*propyl phosphines were used, in order to see the effect that a sterically demanding, strongly electron donating phosphine would have on the catalytic performance of the complexes. The reaction conditions are shown in Figure 65; this time, although the reaction time remained the same, a different base, solvent and temperature were used.

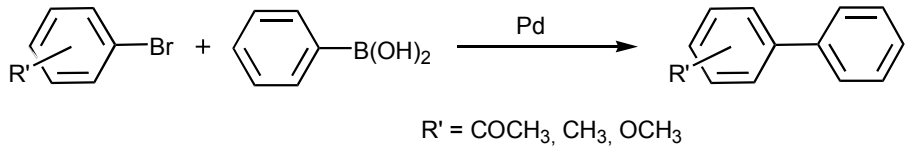

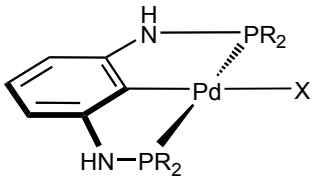

R = Ph, X = Cl: **25a**
R = ^{t}Bu, X = Cl: **25c**
R = Ph, X = TFA: **26a**
R = ^{t}Bu, X = TFA: **26c**

Reaction time (h)	16
Temperature (ºC)	110
Solvent	Toluene
Ar-Br (eqs.)	1.0
$PhB(OH)_2$ (eqs.)	1.5
Base (eqs.)	K_2CO_3 (2.0)

Figure 65. Optimized reaction conditions and catalysts used in the Suzuki-Miyaura coupling of phenylboronic acid with aryl bromides catalyzed by palladium PCP complexes

Like in the case of the PNP complexes, the yields of the reactions were determined by isolation of the final products by flash chromatography (silica gel, petroleum ether) and their characterization with ^{1}H NMR spectroscopy. The catalytic activity of the PCP complexes tested is summarized in Tables 31 and 32.

Table 31. Yields of the Suzuki-Miyaura cross coupling of aryl bromides with phenylboronic acid catalyzed by the Pd(II) PCP complexes **25a** and **25c**[a].

Entry	R'	Catalyst	Catalyst Loading (mol%)	Isolated Yield (%)[b]	TON[c]	TOF (h^{-1})[d]
1	4-CH_3	**25a**	0.01	>99	10.000	625
2	4-CH_3	**25a**	0.001	72	72.000	4.500
3	4-CH_3	**25a**	0.0001	44	440.000	27.500
4	4-$COCH_3$	**25a**	0.01	>99	10.000	625
5	4-$COCH_3$	**25a**	0.001	>99	100.000	6.250
6	4-$COCH_3$	**25a**	0.0001	>99	1.000.000	62.500
7	4-$COCH_3$	**25a**	0.00001	97	9.700.000	625
8	4-$COCH_3$	**25c**	0.01	>99	10.000	625
9	4-$COCH_3$	**25c**	0.001	0	0	0
10	4-OCH_3	**25a**	0.01	>99	10.000	625
11	4-OCH_3	**25a**	0.001	77	77.000	4.813
12	4-OCH_3	**25a**	0.0001	18	180.000	11.250
13	4-OCH_3	**25c**	0.01	>99	10.000	625
14	4-OCH_3	**25c**	0.001	0	0	0

[a]Unless stated otherwise, the experimental conditions are those described in Figure 65. [b]The isolated yield is the average of at least two experiments. [c]Defined as mol product per mol catalyst. [d]Defined as mol product per mol catalyst and reaction time.

As can be seen from Table 31, the Pd(II) PCP complexes are much better catalysts for the coupling af aryl bromides with phenylboronic acid than their PNP analogues; while with these the catalyst loading could be lowered to 0.05 mol%, with the PCP complexs it is possible to go down to catalyst loadings as low as 0.00001 mol% for the activated substrate 4-bromoacetophenone and still obtain almost quantitative yields (entry 7). In the case of neutral and deactivated substrates, catalyst loadings of 0.001 mol% still give high yields (entries 2 and 11). Another measure of the elevated activity of these complexes are the turnover frequencies (TOFs). With the PCP complexes, turnover frequencies as high as 600.000 h^{-1} can be achieved, meaning that the catalyst undergoes a whole catalytic cycle 600.000 times per hour, that is, 170 times per second. These figures (catalyst loadings and TOFs) are among the best ever reported for pincer complexes in the Suzuki reaction[3]. It has to be noted that the *tert*butyl complex **25c** is less active than its phenyl containing counterpart **25a**; just like in the case of the PNP complexes, the steric as well as the electronic properties of the *tert*butyl group may be the cause for such a lower activity. Interestingly, the catalyst remains active after the reaction is complete; upon addition of more substrates to the reaction of 4-bromotoluene with phenylboronic acid catalyzed by 0.01 mol% **25a**, the reaction is resumed, leading again to the coupling product in a quantitative yield at essentially the same rate. Contrarily to the reactions catalyzed by Pd(II) PNP complexes, no palladium black can be observed in the reaction vessel once the catalysis is terminated.

Table 32. Yields of the Suzuki-Miyaura cross coupling of different aryl bromides with phenylboronic acid catalyzed by Pd(II) PCP complexes **26a** and **26c**[a].

Entry	R'	Catalyst	Catalyst Loading (mol%)	Isolated Yield (%)[b]	TON[c]	TOF (h^{-1})[d]
1	4-CH_3	**26a**	0.01	70	7.000	438
2	4-$COCH_3$	**26a**	1.0	>99	100	6.25
3	4-$COCH_3$	**26a**	0.1	>99	1.000	62.5
4	4-$COCH_3$	**26a**	0.01	>99	10.000	625
5	4-$COCH_3$	**26a**	0.001	15	15.000	938
6	4-$COCH_3$	**26c**	0.01	>99	10.000	625
7	4-$COCH_3$	**26c**	0.001	>99	100.000	6.250
8	4-OCH_3	**26a**	1.0	>99	100	6.25
9	4-OCH_3	**26a**	0.1	88	880	55
10	4-OCH_3	**26c**	0.01	68	6.800	425

[a]Unless stated otherwise, the experimental conditions are those described in Figure 65. [b]The isolated yield is the average of at least two experiments. [c]Defined as mol product per mol catalyst. [d]Defined as mol product per mol catalyst and reaction time.

In the case of the trifluoroacetic complexes **26a** and **26c**, their activity is lower than the chloride complexes **25a** and **25c**, but they are still superior than the Pd(II) PNP complexes. This is somewhat surprising, since TFA is more labile than Cl, and a higher activity of **26a** and **26c** could be expected; however, since no details are known about the catalytic cycle or the catalytically active species, any interpretation of the results in such terms would be merely speculative. Catalyst loadings of 0.001 mol % can be used with quantitative yields in the case of activated substrates, while the limit is at 0.01 mol% catalyst loading for neutral and deactivated substrates. Although the TOFs do not reach those observed for the chloride complexes, they are still high. Finally, the activity of **25a** as a catalyst in the coupling of phenylboronic acid with other bromides was also tested; the results are summarized in Table 33.

Table 33. Yields of the Suzuki-Miyaura cross coupling of phenylboronic acid with various alkyl and aryl bromides catalyzed by **25a**[a].

Entry	Bromide	Isolated Yield (%)[b]	TON[c]	TOF (h^{-1})[d]
1	4-nitrobromobenzene	81	8.100	507
2	1-bromo-2-ethylbenzene	65	6.500	407
3	1-bromododecane	74	7.400	463
4	2-bromopyridine	68	6.800	425

[a]Unless stated otherwise, the experimental conditions are those described in Figure 65; the catalyst loading is 0.01 mol%. [b]The isolated yield is the average of at least two experiments. [c]Defined as mol product per mol catalyst. [d]Defined as mol product per mol catalyst and reaction time.

The results in Table 33 show that the activity of **25a** is not limited to the coupling of *para*-substituted aryl bromides; heterocyclic, sterically hindered and also alkyl bromides can be coupled with reasonable yields with 0.01 mol% catalyst. Compared to [Pd(PNP-Ph)Cl]Cl (**21a**), where similar yields were obtained using 2 mol% catalyst, this is another evidence for the better performance of the PCP complexes. However, despite their remarkable activity and the fact that very low catalyst loadings can be used, the PCP complexes were not successful in the coupling of aryl chlorides with phenylboronic acids either.

Finally, the catalytic acitvity of palladium(II) phosphoramidite PCP pincer complexes in the Suzuki-Miyaura and Heck couplings has also been studied in our research group[73]; the results, indicate that these complexes are less effective catalysts than the palladium PCP pincer complexes **25a** and **25b**.

3.3.5 Summary

Cationic, tetracoordinated nickel(II) PNP complexes could only be prepared with aryl- and alkyl-phosphine containing PNP ligands; when phosphoramidite ligands were used, neutral, pentacoordinated nickel(II) complexes were obtained. The stioichiometry of the reaction and the isolation of a reaction intermediate and of a ligand decomposition product made it possible to tentatively suggest a mechanism for the formation of these complexes. This mechanism proceeds via the cleavage of the two P-N bonds of one molecule of a PNP ligand followed by the oxidation of the released neutral phosphines to anionic phosphinite ligands. Tetracoordinated, neutral nickel(II) PCP ligands were prepared by direct metalation of the ligands with $NiCl_2 \cdot 6H_2O$.

Palladium and platinum pincer complexes both with aminophosphine and phosphoramidite moieties were also prepared; cationic and neutral complexes were obtained when the PNP or the PCP ligands were used, respectively. The palladium(II) PCP complexes could be prepared both by direct metalation of the ligands and by oxidative addition. The same decomposition reaction that led to pentacoordinated nickel(II) complexes was observed in the case of the palladium(II) PNP complexes, but the cleavage of the P-N bond of the ligands takes place much more slowly.

Nickel and palladium PN complexes were also prepared; in the case of the nickel complexes, their characterization revealed that they possess different coordination geometries in the solid state and in solution, a feature that was supported by theoretical calculations. η^1- and η^3-palladium allyl complexes were synthesized by reacting the dimeric precursor $[Pd(allyl)(CH_3CN)_2](BF_4)_2$ with the PN ligands both in the absence and in the presence of a silver salt as halide scavenger.

Several palladium(II) PNP and PCP pincer complexes were tested as catalysts in the Suzukki-Miyaura coupling of aryl and alkyl bromides with phenylboronic acid; while the PNP complexes turned out to be mediocre catalysts, the PCP complexes showed very high activities and were able to catalyze the coupling of neutral, deactivated and activated bromides with phenylboronic acid even at very low catalyst loadings.

3.4 Copper(I) catalyzed diastereoselective formation of oxazolines and N-sulfonyl-2-imidazolines

Oxazolines and imidazolines are interesting organic frameworks due to their applicability in the synthesis of biologically active compounds (e.g. β-hydroxy-α–amino acids, α,β-diamino acids[141] and β–substituted serines[142]) and their presence in the structure of several biologically active natural products, such as marine cyclopeptides[143] (e.g. Bistratamides C and D[144]).

The reaction of aldehydes and imines with isocyanocarboxylates is one of the methods for the preparation of oxazolines and imidazolines bearing a heterocyclic 1,3-*O,N*- and 1,3-*N,N*-ring system, respectively (Scheme 65).

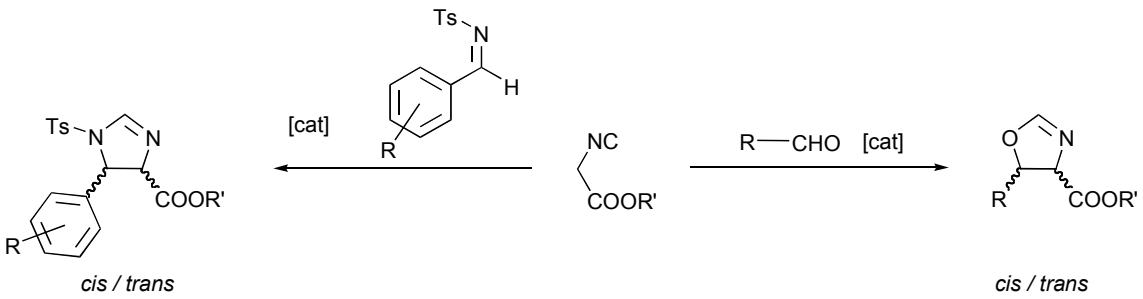

Scheme 65. Reaction between isocyanoacetates and aldehydes (right) or imines (left) yielding oxazolines and *N*-sulfonyl-2-imidazolines, respectively

Whereas there are several examples covering the synthesis of oxazolines using strong proazaphosphatrane bases[145] and transition metal complexes such as Au(I)[146], Ag(I)[147],

---

[141] (a) Potts, K. T. in *Comprehensive Heterocyclic Chemistry*, Katritzky, A., Rees, C. W., Eds.; Pergamon Press: Oxford, 1984; Vol. 5, p 457. (b) Grimmett, M. R. *Adv. Heterocycl. Chem.* **1980**, *27*, 241-326. (c) Volkmann, R. A. in *Comprehensive Organic Synthesis*, Trost, B. M., Fleming, I., Eds.; Pergamon Press: Oxford, 1991; Vol. 1, p 355. (d) Hoppe, D. *Angew. Chem. Int. Ed.* **1974**, *13*, 789-804. (e) Matsumoto, K.; Moriya, T.; Suzuki, M. *Synth. Org. Chem. Jpn.*, **1985**, *43*, 764-776.

[142] (a) Hining, H.; Seufer-Waserthal, P.; Weber, H. *Tetrahedron* **1990**, 46, 3841-3850. (b) Gaparski, C. M.; Miller, M. J. *Tetrahedron* **1991**, 47, 5367-5378. (c) Togni, A.; Pastor, S. D.; Ribs, G. *J. Organomet. Chem.* **1990**, 381, C21-C25.

[143] For reviews, see: (a) Wipf, P. *Chem. Rev.* **1995**, *95*, 2115-2134. (b) Michael, J. P.; Pattenden, G. *Angew. Chem. Int. Ed. Engl.* **1993**, *32*, 1-23 and references therein.

[144] (a) Foster, M. P.; Concepción, G. P.; Caraan, G. B.; Ireland, C. M. *J. Org. Chem.* **1992**, *57*, 6671-6675. (b) Aguilar, E.; Meyers, A. I. *Tetrahedron Lett.* **1994**, *35*, 2477-2480. (c) Downing, S. V.; Aguilar, E.; Meyers, A. I. *J. Org. Chem.* **1999**, *64*, 826-831.

[145] Kisanga, P.; Ilankumaran, P.; Verkade, J. G. Tetrahedron Lett. 2001, 42, 6263-6266.

Pd(II)[116,148] and Pt(II)[149] complexes, there have been few reports on the catalytic reaction of imines with isocyanocarboxylates due to the low reactivity of imines. These include the use of Au(I)[150] and Ru(II)[151] complexes. It has to be noted that imidazolines have also been prepared via a multicomponent reaction (MCR) between amines, aldehydes and isocyanides using AgOAc as the catalyst[152]. However, such methods require the use of relatively expensive transition metals, and long reaction times (typically over 16 hours) are needed in order to achieve reasonable yields. Surprisingly, the use of copper compounds, as copper belongs to the same group as the established catalysts (i.e. silver and gold) for the aldol synthesis of oxazolines and imidazolines, was reported only once over 30 years ago in the literature[153]. In this case, when Cu_2O was used as the catalyst, 1:1 mixtures of *cis*- and *trans*-oxazolines were obtained.

This problem could be easily solved by using a different copper(I) salt, CuCl: the reaction between benzaldehyde and methyl isocyanoacetate now proceeds in 80% yield within two hours with the selective formation of the *trans* product. The yield of the reaction was improved to quantitative by adding triphenylphosphine in a 1:2 ratio in respect to CuCl (Table 34, entry 1). The same procedure was then applied to other aldehydes (entries 2-8). In all cases, the reaction proceeded quantitatively to give *trans* oxazolines with over 86% diastereoselectivity both with aliphatic and aromatic aldehydes. All the reactions were carried out in methylene chloride in the presence of 10 mol% $(^iPr)_2EtN$, using 5 mol% copper(I) chloride and 10 mol% triphenylphosphine as the catalysts. The products were isolated by column chromatography (silica gel, CH_2Cl_2) and the *trans:cis* ratio was determined by ^1H NMR

---

[146] (a) Hayashi, T. *Pure Appl. Chem.* **1988**, *60*, 7-12. (b) Ito, Y.; Sawamura, M.; Hayashi, T. *J. Am. Chem. Soc.* **1986**, *108*, 6405-646. (c) Ito, Y.; Sawamura, M.; Hayashi, T. *Tetrahedron Lett.* **1987**, *28*, 6215-6218. (d) Pastor, S. D.; Togni, A. *J. Am. Chem. Soc.* **1989**, *111*, 2333-2334. (e) Yoshihiko, I.; Sawamura, M.; Shirakawa, E.; Hayashizaki, K.; Hayashi, T. *Tetrahedron* **1988**, *44*, 5253-5262. (f) Togni, A.; Pastor, S. D.*; J. Org. Chem.* **1990**, *55*, 1649-1664. (g) Pastor, S. D.; Togni, A.; *Tetrahedron Lett.* **1990**, *31*, 839-840. (h) Hayashi, T.; Sawamura, M.; Yoshihiko, I. *Tetrahedron* **1992**, *48*, 1999-2012.

[147] (a) Sawamura, M.; Hamashima, H.; Ito, Y. *J. Org. Chem.* **1990**, *55*, 5935-5936. (b) Hayashi, T.; Uozumi, Y.; Yamazaki, A.; Sawamura, M.; Hamashima, H.; Ito, Y. *Tetrahedron Lett.* **1991**, *32*, 2799-2802.

[148] (a) Longmire, J. M.; Zhang, X.; Shang, M. *Organometallics* **1998**, *17* 4374-4379. (b) Motoyama, Y.; Kawakami, H.; Shimozono, K.; Aoki, K.; Nishiyama, H. *Organometallics* **2002**, *21*, 3408-3416. (c) Fossey, J. S.; Richards, C. J. *Organometallics* **2002**, *21*, 5259-5264. (d) Gosiewska, S.; Veld, M. H.; De Pater, J. M.; Bruijnincx, P. C. A.; Lutz, M.; Spek, A. L.; Van Koten, G.; Gebbink, K.; Robertus, J. M. *Tetrahedron: Assymetry* **2006**, *17*, 674-686. (e) Giménez, R.; Swager, T. M. *J. Mol. Cat. A* **2001**, *166*, 265-273.

[149] (a) Horne, D. A.; Yakusijin, K.; Büchi, G. Heterocycles 1994, 39, 139-153.

[150] (a) Hayashi, T.; Kishi, E.; Soloshonok, V.; Uozumi, Y. *Tetrahedron Lett.* **1996**, *37*, 4969-4972. (b) Zhou, X.-T.; Lin, Y.-R.; Dai, L.-X.; Sun, J.; Xia, L.-J.; Tang, M.-H. *J. Org. Chem.* **1999**, *64*, 1331-1334. (c) Zhou, X.-T.; Lin, Y.-R.; Dai, L.-X. *Tetrahedron: Assymetry* **1999**, *10*, 855-862.

[151] Lin, Y.-R.; Zhou, X.-T.; Dai, L.-X.; Sun, J. *J. Org. Chem.* **1997**, *62*, 1799-1803.

[152] (a) Bon, R. S.; Hong, C.; Bouma, M. J.; Schmitz, R. F.; de Kanter, F. J. J.; Lutz, M.; Spek, A. L.; Orru, R. V. A. *Org. Lett.* **2003**, *5*, 3759-3762. (b) Bon, R. S.; van Vliet, B.; Sprenkels, N. E.; Schmitz, R. F.; de Kanter, F. J. J.; Stevens, C. V.; Swart, M.; Bickelhaupt, F. M.; Groen, M. B.; Orru, R. V. A. *J. Org. Chem.* 2005, *70*, 3542-3553.

[153] Saegusa, T.; Ito, Y.; Kinoshita, H.; Tomita, S. *J. Org. Chem.* **1971**, *36*, 3316.

spectroscopy. In the absence of copper salt, the reaction did not take place under otherwise the same reaction conditions.

Table 34. $CuCl/PPh_3$ catalyzed synthesis of oxazolines from aldehydes and methylisocyanoacetate[a].

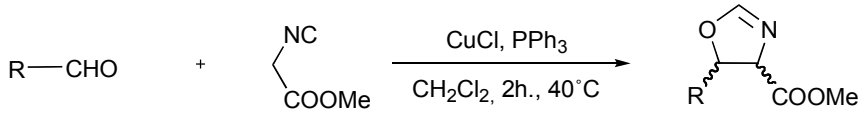

Entry	R	Yield[b] (%)	Ratio[c] of trans/cis
1	phenyl	>99	>99/<1
2	4-chlorophenyl	>99	86/14
3	4-nitrophenyl	>99	90/10
4	4-methoxyphenyl	>99	91/9
5	2-chloro-5-nitrophenyl	>99	86/14
6	2-chloro-6-fluorophenyl	>99	96/4
7	2-methylphenyl	>99	88/12
8	isobutyl	>99	>99/<1

[a]Reaction conditions: 1 equiv. aldehyde, 1 equiv. methyl isocyanoacetate, 10 mol% $(^iPr)_2EtN$, 5 mol% CuCl, 10 mol% PPh_3, CH_2Cl_2, 40ºC, 2 h. [b]Isolated yield by silica gel column chromatography. [c]Determined by ^1H NMR spectroscopy.

For the synthesis of imidazolines, when the *N*-aryl-substituted benzaldehyde-*N*-phenylimine was used, only traces of the coupling product were obtained; due to the low reactivity of imines towards nucleophilic addition, a strong electron withdrawing group, *i.e.,* tosyl, was introduced on the nitrogen atom of the imines in order to activate the C=N bond. If the reaction is performed solely with CuCl, a nearly 50:50 *trans:cis* ratio was observed for the resulting imines (Table 35, entries 1-2). Contrary to the synthesis of oxazolines, where PPh_3 only seemed to influence the yield of the reaction, the use of an additive proved to be crucial for the diastereoselective preparation of imidazolines. It is known that, depending on the metal salt/ligand ratio, CuCl can form several complexes with different stoichiometries and geometries with triphenylphosphine[154]. The trigonal planar complex $[(PPh_3)_2CuCl]$, formed in situ in the course of the reaction, seems to offer the best steric and electronic properties for the reaction between *N*-sulfonylimines and methylisocyanoacetate: when CuCl and PPh_3 were used in a 1:2 ratio, the reaction proceeded selectively to give exclusively the *trans* product (Table 35, entry 4). Other $CuCl:PPh_3$ ratios, including the use of equimolar amounts of metal salt and phosphine and larger excesses of phosphine, resulted either in decreased yields or in decreased diastereoselectivities, probably due to the formation of copper complexes with different geometries (entries 3-7). When these conditions were applied to other *N*-sulfonylimines,

[154] Kräuter, T.; Neumüller, B. *Polyhedron* **1996**, *15*, 2851.

however, the diastereoselectivity decreased (entry 5). Thus, an optimization of the catalyst was performed by screening the activity of several CuCl/Ligand systems (Table 35).

Table 35. Ligand optimization in the CuCl catalyzed synthesis of *N*-sulfonyl-2-imidazolines[a].

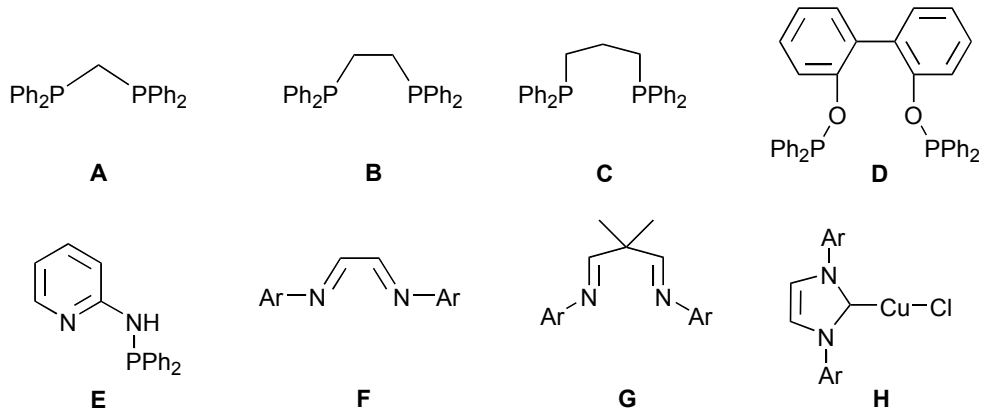

Ar: 2,6-^{i}Pr-Ph

Entry	R	Catalyst	Yield[b] (%)	Ratio[c] of trans/cis
1	phenyl	CuCl (5 mol%)	>99	52/48
2	4-chlorophenyl	CuCl (5 mol%)	>99	40/60
3	phenyl	CuCl (5 mol%) + PPh_3 (5 mol%)	54	84/16
4	phenyl	CuCl (5 mol%) + PPh_3 (10 mol%)	>99	>99/<1
5	4-chlorophenyl	CuCl (5 mol%) + PPh_3 (10 mol%)	96	64/36
6	phenyl	CuCl (5 mol%) + PPh_3 (15 mol%)	97	90/10
7	phenyl	CuCl (5 mol%) + PPh_3 (20 mol%)	75	84/16
8	phenyl	CuCl (5 mol%) + $P(OPh)_3$ (10 mol%)	>99	83/17
9	phenyl	CuCl (5 mol%) + **A** (5 mol%)	31	98/2
10	phenyl	CuCl (5 mol%) + **B** (5 mol%)	76	97/3
11	phenyl	CuCl (5 mol%) + **C** (5 mol%)	92	86/14
12	phenyl	CuCl (5 mol%) + **D** (5 mol%)	57	67/33
13	phenyl	CuCl (5 mol%) + **E** (5 mol%)	14	98/2
14	phenyl	CuCl (5 mol%) + **F** (5 mol%)	Traces	-
15	phenyl	CuCl (5 mol%) + **G** (5 mol%)	Traces	-
16	phenyl	**H** (5 mol%)	>99	96/4
17	4-chlorophenyl	**H** (5 mol%)	>99	95/5

[a]Reaction conditions: 1 equiv. imine, 1 equiv. methyl isocyanoacetate, catalyst (5-20 mol%), CH_2Cl_2, 40ºC, 2 h. [b]Isolated yield by silica gel column chromatography. [c]Determined by ^{1}H NMR spectroscopy.

The best catalyst turned out to be the *N*-heterocyclic carbene complex **H**[155], which gave good yields and selectivities for two different *N*-sulfonylimines (Table 35, entries 16 and 17).

[155] Kaur, H.; Zinn, F. K.; Stevens. E. D.; Nolan, S. P. *Organometallics* **2004**, *23*, 1157.

With these conditions in hand, several other *N*-sulfonylimines were tested, all of which gave the corresponding imidazolines in a quantitative yield and over 85% *trans* diastereoselectivity (Table 36). In this case, the reactions were also carried out in methylene chloride in the presence of 5 mol% **H** as the catalyst, but no $(^{i}Pr)_2EtN$ was used. The products were isolated by column chromatography and the *trans:cis* ratio was determined by ^{1}H NMR spectroscopy. Like in the case of the oxazoline synthesis, no reaction took place if the reaction was performed in the absence of copper catalyst.

Table 36. Copper(I) catalyzed synthesis of *N*-sulfonyl imidazolines from *N*-sulfonylimines and methylisocyanoacetate[a].

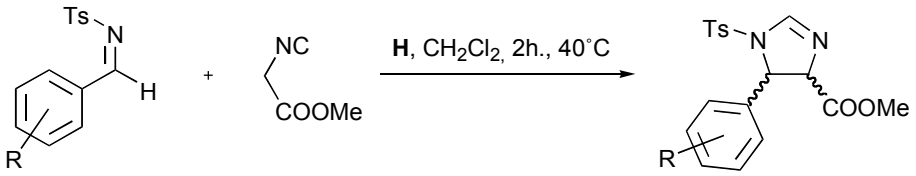

Entry	R	Yield[b] (%)	Ratio[c] of trans/cis
1	phenyl	>99	96/4
2	4-chlorophenyl	>99	95/5
3	4-nitrophenyl	>99	85/15
4	4-methoxyphenyl	>99	76/24
5	2-chloro-5-nitrophenyl	>99	89/11
6	2-chloro-6-fluorophenyl	>99	85/15

[a]Reaction conditions: 1 equiv. imine, 1 equiv. methyl isocyanoacetate, 5 mol% **H**, CH_2Cl_2, 40ºC, 2 h. [b]Isolated yield by silica gel column chromatography. [c]Determined by ^{1}H NMR spectroscopy.

4 Experimental Section

4.1 Abbreviations

AN / CH_3CN	acetonitrile
BArF	tetrakis[(3,5-trifluoromethyl)phenyl]borate
bipy	2,2' bipyridine
^{t}Bu	tert-butyl
n-BuLi	*n*-butyllithium
CCDC	Cambridge Structural Database
CH_2Cl_2	methylene chloride
$CHCl_3$	chloroform
CH_3NO_2	nitromethane
COD	1,5 cyclooctadiene
DEPT	Distorsionless Enhancement by Polarisation Transfer
DME	1,2 dimethoxyethane
DMF	N,N-dimethylformamide
DMSO	dimethyl sulfoxide
EDA	ethyl diazoacetate ($N_2CHCOOEt$)
EtOH	ethanol
Et_2O	diethylether
MeOH	methanol
MW	Molecular Weight
NEt_3	triethylamine
NMP	N-methylpyrrolidone
PCl_3	phosphorus trichloride
Ph	phenyl
^{i}Pr	isopropyl
Py	pyridine
PE	petroleum ether
RT	Room Temperature
terpy	2,2':6',2'' terpyridine
THF	tetrahydrofurane
TFA	trifluoroacetic acid / trifluoroacetate

4.2 General

Unless stated differently, all manipulations were performed under an inert atmosphere of argon by using Schlenk techniques. The solvents were purified according to standard procedures[156]. Deuterated solvents were purchased from Aldrich and Eurisotop, degassed using the freeze-pump-thaw technique and stored over 4Å molecular sieves. ^{1}H, $^{13}C\{^{1}H\}$, and $^{31}P\{^{1}H\}$ NMR spectra were recorded on a Bruker AVANCE-250 spectrometer operating at 250.13 (^{1}H), 62.86 (^{13}C) and 101.26 (^{31}P) MHz and were referenced to $SiMe_4$ and H_3PO_4 (85%), respectively. IR spectra were recorded on a Perkin Elmer 16PC-IR spectrometer.

4.3 Computational Details

All calculations were performed using the Gaussian03 software package on the Silicon Graphics Origin 2000 of the Vienna University of Technology[157]. The geometry and energy of the model complexes and the transition states were optimized at the B3LYP level with the Stuttgart/Dresden ECP (SDD) basis set[158] to describe the electrons of the metal centers. For the C, N, P, Cl, and H atoms the 6-31g** basis set was employed[159]. A vibrational analysis was performed to confirm that the structures of the model compounds have no imaginary frequency. All geometries were optimized without symmetry constraints. Solvation effects were evaluated with the DPCM method[160].

---

[156] Perrin, D. D.; Armarego, W. L. F. Purification of Laboratory Chemicals, 3rd ed., Pergamon, New York, **1988**.

[157] Frisch, M. J.; Trucks, G. W.; Schlegel, H. B.; Scuseria, G. E.; Robb, M. A.; Cheeseman, J. R.; Montgomery, Jr., J. A.; Vreven, T.; Kudin, K. N.; Burant, J. C.; Millam, J. M.; Iyengar, S. S.; Tomasi, J.; Barone, V.; Mennucci, B.; Cossi, M.; Scalmani, G.; Rega, N.; Petersson, G. A.; Nakatsuji, H.; Hada, M.; Ehara, M.; Toyota, K.; Fukuda, R.; Hasegawa, J.; Ishida, M.; Nakajima, T.; Honda, Y.; Kitao, O.; Nakai, H.; Klene, M.; Li, X.; Knox, J. E.; Hratchian, H. P.; Cross, J. B.; Bakken, V.; Adamo, C.; Jaramillo, J.; Gomperts, R.; Stratmann, R. E.; Yazyev, O.; Austin, A. J.; Cammi, R.; Pomelli, C.; Ochterski, J. W.; Ayala, P. Y.; Morokuma, K.; Voth, G. A.; Salvador, P.; Dannenberg, J. J.; Zakrzewski, V. G.; Dapprich, S.; Daniels, A. D.; Strain, M. C.; Farkas, O.; Malick, D. K.; Rabuck, A. D.; Raghavachari, K.; Foresman, J. B.; Ortiz, J. V.; Cui, Q.; Baboul, A. G.; Clifford, S.; Cioslowski, J.; Stefanov, B. B.; Liu, G.; Liashenko, A.; Piskorz, P.; Komaromi, I.; Martin, R. L.; Fox, D. J.; Keith, T.; Al-Laham, M. A.; Peng, C. Y.; Nanayakkara, A.; Challacombe, M.; Gill, P. M. W.; Johnson, B.; Chen, W.; Wong, M. W.; Gonzalez, C.; Pople, J. A. *Gaussian 03*, Revision C.02; Gaussian, Inc., Wallingford, CT, **2004**.

[158] (a) Haeusermann, U.; Dolg, M.; Stoll, H.; Preuss, H. *Mol. Phys.* **1993**, *78*, 1211. (b) Kuechle, W.; Dolg, M.; Stoll, H.; Preuss, H. *J. Chem. Phys.* **1994**, *100*, 7535. (c) Leininger, T.; Nicklass, A.; Stoll, H.; Dolg, M.; Schwerdtfeger, P. *J. Chem. Phys.* **1996**, *105*, 1052.

[159] (a) McLean, A. D.; Chandler, G. S. *J. Chem. Phys.* **1980**, *72*, 5639. (b) Krishnan, R.; Binkley, J. S.; Seeger, R.; Pople, J. A. *J. Chem. Phys.* **1980**, *72*, 650. (c) Wachters, A. J. H. *Chem. Phys.* **1970**, *52*, 1033. (d) Hay, P. J. *J. Chem. Phys.* **1977**, *66*, 4377. (e) Raghavachari, K.; Trucks, G. W. *J. Chem. Phys.* **1989**, *91*, 1062. (f) Binning, R. C.; Curtiss, L. A. *J. Comput. Chem.* **1995**, *103*, 6104. (g) McGrath, M. P.; Radom, L. *J. Chem. Phys.* **1991**, *94*, 511.

[160] (a) Miertus, S.; Scrocco, E.; Tomasi, J. *Chem. Phys.* **1981**, *55*, 117. (b) Pascual-Ahuir, J. L.; Silla, E.; Tomasi, J.; Bonaccorsi, R. *J. Comput. Chem.* **1987**, *8*, 778. (c) Floris, F.; Tomasi, J. *J. Comput. Chem.* **1989**, *10*, 616. (d) Tomasi, J.; Persico, M. *Chem. Rev.* **1994**, *94*, 2027.

4.4 Metal precursors

$[Fe(H_2O)_6](BF_4)_2$ [161]

HBF_4 (25 mL of a 48% solution in H_2O, 0.14 mol) was added dropwise under ice cooling to a suspension of iron powder (5 g, 90 mmol) in 100 mL H_2O. The reaction mixture was stirred at room temperature overnight and then filtered twice. The solvent was evaporated under vacuum until crystallization set in and the mixture was allowed to stand in the fridge overnight. The resulting colorless to pale green crystals were then filtered, washed with Et_2O and dried under vacuum.
Yield: 24 g (79%) colorless to pale green crystals; $H_{12}B_2F_8FeO_6$ (MW: 337.54).

$Fe(CO)_4Br_2$ [162]

Bromine (0.8 mL, 15 mmol) was dissolved in 10 mL of PE and added dropwise and under ice cooling to a solution of $Fe(CO)_5$ (2.0 mL, 15 mmol) in 20 mL PE. A dark red to brown precipitate formed immediately, which was collected on a Schlenk frit, washed with PE and dried under vacuum.
Yield: 4.7 g (95%) dark red to brown solid; $C_4Br_2FeO_4$ (MW: 327.70).

$Fe(py)_4Cl_2$ [163]

$FeCl_2$ (6.2 g, 50 mmol) was added under Argon to a three-necked 50 mL round-bottom flask containing 20 mL pyridine (excess). An intense yellow precipitate was formed immediately. The mixture was allowed to stand at room temperature for twelve hours and the yellow solid was collected on a glass frit and washed with a small amount of pyridine and dried under vacuum.
Yield: 19.7 g (89%) yellow solid; $C_{20}H_{20}Cl_2FeN_4$ (MW: 443.16); 54.21% C, 4.55% H, 12.64% N.

$Ni(DME)Cl_2$ [164]

A three-necked round bottom 100 mL flask equipped with a reflux condenser was charged with $NiCl_2{\cdot}6H_2O$ (10g, 66 mmol), 35 mL DME (excess) and 22 mL (145 mmol) of triethyl orthoformate. The slurry was stirred rapidly and refluxed for two hours. The reaction mixture was then allowed to cool down and the orange solid was collected on a Schlenk frit, washed with DME and pentane and dried under vacuum.

---

[161] Kirchner, K. *Ph.D. Thesis*, Vienna University of Technolgy, **1987**.
[162] Hales, L. A. W.; Roger, I. J. *J. Chem. Soc. (A)* **1967**, *8*, 1389.
[163] Baudisch, O; Hartung, W. H. *Inorg. Synth.* **1939**, *1*, 184.
[164] Ward, L. G. L. *Inorg. Synth.* **1971**, *13*, 154.

Yield: 13.2 g (91%) yellow solid; $C_4H_{10}Cl_2NiO_2$ (MW: 219.74); 21.86% C, 4.59% H.

Ni(DME)Br$_2$ [165]

Bromine (4.16 g, 26 mmol) was added dropwise to a slurry of nickel powder (1.5 g, 26 mmol) in 100 mL DME (excess). After one day, the orange slurry was heated to reflux, whereupon a peach colored solid precipitated. This was collected on a glass frit and dried under vacuum.
Yield: 7.36 g (92%) pale orange solid; $C_4H_{10}Br_2NiO_2$ (MW: 308.64); 15.57% C, 3.27% H.

Pd(COD)Cl$_2$

1,5-cyclooctadiene (10 mL, 84.6 mmol) was added dropwise to a suspension of $PdCl_2$ (5.0 g, 28.2 mmol) in 150 mL MeOH, whereupon a yellow solid precipitated. The reaction mixture was stirred overnight at room temperature, filtered, and the resulting yellow solid was washed with MeOH and dried under vacuum.
Yield: 7.29 g (91%) yellow solid; $C_8H_{12}Cl_2Pd$ (MW: 285.50); 33.66% C, 4.24% H.
^{1}H NMR (δ, $CDCl_3$, 20°C): 6.32 (s, 4H, C*H*=C*H*), 2.92 (m, 4H CH_2CH_2), 2.57 (m, 4H CH_2CH_2).

Pd(TFA)$_2$ [166]

$Pd(OAc)_2$ (0.6 g, 2.7 mmol) was dissolved in 30 mL TFA (excess) and the solution was evaporated under vacuum in the rotary evaporator. Another 15 mL of TFA were added and the solvent was again evaporated in the rotary evaporator to give a dark brown powder.
Yield: 645 mg (72%) brown solid; $C_4F_6O_4Pd$ (MW: 332.43).

Pt(COD)Br$_2$

K_2PtBr_4 (5 g, 8.4 mmol) was dissolved in 100 mL EtOH and 1,5-cyclooctadiene (2.1 mL, 16.8 mmol) was added. The mixture was stirred at RT overnight, whereupon an off-white solid precipitated, which was collected on a glass frit and filtered.
Yield: 3.2 g (82%) off-white solid; $C_8H_{12}Br_2Pt$ (MW: 463.10); 20.75% C, 2.61% H.

---

[165] Casalnuovo, A. L; RajanBabu, T. V.; Ayers, T. A.; Warren, T. H. *J. Am. Chem. Soc.* **1994**, *116*, 9869.
[166] Stephenson, T. A.; Morehouse, S. M.; Powell, A. R.; Heffer, J. P.; Wilkinson, G. *Inorg. Synth.* **1965**, 3632.

4.5 Phosphites

2-chloro-1,3,2-dioxaphospholane (ETOL-PCl)[61a] (1a)

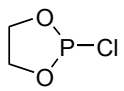

Ethylene glycol (7.0 mL, 0.12 mol) was added under inert atmosphere to a solution of PCl_3 (11.0 mL, 0.12 mol) in CH_2Cl_2 so that gentle refluxing took place. The reaction flask was then adapted for distillation and the solvent first and then **1a** were distilled.

Yield: 11.2 g (69%) colourless oil; $C_2H_4ClO_2P$ (MW: 126.48); 18.99% C, 3.19% H.

^{1}H NMR (δ, $CDCl_3$, 20°C): 4.41 (s, 2H, C*H*$_2$), 4.25 - 4.19 (m, 2H, C*H*$_2$).

^{31}P{^{1}H} NMR (δ, $CDCl_3$, 20°C): 169.0.

2,2'-biphenylylenephosphochloridite (BIPOL-PCl)[61b] (1b)

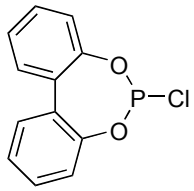

Method 1: Triethylamine (14.0 mL, 105 mmol) was added dropwise to a suspension of 2,2'-biphenyl (10.9 g, 42 mmol) in 50 mL of toluene. The mixture was cooled to 0ºC and PCl_3 (3.9 mL, 45 mmol) was added dropwise. A white solid was formed immediately. The mixture was allowed to reach RT and stirred overnight. Insoluble materials were filtered off, the solvent was removed under vacuum and the remaining oil was dried under vacuum.

Yield: 8.3 g (79%)

Method 2: A mixture of 2,2'-biphenyl (6.0 g, 32.2 mmol), PCl_3 (10 mL, 113.0 mmol) and NMP (31 µL, 0.3 mmol) were refluxed for 30 min (due to heavy HCl formation, the reflux condenser was connected to the extractor hood). After removal of the excess PCl_3 from the orange residue, the product was purified by bulb-to-bulb distillation (10^{-4} mbar, 200ºC, 1h.).

Yield: 6.5 g (81%) colorless oil, crystallizes in the fridge

$C_{12}H_8ClO_2P$ (MW: 250.62); 57.51% C, 3.22% H.

^{1}H NMR (δ, $CDCl_3$, 20°C): 7.52 – 7.25 (m, 8H, Ph).

^{31}P{^{1}H} NMR (δ, $CDCl_3$, 20°C): 181.1.

S-2-chloro-dinaphto[2,1-d:1'2'-f][1,3,2]dioxaphosphepine (BINOL-PCl)[61c] (1c)

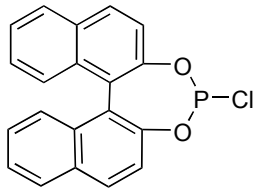

A PCl_3 (3.4 mL, 39.0 mmol) solution in 10 mL THF was added dropwise at -40ºC to a suspension of (S)-(-)-1,1'-bi-2-naphtol (10.0 g, 35.0 mmol) in 30 mL THF. After the mixture was stirred for 10 min., triethylamine (10.8 mL, 77.6 mmol) was added, and the mixture was allowed to come to RT and stirred for further 30 min. Insoluble materials were filtered off, the solvent was removed under vacuum and the remaining yellow solid was dried under vacuum.

Yield: 11.0 g (89%) yellow solid; $C_{20}H_{12}ClO_2P$ (MW: 354.77); 67.71% C, 4.55% H.

^{1}H NMR (δ, $CDCl_3$, 20°C): 8.04 – 7.95 (m, 4H, Ph), 7.56 – 7.21 (m, 8H, Ph).

$^{31}P\{^1H\}$ NMR (δ, $CDCl_3$, 20°C): 179.8.

2-chloro-(4S,5S)-dicarbomethoxy-1,3,2-dioxaphospholane (^{Me}TAR-PCl)[61d] (1d)

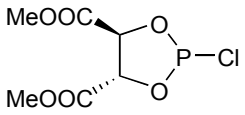

A mixture of D-(-)-methyl tartrate (10.0 g, 56.1 mmol), PCl_3 (14.7 mL, 168.4 mmol) and NMP (0.5 mL, 5.6 mmol) were refluxed for 30 min (due to heavy HCl formation, the reflux condenser was connected to the extractor hood). After removal of the excess PCl_3 from the orange residue, the product was purified by bulb-to-bulb distillation (10^{-4} mbar, 150ºC, 30 min.).

Yield: 11.2 g (82%) colorless oil; $C_6H_8ClO_6P$ (MW: 242.55); 29.71% C, 3.32% H.

^{1}H NMR (δ, $CDCl_3$, 20°C): 5.45 (d, *J* = 6.2 Hz, 1H, C*H*), 5.00 (dd, *J* = 6.2 Hz, *J* = 9.6 Hz, 1H, C*H*), 3.83 (s, 6H, CH_3).

$^{31}P\{^1H\}$ NMR (δ, $CDCl_3$, 20°C): 176.3.

2-chloro-(4R,5R)-dicarboisopropoxi-1,3,2-dioxaphospholane (^{iPr}TAR-PCl)[61d] (1e)

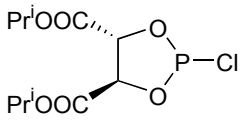

This chlorophosphite was prepared analogously to **1d** with L-(+)-isopropyl tartrate (5.0 mL, 24.0 mmol), PCl_3 (6.3 mL, 72.0 mmol) and NMP (24 µL, 0.2 mmol) as the starting materials.

Yield: 5.4 g (75%) colorless oil; $C_{10}H_{16}ClO_6P$ (MW: 298.66); 40.22% C, 5.40% H.

^{1}H NMR (δ, $CDCl_3$, 20°C): 5.35 (d, *J* = 6.7 Hz, 1H, C*H*), 5.14 (m, *J* = 6.1 Hz, 2H, C*H*$(CH_3)_2$), 5.00 (dd, *J* = 6.7 Hz, *J* = 8.8 Hz, 1H, C*H*), 1.33 – 1.28 (m, 12H, CH(C*H*$_3)_2$).
^{31}P{^{1}H} NMR (δ, $CDCl_3$, 20°C): 176.4.

(4S,5S)-2-chloro-4,5-diphenyl-1,3,2-dioxaphospholane (HBz-PCl)[61e] (1f)

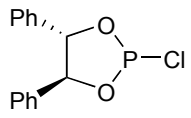

This chlorophosphite was prepared analogously to **1d** with (S,S)-(-)-Hydrobenzoine (5.0 g, 23.3 mmol), PCl_3 (7.1 mL, 81.6 mmol) and NMP (22 µL, 0.2 mmol) as the starting materials.
Yield: 4.7 g (72%) pale yellow solid; $C_{14}H_{12}ClO_2P$ (MW: 278.67); 60.34% C, 4.34% H.
^{1}H NMR (δ, $CDCl_3$, 20°C): 7.45 – 7.35 (m, 10H, Ph), 5.31 (s, 2H, C*H*).
^{31}P{^{1}H} NMR (δ, $CDCl_3$, 20°C): 174.6.

(4S,5R)-2-chloro-3,4-dimethyl-5-phenyl-1,3,2-oxazaphospholidine (Eph-PCl)[61f] (1g)

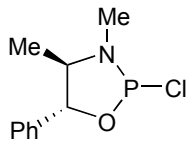

A solution of (1R,2S)-(-)-ephedrine (5.0 g, 30.5 mmol) in 20 mL toluene was added at -78ºC to a mixture of PCl_3 (2.7 mL, 30.5 mmol) and N-methylmorpholine (10.0 mL, 91.5 mmol) in 10 mL toluene. The mixture was allowed to reach RT and stirred overnight. Insoluble materials were filtered off and the product was purified by bulb-to-bulb distillation (10^{-4} mbar, 200ºC, 2 h.).
Yield: 7.0 g (92%) pale yellow solid; $C_{10}H_{13}ClNOP$ (MW: 229.65); 52.30% C, 5.71% H, 6.10% N.
^{1}H NMR (δ, $CDCl_3$, 20°C): 7.36 – 7.22 (m, 5H, Ph), 5.83 (dd, *J* = 1.1 Hz, *J* = 8.0 Hz, 1H, C*H*Ph), 3.69 – 3.61 (m, 1H, C*H*CH_3), 2.70 (d, *J* = 16.0 Hz, 3H, NC*H*$_3$), 0.72 (d, *J* = 6.6 Hz, 3H, CHC*H*$_3$).
^{31}P{^{1}H} NMR (δ, $CDCl_3$, 20°C): 172.7.

4.6 Ligands

4.6.1 PNP Ligands

***N,N'*-Bis(diphenylphosphino)-2,6-diaminopyridine (PNP-Ph)[60] (2a)**.

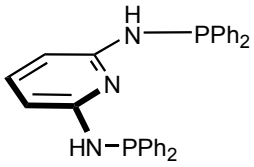

Triethylamine (16.5 mL, 92 mmol) was added to a suspension of 2,6-diaminopyridine (5.0 g, 46 mmol) in toluene (250 mL). The mixture was then cooled to 0°C and PPh_2Cl (11.2 mL, 92 mmol) was added dropwise. The solution was allowed to reach room temperature and was then stirred overnight at 80°C. After that, insoluble materials were filtered off and the solvent was removed under vacuum. The remaining yellow oil was recrystallized from toluene/*n*-hexane (1:1).

Yield: 34.6 g (79%) white solid; $C_{29}H_{25}N_3P_2$ (MW: 477.48); 72.95% C, 5.28% H, 8.80% N.

^{1}H NMR (δ, $CDCl_3$, 20°C): 7.36 – 7.34 (m, 21H, Ph, py^4), 6.53 (dd, *J* = 7.9 Hz, *J* = 1.6 Hz, 2H, py^{3,5}), 5.39 (s, 2H, N*H*).

^{13}C{^{1}H} NMR (δ, $CDCl_3$, 20°C): 157.6 (d, *J* = 20.2 Hz, py^{2,6}), 139.9 (d, *J* = 12.1 Hz, py^4), 134.0 (Ph^1), 131.3 (d, *J* = 20.9 Hz, Ph^{2,6}), 129.2 (Ph^4), 128.5 (d, *J* = 6.7 Hz, Ph^{3,5}), 99.2 (d, *J* = 14.8 Hz, py^{3,5}).

^{31}P{^{1}H} NMR (δ, $CDCl_3$, 20°C): 28.0.

***N,N'*-bis(diisopropylphosphino)-2,6-diaminopyridine (PNP-^{i}Pr) (2b)**

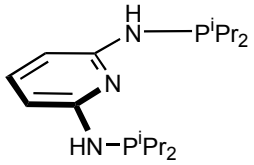

To a suspension of 2,6-diaminopyridine (1.8 g, 16.4 mmol) in toluene NEt_3 (4.0 mL, 32.8 mmol) was added. The mixture was then cooled to 0°C and PPr^i_2Cl (5.0 g, 32.8 mmol) was added dropwise. Upon further cooling to -70°C, *n*-BuLi (32.8 mmol, 14.0 mL of a 2.3 M solution in hexane) was slowly added. The solution was allowed to reach room temperature and was then stirred overnight at 80°C. After that, the solution was filtered and the solvent was removed under vacuum. The remaining yellow oil was recrystallized from toluene/*n*-hexane (1:1).

Yield: 4.3 g (78%) white solid; $C_{17}H_{33}N_3P_2$ (MW: 341.41); 59.81%C, 9.74% H, 12.31% N.

^{1}H NMR (δ, $CDCl_3$, 20°C): 7.23 (t, *J* = 7.9 Hz, 1H, py^4), 6.42 (dd, *J* = 7.9 Hz, *J* = 2.3 Hz, 2H, py^{3,5}), 4.29 (d, *J* = 11.2 Hz, 2H, N*H*), 1.78-1.67 (m, *J* = 7.0 Hz, *J* = 2.0 Hz, 4H, C*H*$(CH_3)_2$), 1.08-0.99 (m, 24H, CH(C*H*$_3)_2$).

^{13}C{^{1}H} NMR (δ, $CDCl_3$, 20°C): 159.5 (d, *J* = 20.3 Hz, py^{2,6}), 139.1 (py^4), 98.1 (d, *J* = 18.4 Hz, py^{3,5}), 26.3 (d, *J* = 10.7 Hz, *C*H$(CH_3)_2$), 18.6 (d, *J* = 19.6 Hz, CH(*C*H$_3)_2$), 17.1 (d, *J* = 7.7 Hz, CH(*C*H$_3)_2$).

^{31}P{^{1}H} NMR (δ, $CDCl_3$, 20°C): 49.0.

***N,N'*-bis(di-*tert*-butylphosphino)-2,6-diaminopyridine (PNP-^{t}Bu) (2c)**

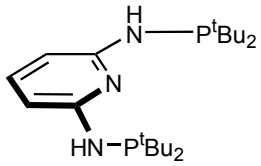

This ligand was prepared analogously to **2b** with NEt_3 (3.4 mL, 27.6 mmol), 2,6-diaminopyridine (1.5 g, 13.8 mmol), PBu^t_2Cl (5.0 g, 27.6 mmol), and *n*-BuLi (27.6 mmol, 15.0 mL of a 1.9 M solution in hexane) as the starting materials.

Yield: 3.9 g (73 %) white solid; $C_{21}H_{41}N_3P_2$ (MW: 397.52); 63.45% C, 10.40% H, 10.57% N.

^{1}H NMR (δ, $CDCl_3$, 20°C): 7.25 (t, *J* = 7.6 Hz, 1H, py^4), 6.48 (dd, *J* = 7.6 Hz, *J* = 2.5 Hz, 2H, py^{3,5}), 4.64 (d, *J* = 11.2 Hz, 2H, N*H*), 1.22-1.15 (m, 36H, C(C*H*$_3)_3$).

^{13}C{^{1}H} NMR (δ, $CDCl_3$, 20°C): 155.1(py^{2,6}), 138.7 (py^4), 98.2 (d, *J* = 18.5 Hz, py^{3,5}), 29.4 (d, *J* = 13.9 Hz, *C*$(CH_3)_3$), 27.8 (d, *J* = 15.0 Hz, C(*C*H$_3)_3$).

^{31}P{^{1}H} NMR (δ, $CDCl_3$, 20°C): 60.2.

***N,N'*-bis(1,2-ethandiolphosphino)-2,6-diaminopyridine (PNP-ETOL) (2d)**

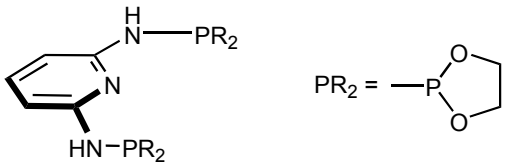

To a suspension of 2,6-diaminopyridine (0.6 g, 5.6 mmol) in toluene NEt_3 (1.6 mL, 11.2 mmol) was added and the mixture was cooled to 0°C. Upon addition of 2-chloro-1,3,2-dioxaphospholane (**1a**, 1.4 g, 11.2 mmol) the mixture was stirred at 80°C overnight whereupon a white solid precipitated. After removal of insoluble materials by filtration, the solvent was removed under vacuum affording a white solid.

Yield: 1.4 g (64 %) white solid; $C_9H_{13}N_3O_4P_2$ (MW: 289.17); 37.38%C, 4.53%H, 14.53%N.

^{1}H NMR (δ, $CDCl_3$, 20°C): 7.28 (t, *J* = 7.9 Hz, 1H, py^4), 6.29 (d, *J* = 7.9 Hz, 2H, py^{3,5}), 5.70 (s, 2H, N*H*), 4.20-4.13 (m, 4H, C*H*$_2$), 4.01-3.91 (m, 4H, C*H*$_2$).

$^{13}C\{^1H\}$ NMR (δ, $CDCl_3$, 20°C): 157.0 ($py^{2,6}$), 139.6 (py^4), 100.8 (d, *J* = 12.1 Hz, $py^{3,5}$), 63.7 (CH_2), 63.5 (CH_2).
$^{31}P\{^1H\}$ NMR (δ, $CDCl_3$, 20°C): 129.9.

***N,N'*-bis(dibenzo[d,f][1,3,2]dioxaphosphepine)-2,6-diaminopyridine (PNP-BIPOL) (2e)**

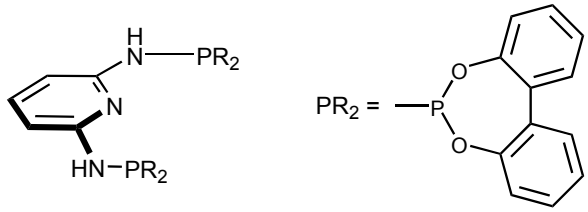

This ligand was prepared analogously to **2d** with NEt_3 (1.5 mL, 12.0 mmol), 2,6-diaminopyridine (0.6 g, 6.0 mmol), and 2,2'-biphenylylenephosphochloridite (**1b**, 3.0 g, 12.0 mmol) as the starting materials.
Yield: 3.4 g (79 %) white solid; $C_{29}H_{21}N_3O_4P_2$ (MW: 537.45); 64.81% C, 3.94% H, 7.82% N.
^1H NMR (δ, $CDCl_3$, 20°C): 7.49-7.15 (m, 15H, $Ph^{3,5}$, Ph^4 and py4), 6.11 (dd, *J* = 31.6 Hz, *J* = 7.9 Hz, 2H, $Ph^{2,6}$), 5.89 (d, *J* = 7.8 Hz, 2H, $py^{3,5}$), 4.32 (s, 2H, N*H*).
$^{13}C\{^1H\}$ NMR (δ, $CDCl_3$, 20°C): 154.2 (d, *J* = 17.3 Hz, $py^{2,6}$), 149.5 (d, *J* = 3.8 Hz, Ph), 140.0 (py^4), 131.6 (d, *J* = 3.1, Ph), 129.8 (Ph), 129.2 (Ph), 125.3 (Ph), 122.3 (Ph), 101.5 (d, *J* = 12.3 Hz, $py^{3,5}$).
$^{31}P\{^1H\}$ NMR (δ, $CDCl_3$, 20°C): 147.5.

***N,N'*-bis(S-dinaphto[2,1-d:1'2'-f][1,3,2]dioxaphosphepine)-2,6-diaminopyridine (PNP-BINOL) (2f)**

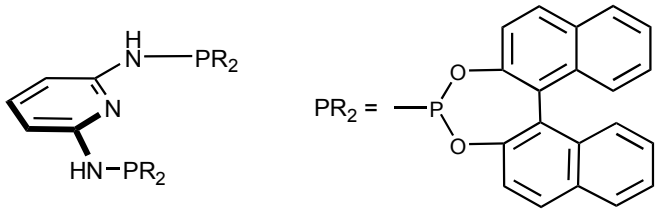

A solution of 2,6-diaminopyridine (46 mg, 0.42 mmol) in THF (10 mL) was cooled to -70°C, and *n*-BuLi (0.85 mmol, 0.47 mL of a 2.10 M solution in hexane) was added. The reaction was stirred until the temperature reached -20°C, and S-2-chloro-dinaphto[2,1-d:1'2'-f][1,3,2]dioxaphosphepine (**1c**, 300 mg, 0.85 mmol) in 2 mL THF was added. After allowing the reaction to stir overnight at room temperature, the mixture was filtered, and the solvent removed under vacuum.
Yield: 350 mg (94 %) white solid; $C_{45}H_{29}N_3O_4P_2$ (MW: 737.69); 73.27% C, 3.96% H, 5.70% N.

^{1}H NMR (δ, $CDCl_3$, 20°C): 8.00-7.85 (m, 8H, Ph), 7.54-7.29 (m, 17H, Ph and py^{4}), 6.06 (d, *J* = 7.9 Hz, 2H, py^{3,5}), 5.72 (d, *J* = 8.2 Hz, 2H, N*H*).
^{13}C{^{1}H} NMR (δ, $CDCl_3$, 20°C): 162.2 (py^{2,6}), 139.7 (py^{4}), 130.4 (Ph), 129.9 (Ph), 129.8 (Ph), 128.5 (Ph), 128.4 (Ph), 126.9 (Ph), 126.7 (Ph), 126.4 (Ph), 126.2 (Ph), 125.0 (Ph); 100.6 (py^{3,5}).
^{31}P{^{1}H} NMR (δ, $CDCl_3$, 20°C): 146.1.

***N,N'*-bis(4S,5S-dicarbomethoxy-1,3,2-dioxaphospholane)-2,6-diaminopyridine (PNP-TAR^{Me}) (2g)**

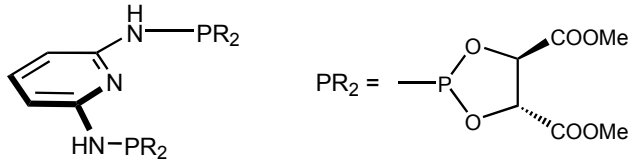

This ligand was prepared analogously to **2d** with NEt_3 (2.3 mL, 16.4 mmol), 2,6-diaminopyridine (0.9 g, 8.2 mmol), and 2-chloro-(4S,5S)-dicarbomethoxy-1,3,2-dioxaphospholane (**1d**, 4.0 g, 16.4 mmol) as the starting materials.
Yield: 1.6 g (66 %) white solid; $C_{17}H_{21}N_3O_{12}P_2$ (MW: 521.31); 39.17%C, 4.06%H, 8.06%N.
^{1}H NMR (δ, $CDCl_3$, 20°C): 7.30 (t, *J* = 7.9 Hz, 1H, py^{4}) 6.45 (s, 2H, N*H*), 6.28 (d, *J* = 7.9 Hz, 2H, py^{3,5}), 5.06-5.03 (m, 2H, C*H*), 4.81-4.75 (m, 2H, C*H*), 3.83 (s, 6H, CH_3).
^{13}C{^{1}H} NMR (δ, $CDCl_3$, 20°C): 171.3 (*C*O), 169.0 (*C*O), 153.8 (d, *J* = 14.9 Hz, py^{2,6}), 139.7 (py^{4}), 101.9 (d, *J* = 10.3 Hz, py^{3,5}), 77.6 (*C*H), 77.1 (*C*H), 76.7 (t, *J* = 10.1 Hz, *C*H_3), 53.2 (d, *J* = 15.5 Hz, *C*H_3).
^{31}P{^{1}H} NMR (δ, $CDCl_3$, 20°C): 142.9.

***N,N'*-bis(4R,5R-dicarboisopropoxy-1,3,2-dioxaphospholane)-2,6-diaminopyridine (PNP-TAR^{Pr}) (2h)**

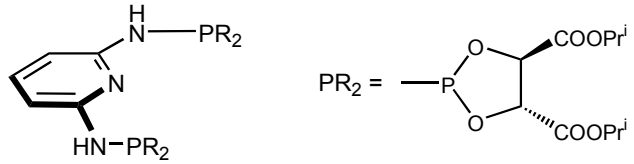

This ligand was prepared analogously to **2d** with NEt_3 (2.3 mL, 16.4 mmol), 2,6-diaminopyridine (0.9 g, 8.2 mmol), and 2-chloro-(4R,5R)-dicarboisopropoxi-1,3,2-dioxaphospholane (**1e**, 5.0 g, 16.4 mmol) as the starting materials.
Yield: 5.0 g (95 %) pale brown oil; $C_{25}H_{37}N_3O_{12}P_2$ (MW: 633.53); 47.40% C, 5.89% H, 6.63% N.
^{1}H NMR (δ, $CDCl_3$, 20°C): 7.28 (t, *J* = 7.9 Hz, 1H, py^{4}) 6.54 (d, *J* = 4.0 Hz, 2H, N*H*), 6.26 (d, *J* = 7.9 Hz, 2H, py^{3,5}), 5.20-5.06 (m, 4H, $(CH_3)_2$C*H*), 4.86-4.84 (m, 2H, C*H*), 4.62-4.56 (m, 2H, C*H*), 1.32-1.27 (m, 24H, (CH_3)$_2$CH).

$^{13}C\{^1H\}$ NMR (δ, $CDCl_3$, 20°C): 170.4 (*C*O), 167.8 (*C*O), 154.1 (d, *J* = 16.1 Hz, $py^{2,6}$), 139.6 (py^4), 101.5 (d, *J* = 10.1 Hz, $py^{3,5}$), 77.4 (*C*H), 76.5 (*C*H), 70.8 ($(CH_3)_2$*C*H), 70.2 ($(CH_3)_2$*C*H), 21.6 ($(CH_3)_2$*C*H).
$^{31}P\{^1H\}$ NMR (δ, $CDCl_3$, 20°C): 142.7.

***N,N'*-bis(4S,5S-2-chloro-4,5-diphenyl-1,3,2-dioxaphospholane)-2,6-diaminopyridine (PNP-HBz) (2i)**

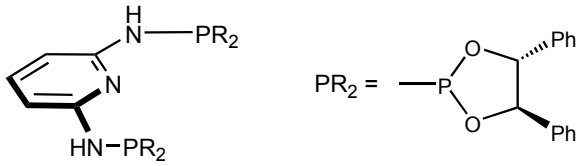

This ligand was prepared analogously to **2d** with 2,6-diaminopyridine (98 mg, 0.9 mmol), triethylamine (0.25 mL, 1.8 mmol) and (4S,5S)-2-chloro-4,5-diphenyl-1,3,2-dioxaphospholane (**1f**, 500 mg, 1.8 mmol) as the starting materials.
Yield: 363 mg (68%) white solid; $C_{33}H_{29}N_3O_4P_2$ (MW: 593.56); 66.78% C, 4.92% H, 7.08% N.
^1H NMR (δ, $CDCl_3$, 20°C): 7.38 – 7.11 (m, 21H, Ph and py^4), 6.43 (d, *J* = 7.9 Hz, 2H, $py^{3,5}$), 6.05 (d, *J* = 8.2 Hz, 2H, N*H*), 5.24 – 5.15 (m, 2H, C*H*), 5.00 – 4.81 (m, 2H, C*H*).
$^{13}C\{^1H\}$ NMR (δ, $CDCl_3$, 20°C): 157.6 ($py^{2,6}$), 140.2 (py^4), 136.5 (Ph^1), 129.0 ($Ph^{2,6}$), 128.5 (Ph^4), 126.7 ($Ph^{3,5}$), 100.7 ($py^{3,5}$), 87.2 (*C*H).
$^{31}P\{^1H\}$ NMR δ, $CDCl_3$, 20°C): 130.0.

***N,N'*-bis(4S,5R-2-chloro-3,4-dimethyl-5-phenyl-1,3,2-oxazaphospholidine)-2,6-diamino-pyridine (PNP-Eph) (2j)**

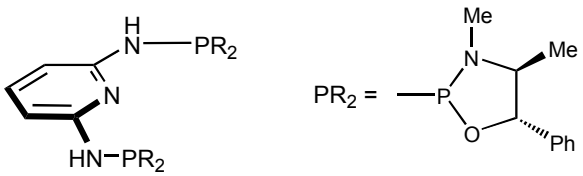

This ligand has been prepared analogously to **2d** with (4S,5R)-2-chloro-3,4-dimethyl-5-phenyl-1,3,2-oxazaphospholidine (**1g**, 500 mg, 2.2 mmol), 2,6-diaminopyridine (118 mg, 1.1 mmol) and triethylamine (0.30 mL, 2.2 mmol) as the starting materials.
Yield: 283 mg (52%) white solid; $C_{25}H_{31}N_5O_2P_2$ (MW: 495.50); 60.60% C, 6.31% H, 14.13% N.
^1H NMR (δ, $CDCl_3$, 20°C): 7.37 – 7.15 (m, 13H, Ph, $py^{3,5}$ and py^4), 5.86 (d, *J* = 7.8 Hz, 2H, N*H*), 4.71 – 4.60 (m, 2H, C*H*Ph), 3.77 – 3.60 (m, 2H, C*H*CH_3), 2.84 – 2.63 (m, 6H, NCH_3), 0.84 – 0.63 (m, 6H, CHCH_3).
$^{13}C\{^1H\}$ NMR (δ, $CDCl_3$, 20°C): 157.0 ($py^{2,6}$), 140.1 (py^4), 139.6 (Ph^1), 128.5 ($Ph^{2,6}$), 126.8 (Ph^4), 125.8 ($Ph^{3,5}$), 99.7 ($py^{3,5}$), 81.7 (*C*HPh), 60.2 (*C*HCH_3), 29.1 (N*C*H_3), 14.6 (CH*C*H_3).

$^{31}P\{^1H\}$ NMR (δ, $CDCl_3$, 20°C): 119.0.

4.6.2 PCP Ligands

***N,N'*-bis(diphenylphosphino)-1,3-benzenediamine (PCP-Ph) (3a)**

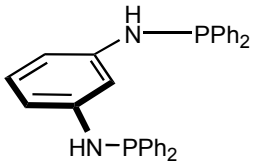

To a suspension of m-phenylenediamine (5.0 g, 46 mmol) in 75 mL toluene NEt_3 (11.2 mL, 92 mmol) was added. The mixture was then cooled to 0°C, PPh_2Cl (16.5 mL, 92 mmol) was added dropwise and the solution was allowed to reach room temperature and stirred overnight at 80°C. Insoluble materials were filtered off and the solvent was removed under vacuum. The remaining yellow oil was recrystallized from toluene/*n*-hexane (1:1).

Yield: 13.2 g (84%) white solid; $C_{30}H_{26}N_2P_2$ (MW: 476.50); 75.62% C, 5.50% H, 5.88% N.

^1H NMR (δ, $CDCl_3$, 20°C): 7.43 - 7.32 (m, 20H, PPh), 6.99 (t, *J* = 8.0 Hz, 1H, Ph^4), 6.72 (t, *J* = 2.1 Hz, 1H, Ph^{ipso}), 6.50 (d, *J* = 8.0 Hz, 2H, $Ph^{3,5}$), 4.39 (d, *J* = 8.2 Hz, 2H, N*H*).

$^{13}C\{^1H\}$ NMR (δ, $CDCl_3$, 20°C): 147.7 (d, *J* = 16.5 Hz, $Ph^{2,6}$), 140.2 (d, *J* = 11.9 Hz, PPh), 131.3 (d, *J* = 20.7 Hz, $PPh^{2,6}$), 130.1 (Ph^4), 129.1 (PPh^4), 128.6 (d, *J* = 6.5 Hz, $PPh^{3,5}$), 107.3 (d, *J* = 13.8 Hz, $Ph^{3,5}$), 103.3 (t, *J* = 13.4 Hz, Ph^{ipso}).

$^{31}P\{^1H\}$ NMR δ, $CDCl_3$, 20°C): 28.6.

***N,N'*-bis(diisopropylphosphino)-1,3-benzenediamine (PCP-^{i}Pr) (3b)**

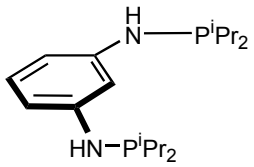

This ligand has been prepared analogously to **3a** with NEt_3 (8.0 mL, 66 mmol), m-phenylenediamine (3.6 g, 33 mmol) and P^iPr_2Cl (10.0 g, 66 mmol) as the starting materials.

Yield: 8.8 g (79 %) white solid; $C_{18}H_{33}N_2P_2$ (MW: 339.42); 63.70% C, 9.80% H, 8.25% N.

^1H NMR (δ, $CDCl_3$, 20°C): 6.92 (t, *J* = 8.0 Hz, 1H, Ph^4), 6.64 (t, *J* = 2.2 Hz, 1H, Ph^{ipso}), 6.37 (d, *J* = 8.0 Hz, 2H, $Ph^{3,5}$), 3.63 (d, *J* = 10.5 Hz, 2H, N*H*), 1.75 - 1.68 (m, 4H, C*H*$(CH_3)_2$), 1.12 - 1.02 (m, 24 H, CH(C*H*$_3$)$_2$).

$^{13}C\{^1H\}$ NMR (δ, $CDCl_3$, 20°C): 149.6 (d, *J* = 17.2 Hz, $Ph^{2,6}$), 129.5 (Ph^4), 106.5 (d, *J* = 12.1 Hz, $Ph^{3,5}$), 103.4 (t, *J* = 12.4 Hz, Ph^{ipso}), 26.6 (d, *J* = 9.8 Hz, $CH(CH_3)_2$), 18.7 (d, *J* = 20.1 Hz, $CH(CH_3)_2$), 17.1 (d, *J* = 7.5 Hz, $CH(CH_3)_2$).
$^{31}P\{^1H\}$ NMR δ, $CDCl_3$, 20°C): 48.9.

***N,N'*-bis(di-*tert*-butylphosphino)-1,3-benzenediamine (PCP-^{t}Bu) (3c)**

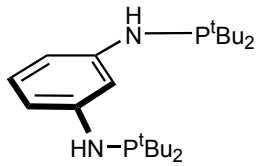

Triethylamine (6.0 mL, 42 mmol) was added to a solution of m-phenylenediamine (0.6 g, 5.3 mmol) in 100 mL THF; the reaction mixture was then cooled to 0°C and PBu^t_2Cl (2.0 mL, 10.5 mmol) was added. Upon cooling to -80°C, *n*-BuLi (10.5 mmol, 5.0 mL of a 2.1 M solution in hexane) was added and the reaction was allowed to reach room temperature and stirred overnight. After that, the solution was filtered and the solvent was removed under vacuum; the white solid obtained was used without further purification.
Yield: 2.0 g (96 %) white solid; $C_{22}H_{42}N_2P_2$ (MW: 396.54); 66.64% C, 10.68% H, 7.06% N.
^1H NMR (δ, CD_2Cl_2, 20°C): 6.89 (t, *J* = 7.9 Hz, 1H, Ph^4), 6.73 (t, *J* = 2.3 Hz, 1H, Ph^{ipso}), 6.36 (d, *J* = 7.9 Hz, 2H, $Ph^{3,5}$), 3.96 (d, *J* = 11.0 Hz, 2H, N*H*), 1.12 (d, *J* = 11.9 Hz, 36H, $C(CH_3)_3$).
$^{13}C\{^1H\}$ NMR (δ, CD_2Cl_2, 20°C): 150.1 (d, *J* = 16.7 Hz, $Ph^{2,6}$), 129.6 (Ph^4), 106.5 (d, *J* = 12.1 Hz, $Ph^{3,5}$), 103.5 (t, *J* = 11.2 Hz, Ph^{ipso}), 34.2 (d, *J* = 19.0 Hz, $C(CH_3)_3$), 28.1 (d, *J* = 14.9 Hz, $C(CH_3)_3$).
$^{31}P\{^1H\}$ NMR (δ, CD_2Cl_2, 20°C): 59.3.

***N,N'*-bis(diphenylphosphino)-5-(trifluoromethyl)-1,3-benzenediamine (PCP-Ph^F) (3d)**

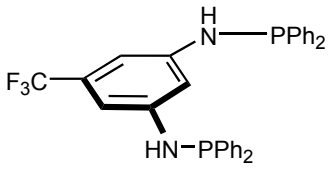

Triethylamine (0.4 mL, 2.84 mmol) was added to a solution of 5-(trifluoromethyl)-1,3-benzenediamine (250 mg, 1.42 mmol) in 80 mL THF; the reaction mixture was then cooled to 0ºC and PPh_2Cl (0.5 mL, 2.84 mmol) was added, whereupon a white solid immediately precipitated. The mixture was stirred overnight at RT, filtered, and the solvent was removed under vacuum, yielding a white solid.
Yield: 725 mg (94 %) white solid; $C_{31}H_{24}F_3N_2P_2$ (MW: 543.49); 68.51% C, 4.45% H, 5.15% N.

^{1}H NMR (δ, $CDCl_3$, 20°C): 7.81 – 7.75 (m, 2H, PPh), 7.63 – 7.57 (m, 2H, PPh), 7.43 – 7.24 (m, 16H, PPh), 6.88 (s, 1H, Ph^{ipso}), 6.76 (s, 1H, $Ph^{3,5}$), 4.56 (d, *J* = 8.2 Hz, 2H, N*H*).
^{13}C{^{1}H} NMR (δ, $CDCl_3$, 20°C): 148.2 (d, *J* = 18.3 Hz, $Ph^{2,6}$), 139.5 (d, *J* = 11.4 Hz, PPh), 131.2 (d, *J* = 20.85 Hz, $PPh^{2,6}$), 130.3 (Ph^{4}), 129.3 (PPh^{4}), 128.6 (t, *J* = 5.4 Hz, $PPh^{3,5}$), 105.5 (t, *J* = 16.4 Hz, $Ph^{3,5}$), 103.7 (t, *J* = 4.4 Hz, Ph^{ipso}).
^{31}P{^{1}H} NMR (δ, $CDCl_3$, 20°C): 27.0.

***N,N'*-bis(diphenylphosphino)-3,5-Diamino-benzoic acid isopropyl ester (PCP-Ph^{E}) (3e)**

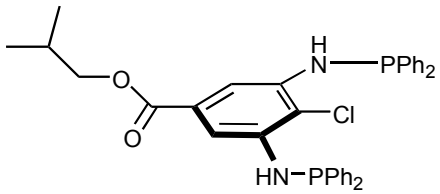

Triethylamine (0.3 mL, 2.10 mmol) was added to a solution of 3,5-diamino-4-chloroisobutylbenzoate (250 mg, 1.03 mmol) in THF; the reaction mixture was then cooled to 0ºC and PPh_2Cl (0.4 mL, 2.10 mmol) was added, whereupon a white solid immediately precipitated. The mixture was stirred overnight at 50ºC, filtered, and the solvent was removed under vacuum, yielding a white solid.
Yield: 486 mg (82 %) white solid; $C_{35}H_{33}ClN_2O_2P_2$ (MW: 611.06); 68.80% C, 5.44% H, 4.58% N.
^{1}H NMR (δ, $CDCl_3$, 20°C): 7.61 – 7.36 (m, 22H, PPh, $Ph^{3,5}$), 5.10 (d, *J* = 7.3 Hz, 2H, N*H*), 4.02 (q, *J* = 6.7 Hz, 2H, CH_2), 2.0 (m, *J* = 6.7 Hz, 1H, C*H*(CH_3)$_2$), 0.95 (d, *J* = 6.7 Hz, 6H, CH(CH_3)$_2$).
^{13}C{^{1}H} NMR (δ, $CDCl_3$, 20°C): 166.3 (*C*O), 143.4 (t, *J* = 19.6 Hz, $Ph^{2,6}$), 139.4 (d, *J* = 12.6 Hz, PPh), 131.2 (d, *J* = 20.9 Hz, $PPh^{2,6}$), 130.3 (Ph^{4}), 129.3 (PPh^{4}), 128.6 (t, *J* = 6.3 Hz, $PPh^{3,5}$), 107.2 ($Ph^{3,5}$), 106.4 (Ph^{ipso}), 70.9 (*C*H_2), 27.8 (*C*H(CH_3)$_2$), 19.1 (CH(*C*H_3)$_2$).
^{31}P{^{1}H} NMR (δ, $CDCl_3$, 20°C): 30.6.

4.6.3 PN Ligands

***N*-diphenylphosphino-2-aminopyridine (PN^{py}-Ph) (4a)**

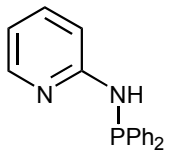

PPh_2Cl (9.5 mL, 53.1 mmol) was added dropwise to a solution of 2-aminopyridine (5.0 g, 53.1 mmol) and triethylamine (7.4 mL, 53.1 mmol) in toluene (50 mL) at 0°C. The mixture was stirred for 3 h. at 80°C, filtered and the solvent was removed under vacuum to give **4a** as a pale yellow

solid.

Yield: 12.9 g (87%) pale yellow solid; $C_{17}H_{15}N_2P$ (MW: 278.29); 73.37% C, 5.43% H, 10.07% N.

^{1}H NMR (δ, $CDCl_3$, 20ºC): 7.93 (d, *J* = 4.6 Hz, 1H, py^6), 7.51 – 7.42 (m, 5H, Ph), 7.36 – 7.33 (m, 6H, Ph and py^4), 7.06 (d, *J* = 8.2 Hz, 1H, py^3), 6.64 (dd, *J* = 5.2 Hz, *J* = 6.4 Hz, 1H, py^5), 5.93 (d, *J* = 8.4 Hz, 1H, N*H*).

^{13}C {^{1}H} NMR (δ, $CDCl_3$, 20ºC): 158.7 (d, *J* = 20.7 Hz, py^2), 148.1 (d, *J* = 1.5 Hz, py^6), 139.6 (d, *J* = 11.1 Hz, Ph^1), 137.82 (d, *J* = 2.3 Hz, py^4), 131.3 (d, *J* = 20.7 Hz, Ph^{2,6}), 129.2 (Ph^4), 128.6 (d, *J* = 6.9 Hz, Ph^{3,5}), 115.0 (py^5), 108.9 (d, *J* = 15.7 Hz, py^3).

^{31}P {^{1}H} NMR (δ, $CDCl_3$, 20ºC): 27.5.

_N_-diisopropylphosphino-2-aminopyridine (PN^{py}-^{i}Pr) (4b)

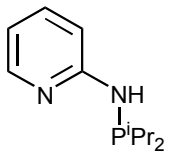

This ligand was prepared analogously to **4a** with 2-aminopyridine (5.0 g, 53.1 mmol), ^{i}Pr$_2$PCl (8.5 mL, 53.1 mmol) and triethylamine (7.4 mL, 53.1 mmol) as the starting materials.

Yield: 10.6 g (95%) pale yellow solid; $C_{11}H_{19}N_2P$ (MW: 210.26); 62.84% C, 9.11% H, 13.32% N.

^{1}H NMR (δ, $CDCl_3$, 20ºC): 8.00 (d, *J* = 3.9 Hz, 1H, py^6), 7.42 (dt, *J* = 1.5 Hz, *J* = 2.0 Hz, 1H, py^4), 7.08 (s, 1H, py^3), 6.61 (m, 1H, py^5), 4.94 (d, *J* = 10.5 Hz, 1H, N*H*), 1.77 (dh, *J* = 2.3 Hz, *J* = 7.0 Hz, 2H, C*H*(CH$_3$)$_2$), 1.09 – 0.99 (m, 12H, CH(C*H*$_3$)$_2$).

^{13}C {^{1}H} NMR (δ, $CDCl_3$, 20ºC): 160.7 (d, *J* = 19.6 Hz, py^2), 147.5 (d, *J* = 1.2 Hz, py^6), 137.6 (d, *J* = 2.0 Hz, py^4), 114.1 (py^5), 108.9 (d, *J* = 18.0 Hz, py^3), 26.3 (d, *J* = 11.1 Hz, *C*H(CH$_3$)$_2$), 18.6 (d, *J* = 19.5 Hz, CH(*C*H$_3$)$_2$), 17.0 (d, *J* = 7.7 Hz, CH(*C*H$_3$)$_2$).

^{31}P {^{1}H} NMR (δ, $CDCl_3$, 20ºC): 50.1.

_N_-dibenzo[d,f][1,3,2]dioxaphosphepine-2-aminopyridine (PN^{py}-BIPOL) (4c)

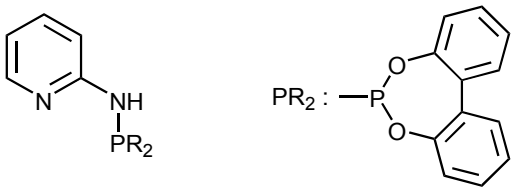

This ligand was prepared analogously to **4a** with 2,2'-biphenylylenephosphochloridite (**1b**, 1.1 g, 4.3 mmol), triethylamine (0.60 mL, 4.3 mmol) and 2-aminopyridine (405 mg, 4.3 mmol) as the starting materials.

Yield: 1.2 g (92%) white solid, $C_{17}H_{13}N_2O_2P$ (MW: 308.28); 66.24% C, 4.25% H, 9.09% N.

^{1}H NMR (δ, $CDCl_3$, 20ºC): 8.12 (d, *J* = 5.0 Hz, 1H, py^{6}), 7.54 – 7.47 (m, 3H, Ph and py^{4}), 7.39 – 7.24 (m, 6H, Ph), 6.84 – 6.79 (m, 2H, py^{3} and py^{5}), 6.38 (s, 1H, N*H*).
^{13}C {^{1}H} NMR (δ, $CDCl_3$, 20ºC): 155.4 (d, *J* = 16.9 Hz, py^{2}), 149.6 (d, *J* = 4.2 Hz, Ph), 148.3 (py^{6}), 138.0 (d, *J* = 1.6 Hz, py^{4}), 131.6 (d, *J* = 3.1 Hz, Ph), 129.8 (d, *J* = 1.1 Hz, Ph), 129.2 (Ph), 125.3 (Ph), 122.2 (d, *J* = 1.5 Hz, Ph), 116.6 (py^{5}), 110.2 (d, *J* = 11.1 Hz, py^{3}).
^{31}P {^{1}H} NMR (δ, $CDCl_3$, 20ºC): 147.3.

_N_-(4R,5R)-dicarbomethoxy-1,3,2-dioxaphospholane-2-aminopyridine (PN-^{Me}TAR) (4d)

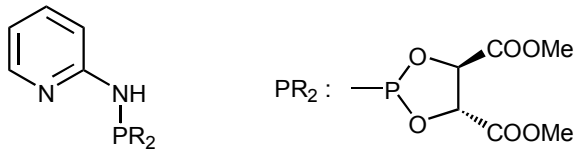

This ligand was prepared analogously to **1a** with 2-chloro-(4S,5S)-dicarbomethoxy-1,3,2-dioxaphospholane (**1d**, 1.5 g, 6.1 mmol), triethylamine (0.85 mL, 6.1 mmol) and 2-aminopyridine (577 mg, 6.1 mmol) as the starting materials.
Yield: 1.6 g (88%) white solid; $C_{11}H_{13}N_2O_2P$ (MW: 236.21); 55.93% C, 5.55% H, 11.86% N.
^{1}H NMR (δ, $CDCl_3$, 20ºC): 8.14 (d, *J* = 5.0 Hz, 1H, py^{6}), 7.48 (m, 1H, py^{4}), 6.80 (m, 1H, py^{3}), 6.70 (d, *J* = 8.2 Hz, py^{5}), 6.60 (s, 1H, N*H*), 5.10 (dd, *J* = 1.6 Hz, *J* = 5.2 Hz, 1H, C*H*), 4.84 (dd, *J* = 5.2 Hz, *J* = 10.0 Hz, 1H, C*H*), 3.83 (s, 3H, CH_3), 3.81 (s, 3H, CH_3).
^{13}C {^{1}H} NMR (δ, $CDCl_3$, 20ºC): 171.4 (*C*O), 169.2 (*C*O), 155.7 (d, *J* = 20.0 Hz, py^{2}), 148.0 (py^{6}), 140.0 (py^{4}), 116.6 (py^{5}), 110.3 (d, *J* = 6.9 Hz, py^{3}), 77.2 (*C*H), 77.0 (*C*H), 53.2 (*C*H_3), 53.1 (*C*H_3).
^{31}P {^{1}H} NMR (δ, $CDCl_3$, 20ºC): 142.6.

_O_-diphenylphosphino-2-hydroxyquinoline (PN^{ox}-Ph) (5a)

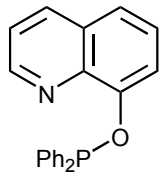

This ligand was prepared analogously to **4a** with 2-hydroxyquinoline (1.6 g, 11.1 mmol), Ph_2PCl (2.0 mL, 11.1 mmol) and triethylamine (1.6 mL, 11.1 mmol) as the starting materials.
Yield: 2.8 g (77%) yellow oil; $C_{21}H_{16}NOP$ (MW: 329.34); 76.59% C, 4.90% H, 4.25% N.
^{1}H NMR (δ, $CDCl_3$, 20ºC): 8.96 (dd, *J* = 1.5 Hz, *J* = 4.3 Hz, 1H, quin^{2}), 8.13 (dd, *J* = 1.8 Hz, *J* = 8.2 Hz, quin^{4}), 7.87 – 7.81 (m, 4H, quin), 7.52 – 7.26 (m, 10H, Ph).
^{13}C {^{1}H} NMR (δ, $CDCl_3$, 20ºC): 149.4 (quin), 147.9 (quin), 141.8 (d, *J* = 18.4 Hz, quin), 135.8 (Ph), 130.8 (d, *J* = 21.0 Hz, Ph^{2,6}), 129.6 (Ph^{4}), 128.4 (d, *J* = 6.9 Hz, Ph^{3,5}), 126.5 (quin), 122.1 (quin), 121.5 (quin), 117.9 (quin), 117.3 (d, *J* = 13.4 Hz, quin), 110.0 (quin).

$^{31}P\ \{^1H\}$ NMR (δ, $CDCl_3$, 20ºC): 118.4.

***O*-diisopropylphosphino-2-hydroxyquinoline (PN^{ox}-^{i}Pr) (5b)**

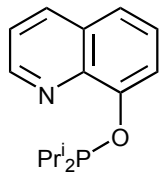

This ligand has been prepared analogously to **4a** with 2-hydroxyquinoline (1.6 g, 11.1 mmol), $^iPr_2PCl$ (1.8 mL, 11.1 mmol) and triethylamine (1.6 mL, 11.1 mmol) as the starting materials.
Yield: 1.9 g (66%) yellow oil; $C_{15}H_{20}NOP$ (MW: 261.30); 68.95% C, 7.71% H, 5.36% N.
^1H NMR (δ, $CDCl_3$, 20ºC): 8.92 (dd, *J* = 1.5 Hz, *J* = 4.0 Hz, 1H, quin^2), 8.07 (dd, *J* = 1.5 Hz, *J* = 8.2 Hz, 1H, quin^4), 7.55 - 7.41 (m, 1H, quin), 7.39 – 7.32 (m, 3H, quin), 2.17 (m, *J* = 7.2 Hz, 2H, C*H*$(CH_3)_2$), 1.30 (m, 6H, CH(C*H*$_3)_2$), 1.14 (m, 6H, CH(C*H*$_3)_2$).
$^{13}C\ \{^1H\}$ NMR (δ, $CDCl_3$, 20ºC): 149.3 (quin), 147.8 (quin), 141.5 (quin), 129.6 (quin), 126.5 (quin), 121.3 (quin), 120.8 (quin), 116.3 (d, J = 18.8 Hz, quin), 109.9 (quin), 28.8 (d, *J* = 17.6 Hz, *C*H$(CH_3)_2$), 17.8 (d, *J* = 23.4 Hz, CH(*C*H$_3)_2$), 17.5 (d, *J* = 11.1 Hz, CH(*C*H$_3)_2$).
$^{31}P\ \{^1H\}$ NMR (δ, $CDCl_3$, 20ºC): 158.2.

4.6.4 NPN Ligands

NPN^{py}-Ph^{75} (6)

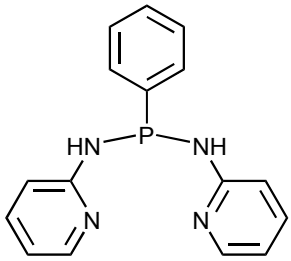

Cl_2PPh (2.8 mL, 20 mmol) was added at 0ºC to a solution of 2-aminopyridine (7.5 g, 80 mmol) in 150 mL THF; the reaction mixture was allowed to reach RT and stirred for 2 h. The solution was then filtered and the solvent was removed under vacuum to give a white solid.
Yield: 3.5 g (60 %) white solid; $C_{16}H_{15}N_4P$ (MW: 294.30); 65.30% C, 5.14% H, 19.04% N.
^1H NMR (δ, $CDCl_3$, 20ºC): 8.00 (d, *J* = 4.0 Hz, 2H, py^6), 7.70 (t, *J* = 6.9 Hz, 2H, py^4), 7.53 (t, *J* = 7.6 Hz, 2H, py^3), 7.49 – 7.07 (m, 7H, py^5 and Ph), 6.58 (t, *J* = 6.1 Hz, 2H, N*H*).

$^{13}C\ \{^1H\}$ NMR (δ, $CDCl_3$, 20ºC): 157.2 (d, *J* = 15.2 Hz, py^2), 145.7 (py^6), 142.1 (Ph^1), 138.8 (py^4), 129.9 (d, *J* = 19.4 Hz, $Ph^{2,6}$), 129.3 (Ph^4), 128.6 (d, *J* = 5.9 Hz, $Ph^{3,5}$), 115.4 (py^5), 111.2 (d, *J* = 11.4 Hz, py^3).

$^{31}P\ \{^1H\}$ NMR (δ, $CDCl_3$, 20ºC): 45.5.

4.7 Complexes

4.7.1 Iron(II) PNP complexes

$[Fe(PNP\text{-}Ph)(CH_3CN)_3](BF_4)_2$ (7a)

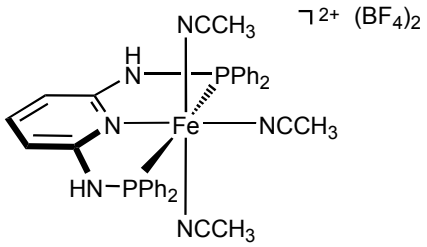

A solution of **2a** (500 mg, 1.05 mmol) and $[Fe(H_2O)_6](BF_4)_2$ (354 mg, 1.05 mmol) in acetonitrile (10 mL) was stirred at room temperature for 2 h. Insoluble materials were then removed by filtration and the volume of the solution was reduced to about 2 mL. Upon addition of Et_2O an orange precipitate was formed, which was washed twice with Et_2O and dried under vacuum.

Yield 805 mg (97%) orange solid; $C_{35}H_{37}B_2F_8FeN_6P_2$ (MW: 833.12); 50.46% C, 4.48% H, 10.09% N.

^1H NMR (δ, CD_3CN, 20°C): 8.36 (s, 2H, N*H*), 7.91-7.62 (m, 21H, Ph, py^4), 6.64 (d, *J* = 8.0 Hz, 2H, $py^{3,5}$), 1.97 (s, 9H, C*H*$_3$CN).

$^{13}C\{^1H\}$ NMR (δ, CD_3CN, 20°C): 163.2 (t, *J* = 9.8 Hz, $py^{2,6}$), 141.2 (py^4), 137.7 (CH_3CN), 136.7 (Ph^1), 131.5 ($Ph^{2,6}$), 131.0 (Ph^4), 129.2 ($Ph^{3,5}$), 100.9 ($py^{3,5}$), 3.4 (*C*H$_3$CN).

$^{31}P\{^1H\}$ NMR (δ, CD_3CN, 20°C): 103.9.

[Fe(PNP-^{i}Pr)(CH$_3$CN)$_3$](BF$_4$)$_2$ (7b)

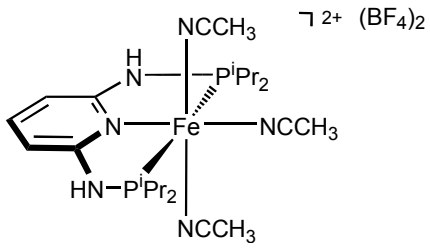

This complex was prepared analogously to **7a** with **2b** (1.0 g, 2.9 mmol) and [Fe(H$_2$O)$_6$](BF$_4$)$_2$ (1.0 g, 2.9 mmol) as the starting materials.

Yield: 1.9 g (94%) orange solid; $C_{23}H_{42}B_2F_8FeN_6P_2$ (MW: 694.03); 39.80% C, 6.10% H, 12.11% N.

^{1}H NMR (δ, CD$_3$CN, 20°C): 7.30 (s, 2H, N*H*), 7.16 (s, 1H, py^4), 6.30 (s, 2H, py^{3,5}), 2.97 (s, 4H, C*H*(CH$_3$)$_2$), 1.97 (s, 9H, C*H*$_3$CN), 1.60 (s, 12H, CH(C*H*$_3$)$_2$), 1.42 (s, 12H, CH(C*H*$_3$)$_2$).

^{13}C{^{1}H} NMR (δ, CD$_3$CN, 20°C): 164.1 (t, *J* = 8.1 Hz, py^{2,6}), 140.6 (py^4), 138.3 (CH$_3$*C*N), 99.1 (py^{3,5}), 26.8 (t, *J* = 10.1 Hz, *C*H(CH$_3$)$_2$), 17.6 (CH(*C*H$_3$)$_2$), 17.3 (CH(*C*H$_3$)$_2$). 4.4 (*C*H$_3$CN).

^{31}P{^{1}H} NMR (δ, CD$_3$CN, 20°C): 115.1.

[Fe(PNP-ETOL)(CH$_3$CN)$_3$](BF$_4$)$_2$ (7c)

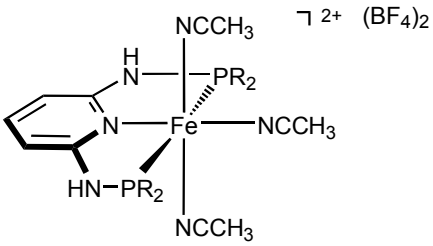

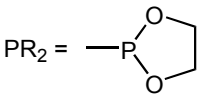

This complex was prepared analogously to **7a** with **2d** (300 mg, 1.51 mmol) and [Fe(H$_2$O)$_6$](BF$_4$)$_2$ (511 mg, 1.51 mmol) as the starting materials.

Yield: 600 mg (72 %) orange solid; $C_{15}H_{22}B_2F_8FeN_6O_4P_2$ (MW: 641.778); 28.07% C, 3.46% H, 13.09% N.

^{1}H NMR (δ, CD$_3$CN, 20°C): 8.14 (s, 2H, NH), 7.36 (t, *J* = 7.6 Hz, 1H, py^4), 6.22 (d, *J* = 7.6 Hz, 1H, py^{3,5}), 5.90 (d, *J* = 7.6 Hz, 1H, py^{3,5}), 4.71-4.59 (m, 4H, C*H*$_2$), 3.28-3.00 (m, 3H, C*H*$_3$CN), 1.13-0.95 (m, 6H, C*H*$_3$CN).

^{13}C{^{1}H} NMR (δ, CD$_3$CN, 20°C): 159.5 (t, *J* = 12.1 Hz, py^{2,6}), 146.0 (CH$_3$*C*N), 141.8 (py^4), 101.2 (py^{3,5}), 67.3 (*C*H$_2$), 8.1 (*C*H$_3$CN).

^{31}P{^{1}H} NMR (δ, CD$_3$CN, 20°C): 183.6.

[Fe(PNP-BIPOL)(CH_3CN)$_3$](BF_4)$_2$ (7d)

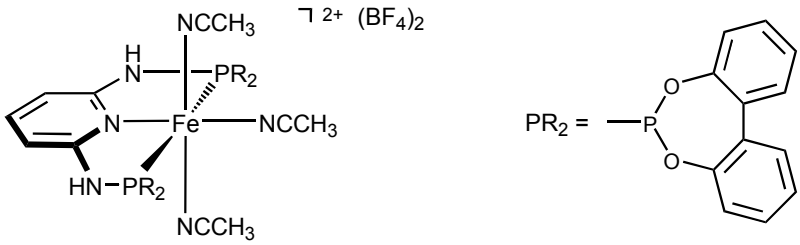

This complex was prepared analogously to **7a** with **2e** (2.0 g, 3.7 mmol) and [Fe(H_2O)$_6$](BF_4)$_2$ (1.3 g, 3.7 mmol) as the starting materials.

Yield: 2.7 g (80 %) orange solid; $C_{35}H_{30}B_2F_8FeN_6O_4P_2$ (MW: 890.062); 47.23%C, 3.40% H, 9.44% N.

^{1}H NMR (δ, CD_3CN, 20°C): 8.89 (s, 2H, N*H*), 7.84-7.81 (m, 14H, Ph), 7.23 (s, 1H, py^4), 7.00-6.93 (m, 2H, Ph), 6.52 (d, *J* = 8.2 Hz, 2H, py^{3,5}), 2.32 (s, 6H, C*H*$_3$CN), 1.59 (s, 3H, C*H*$_3$CN).

^{13}C{^{1}H} NMR (δ, CD_3CN, 20°C): 159.9 (t, *J* = 13.2 Hz, py^{2,6}), 151.4 (Ph), 148.6 (Ph), 146.1 (py^4), 142.7 (Ph), 137.7 (CH_3*C*N), 130.5 (Ph), 127.4 (Ph), 122.1 (Ph), 102.6 (py^{3,5}), 4.3 (*C*H$_3$CN).

^{31}P{^{1}H} NMR (δ, CD_3CN, 20°C): 186.7.

[Fe(PNP-BINOL)(CH_3CN)$_3$](BF_4)$_2$ (7e)

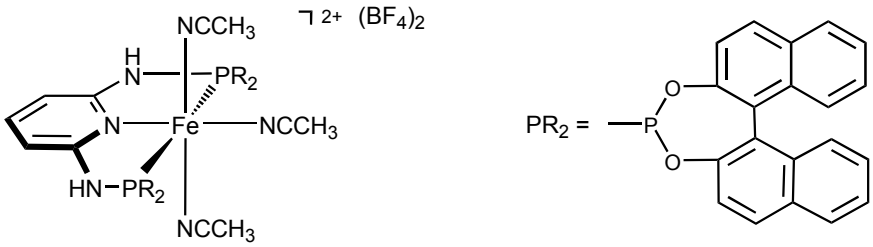

This complex was prepared analogously to **7a** with **2f** (300 mg, 0.40 mmol) and [Fe(H_2O)$_6$](BF_4)$_2$ (137 mg, 0.40 mmol) as the starting materials.

Yield: 157 mg (36%) orange solid; $C_{51}H_{38}B_2F_8FeN_6O_4P_2$ (MW: 1090.30); 56.18% C, 3.51% H, 7.71% N.

^{1}H NMR (δ, CD_3CN, 20°C): 8.35-8.02 (m, 10H, Ph, N*H*), 7.48-7.27 (m, 17H, Ph, py^4), 5.97-5.80 (m, 2H, py^{3,5}), 1.33 (s, 9H, C*H*$_3$CN).

^{13}C{^{1}H} NMR (δ, CD_3CN, 20°C): 158.2 (py^{2,6}), 144.9 (py^4), 134.1 (CH_3*C*N), 133.4 (Ph), 132.0 (Ph), 131.1 (Ph), 130.7 (Ph), 129.9 (Ph), 129.0 (Ph), 128.6 (Ph), 128.0 (Ph), 126.5 (Ph), 124.9 (Ph), 95.7 (py^{3,5}), 8.1 (*C*H$_3$CN).

^{31}P{^{1}H} NMR (δ, CD_3CN, 20°C): 189.9.

[Fe(PNP-^{Me}TAR)(CH_3CN)$_3$](BF_4)$_2$ (7f)

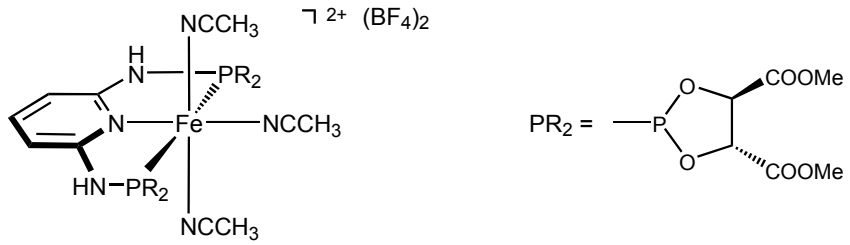

This complex was prepared analogously to **7a** with **2g** (200 mg, 0.38 mmol), and [Fe(H_2O)$_6$](BF_4)$_2$ (128 mg, 0.38 mmol) as the starting materials.

Yield: 294 mg (88 %) orange solid; $C_{23}H_{30}B_2F_8FeN_6O_{12}P_2$ (MW: 873.93); 31.61% C, 3.46% H, 9.62% N.

^{1}H NMR (δ, CD_3CN, 20°C): 8.17 (s, 2H, N*H*), 7.57 (t, *J* = 7.7 Hz, 1H, py^4), 6.64 (d, *J* = 7.7 Hz, 2H, py^{3,5}), 5.74 (t, *J* = 6.7 Hz, 1H, C*H*), 5.63 (t, *J* = 8.6 Hz, 1H, C*H*), 4.01 (s, 6H, C*H*$_3$), 3.87 (s, 6H, C*H*$_3$), 1.97 (s, 9H, C*H*$_3$CN).

^{13}C{^{1}H} NMR (δ, CD_3CN, 20°C): 168.6 (*C*O), 167.7 (*C*O), 159.1 (t, *J* = 12.1 Hz, py^{2,6}), 146.1 (py^4), 136.9 (CH_3*C*N), 103.0 (t, *J* = 4.4 Hz, py^{3,5}), 78.5 (t, *J* = 3.0 Hz, *C*H), 77.2 (t, *J* = 3.7 Hz, *C*H), 53.7 (*C*H$_3$), 53.3 (*C*H$_3$), 8.2 (*C*H$_3$CN).

^{31}P{^{1}H} NMR (δ, CD_3CN, 20°C): 193.8.

[Fe(PNP-Ph)(bipy)(CH_3CN)](BF_4)$_2$ (8a)

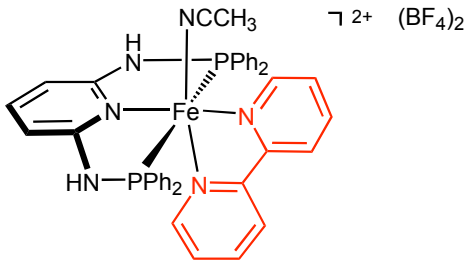

2,2'-Bipyridine (28 mg, 0.18 mmol) was added to a solution of **7a** (150 mg, 0.18 mmol) in CH_3NO_2. After the mixture was stirred at room temperature for 2 h., the solvent was evaporated in vacuum, the solid precipitated and washed twice with Et_2O and evaporated to dryness.

Yield: 154 mg (95%) deep red solid; $C_{42}H_{39}B_2F_8FeN_7O_2P_2$ (MW: 965.22); 52.26% C, 4.07% H, 10.16% N.

^{1}H-NMR (δ, CD_3NO_2, 20°C): 8.66-8.64 (m, 2H, bipy^1), 8.56 (d, *J* = 8.2 Hz, 2H, N*H*), 8.11 - 8.06 (m, 2H, bipy^4), 7.72 - 7.53 (m, 10H, Ph, py^4), 7.43 - 7.37 (m, 2H, bipy^{2,3}), 7.18 - 6.75 (m, 11H, Ph), 6.49 (s, 2H, py^{3,5}), 1.68 (t, *J* = 1.48 Hz, 3H, C*H*$_3$CN).

$^{13}C\{^1H\}$NMR (CD_3NO_2, δ): 163.2 (py^{2,6}), 156.8 (bipy^5), 154.0 (bipy^1), 141.5 (py^4), 138.0 (bipy^3), 131.5 (Ph), 130.6 (Ph^{2,6}), 130.0 (Ph^4), 129.3 (Ph^{3,5}), 128.7 (bipy^4), 127.2 (CH_3CN), 123.6 (bipy^2), 101.8 (py^{3,5}), 12.7 (CH_3CN).

$^{31}P\{^1H\}$NMR (δ, CD_3NO_2, 20°C): 101.8.

[Fe(PNP-Ph)(terpy)](BF_4)$_2$ (8b)

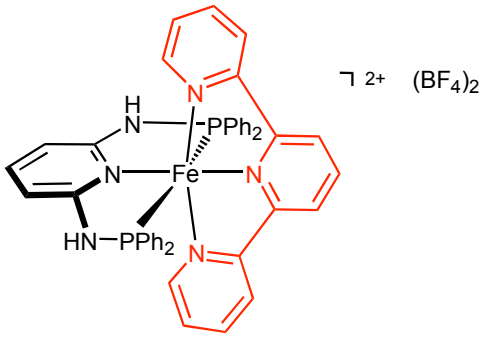

This complex was prepared analogously to **8a** with 2, 2':6', 2''-Terpyridine (42 mg, 0.18 mmol) and **7a** (150 mg, 0.18 mmol) as the starting materials.

Yield: 139 mg (83%) deep red solid; $C_{45}H_{39}B_2F_8FeN_7O_2P_2$ (MW: 1001.25); 53.98% C, 3.93% H, 9.79% N.

^{1}H NMR (δ, CD_3NO_2, 20°C): 8:38 (m, 4H, terpy^{1,4}), 8.15 (s, 2H, N*H*), 7.74 (d, *J* = 7.8 Hz, 3H, terpy^{3,7}), 7.46 (t, *J* = 8.1Hz, 2H, terpy^6), 7.19 - 7.16 (m, 4H, terpy^2, py^{3,5}), 7.05 - 6.99 (m, 10H, Ph), 6.89 - 6.83 (m, 11H, Ph, py^4).

$^{13}C\{^1H\}$NMR (δ, CD_3NO_2, 20°C): 163.3 (py^{2,6}), 157.64 (terpy^8), 156.80 (terpy^5), 152.75 (terpy^1), 141.62 (py^4), 136.66 (terpy^3), 136.26 (terpy^7), 130.60 (Ph^{2,6}), 128.80-128.72 (Ph^4, Ph), 127.04 (Ph^{3,5}), 123.20 (terpy^4), 122.98 (terpy^6), 122.01 (terpy^2), 102.20 (py^{3,5}).

$^{31}P\{^1H\}$NMR (δ, CD_3NO_2, 20°C): 100.3.

[Fe(PNP-Ph)$_2$](BF_4)$_2$ (8c)

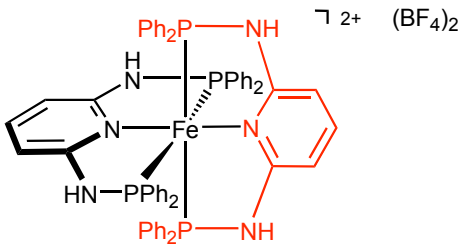

Method 1: $Fe(H_2O)_6(BF_4)_2$ (300 mg, 0.90 mmol) was added to a solution of **2a** (848 mg, 1.80 mmol) in 10 mL THF, whereupon the colour of the solution turned purple. After the mixture was stirred at room temperature for 2 h., the solvent was evaporated in vacuum, the solid precipitated and washed twice with Et_2O and evaporated to dryness.

Yield: 960 mg (90%)

Method 2: **2a** (172 mg, 0.36 mmol) was added to a solution of **7a** (300 mg, 0.36 mmol) in 10 mL CH_3NO_2 and the purple solution was stirred at RT for 2 h. The solvent was removed under vacuum and the resulting purple solid was washed twice with Et_2O and dried.

Yield: 375 mg (88%) purple solid; $C_{58}H_{50}B_2F_8FeN_6P_4$ (MW: 1184.42); 58.82% C, 4.25% H, 7.10% N.

^{1}H NMR (δ, CD_3NO_2, 20°C): 7.95 (t, *J* = 8.0 Hz, 2H, py^4), 7.25-6.48 (m, 46H, Ph, py^{3,5}, N*H*).

^{13}C{^{1}H}NMR (δ, CD_3NO_2, 20°C): 163.0 (s, py^{2,6}), 142.1 (s, py^4), 136.8 (s, Ph), 129.9 (s, Ph^{2,6}), 129.1 (s, Ph^4), 128.8 (s, Ph^{3,5}), 101.6 (s, py^{3,5}).

^{31}P{^{1}H}NMR (δ, CD_3NO_2, 20°C): 92.0.

[Fe(PNP-Ph)(CO)(CH$_3$CN)$_2$](BF$_4$)$_2$ (9a)

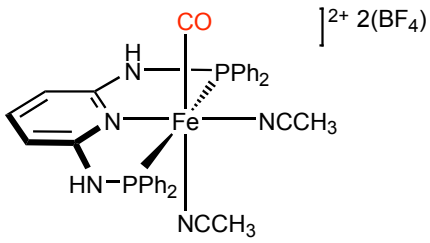

Carbon monoxide was bubbled into a solution of **7a** (0.5 g, 0.6 mmol) in acetone (30 mL) for 15 min, whereupon the colour of the solution turned from orange to yellow, and the mixture was stirred overnight at RT under CO atmosphere. After removal of the solvent under reduced pressure, the remaining yellow solid was washed twice with Et_2O (20 mL) and dried under vacuum.

Yield: 400 mg (88%) yellow solid; $C_{34}H_{31}B_2F_8FeN_5OP_2$ (MW:) 49.98% C, 3.82% H, 8.57% N.

^{1}H NMR (δ, acetone-d$_6$, 20°C): 9.21 (s, 2H, N*H*), 7.99 – 7.84 (m, 7H, Ph and py^4), 7.56 – 7.40 (m, 14H, Ph), 6.70 (d, *J* = 7.4 Hz, 2H, py^{3,5}), 2.58 (s, 3H, C*H*$_3$CN), 1.58 (s, 3H, C*H*$_3$CN).

^{13}C{^{1}H} NMR (δ, acetone-d$_6$, 20°C): 212.4 (t, *J* = 27.0 Hz, *C*O), 162.6 (t, *J* = 8.3 Hz, py^{2,6}), 143.6 (py^4), 140.2 (Ph^1), 133.4 (CH$_3$*C*N), 133.1 (CH$_3$*C*N), 132.1 – 131.7 (m, Ph), 130.7 – 130.4 (m, Ph), 103.2 (t, *J* = 4.1 Hz, py^{3,5}), 5.1 (*C*H$_3$CN), 3.4 (*C*H$_3$CN).

^{31}P{^{1}H} NMR (δ, acetone-d$_6$, 20°C): 95.9.

IR (KBr, cm^{-1}): 2021 ($\nu_{C=O}$).

[Fe(PNP-^{i}Pr)(CO)(CH$_3$CN)$_2$](BF$_4$)$_2$ (9b)

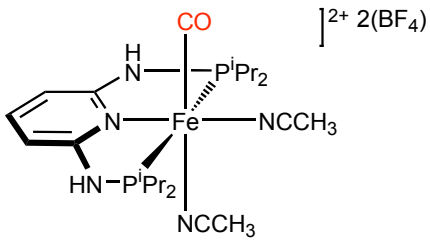

This complex was prepared analogously to **9a** with **7b** (1.5 g, 2.2 mmol) as the starting material. Yield: 1.4 g (93%) yellow solid; $C_{22}H_{39}B_2F_8FeN_5OP_2$ (MW: 681.00); 38.80%C, 5.77% H, 10.28% N.

^{1}H NMR (δ, Acetone-d$_6$, 20°C): 7.39 (s, 1H, py^4), 6.90 (s, 2H, N*H*), 6.34 (s, 2H, py^{3,5}), 3.17 (s, 4H, C*H*(CH$_3$)$_2$), 2.53 (s, 3H, C*H*$_3$CN), 2.40 (s, 3H, C*H*$_3$CN), 1.56 – 1.50 (m, 24H, CH(C*H*$_3$)$_2$).

^{13}C{^{1}H} NMR (δ, Acetone-d$_6$, 20°C): 215.4 (t, *J* = 25.9 Hz, *C*O), 162.1 (t, *J* = 6.6 Hz, py^{2,6}), 141.8 (t, *J* = 38.8 Hz, py^4), 139.8 (CH$_3$*C*N), 100.59 (t, *J* = 3.5 Hz, py^{3,5}), 27.87 (t, *J* = 13.0 Hz, *C*H(CH$_3$)$_2$), 17.7 (d, *J* = 29.7 Hz, CH(*C*H$_3$)$_2$), 17.0 (d, *J* = 29.1 Hz, CH(*C*H$_3$)$_2$), 3.8 (*C*H$_3$CN), 3.7 (*C*H$_3$CN).

^{31}P{^{1}H} NMR (δ, Acetone-d$_6$, 20°C): 114.7.

IR (KBr, cm^{-1}): 1995 ($_{C=O}$).

[Fe(PNP-^{i}Pr)(CO)(CH$_3$CN)$_2$](BArF)$_2$ (9b')

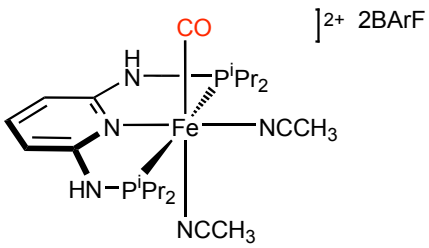

BArF$^-$ =

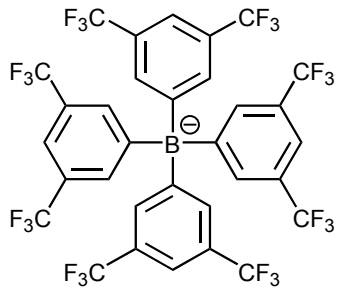

NaBArF (260 mg, 0.29 mmol) was added to a suspension of **9b** (100 mg, 0.14 mmol) in CH$_2$Cl$_2$ (10 mL), whereupon a yellow solution formed and a white solid precipitated. The mixture was stirred at room temperature for 2 h. and the solution was filtered and dried under vacuum.

Yield: 275 mg (88%) brown solid; $C_{86}H_{63}B_2F_{48}FeN_5OP_2$ (MW: 2233.81); 46.24% C, 2.84% H, 3.14% N.

^{1}H NMR (δ, CD$_2$Cl$_2$, 20°C): 7.72 (m, 16 H, BArF), 7.57 (m, 8H, BArF), 7.33 (t, *J* = 8.4 Hz, 1H, py^4), 6.30 (d, *J* = 8.4 Hz, 2H, py^{3,5}), 5.68 (s, 2H, N*H*), 3.08 (m, 2H, C*H*(CH$_3$)$_2$), 2.90 (bs, 2H, C*H*(CH$_3$)$_2$), 2.46 (s, 3H, C*H*$_3$CN), 2.30 (s, 3H, C*H*$_3$CN), 1.55 – 1.24 (m, 24H, CH(C*H*$_3$)$_2$.

^{13}C{^{1}H} NMR (δ, CD$_2$Cl$_2$, 20°C): 219.9 (*C*O), 161.7 (q, *J* = 49.7 Hz, BArF), 161.1 (py^{2,6}), 143.1 (py^4), 134.7 (BArF), 133.6 (CH$_3$*C*N), 128.8 (q, *J* = 32.2 Hz, BArF), 124.5 (q, *J* = 270.7 Hz, BArF),

117.5 (BArF), 102.1 (py^{3,5}), 29.6 (t, *J* = 10.4 Hz, *C*H(CH_3)$_2$), 28.9 (t, *J* = 12.3 Hz, *C*H(CH_3)$_2$), 17.6 (t, *J* = 5.7 Hz, CH(*C*H_3)$_2$), 4.65 (*C*H_3CN), 4.47 (*C*H_3CN).

^{31}P{^{1}H} NMR (δ, CD_2Cl_2, 20°C): 114.5.

Deprotonation of [Fe(PNP-BIPOL)(CH_3CN)$_3$](BF_4)$_2$ (7d).
Formation of [Fe(PNP-BIPOL)(CH_3CN)$_3$]BF_4 (10)

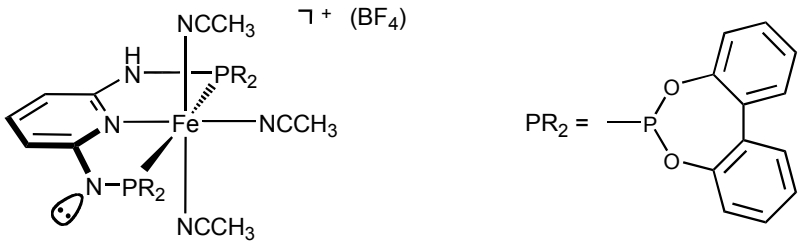

Method 1**.** A solution of **7d** (150 mg, 0.17 mmol) in acetonitrile was treated with an excess of NaHg (3%) whereupon an immediate formation of gas (H_2) took place. The mixture was stirred until the evolution of dihydrogen had ceased. Insoluble materials were then removed by filtration and the solvent was evaporated under reduced pressure. The resulting dark brown solid was washed twice with Et_2O and dried under vaccum Yield: 104 mg (76%).

Method 2. A solution of **7d** (500 mg, 0.56 mmol) in acetonitrile was chromatographed over basic Al_2O_3 yielding a dark brown solution. Removal of the solvent under reduced pressure gave **10** as a dark brown solid.

Yield: 367 mg (81%) dark brown solid; $C_{35}H_{29}BF_4FeN_6O_4P_2$ (MW: 802.250); 52.40% C, 3.64% H, 10.48% N.

^{13}C{^{1}H} NMR (δ, CD_3CN, 20°C): 158.9 (py^{2,6}), 149.0 (py^4), 141.7 (CH_3*C*N), 130.3 (Ph), 129.8 (Ph), 127.0 (Ph), 122.2 (Ph), 101.7 (py^{3,5}), 4.1 (*C*H_3CN). Quaternary carbons could not be detected.

^{31}P{^{1}H} NMR (δ, CD_3CN, 20°C): 194.4.

Reaction of 10 with HBF_4·OEt_2. Formation of [Fe(PNP-BIPOL)(CH_3CN)$_3$](BF_4)$_2$ (7d)

A 5 mm NMR tube was charged with **10** (30 mg, 0.04 mmol) in CD_3CN (0.5 mL). Upon addition of HBF_4·OEt_2 (2.3 µL, 0.04 mmol), the color of the solution changed from brown to orange. The reaction was monitored by ^{1}H and ^{31}P{^{1}H} NMR spectroscopy and quantitative formation of **7d** was observed.

[Fe(PNP-Ph)(CO)$_2$(Br)]BPh$_4$ (11)

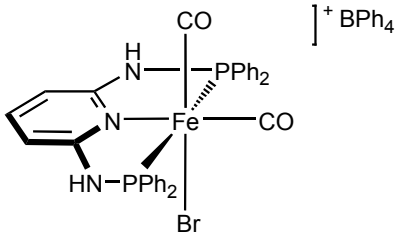

2a (364 mg, 0.76 mmol) was added to a solution of $Fe(CO)_4Br_2$ (250 mg, 0.76 mmol) and $NaBPh_4$ (261 mg, 0.76 mmol) in CH_2Cl_2; after CO evolution was complete (~30 min.), the solution was filtered to remove the NaBr and evaporated to dryness.

Yield: 417 mg (82%) dark brown solid; $C_{55}H_{45}BBrFeN_3O_2P_2$ (MW: 988.49); 66.83% C, 4.59% H, 4.25% N.

^{1}H NMR (δ, CD_2Cl_2, 20°C): 7.90 (s, 2H, N*H*), 7.79 - 7.77 (m, 3H, Ph), 7.66 - 7.64 (m, 4H, Ph), 7.48 - 7.45 (m, 20H, Ph and py^4), 7.02 - 7.00 (m, 10H, Ph), 6.85 - 6.82 (m, 4H, Ph), 6.58 (d, *J* = 7.9 Hz, py^{3,5}).

^{13}C{^{1}H} NMR (δ, CD_2Cl_2, 20°C): 209.8 (t, *J* = 20.2 Hz, *C*O), 206.5 (t, *J* = 23.1 Hz, *C*O), 164.0 (q, *J* = 49.32 Hz, BPh$_4$-Ph^1), 159.3 (t, *J* = 8.67 Hz, py^{2,6}), 142.4 (py^4), 136.0 (BPH$_4$-Ph^{2,6}), 132.2 (PPh^{2,6}), 132.0 (PPh^1), 130.0 (PPh^4), 129.9 (PPh^{3,5}), 125.8 (BPh$_4$-Ph^4), 122.0 (BPh$_4$-Ph^{3,5}), 102.7 (py^{3,5}).

^{31}P{^{1}H} NMR (δ, CD_2Cl_2, 20°C): 100.5.

[Fe(PNP-^{i}Pr)(Cl)$_2$] (12a)

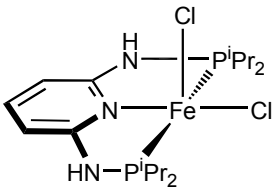

$FeCl_2$ (180 mg, 1.46 mmol) was added to a solution of **2b** (500 mg, 1.46 mmol) in 20 mL THF, and the reaction mixture was stirred overnight at RT. The yellow solution was then filtered and the solvent was evaporated under reduced pressure. The residue was washed twice with Et_2O (10 mL) and dried under vacuum.

Yield: 615 mg (90%) yellow solid; $C_{17}H_{33}Cl_2FeN_3P_2$ (MW: 468.19); 43.61% C, 7.10% H, 8.98% N.

^{1}H NMR (δ, Acetone-d$_6$, 20°C, all peaks appear as broad singlets): 140.35 (C*H*(CH$_3$)$_2$), 75.30 (N*H*), 47.49 (py^{3,5}), 13.13 (CH(C*H*$_3$)$_2$), 7.00 (CH(C*H*$_3$)$_2$), -21.26 (py^4). The identity of the N*H* protons was determined by adding 0.2 mL D_2O to the NMR tube, whereupon the signal at 75.30 ppm disappeared.

[Fe(PNP-^{t}Bu)(Cl)$_2$] (12b)

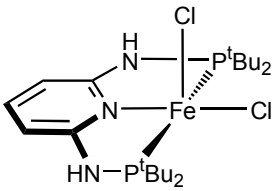

This complex was prepared analogously to **12a** with $FeCl_2$ (100 mg, 0.78 mmol) and **2c** (314 mg, 0.78 mmol) as the starting materials.

Yield: 343 mg (84%) yellow solid; $C_{21}H_{41}Cl_2FeN_3P_2$ (MW: 524.28); 48.11% C, 7.88% H, 8.01% N.

^{1}H NMR (δ, Acetone-d$_6$, 20°C, all peaks appear as broad singlets): 64.68 (N*H*), 51.57 (py^{3,5}), 17.46 (C*H*$_3$), -20.18 (py^4).

4.7.2 Iron(II) PN Complexes

[Fe(PN^{py}-Ph)$_2$(AN)$_2$](BF$_4$)$_2$ (13)

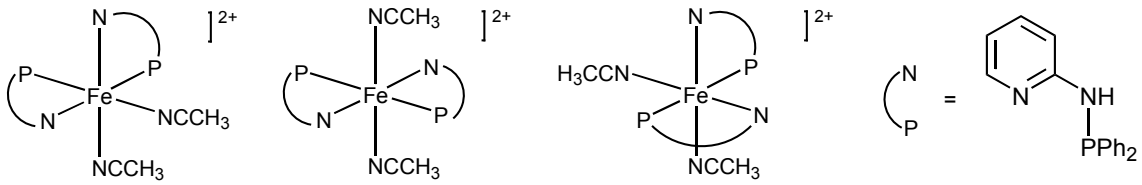

A **B** **C**

4a (200 mg, 0.72 mmol) was added to a solution of $[Fe(H_2O)_6](BF_4)_2$ (121 mg, 0.36 mmol) in 15 mL CH_3CN, whereupon the solution turned violet. After the reaction mixture was stirred at RT for 2 h., the solvent was removed under vacuum, the residue washed twice with Et_2O and dried.

Yield: 381 mg (61%) violet solid; $C_{38}H_{36}B_2F_8FeN_6P_2$ (MW: 868.14); 52.57% C, 4.18% H, 9.68% N.

^{1}H NMR (δ, CD_3NO_2, 20ºC): 9.00 (s, 1H, py^6, **A, C**), 8.04 – 7.00 (m, 14 H, py and N*H*, **A, C**), 2.17 (s, 3H, C*H*$_3$CN, **A, C**), 2.08 (s, C*H*$_3$CN, **B**), 1.87 (s, 3H, C*H*$_3$CN, **A, C**).

^{13}C {^{1}H} NMR (δ, $CDCl_3$, 20ºC): 163.9 (d, *J* = 12.9 Hz, py^2, **A, C**), 162.7 (d, *J* = 10.5 Hz, py^2, **B**), 152.0 (py^6, **A, C**), 150.1 (py^6, **B**), 140.9 (py^4, **A, C**), 139.3 (py^4, **B**), 137.1 (Ph^1, **A, C**), 135.9 (CH$_3$*C*N, **A, C**), 135.1 (CH$_3$*C*N, **B**), 133.5 (Ph^1, **B**), 130.8 (d, *J* = 7.2 Hz, Ph^{2,6}, **B**), 130.6 (d, *J* = 7.7 Hz, Ph^{2,6}, **A, C**), 130.1 (d, *J* = 11.5 Hz, Ph^4, **A, C**), 129.3 (t, *J* = 11.2, Ph^{3,5}, **A, C**), 129.0 (t, *J* = 9.8 Hz, Ph^{3,5}, **B**), 128.4 (d, *J* = 10.5 Hz, Ph^4, **B**), 118.1 (py^5, **A, C**), 117.3 (py^5, **B**), 111.8 (py^3, **A, C**), 111.6 (py^3, **B**), 3.2 (*C*H$_3$CN, **A, C**), 2.7 (*C*H$_3$CN, **B**), 2.5 (*C*H$_3$CN, **A, C**).

$^{31}P\ \{^1H\}$ NMR (δ, $CDCl_3$, 20ºC): 119.0 (d, *J* = 53.5 Hz, **A, C**), 113.6 (d, *J* = 53.5 Hz, **A, C**), 110.8 (s, **B**).

Fe(PN^{py}-Ph)(CO)$_2$Br$_2$ (14a)

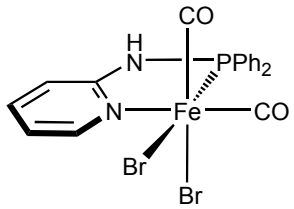

4a (200 mg, 0.72 mmol) was added to a solution of $Fe(CO)_4Br_2$ (235 mg, 0.72 mmol) in 15 mL toluene; once the CO evolution subsided, the reaction mixture was stirred at RT for 1 h., and the solvent was decanted from the resulting brown solid, which was washed twice with Et_2O and dried under vacuum.

Yield: 332 mg (81%) brown solid; $C_{19}H_{15}Br_2FeN_2O_2P$ (MW: 550.00); 41.49% C, 2.75% H, 5.09% N.

^1H NMR (δ, acetone-d_6, 20ºC): 9.40 (d, *J* = 4.9 Hz, 1H, py^6), 9.20 (d, *J* = 7.0 Hz, 1H, N*H*), 7.81 – 7.05 (m, 12H, Ph).

$^{13}C\ \{^1H\}$ NMR (δ, acetone-d_6, 20ºC): 214.0 (d, *J* = 24.0 Hz, *C*O), 211.9 (d, *J* = 23.0 Hz, *C*O), 161.4 (py^2), 151.4 (py^6), 141.0 (py^4), 136.4 (Ph^1), 132.2 (d, *J* = 11.0 Hz, Ph^{2,6}), 129.0 (Ph^4), 128.4 (d, *J* = 11.5 Hz, Ph^{3,5}), 117.2 (py^5), 112.1 (d, *J* = 9.2 Hz, py^3).

$^{31}P\ \{^1H\}$ NMR (δ, acetone-d_6, 20ºC): 123.1

IR (KBr, cm^{-1}): 1997 and 2048 ($_{C=O}$).

Fe(PN^{py}-^{i}Pr)(CO)$_2$Br$_2$ (14b)

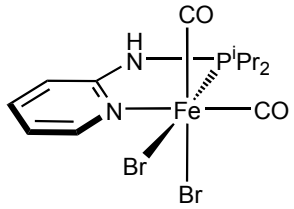

This complex was prepared analogously to **14a** with **4b** (152 mg, 0.72 mmol) and $Fe(CO)_4Br_2$ (235 mg, 0.72 mmol) as the starting materials.

Yield: 297 mg (77%) brown solid; $C_{13}H_{19}Br_2FeN_2O_2P$ (MW: 481.93); 32.40% C, 3.97% H, 5.81% N.

^1H NMR (δ, acetone-d_6, 20ºC): 9.40 (s, 1H, py^6), 7.96 (s, 1H, py^4), 7.76 (s, 1H, py^3), 6.93 (s, 2H, py^5 and N*H*), 3.36 (s, 1H, C*H*$(CH_3)_2$), 2.79 (s, 1H, C*H*$(CH_3)_2$), 1.44 – 1.25 (m, 12H, CH(C*H*$_3$)$_2$).

^{13}C {^{1}H} NMR (δ, acetone-d_6, 20ºC): 214.0 (d, *J* = 24.0 Hz, *C*O), 211.9 (d, *J* = 23.0 Hz, *C*O), 162.0 (d, *J* = 8.6 Hz, py^2), 151.5 (py^6), 141.4 (py^4), 116.9 (py^5), 112.2 (d, *J* = 9.2 Hz, py^3), 31.6 (*C*H(CH_3)$_2$), 29.5 (*C*H(CH_3)$_2$), 19.1 (CH(*C*H_3)$_2$), 18.8 (CH(*C*H_3)$_2$).

^{31}P {^{1}H} NMR (δ, acetone-d_6, 20ºC): 153.1

Fe(PN^{py}-BIPOL)(CO)$_2$Br$_2$ (14c)

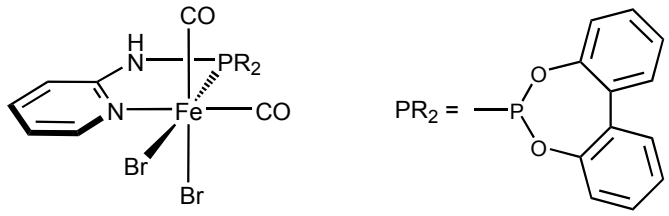

This complex was prepared analogously to **14a** with **4c** (100 mg, 0.32 mmol) and $Fe(CO)_4Br_2$ (106 mg, 0.32 mmol) as the starting materials.

Yield: 108 mg (58%) brown solid; $C_{19}H_{13}Br_2FeN_2O_4P$ (MW: 579.95); 39.35% C, 2.26% H, 4.83% N.

^{1}H NMR (δ, acetone-d_6, 20ºC): 9.45 (s, 1H, py^6), 8.00 – 7.58 (m, 8H, Ph), 7.30 – 7.19 (m, 4H, Ph and N*H*).

^{13}C {^{1}H} NMR (δ, acetone-d_6, 20ºC): 210.3 (d, *J* = 34.0 Hz, *C*O), 209.2 (d, *J* = 34.0 Hz, *C*O), 158.9 (d, *J* = 20.7 Hz, py^2), 151.5 (Ph), 149.6 (d, *J* = 14.4 Hz, py^6), 147.9 (Ph), 141.8 (py^4), 130.4 (Ph), 129.0 (Ph), 122.7 (Ph), 122.1 (Ph), 1184 (py^5), 112.5 (py^3).

^{31}P {^{1}H} NMR (δ, acetone-d_6, 20ºC): 207.0.

IR (KBr, cm^{-1}): 2035 and 2065 ($_{C=O}$).

Fe(PN^{ox}-Ph)(CO)$_2$Br$_2$ (15)

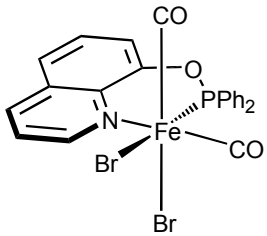

This complex was prepared analogously to **14a** with **5a** (318 mg, 1.0 mmol) and $Fe(CO)_4Br_2$ (328 mg, 1.0 mmol) as the starting materials.

Yield: 493 mg (82%) brown solid; $C_{23}H_{16}Br_2FeNO_3P$ (MW: 601.01); 45.96% C, 2.68% H, 2.33% N.

^{1}H NMR (δ, acetone-d_6, 20ºC): 10.57 (s, 1H, $quin^2$), 8.80 (s, 1H, $quin^4$), 7.88 – 7.73 (m, 10H, Ph), 7.35 – 7.18 (m, 4H, quin).

^{31}P {^{1}H} NMR (δ, acetone-d$_6$, 20ºC): 172.3.

[Fe(NPN^{py}-Ph)$_2$](BF$_4$)$_2$ (16)

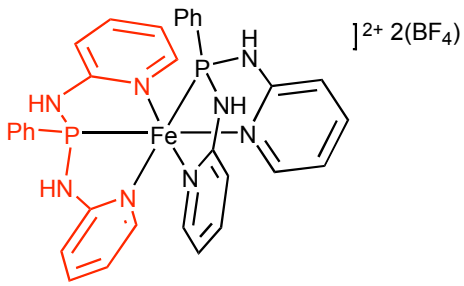

[Fe(H$_2$O)$_6$](BF$_4$)$_2$ (172 mg, 0.5 mmol) and **6** (300 mg, 1.1 mmol) were stirred at RT in 15 mL CH$_3$CN for 2 h. The solvent was then removed under vacuum and the remaining solid was washed twice with Et$_2$O and dried.

Yield: 352 mg (86%) deep red solid; C$_{32}$H$_{30}$B$_2$F$_8$FeN$_8$P$_2$ (MW: 818.04); 46.98% C, 3.70% H, 13.70% N.

^{1}H NMR (δ, CD$_3$NO$_2$, 20ºC): 8.25 (s, 4H, py^{6}), 7.50 – 7.40 (m, 8H, Ph), 7.25 – 7.12 (m, 2H, Ph), 6.95 – 6.77 (m, 2H, py), 6.62 – 6.46 (m, 6H, py), 6.33 – 6.25 (m, 4H, N*H*).

^{13}C {^{1}H} NMR (δ, CD$_3$NO$_2$, 20ºC): 162.0 (py^{2}), 151.5 (py^{6}), 150.3 (Ph^{1}), 140.5 (py^{4}), 133.2 (Ph^{4}), 131.1 (Ph^{2,6}), 129.2 (Ph^{3,5}), 118.0 (d, *J* = 39.2 Hz, py^{5}), 112.7 (py^{3}).

^{31}P {^{1}H} NMR (δ, CD$_3$NO$_2$, 20ºC): 164.5.

4.7.3 Tetracoordinated nickel(II) PNP complexes

[Ni(PNP-Ph)Cl]Cl (17a) and [Ni(PNP-Ph)Br]Br (17a').

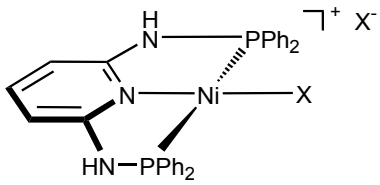

X = Cl: To a solution of **2a** (150 mg, 0.30 mmol) in CH$_2$Cl$_2$ (10 mL) NiCl$_2$(DME) (70 mg, 0.30 mmol) was added and the mixture was stirred overnight at room temperature, whereupon an orange solid precipitated, which was collected on a glass frit, washed twice with Et$_2$O and dried under vacuum.

Yield: 162 mg (89 %) light orange solid; C$_{29}$H$_{25}$Cl$_2$N$_3$NiP$_2$ (MW: 607.10); 57.37% C, 4.15% H, 6.92% N.

^{1}H NMR (δ, CD_3OD, 20ºC): 7.48 - 7.35 (m, 8H, Ph), 7.17 - 7.11 (m, 13H, Ph, py^{4}), 6.00 (s, 2H, py^{3,5}), 3.18 (s, 2H, N*H*).

^{13}C{1H} NMR (δ, CD_3OD, 20ºC): 161.3 (py^{2,6}), 145.5 (Ph), 143.3 (py^{4}), 132.0 (Ph^{4}), 131.8 (Ph^{2,6}), 128.6 (Ph^{3,5}), 99.7 (py^{3,5}).

^{31}P{^{1}H} NMR (δ, CD_3OD, 20ºC): 60.7

X = Br: This complex has been prepared analogously to **17a** with $NiBr_2$(DME) (300 mg, 0.97 mmol) and **2a** (463 mg, 0.97 mmol) as the starting materials.

Yield: 620 mg (94 %) light orange solid; $C_{29}H_{25}Br_2N_3NiP_2$ (MW: 696.00); 50.05% C, 3.62% H, 6.04% N.

^{1}H NMR (δ, CD_3OD, 20ºC): 7.89 - 7.48 (m, 21H, Ph, py^{4}) 6.41 (d, *J* = 8.0 Hz, 2H, py^{3,5}), 3.30 (s, 2H, N*H*).

^{13}C{1H} NMR (δ, CD_3OD, 20ºC): 161.6 (py^{2,6}), 145.3 (Ph), 143.6 (py^{4}), 132.5 (Ph^{2,6}), 132.3 (Ph^{4}), 128.8 (Ph^{3,5}), 99.7 (py^{3,5}).

^{31}P{^{1}H} NMR (δ, CD_3OD, 20ºC): 66.1.

[Ni(PNP-^{i}Pr)Cl]Cl (17b) and [Ni(PNP-^{i}Pr)Br]Br (17b')

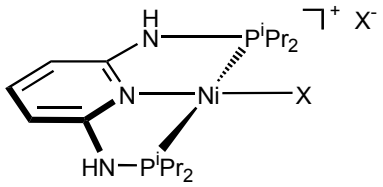

X = Cl: This complex has been prepared analogously to **17a** with $NiCl_2$(DME) (129 mg, 0.58 mmol) and **2b** (200 mg, 0.58 mmol) as the starting materials.

Yield: 229 mg (84 %) yellow-brown solid; $C_{17}H_{33}Cl_2N_3NiP_2$ (MW: 471.03); 43.35% C, 7.06% H, 8.92% N.

^{1}H NMR (δ, CD_3OD, 20ºC): 7.51 (t, *J* = 8.0 Hz, 1H, py^{4}), 6.26 (d, *J* = 8.0 Hz, 2H, py^{3,5}), 3.30 (s, 2H, N*H*), 2.46 - 2.38 (m, 4H, C*H*(CH_3)$_2$), 1.53-1.36 (m, 24 H, CH(C*H*$_3$)$_2$).

^{31}P{^{1}H} NMR (δ, CD_3OD, 20ºC): 97.8.

X = Br: This complex has been prepared analogously to **17a** with $NiBr_2$(DME) (271 mg, 0.88 mmol) and **2b** (300 mg, 0.88 mmol) as the starting materials.

Yield: 450 mg (81 %) yellow-brown solid; $C_{17}H_{33}Br_2N_3NiP_2$ (MW: 559.93); 36.47% C, 5.94% H, 7.50% N.

^{1}H NMR (δ, CD_3OD, 20ºC): 7.54 (t, *J* = 8.0 Hz, 1H, py^{4}), 6.32 (d, *J* = 8.0 Hz, 2H, py^{3,5}), 3.30 (s, 2H, N*H*), 2.51 - 2.46 (m, 4H, C*H*(CH_3)$_2$), 1.53 - 1.36 (m, 24 H, CH(C*H*$_3$)$_2$).

^{13}C{1H} NMR (δ, CD_3OD, 20ºC): 161.8 (t, *J* = 8.9 Hz, py^{2,6}), 141.7 (py^{4}), 97.4 (py^{3,5}), 24.9 (t, *J* = 13.7 Hz, *C*H(CH_3)$_2$), 14.2 (CH(*C*H$_3$)$_2$).

^{31}P{^{1}H} NMR (δ, CD_3OD, 20ºC): 100.6.

[Ni(PNP-^{t}Bu)Cl]Cl (17c) [Ni(PNP-^{t}Bu)Br]Br (17c')

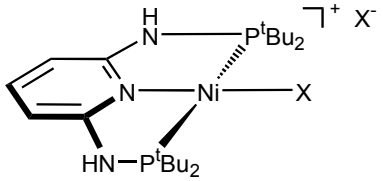

X = Cl: This complex has been prepared analogously to **17a** with $NiCl_2$(DME) (166 mg, 0.75 mmol) and **2c** (300 mg, 0.75 mmol) as the starting materials.

Yield: 276 mg (70 %) yellow-brown solid; $C_{21}H_{41}Cl_2N_3NiP_2$ (MW: 527.14); 47.85% C, 7.84% H, 7.97% N.

^{1}H NMR (δ, CD_3OD, 20ºC): 7.14 (s, 1H, py^4) 6.01 (s, 2H, py^{3,5}), 3.15 (s, 2H, N*H*), 1.27 - 1.16 (m, 36H, C(C*H*$_3$)$_3$).

^{31}P{^{1}H} NMR (δ, CD_3OD, 20ºC): 99.8.

X = Br: This complex has been prepared analogously to **17a** with $NiBr_2$(DME) (233 mg, 0.75 mmol) and **2c** (300 mg, 0.75 mmol) as the starting materials.

Yield: 440 mg (72 %) yellow-brown solid; $C_{21}H_{41}Br_2N_3NiP_2$ (MW: 616.04); 40.94% C, 6.71% H, 6.82% N.

^{1}H NMR (δ, CD_3OD, 20ºC): 7.51 (t, *J* = 8.0 Hz, 1H, py^4) 6.36 (d, *J* = 8.0 Hz, 2H, py^{3,5}), 3.30 (s, 2H, N*H*), 1.59 - 1.52 (m, 36H, C(C*H*$_3$)$_3$).

^{13}C{1H} NMR (δ, CD_3OD, 20ºC): 163.4 (py^{2,6}), 143.0 (py^4), 98.5 (py^{3,5}), 39.3 (t, *J* = 9.2 Hz, *C*(CH$_3$)$_3$), 27.3 (C(*C*H$_3$)$_3$).

^{31}P{^{1}H} NMR (δ, CD_3OD, 20ºC): 103.7.

4.7.4 Pentacoordinated nickel(II) PNP complexes

[Ni(PNP-BIPOL)(κ^1(P)-BIPOL-P=O)Br] (18a)

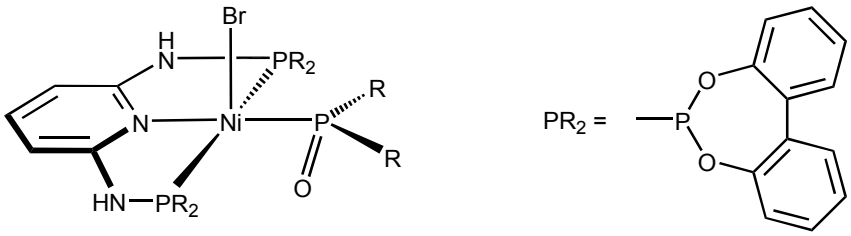

$NiBr_2$ (150 mg, 0.46 mmol) was suspended in a solution of **2e** (500 mg, 0.93 mmol) in CH_2Cl_2 (5 mL). Upon addition of DMSO (33 µL, 0.46 mmol) the solution turned deep orange. The mixture

was stirred at room temperature for 1h and the volume of the solution was concentrated under vacuum. The orange product was precipitated with Et_2O and dried under vacuum.

Yield: 371 mg (89%) orange solid; $C_{41}H_{29}BrN_3NiO_7P_3$ (MW: 907.23); 54.28% C, 3.22% H, 4.63% N.

^{1}H NMR (δ, dmso-d_6, 20°C): 7.33 – 7.09 (m, 20 H, Ph), 6.93 – 6.88 (m, 4H, Ph), 6.70 (t, *J* = 7.3 Hz, 1H, py^4), 6.36 (d, *J* = 7.3 Hz, 2H, py^{3,5}), 5.80 (d, *J* = 8.0 Hz, 2H, N*H*).

^{13}C{^{1}H} NMR (δ, dmso-d_6, 20°C): 155.1 (Ph), 154.3 (py^{2,6}), 142.2 (py^4), 132.3 – 124.4 (Ph), 100.8 (py^{3,5}).

^{31}P{^{1}H} NMR (δ, dmso-d_6, 20°C): 147.7 (d, *J* = 98.6 Hz, BIPOL-*P*N*P*), 86.6 (t, *J* = 98.6 Hz, BIPOL-*P*O).

[Ni(PNP-TAR^{Me})(κ^1(P)-TAR^{Me}-P=O)Br] (18b)

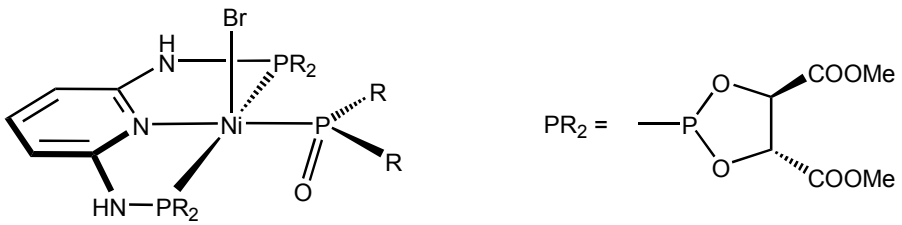

This complex was prepared analogously to **18a** with $NiBr_2$ (205 mg, 0.94 mmol), **2g** (980 mg, 1.87 mmol) and DMSO (68 µL, 0.94 mmol) as the starting materials.

Yield: 672 mg (81%) orange solid; $C_{23}H_{29}BrN_3NiO_{19}P_3$ (MW: 883.03); 31.28% C, 3.31% H, 4.76% N.

^{1}H NMR (δ, dmso-d_6, 20°C): 7.44 (t, *J* = 8.0 Hz, 1H, py^4), 6.40 (d, *J* = 8.0 Hz, 2H, py^{3,5}), 5.83 (d, *J* = 8.3 Hz, 2H, N*H*), 5.03 – 4.89 (m, 4H, C*H*), 4.80 – 4.61 (m, 2H, C*H*), 1.23 – 1.14 (m, 18H, CH_3).

^{13}C{^{1}H} NMR (δ, dmso-d_6, 20°C): 170.2 (*C*O), 166.3 (*C*O), 159.6 (py^{2,6}), 142.1 (py^4), 100.8 (py^{3,5}), 95.1 (*C*H), 76.7 (*C*H), 45.9 (*C*H_3), 45.3 (*C*H_3).

^{31}P{^{1}H} NMR (δ, dmso-d_6, 20°C): 146.2 (d, *J* = 104.2 Hz, TAR^{Me}-*P*N*P*), 85.3 (t, *J* = 104.2 Hz, TAR^{Me}-*P*=O).

[Ni(PNP-TAR^{Pr})(κ^1(P)-TAR^{Pr}-PO)Br] (18c)

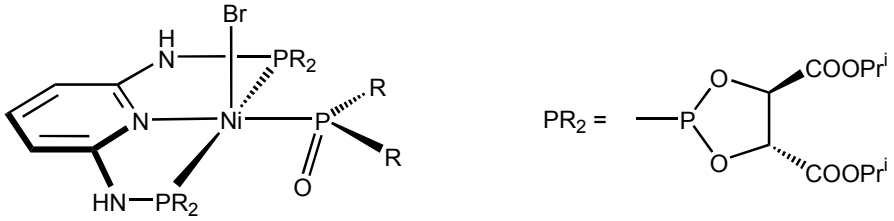

This complex has been prepared analogously to **18a** with $NiBr_2$ (290 mg, 1.33 mmol), **2h** (1.6 g, 2.7 mmol) and DMSO (96 µL, 1.33 mmol) as the starting materials.

Yield: 979 mg (70%) orange solid; $C_{35}H_{53}BrN_3NiO_{19}P_3$ (MW: 1051.35); 40.00% C, 5.08% H, 4.00% N.

^{1}H NMR (δ, dmso-d$_6$, 20°C): 7.42 (t, *J* = 7.8 Hz, 1H, py^4), 6.41 (d, *J* = 7.8 Hz, 2H, py^{3,5}), 5.81 (d, *J* = 8.2 Hz, 2H, NH), 5.06 – 4.40 (m, 12H, C*H* and C*H*(CH$_3$)$_2$), 1.23 – 1.12 (m, 36H, (CH(C*H*$_3$)$_2$).

^{13}C{^{1}H} NMR (δ, dmso-d$_6$, 20°C): 170.2 (*C*O), 168.3 (*C*O), 159.8 (py^{2,6}), 145.1 (py^4), 100.8 (py^{3,5}), 95.2 (*C*H), 80.0 (*C*H), 69.1 (*C*H(CH$_3$)$_2$), 68.8 (*C*H(CH$_3$)$_2$), 21.9 (CH(*C*H$_3$)$_2$), 21.7 (CH(*C*H$_3$)$_2$).

^{31}P{^{1}H} NMR (δ, dmso-d$_6$, 20°C): 146.1 (d, *J* = 100.8 Hz, TAR^{Pr}-*P*N*P*), 85.5 (t, *J* = 100.8 Hz, TAR^{Pr}-*P*=O).

[Ni(PNP-HBz)(κ^1(P)-HBz-P=O)Br] (18d)

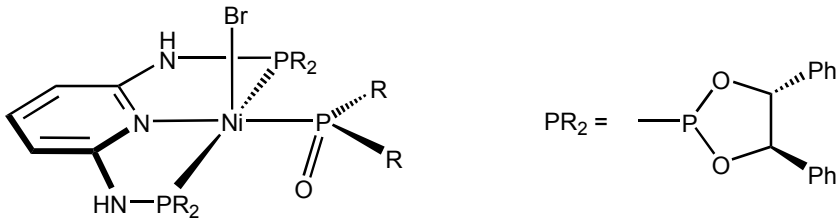

This complex has been prepared analogously to **18a** with $NiBr_2$ (54 mg, 0.24 mmol), **2i** (300 mg, 0.49 mmol) and DMSO (18.0 µL, 0.24 mmol) as the starting materials.

Yield: 132 mg (55%) orange solid; $C_{47}H_{41}BrN_3NiO_7P_3$ (MW: 991.39); 56.94% C, 4.17% H, 4.24% N.

^{1}H NMR (δ, dmso-d$_6$, 20°C): 7.29 – 7.00 (m, 33H, Ph, py^4 and py^{3,5}), 5.70 (d, *J* = 8.0 Hz, 2H, N*H*), 5.24 – 4.90 (m, 6H, C*H*).

^{13}C{^{1}H} NMR (δ, dmso-d$_6$, 20°C): 152.6 (py^{2,6}), 144.3 (Ph), 142.5 (py^4), 130.1 – 127.3 (Ph), 98.8 (py^{3,5}), 95.1 (*C*H), 87.0 (*C*H).

^{31}P{^{1}H} NMR (δ, dmso-d$_6$, 20°C): 143.4 (d, *J* = 107.2 Hz, *P*N*P*-HBz), 87.8 (t, *J* = 107.2 Hz, HBz-*P*=O).

[Ni(PNP-Eph)(κ[1](P)-Eph-P=O)Br] (18e)

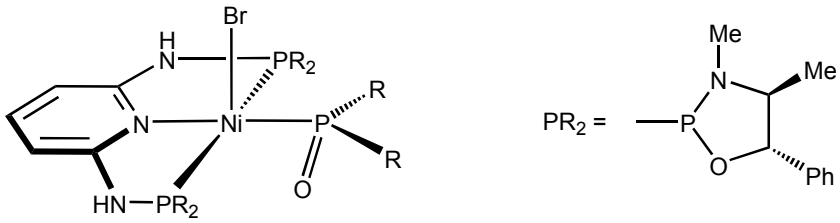

This complex has been prepared analogously to **18a** with $NiBr_2$ (175 mg, 0.40 mmol), **2j** (400 mg, 0.80 mmol) and DMSO (29 µL, 0.40 mmol) as the starting materials.

Yield: 213 mg (63%) orange solid; $C_{35}H_{44}BrN_6NiO_4P_3$ (MW: 844.31); 49.79% C, 5.25% H, 9.95% N.

^{1}H NMR (δ, dmso-d_6, 20°C): 7.40 – 7.02 (m, 18H, Ph, py^4 and py^{3,5}), 5.60 (s, 2H, N*H*), 4.90 – 4.74 (m, 3H, C*H*Ph), 3.64 – 3.47 (m, 3H, C*H*CH_3), 3.22 – 3.11 (m, 9H, NC*H*$_3$), 0.94 – 0.72 (m, 9H, CHC*H*$_3$).

^{13}C{^{1}H} NMR (δ, dmso-d_6, 20°C): 155.7 (py^{2,6}), 143.9 (py^4), 141.3 (Ph), 128.6 – 126.1 (Ph), 99.7 (py^{3,5}), 84.5 (*C*HPh), 81.6 (*C*HPh), 65.2 (*C*HCH_3), 59.2 (*C*HCH_3), 30.9 (N*C*H$_3$), 28.8 (N*C*H$_3$), 15.5 (CH*C*H$_3$), 9.5 (CH*C*H$_3$).

^{31}P{^{1}H} NMR (δ, dmso-d_6, 20°C): 116.8 (d, *J* = 114.1, *P*N*P*-Eph), 74.5 (t, *J* = 114.1, Eph-*P*=O).

4.7.5 Nickel(II) PCP complexes

[Ni(PCP-Ph)Cl] (19a)

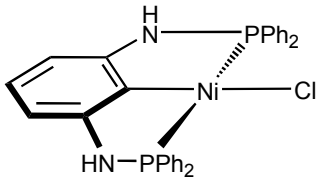

To a suspension of **3a** (300 mg, 0.63 mmol) in EtOH (10 mL) $NiCl_2{\cdot}6H_2O$ (78 mg, 0.63 mmol) was added, whereupon the solution turned orange. The mixture was refluxed overnight. The orange solid was collected on a glass frit, washed twice with pentane and dried under vacuum.

Yield: 316 mg (88 %) orange solid; $C_{30}H_{25}ClN_2NiP_2$ (MW: 569.65); 63.25% C, 4.42% H, 4.92% N.

^{1}H NMR (δ, C_6D_6, 20°C): 8.08 (d, *J* = 5.5 Hz, 2H, N*H*), 7.56 (q, *J* = 6.3 Hz, 8H, Ph), 7.07 - 7.04 (m, 12H, Ph), 6.90 (s, 1H, Ph^4), 6.39 (d, *J* = 7.6 Hz, 2H, Ph^{3,5}).

$^{13}C\{^1H\}$ NMR (δ, C_6D_6, 20°C): 159.2 (t, *J* = 17.0 Hz, C^{Ph}), 134.2 (t, *J* = 23.9 Hz, C^{PPh}), 132.5 (t, *J* = 6.9 Hz, C^{PPh}), 131.8 (d, *J* = 2.3 Hz, C^{PPh}), 130.7 (d, *J* = 11.5 Hz, C^{Ph}), 128.5 (t, *J* = 12.4 Hz, C^{PPh}), 103.0 (t, *J* = 8.3 Hz, C^{Ph}).
$^{31}P\{^1H\}$ NMR (δ, C_6D_6, 20°C): 77.8.

[Ni(PCP-^{i}Pr)Cl] (19b)

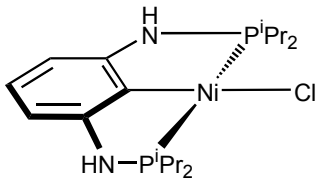

This complex has been prepared analogously to **19a** with $NiCl_2{\cdot}6H_2O$ (137 mg, 0.58 mmol) and **3b** (200 mg, 0.58 mmol) as the starting materials.
Yield: 181 mg (72 %) orange solid; $C_{18}H_{33}ClN_2NiP_2$ (MW: 433.58); 49.86% C, 7.67% H, 6.46% N.
^1H NMR (δ, CD_2Cl_2, 20°C): 6.61 (s, 1H, Ph^4), 5.94 (s, 2H, $Ph^{3,5}$), 3.95 (s, 2H, N*H*), 2.22 (s, 4H, C*H*$(CH_3)_2$, 1.36 (s, 24H, CH(C*H*$_3$)$_2$).
$^{13}C\{^1H\}$ NMR (δ, CD_2Cl_2, 20°C): 160.7 (C^{Ph}), 131.1 (C^{Ph}), 127.3 (C^{Ph}), 101.1 (C^{Ph}), 26.3 (*C*H$(CH_3)_2$), 17.8 (CH(*C*H$_3$)$_2$).
$^{31}P\{^1H\}$ NMR (δ, CD_2Cl_2, 20°C): 110.8.

[Ni(PCP-^{t}Bu)Cl] (19c)

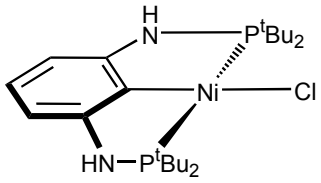

This complex has been prepared analogously to **19a** with $NiCl_2$ (65 mg, 0.50 mmol) and **3c** (200 mg, 0.50 mmol) as the starting materials.
Yield: 220 mg (90 %) orange solid; $C_{22}H_{41}ClN_2NiP_2$ (MW: 489.69); 53.96%C, 8.44% H, 5.72% N.
^1H NMR (δ, CD_2Cl_2, 20°C): 6.67 (s, 1H, Ph^4), 5.95 (d, *J* = 6.7 Hz, 2H, $Ph^{3,5}$), 4.12 (s, 2H, N*H*), 1.47 (s, 36H, C(C*H*$_3$)$_3$).
$^{13}C\{^1H\}$ NMR (δ, CD_2Cl_2, 20°C): 160.1 (t, *J* = 14.4 Hz, C^{Ph}), 134.6 (C^{Ph}), 127.1 (C^{Ph}), 103.0 (t, *J* = 6.0 Hz, C^{Ph}), 37.7 (*C*$(CH_3)_3$), 28.2 (t, *J* = 2.6 Hz, C(*C*H$_3$)$_3$).
$^{31}P\{^1H\}$ NMR (δ, CD_2Cl_2, 20°C): 113.5.

4.7.6 Nickel(II) PN complexes

[Ni(PN^{py}-Ph)Cl$_2$] (20a)

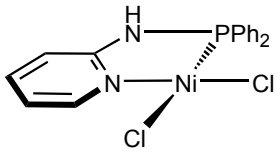

4a (91 mg, 0.32 mmol) was added to a suspension of Ni(DME)Cl$_2$ (100 mg, 0.32 mmol) in CH$_2$Cl$_2$ and the mixture was stirred at room temperature for 2 h. The solvent was evaporated vacuum and the remaining violet solid was washed twice with Et$_2$O and dried.
Yield: 108 mg (83%) violet solid; C$_{17}$H$_{15}$Cl$_2$N$_2$NiP (MW: 407.91); 50.06% C, 3.71% H, 6.87% N.

[Ni(PN^{py}-^{i}Pr)Cl$_2$] (20b).

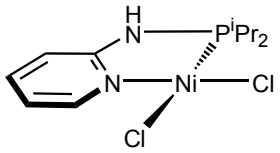

This complex has been prepared analogously to **20a** with **4b** (390 mg, 1.85 mmol) and Ni(DME)Cl$_2$ (405 mg, 1.85 mmol) as the starting materials.
Yield: 490 mg (78%) deep red solid; C$_{11}$H$_{19}$Cl$_2$N$_2$NiP (MW: 339.87); 38.87% C, 5.63% H, 8.24% N.

4.7.7 Palladium (II) PNP complexes

[Pd(PNP-Ph)Cl]Cl (21a).

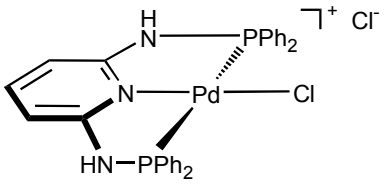

To a solution of Pd(COD)Cl$_2$ (0.6 g, 2.1 mmol) in CH$_2$Cl$_2$ (10 mL) **2a** (1.0 g, 2.1 mmol) was added. After the mixture was stirred for 2 h., the solvent was removed under vacuum and the product was precipitated with Et$_2$O, collected on a glass frit and washed twice with Et$_2$O (10 mL).

Yield: 1.3 g (95 %) yellow solid; $C_{29}H_{25}Cl_2N_3P_2Pd$ (MW: 654.79); 53.20% C, 3.85% H, 6.42% N.
^{1}H NMR (δ, CD_2Cl_2, 20ºC): 10.47 (s, 2H, N*H*), 8.00 - 7.28 (m, 21H, Ph, py^4), 6.84 (d, *J* = 8.0 Hz, py^{3,5}).
^{13}C{^{1}H} NMR (δ, CD_2Cl_2, 20ºC): 160.6 (t, *J* = 7.5 Hz, py^{2,6}), 151.1 (Ph), 142.0 (py^4), 132.3 (t, *J* = 7.8 Hz, Ph^{2,6}), 130.1 (Ph^4), 129.1 (t, *J* = 6.0 Hz, Ph^{3,5}), 101.7 (py^{3,5}).
^{31}P{^{1}H} NMR (δ, CD_2Cl_2, 20ºC): 69.9.

[Pd(PNP-^{i}Pr)Cl]Cl (21b).

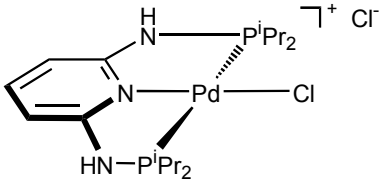

This complex has been prepared analogously to **21a** with $Pd(COD)Cl_2$ (337 mg, 1.18 mmol) and **2b** (400 mg, 1.18 mmol) as the starting materials.
Yield: 600 mg (98 %) yellow solid; $C_{17}H_{33}Cl_2N_3P_2Pd$ (MW: 518.72); 39.36% C, 6.41% H, 8.10% N.
^{1}H NMR (δ, CD_2Cl_2, 20ºC): 9.44 (s, 2H, N*H*), 7.20 (t, *J* = 7.6 Hz, 1H, py^4), 6.81 (d, *J* = 7.6 Hz, 2H, py^{3,5}), 2.67 - 2.56 (m, *J* = 6.8 Hz, 4H, C*H*$(CH_3)_2$), 1.44 - 1.32 (m, *J* = 8.7 Hz, 24 H, CH(C*H*$_3)_2$).
^{13}C{^{1}H} NMR (δ, CD_2Cl_2, 20ºC): 162.4 (t, *J* = 6.1 Hz, py^{2,6}), 141.1 (py^4), 100.4 (py^{3,5}), 27.3 (t, *J* = 13.4 Hz, *C*H$(CH_3)_2$), 17.3 (CH(*C*H$_3)_2$).
^{31}P{^{1}H} NMR (δ, CD_2Cl_2, 20ºC): 108.4.

[Pd(PNP-^{t}Bu)Cl]Cl (21c).

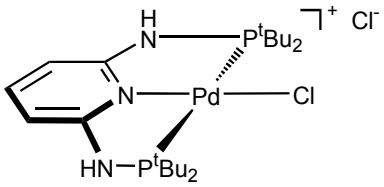

This complex has been prepared analogously to **21a** with $Pd(cod)Cl_2$ (156 mg, 0.88 mmol) and **2c** (300 mg, 0.88 mmol) as the starting materials.
Yield: 420 mg (81 %) yellow solid; $C_{21}H_{41}Cl_2N_3P_2Pd$ (MW: 574.23); 43.88% C, 7.19% H, 7.31% N.
^{1}H NMR (δ, CD_2Cl_2, 20ºC): 9.43 (s, 2H, N*H*), 7.16 (d, *J* = 7.5 Hz, 2H, py^{3,5}), 6.95 (t, *J* = 7.5 Hz, 1H, py^4), 1.55 - 1.49 (m, 36H, C(C*H*$_3)_3$).

$^{13}C\{^1H\}$ NMR (δ, CD_2Cl_2, 20ºC): 163.0 (t, *J* = 5.8 Hz, $py^{2,6}$), 140.6 (py^4), 100.2 ($py^{3,5}$), 39.5 (t, *J* = 9.2 Hz, *C*$(CH_3)_3$), 28.0 (t, *J* = 3.2 Hz, C(*C*$H_3)_3$).
$^{31}P\{^1H\}$ NMR (δ, CD_2Cl_2): 115.7.

[Pd(PNP-ETOL)Cl]CF_3SO_3 (21d).

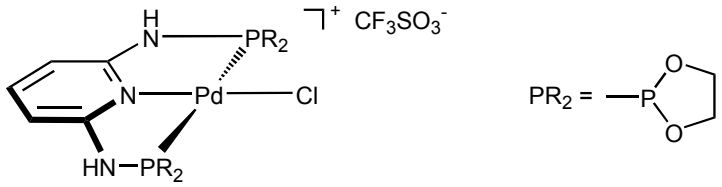

KCF_3SO_3 (130 mg, 0.70 mmol) and $Pd(COD)Cl_2$ (182 mg, 0.64 mmol) were added to a solution of **2d** (185 mg, 0.64 mmol) in CH_3CN. The mixture was stirred for 2 h. and filtered. The yellow filtrate was evaporated to dryness and the product was precipitated with Et_2O, collected on a glass frit and washed twice with Et_2O (10 mL).
Yield: 282 mg (76%) yellow solid; $C_{10}H_{13}ClF_3N_3O_7P_2PdS$ (MW: 580.08); 20.71% C, 2.26% H, 7.24% N.
^1H NMR (δ, CD_3CN, 20ºC): 7.54 (t, *J* = 8.2 Hz, 1H, py^4), 6.20 (s, 2H, N*H*), 6.03 (d, *J* = 8.2 Hz, 2H, $py^{3,5}$), 4.36 - 4.30 (m, 8H, CH_2).
$^{13}C\{^1H\}$ NMR (δ, CD_3CN, 20ºC): 151.6 ($py^{2,6}$), 145.9 ($py^{3,5}$), 96.3 (py^4), 67.7 (*C*H_2), 65.2 (*C*H_2).
$^{31}P\{^1H\}$ NMR (δ, CD_3CN, 20ºC): 123.8.

[Pd(PNP-BIPOL)Cl]CF_3SO_3 (21e).

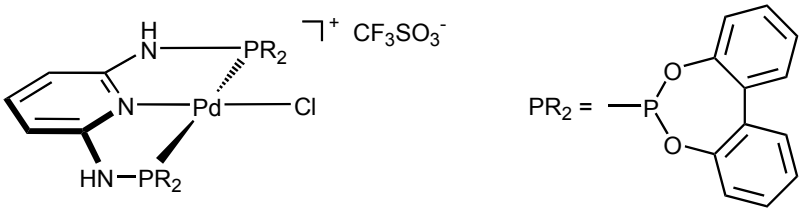

This complex has been prepared analogously to **21d** with KCF_3SO_3 (116 mg, 0.62 mmol), $Pd(COD)Cl_2$ (159 mg, 0.56 mmol) and **2e** (300 mg, 0.56 mmol) as the starting materials.
Yield: 417 mg (90%) yellow solid; $C_{32}H_{24}ClF_3N_4O_7P_2PdS$ (MW: 855.413); 44.93% C, 2.83% H, 4.91% N.
^1H NMR (δ, CD_3CN, 20ºC): 8.97 (s, 2H, N*H*), 7.83 (t, *J* = 8.2 Hz, 1H, py^4), 7.69 - 7.68 (m, 4H, Ph), 7.56 - 7.47 (m, 12H, Ph), 6.67 (d, *J* = 8.2 Hz, 2H, $py^{3,5}$).
$^{13}C\{^1H\}$ NMR (δ, CD_3CN, 20ºC): 154.3 (t, *J* = 11.2 Hz, $py^{2,6}$), 147.7 (t, *J* = 4.9 Hz, Ph), 145.2 (py^4), 130.6 (Ph), 128.5 (Ph), 127.8 (Ph), 122.0 (Ph), 103.2 (t, *J* = 6.6 Hz, $py^{3,5}$).
$^{31}P\{^1H\}$ NMR (δ, CD_3CN, 20ºC): 124.6.

[Pd(PNP-BINOL)Cl]CF_3SO_3 (21f).

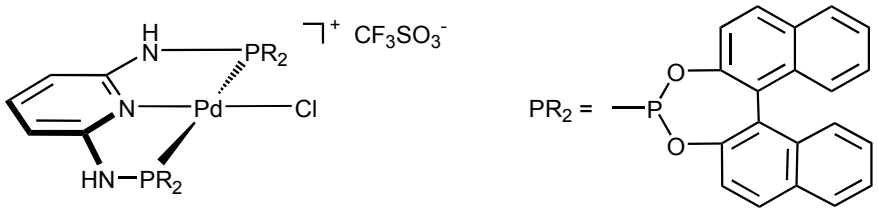

This complex has been prepared analogously to **21d** with KCF_3SO_3 (40 mg, 0.21 mmol), $Pd(COD)Cl_2$ (60 mg, 0.21 mmol) and **2f** (200 mg, 0.21 mmol) as the starting materials.

Yield: 216 mg (77%) yellow solid; $C_{30}H_{21}ClF_3N_3O_7P_2PdS$ (MW: 828.37); 43.50%C, 2.56% H, 5.07% N.

^{1}H NMR (δ, CD_2Cl_2, 20ºC): 8.10 - 7.91 (m, 10H, Ph, N*H*), 7.54 - 7.31 (m, 17H, Ph, py^4), 7.12 (d, *J* = 7.9 Hz, 2H, py^{3,5}).

^{31}P{^{1}H} NMR (δ, CD_2Cl_2, 20ºC): 124.1.

[Pd(PNP-^{Me}TAR)Cl]CF_3SO_3 (21g).

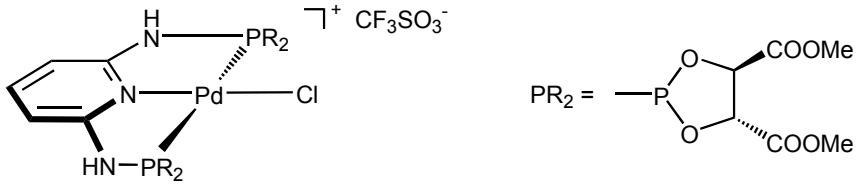

This complex has been prepared analogously to **21d** with KCF_3SO_3 (94 mg, 0.50 mmol), $Pd(COD)Cl_2$ (129 mg, 0.45 mmol) and **2g** (239 mg, 0.45 mmol) as the starting materials.

Yield: 338 mg (92%) yellow solid; $C_{18}H_{21}ClF_3N_3O_{15}P_2PdS$ (MW: 812.231); 26.62% C, 2.61% H, 5.17% N.

^{1}H NMR (δ, CD_3CN, 20ºC): 8.44 (s, 2H, N*H*), 7.83 (t, *J* = 8.2 Hz, 1H, py^4), 6.81 (d, *J* = 8.2 Hz, py^{3,5}), 5.55 - 5.44 (m, 4H, C*H*), 3.89 - 3.83 (m, 12 H, CH_3).

^{13}C{^{1}H} NMR (δ, CD_3CN, 20ºC): 167.3 (*C*O), 166.2 (*C*O), 153.3 (t, *J* = 10.1 Hz, py^{2,6}), 145.0 (py^4), 104.0 (t, *J* = 6.6 Hz, py^{3,5}), 77.8 (*C*H(CH_3)$_2$), 76.9 (*C*H(CH_3)$_2$), 53.6 (d, *J* = 11.0 Hz, CH(*C*H_3)$_2$), 52.7 (d, *J* = 11.5 Hz, CH(*C*H_3)$_2$).

^{31}P{^{1}H} NMR (δ, CD_3CN, 20ºC): 130.2.

[Pd(PNP-^{Pr}TAR)Cl]CF_3SO_3 (21h).

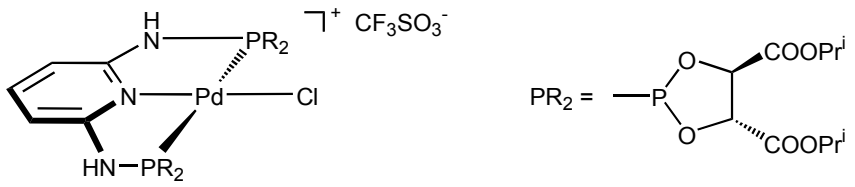

This complex has been prepared analogously to **21d** with KCF_3SO_3 (90 mg, 0.48 mmol), $Pd(COD)Cl_2$ (124 mg, 0.43 mmol) and **2h** (275 mg, 0.43 mmol) as the starting materials.

Yield: 353 mg (89 %) yellow solid; $C_{26}H_{37}ClF_3N_3O_{15}P_2PdS$ (MW: 924.45); 33.78% C, 4.03 H, 4.55 N.

^{1}H NMR (δ, CD_3CN, 20ºC): 8.42 (s, 2H, N*H*), 7.53 (t, *J* = 8.2 Hz, 1H, py^4), 6.79 (d, *J* = 8.2 Hz, py^{3,5}), 5.41 - 5.35 (m, 4H, C*H*$(CH_3)_2$), 5.12 - 5.07 (m, 4H, C*H*), 1.34 - 1.26 (m, 12 H, (CH(C*H*$_3$)$_2$).

^{13}C{^{1}H} NMR (δ, CD_3CN, 20ºC): 166.7 (*C*O), 166.4 (*C*O), 151.7 (py^{2,6}), 145.8 (py^4), 96.2 (py^{3,5}), 75.4 (d, *J* = 4.6 Hz, *C*H), 70.4 (d, *J* = 10.9 Hz, *C*H$(CH_3)_2$), 20.9 (CH(*C*H$_3$)$_2$).

^{31}P{^{1}H} NMR (δ, CD_3CN, 20ºC): 129.7.

[Pd(PNP-Ph)(η^{1}allyl)]BF_4 (23).

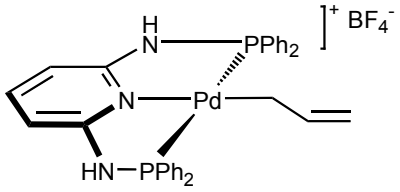

$AgBF_4$ (112 mg, 0.57 mmol) was added to a solution of [Pd(η^{1}allyl)Cl]$_2$ (100 mg, 0.27 mmol) in CH_3CN. A white precipitate was observed immediately. After stirring the mixture in the dark for 15 min., the mixture was filtered under argon and **2a** (275 mg, 0.57 mmol), dissolved in 5 mL CH_3CN, was added, whereupon the solution turned yellow. The mixture was then stirred for another 15 min., and the solvent was removed under vacuum.

Yield: 373 mg (97%) yellow solid; $C_{32}H_{30}BF_4N_3P_2Pd$ (MW: 711.76); 54.00% C, 4.25% H, 5.90% N.

^{1}H NMR (δ, $CDCl_3$, 20ºC): 7.90 (s, 2H, N*H*), 7.72 – 7.64 (m, 8H, Ph), 7.48 – 7.39 (m, 12H, Ph), 6.99 (t, *J* = 8.0 Hz, 1H, py^4), 6.54 (d, *J* = 8.0 Hz, 2H, py^{3,5}), 5.55 (heptuplet, *J* = 8.5 Hz, 1H, C*H*=CH_2), 4.29 (d, *J* = 16.7 Hz, 1H, CH=C*H*$_2^{trans}$), 4.19 (dd, *J* = 9.6 Hz, *J* = 2.1 Hz, 1H, CH=C*H*$_2^{cis}$), 2.66 (dt, *J* = 9.6 Hz, *J* = 4.2 Hz, 2H, C*H*$_2$).

^{13}C{^{1}H} NMR (δ, $CDCl_3$, 20ºC): 156.9 (t, *J* = 7.5 Hz, py^{2,6}), 142.0 (py^4), 141.2 (CH_2=*C*H), 132.5 (t, *J* = 7.9 Hz, Ph^{2,6}), 132.1 (Ph^4), 130.8 (t, *J* = 26.1 Hz, Ph^1), 129.2 (t, *J* = 5.6 Hz, Ph^{3,5}), 109.6 (*C*H$_2$=CH), 101.1 (py^{3,5}), 17.6 (*C*H$_2$).

^{31}P{^{1}H} NMR (δ, $CDCl_3$, 20ºC): 69.1.

4.7.8 Palladium(II) PCP complexes

[Pd(PCP-Ph)Cl] (25a)

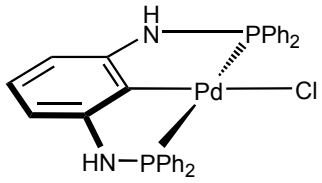

$Pd(COD)Cl_2$ (179 mg, 0.63 mmol) was added to a solution of **3a** (300 mg, 0.63 mmol) in toluene (15 mL) and the mixture was refluxed for 5h, whereupon a yellow solid precipitated, which was collected on a glass frit and washed twice with Et_2O (10 mL).

Yield: 350 mg (90 %) yellow solid; $C_{30}H_{25}ClN_2P_2Pd$ (MW: 617.34); 58.37% C, 4.08% H, 4.54% N.

^{1}H NMR (δ, dmso-d_6, 20°C): 8.00 (s, 2H, N*H*), 7.87 - 7.83 (m, 6H, PPh), 7.50 - 7.48 (m, 14H, PPh), 6.77 (t, *J* = 7.8 Hz, 1H, Ph^4), 6.23 (d, *J* = 7.8 Hz, 2H, $Ph^{3,5}$).

$^{13}C\{^1H\}$ NMR (δ, dmso-d_6, 20°C): 156.9 (t, *J* = 14.1 Hz, C^{Ph}), 135.1 (t, *J* = 25.0 Hz, C^{PPh}), 131.8 (t, *J* = 7.8 Hz, C^{PPh}), 131.4 (C^{PPh}), 129.2 (C^{Ph}), 129.0 (t, *J* = 5.2 Hz, C^{PPh}), 103.2 (t, *J* = 10.1 Hz, C^{Ph}).

$^{31}P\{^1H\}$ NMR ((δ, dmso-d_6, 20°C): 76.9.

[Pd(PCP-^{i}Pr)Cl] (25b)

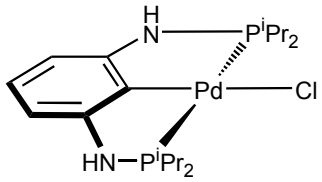

This complex was prepared analogously to **25a** with $Pd(COD)Cl_2$ (208 mg, 0.73 mmol) and **3b** (250 mg, 0.73 mmol) as the starting materials.

Yield: 434 mg (96 %) yellow solid; $C_{18}H_{33}ClN_2P_2Pd$ (MW: 481.27); 44.92% C, 6.91% H, 5.82% N.

^{1}H NMR (δ, CD_2Cl_2, 20°C): 6.76 (t, *J* = 7.7 Hz, 1H, Ph^4), 6.14 (t, *J* = 7.7 Hz, 2H, $Ph^{3,5}$), 3.91 (s, 2H, N*H*), 2.40 - 2.29 (m, 4H C*H*$(CH_3)_2$), 1.42 - 1.20 (m, 24H, CH(C*H*$_3)_2$).

$^{13}C\{^1H\}$ NMR (δ, CD_2Cl_2, 20°C): 157.3 (t, *J* = 12.1 Hz, C^{Ph}), 127.0 (C^{Ph}), 124.0 (C^{Ph}), 101.9 (t, *J* = 7.9 Hz, C^{Ph}), 27.3 (t, *J* = 12.7 Hz, *C*H$(CH_3)_2$), 18.1 (CH(*C*H$_3)_2$), 17.3 (CH(*C*H$_3)_2$).

$^{31}P\{^1H\}$ NMR (δ, CD_2Cl_2, 20°C): 114.3.

[Pd(PCP-^{t}Bu)Cl] (25c)

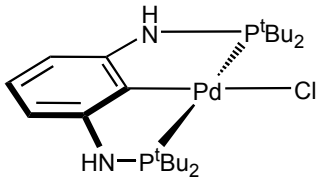

This complex was prepared analogously to **25a** with Pd(COD)Cl_2 (144 mg, 0.50 mmol) and **3c** (200 mg, 0.50 mmol) as the starting materials.

Yield: 233 mg (83 %) yellow solid; $C_{22}H_{41}ClN_2P_2Pd$ (MW: 537.38); 49.17% C, 7.69% H, 5.21% N.

^{1}H NMR (δ, CD_2Cl_2, 20°C): 6.73 (t, *J* = 7.8 Hz, 1H, Ph^4), 6.12 (d, *J* = 7.8 Hz, 2H, Ph^{3,5}), 4.18 (s, 2H, N*H*), 1.45-1.39 (t, *J* = 7.3 Hz, 36H, C(C*H*$_3$)$_3$).

^{13}C{^{1}H} NMR (δ, CD_2Cl_2, 20°C): 157.9 (t, *J* = 11.2 Hz, C^{Ph}), 126.7 (C^{Ph}), 117.0 (t, *J* = 11.5 Hz, C^{Ph}), 101.4 (t, *J* = 7.8 Hz, C^{Ph}), 38.1 (t, *J* = 8.9 Hz, *C*(CH$_3$)$_3$), 28.0 (t, *J* = 3.7 Hz, C(*C*H$_3$)$_3$).

^{31}P{^{1}H} NMR (δ, CD_2Cl_2, 20°C): 120.4.

[Pd(PCP-Ph^F)Cl] (25d)

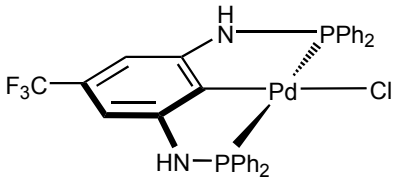

This complex has been prepared analogously to **25a** with Pd(COD)Cl_2 (75 mg, 0.27 mmol) and **3d** (145 mg, 0.27 mmol) as the starting materials.

Yield: 150 mg (81 %) yellow solid; $C_{31}H_{24}ClF_3N_2P_2Pd$ (MW: 685.34); 54.33% C, 3.53% H, 4.09% N.

^{1}H NMR (δ, CD_2Cl_2, 20°C): 7.89 – 7.81 (m, 8H, PPh), 7.55 – 7.49 (m, 12H, PPh), 6.57 (s, 2H, Ph^{3,5}), 5.12 (s, 2H, N*H*).

^{13}C{^{1}H} NMR (δ, CD_2Cl_2, 20°C): 151.3 (C^{Ph}), 139.7 (C^{PPh}), 133.8 (C^{Ph}), 131.8 (C^{PPh}), 131.4 (C^{PPh}), 128.9 (C^{PPh}), 100.9 (C^{Ph}).

^{31}P{^{1}H} NMR (δ, CD_2Cl_2, 20°C): 81.4.

[Pd(PCP-Ph)TFA] (26a)

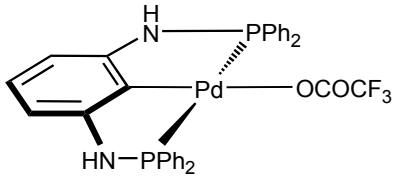

$Pd(TFA)_2$ (100 mg, 0.30 mmol) was added to a solution of **3a** (144 mg, 0.30 mmol) in THF and the mixture was stirred at room temperature for 3h. The solvent was removed under vacuum and the product precipitated with Et_2O, collected on a glass frit and washed twice with Et_2O (10 mL).

Yield: 187 mg (91 %) brown solid; $C_{32}H_{25}F_3N_2O_2P_2Pd$ (MW: 694.90); 55.31% C, 3.63% H, 4.03% N.

^{1}H NMR (δ, CD_2Cl_2, 20°C): 7.81 - 7.72 (m, 8H, PPh), 7.48 - 7.43 (m, 12H, PPh), 6.86 (t, *J* = 7.9 Hz, 1H, Ph^4), 6.26 (d, *J* = 7.9 Hz, 2H, Ph^{3,5}), 4.67 (s, 2H, N*H*).

^{13}C{^{1}H} NMR (δ, CD_2Cl_2, 20°C): 156.0 (t, *J* = 13.8 Hz, C^{Ph}), 133.5 (t, *J* = 25.0 Hz, C^{PPh}), 131.9 (t, *J* = 8.1 Hz, C^{PPh}), 131.4 (C^{PPh}), 128.8 (t, *J* = 5.5 Hz, C^{PPh}), 128.2 (C^{Ph}), 103.5 (t, *J* = 9.2 Hz, C^{Ph}).

^{31}P{^{1}H} NMR (δ, CD_2Cl_2, 20°C): 82.1.

[Pd(PCP-^{i}Pr)TFA] (26b)

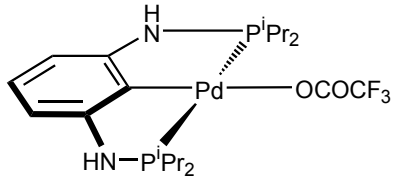

This complex has been prepared analogously to **26a** with $Pd(TFA)_2$ (86 mg, 0.26 mmol) and **3b** (88 mg, 0.26 mmol) as the starting materials.

Yield: 124 mg (88 %) brown solid; $C_{20}H_{32}F_3N_2O_2P_2Pd$ (MW: 577.83); 43.06% C, 5.78% H, 5.02% N.

^{1}H NMR (δ, CD_2Cl_2, 20°C): 6.76 (t, *J* = 7.9 Hz, 1H, Ph^4), 6.11 (t, *J* = 7.9 Hz, 2H, Ph^{3,5}), 3.91 (s, 2H, N*H*), 2.38 - 2.28 (m, 4H C*H*$(CH_3)_2$), 1.32 - 1.20 (m, 24 H, CH(C*H*$_3)_2$).

^{13}C{^{1}H} NMR (δ, CD_2Cl_2, 20°C): 157.7 (C^{Ph}), 127.3 (C^{Ph}), 124.0 (C^{Ph}), 102.1 (C^{Ph}), 27.4 (t, *J* = 12.6 Hz, *C*H$(CH_3)_2$), 17.2 (CH(*C*H$_3)_2$).

^{31}P{^{1}H} NMR (δ, CD_2Cl_2, 20°C): 114.5.

[Pd(PCP-^{t}Bu)TFA] (26c)

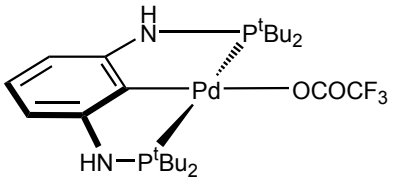

This complex has been prepared analogously to **26a** with $Pd(TFA)_2$ (100 mg, 0.30 mmol) and **3c** (120 mg, 0.30 mmol) as the starting materials.

Yield: 140 mg (78 %) brown solid; $C_{24}H_{41}F_3N_2OP_2Pd$ (MW: 614.94); 46.88% C, 6.72% H, 4.56% N.

^{1}H NMR (δ, CD_2Cl_2, 20°C): 6.73 (t, *J* = 7.9 Hz, 1H, Ph^4), 6.13 (d, *J* = 7.9 Hz, 2H, Ph^{3,5}), 4.18 (s, 2H, N*H*), 1.45 - 1.39 (m, 36H, C(C*H*$_3$)$_3$).

^{13}C{^{1}H} NMR (δ, CD_2Cl_2, 20°C): 158.0 (t, *J* = 11.5 Hz, C^{Ph}), 129.8 (C^{Ph}), 126.7 (C^{Ph}), 101.4 (t, *J* = 8.1 Hz, C^{Ph}), 38.1 (t, *J* = 8.9 Hz, *C*(CH$_3$)$_3$), 28.0 (t, *J* = 3.7 Hz, C(*C*H$_3$)$_3$).

^{31}P{^{1}H} NMR (δ, CD_2Cl_2, 20°C): 120.4.

[Pd(PCP-Ph^E)Cl] (27)

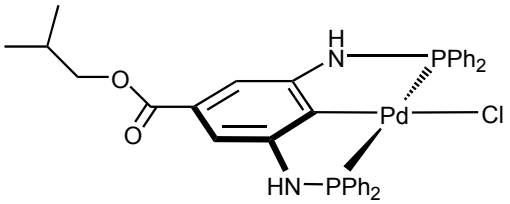

A suspension of $Pd_2(dba)_3$ (172 mg, 0.19 mmol) and **3e** (230 mg, 0.38 mmol) in toluene (10 mL) was stirred overnight at 80ºC. The resulting yellow solution was evaporated under vaccum and the product precipitated with pentane, collected on a glass frit and washed twice with Et_2O.

Yield: 245 mg (90 %) yellow solid; $C_{35}H_{33}ClN_2O_2P_2Pd$ (MW: 717.46); 58.59% C, 4.64% H, 3.90% N.

^{1}H NMR (δ, CD_2Cl_2, 20°C): 7.87 – 7.43 (m, 22H, PPh, Ph^{3,5}), 5.25 (s, 2H, N*H*), 4.00 (d, *J* = 6.7 Hz, 2H, C*H*$_2$), 2.02 (m, *J* = 6.7 Hz, 1H, C*H*(CH$_3$)$_2$), 0.99 (d, *J* = 6.7 Hz, 6H, CH(C*H*$_3$)$_2$).

^{13}C{^{1}H} NMR (δ, CD_2Cl_2, 20°C): 166.1 (*C*O), 155.7 (t, *J* = 13.9 Hz, C^{Ph}), 134.8 (C^{PPh}), 131.9 (t, *J* = 7.9 Hz, C^{PPh}), 130.3 (C^{PPh}), 130.4 (C^{Ph}), 128.8 (t, *J* = 5.7 Hz, C^{PPh}), 104.0 (t, *J* = 9.5 Hz, C^{Ph}), 70.7 (*C*H$_2$), 27.9 (*C*H(CH$_3$)$_2$), 18.9 (CH(*C*H$_3$)$_2$).

^{31}P{^{1}H} NMR (δ, CD_2Cl_2, 20°C): 80.5.

4.7.9 Palladium(II) PN Complexes

[Pd(PN-Ph)Cl_2] (29a).

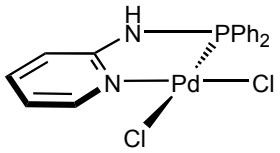

4a (300 mg, 1.1 mmol) was added to a solution of Pd(COD)Cl_2 (307 mg, 1.1 mmol) in 20 mL CH_2Cl_2 and the mixture was stirred at room temperature for 2 h. The solvent was then removed under vacuum and the remaining yellow solid was washed twice with Et_2O and dried.

Yield: 420 mg (88%) yellow solid; $C_{17}H_{15}Cl_2N_2PPd$ (MW: 455.60); 44.82% C, 3.32% H, 6.15% N.

^{1}H NMR (δ, CD_2Cl_2, 20ºC): 10.11 (s, 1H, N*H*), 9.00 (d, *J* = 5.8 Hz, py^6), 7.90 – 7.83 (m, 5H, Ph), 7.71 – 7.61 (m, 6H, Ph and py^4), 7.13 (d, *J* = 8.2 Hz, py^3), 7.03 (t, *J* = 6.5 Hz, py^5).

^{13}C {^{1}H} NMR (δ, CD_2Cl_2, 20ºC): 161.8 (d, *J* = 10.7 Hz, py^2), 148.9 (py^6), 142.1 (py^4), 133.4 (d, *J* = 2.7 Hz, Ph), 132.9 (d, *J* = 12.3 Hz, Ph^{2,6}), 129.6 (d, *J* = 12.3 Hz, Ph^{3,5}), 128.8 (Ph^4), 116.7 (py^5), 111.7 (d, *J* = 11.5 Hz, py^3).

^{31}P {^{1}H} NMR (δ, CD_2Cl_2, 20ºC): 79.5.

[Pd(PN-^{i}Pr)Cl_2] (29b).

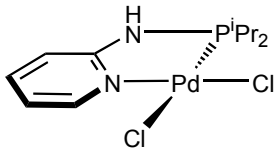

This complex has been prepared analogously to **29a** with Pd(COD)Cl_2 (460 mg, 1.6 mmol) and **4b** (340 mg, 1.6 mmol) as the starting materials.

Yield: 565 mg (91%) yellow solid; $C_{11}H_{19}Cl_2N_2PPd$ (MW: 387,56); 34.09% C, 4.94% H, 7.23% N.

^{1}H NMR (δ, CD_2Cl_2, 20ºC): 8.90 (s, 1H, N*H*), 8.83 (d, *J* = 5.2 Hz, 1H, py^6), 7.84 (t, *J* = 7.8 Hz, 1H, py^4), 7.07 (d, *J* = 8.2 Hz, 1H, py^3), 6.95 (t, *J* = 6.4 Hz, 1H, py^5), 2.47 (m, *J* = 7.1 Hz, 2H, C*H*$(CH_3)_2$), 1.38 – 1.20 (m, 12 H, CH(C*H*$_3)_2$).

^{13}C {^{1}H} NMR (δ, CD_2Cl_2, 20ºC): 163.1 (d, 7.3 Hz, py^2), 148.5 (py^6), 141.8 (py^4), 116.3 (py^5), 111.1 (d, *J* = 9.2 Hz, py^3), 28.1 (d, *J* = 32.2 Hz, *C*H$(CH_3)_2$), 17.8 (d, *J* = 2.0 Hz, CH(*C*H$_3)_2$), 16.8 (d, *J* = 2.5 Hz, CH(*C*H$_3)_2$).

^{31}P {^{1}H} NMR (δ, CD_2Cl_2, 20ºC): 125.7.

[Pd(PN-BIPOL)Cl_2] (29c).

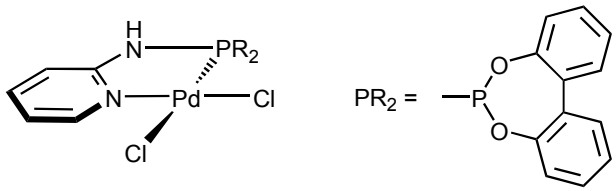

This complex has been prepared analogously to **29a** with Pd(COD)Cl_2 (92 mg, 0.32 mmol) and **4c** (100 mg, 0.32 mmol) as the starting materials.

Yield: 112 mg (74%) yellow solid; $C_{17}H_{13}Cl_2N_2O_2PPd$ (MW: 485.58); 42.05% C, 2.70% H, 5.77% N.

^{1}H NMR (δ, CD_2Cl_2, 20ºC): 9.00 (d, *J* = 5.9 Hz, 1H, py^6), 7.70 (t, *J* = 7.8 Hz, 1H, py^4), 7.50 – 7.32 (m, 8H, Ph), 7.17 (d, *J* = 7.3 Hz, 1H, py^3), 6.94 (t, *J* = 7.3 Hz, 1H, py^5), 6.25 (s, 1H, NH).

^{13}C {^{1}H} NMR (δ, CD_2Cl_2, 20ºC): 155.6 (d, *J* = 22.2 Hz, py^2), 149.3 (Ph), 148.2 (d, *J* = 12.6 Hz, py^6), 141.5 (py^4), 130.2 (Ph), 128.9 (Ph), 127.2 (Ph), 122.5 (d, *J* = 4.2 Hz, Ph), 117.9 (Ph), 117.1 (py^5), 111.6 (d, *J* = 12.6 Hz, py^3).

^{31}P {^{1}H} NMR (δ, CD_2Cl_2, 20ºC): 109.5

[Pd(PN-^{Me}TAR)Cl_2] (29d).

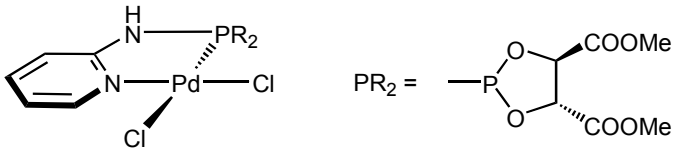

This complex has been prepared analogously to **29a** with Pd(COD)Cl_2 (95 mg, 0.33 mmol) and **4d** (100 mg, 0.33 mmol) as the starting materials.

Yield: 118 mg (75%) yellow solid; for $C_{11}H_{13}Cl_2N_2O_6PPd$ (MW: 4777.51); 27.67% C, 2.74% H, 5.87% N.

^{1}H NMR (δ, CD_2Cl_2, 20ºC): 9.17 (d, *J* = 6.2, 1H, py^6), 7.33 (d, *J* = 8.2 Hz, py^4), 7.06 (t, *J* = 6.5 Hz, 1H, py^3), 6.78 (t, *J* = 6.5 Hz, 1H, py^5), 6.27 (s, 1H, N*H*), 5.58 (dd, *J* = 4.3 Hz, *J* = 14.0 Hz, 1H, C*H*), 5.41 (dd, *J* = 4.3 Hz, *J* = 13.9 Hz, 1H, C*H*), 3.92 (s, 3H, CH_3), 3.86 (s, 3H, CH_3).

^{13}C {^{1}H} NMR (δ, $CDCl_3$, 20ºC): 168.0 (*C*O), 166.1 (*C*O), 149.5 (py^2), 143.8 (py^6), 142.0 (py^4), 117.1 (py^5), 111.7 (d, *J* = 14.6 Hz, py^3), 77.7 (d, *J* = 5 Hz, *C*H), 76.7 (d, *J* = 7.3 Hz, *C*H), 54.0 (*C*H_3), 53.8 (*C*H_3).

^{31}P {^{1}H} NMR (δ, $CDCl_3$, 20ºC): 118.5

[Pd(PN^{ox}-Ph)Cl$_2$] (30)

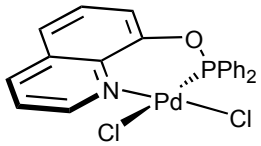

This complex has been prepared analogously to **29a** with Pd(COD)Cl$_2$ (305 mg, 1.1 mmol) and **5a** (340 mg, 1.1 mmol) as the starting materials.

Yield: 501 mg (90%) yellow solid; $C_{21}H_{16}Cl_2NOPPd$ (MW: 506.64); 49.78% C, 3.18% H, 2.76% N.

^{1}H NMR (δ, CD_2Cl_2, 20ºC): 10.54 (dd, *J* = 1.2 Hz, *J* = 5.5 Hz, 1H, quin^2), 8.45 (dd, *J* = 1.21 Hz, *J* = 8.22 Hz, 1H, quin^4), 7.97 – 7.89 (m, 4H, quin), 7.60 – 7.47 (m, 10H, Ph).

^{31}P {^{1}H} NMR (δ, $CDCl_3$, 20ºC): 115.7

[Pd(PN^{py}-Ph)(η^1-allyl)Cl$_2$] (31a)

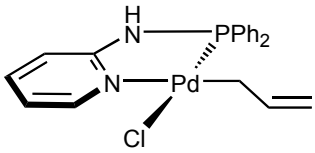

4a (160 mg, 0.58 mmol) was added to a solution of [Pd(η^3-allyl)Cl]$_2$ (100 mg, 0.28 mmol) in 15 mL CH_2Cl_2 and the mixture was stirred at room temperature for 2 h. The solvent was removed under vacuum and the remaining yellow solid was washed twice with Et_2O and dried.

Yield: 217 mg (83%) $C_{20}H_{20}ClN_2PPd$ (MW: 461.22); 52.08% C, 4.37% H, 6.07% N.

^{1}H NMR (δ, CD_2Cl_2, 20ºC): 11.21 (s, 1H, N*H*), 8.37 (d, *J* = 4.8 Hz, py^6), 7.90 – 7.74 (m, 6H, Ph, py^3 and py^4), 7.49 – 7.26 (m, 6H, Ph), 6.69 (t, *J* = 5.8 Hz, py^5), 5.90 (m, *J* = 10.6 Hz, C*H*), 4.67 (bs, 1H, =C*H*), 4.06 (bs, 1H, =C*H*), 3.32 (bs, 2H, C*H*$_2$).

^{13}C {^{1}H} NMR (δ, $CDCl_3$, 20ºC): 159.4 (d, *J* = 13.1 Hz, py^2), 149.6 (s, py^6), 137.8 (py^4), 129.9 (d, *J* = 15.5 Hz, Ph^{2,6}), 129.4 (d, *J* = 2.5 Hz, Ph^4), 129.1 (Ph^1), 126.7 (d, *J* = 12.0 Hz, Ph^{3,5}), 122.8 (*C*H), 113.7 (py^5), 111.8 (d, *J* = 8.1 Hz, py^3), 82.8 (=*C*H$_2$), 45.2 (*C*H$_2$).

^{31}P {^{1}H} NMR (δ, $CDCl_3$, 20ºC): 78.4

[Pd(PN^{py}-^{i}Pr)(η^{1}-allyl)Cl$_2$] (31b)

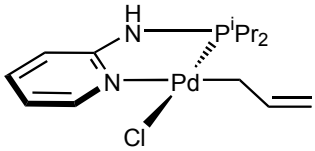

This complex has been prepared analogously to **31a** with **4b** (121 mg, 0.58 mmol) and [Pd(η^{3}-allyl)Cl]$_2$ (100 mg, 0.28 mmol) as the starting materials.

Yield: 155 mg (68%); $C_{14}H_{24}ClN_2PPd$ (MW: 393.18); 42.77% C, 6.15% H, 7.12% N.

^{1}H NMR (δ, CD_2Cl_2, 20ºC): 10.40 (s, 1H, N*H*), 8.23 (bs, 1H, py^{6}), 7.81 (bs, 1H, py^{4}), 7.56 (bs, 1H, py^{3}), 6.65 (bs, 1H, py^{5}), 5.66 (s, 1H, C*H*), 4.66 (s, 1H, =C*H*), 3.96 (s, 1H, =C*H*), 3.19 (s, 2H, C*H*$_2$), 2.56 (s, 2H, C*H*(CH$_3$)$_2$), 1.20 (s, 12H, CH(C*H*$_3$)$_2$).

^{13}C {^{1}H} NMR (δ, $CDCl_3$, 20ºC): 163.4 (d, *J* = 10.0 Hz, py^{2}), 152.5 (py^{6}), 140.1 (py^{4}), 121.5 (d, *J* = 5.5 Hz, *C*H), 115.5 (py^{5}), 113.9 (d, *J* = 7.5 Hz, py^{3}), 82.0 (d, *J* = 29.0 Hz, =*C*H$_2$), 44.1 (*C*H$_2$), 27.5 (d, *J* = 27.4 Hz, *C*H(CH$_3$)$_2$), 18.1 (CH(*C*H$_3$)$_2$).

^{31}P {^{1}H} NMR (δ, $CDCl_3$, 20ºC): 115.3.

[Pd(PN^{py}-Ph)(η^{3}-allyl)Cl$_2$] (32a)

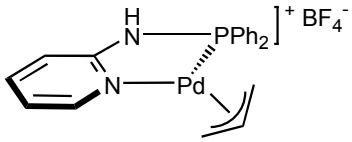

$AgBF_4$ (112 mg, 0.58 mmol) was added to a solution of [Pd(η^{3}-allyl)Cl]$_2$ (100 mg, 0.28 mmol) in CH_3CN (15 mL) and the mixture was stirred at room temperature in the dark for 15 min. The solution was then filtered under argon and **4a** (160 mg, 0.58 mmol), dissolved in 5 ML CH_3CN, was added. The mixture was stirred for further 30 min. at room temperature, after which the solvent was removed under vacuum and the remaining off-white solid was washed twice with Et_2O and dried.

Yield: 273 mg (92%) $C_{20}H_{20}BF_4N_2PPd$ (MW: 512.57) 46.87% C, 3.93% H, 5.47% N.

^{1}H NMR (δ, CD_2Cl_2, 20ºC): 8.34 (d, *J* = 5.3 Hz, 1H, py^{6}), 8.24 (d, *J* = 4.2 Hz, 1H, N*H*), 7.65 – 7.59 (m, 4H, Ph, py^{3} and py^{4}), 7.52 – 7.48 (m, 9H, Ph and py^{5}), 6.79 (t, *J* = 6.4 Hz, =C*H*), 5.90 (m, 1H, C*H*), 4.82 (t, *J* = 6.4 Hz, 1H, =C*H*), 4.13 (d, *J* = 10.1 Hz, 1H, C*H*$_2$), 4.08 (d, *J* = 10.1 Hz, 1H, C*H*$_2$).

^{13}C {^{1}H} NMR (δ, $CDCl_3$, 20ºC): 159.0 (d, *J* = 13.4 Hz, py^{2}), 150.9 (py^{6}), 139.4 (py^{4}), 130.4 (d, *J* = 2.8 Hz, Ph^{2,6}), 130.1 (Ph^{1}), 129.8 (Ph^{4}), 127.5 (d, *J* = 12.4 Hz, Ph^{3,5}), 120.9 (d, *J* = 5.7 Hz, *C*H), 115.0 (py^{5}), 111.9 (d, *J* = 7.4 Hz, py^{3}), 79.6 (d, *J* = 31.4 Hz, =*C*H$_2$), 49.4 (*C*H$_2$).

^{31}P {^{1}H} NMR (δ, $CDCl_3$, 20ºC): 77.6.

[Pd(PN^{py}-^{i}Pr)(η^{3}-allyl)Cl$_2$] (32b).

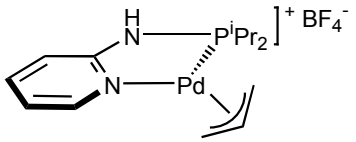

This complex has been prepared analogously to **32a** with $AgBF_4$ (112 mg, 0.58 mmol), [Pd(η^{3}-allyl)Cl]$_2$ (100 mg, 0.28 mmol) and **4b** (121 mg, 0.57 mmol) as the starting materials.

Yield: 93 mg (75%) $C_{14}H_{24}BF_4N_2PPd$ (MW: 444.53); 37.83% C, 5.44% H, 6.30% N.

^{1}H NMR (δ, CD_2Cl_2, 20ºC): 8.30 (d, *J* = 4.6 Hz, 1H, N*H*), 7.63 (d, *J* = 7.0 Hz, 1H, py^{6}), 7.39 – 7.37 (m, 2H, py^{3} and py^{4}), 6.76 (t, *J* = 5.3 Hz, py^{5}), 5.70 (m, *J* = 6.4 Hz, 1H, C*H*), 4.76 (s, 1H, =C*H*), 4.03 – 3.92 (m, 2H, C*H*$_2$), 2.69 – 2.42 (m, 3H, =C*H* and C*H*(CH$_3$)$_2$), 1.22 – 1.14 (m, 12H, CH(C*H*3)2).

^{13}C {^{1}H} NMR (δ, $CDCl_3$, 20ºC): 162.4 (d, *J* = 10.0 Hz, py^{2}), 153.0 (py^{6}), 140.9 (py^{4}), 121.5 (d, *J* = 5.5 Hz, *C*H), 116.3 (py^{5}), 113.1 (d, *J* = 7.0 Hz, py^{3}), 82.2 (d, *J* = 29.4 Hz, =*C*H$_2$), 45.6 (*C*H$_2$), 27.6 (d, *J* = 25.9 Hz, *C*H(CH$_3$)$_2$), 27.2 (d, *J* = 25.9 Hz, *C*H(CH$_3$)$_2$), 18.2 (d, *J* = 8.0 Hz, CH(*C*H$_3$)$_2$), 17.3 (d, *J* = 15.0 Hz, CH(*C*H$_3$)$_2$).

^{31}P {^{1}H} NMR (δ, $CDCl_3$, 20ºC): 115.4.

4.7.10 Platinum(II) PNP complexes

[Pt(PNP-Ph)Br]Br (22a)

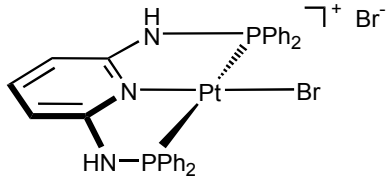

To a solution of Pt(COD)Br$_2$ (194 mg, 0.42 mmol) in CH_2Cl_2 (10mL) **1b** (200 mg, 0.42 mmol) was added. After the mixture was stirred for 2 h, the solvent was removed under vacuum and the product was precipitated with Et_2O, collected on a glass frit and washed twice with Et_2O (10 mL).

Yield: 325 mg (93 %) off-white solid; $C_{29}H_{25}Br_2N_3P_2Pt$ (MW: 832.382); 41.85% C, 3.03% H, 5.05% N.

^{1}H NMR (δ, CD_2Cl_2, 20ºC): 10.54 (s, $J_{HPt(sat)}$ = 26.8 Hz, 2H, N*H*), 8.00 (d, *J* = 6.3 Hz, 6H, Ph), 7.38 - 7.35 (m, 14H, Ph), 7.05 (s, 1H, py^{4}), 5.61 (t, *J* = 8.1 Hz, 2H, py^{3,5}).

$^{31}P\{^1H\}$ NMR (δ, CD_2Cl_2, 20ºC): 65.5 (t, $J_{PPt(sat)}$ = 2686 Hz).

[Pt(PNP-^{i}Pr)Br]Br (22b)

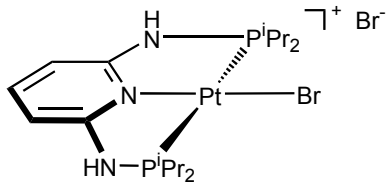

This complex has been prepared analogously to **22a** with $Pt(COD)Br_2$ (100 mg, 0.28 mmol) and **1c** (97 mg, 0.28 mmol) as the starting materials.

Yield: 184 mg (94 %) off-white solid; $C_{17}H_{33}Br_2N_3P_2Pt$ (MW: 696.31); 29.32% C, 4.78% H, 6.03% N.

^1H NMR (δ, CD_2Cl_2, 20ºC): 9.43 (s, $J_{HPt(sat)}$ = 30.4 Hz, 2H, N*H*), 7.16 (t, *J* = 8.0 Hz, 1H, py^4), 6.95 (d, *J* = 8.0 Hz, 2H, py^{3,5}), 2.88 - 2.77 (m, 4H, C*H*$(CH_3)_2$), 1.41 - 1.34 (m, 24H, CH(C*H*$_3)_2$).

$^{13}C\{^1H\}$ NMR (δ, CD_2Cl_2, 20ºC): 161.7 (t, *J* = 5.5 Hz, py^{2,6}), 140.4 (py^4), 100.0 (py^{3,5}), 27.3 (t, *J* = 17.0 Hz, *C*H$(CH_3)_2$), 17.2 (d, *J* = 9.2 Hz, CH(*C*H$_3)_2$).

$^{31}P\{^1H\}$ NMR (δ, CD_2Cl_2, 20ºC): 100.4 (t, $J_{PPt(sat)}$ = 2556 Hz).

[Pt(PNP-^{t}Bu)Br]Br (22c)

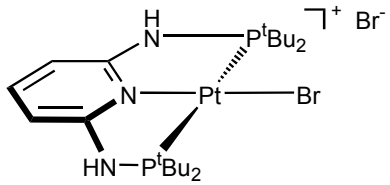

This complex has been prepared analogously to **22a** with $Pt(COD)Br_2$ (100 mg, 0.28 mmol) and **1c** (112 mg, 0.28 mmol) as the starting materials.

Yield: 180 mg (85 %) off-white solid; $C_{21}H_{41}Br_2N_3P_2Pt$ (MW: 752.421); 33.52% C, 5.49% H, 5.58% N.

^1H NMR (δ, CD_2Cl_2, 20ºC): 9.21 (s, $J_{HPt(sat)}$ = 33.6 Hz, 2H, N*H*), 7.42 (t, *J* = 7.8 Hz, 1H, py^4), 6.95 (m, 2H, py^{3,5}), 1.57-1.51 (m, 36H, C(C*H*$_3)_3$).

$^{13}C\{^1H\}$ NMR (δ, CD_2Cl_2, 20ºC): 162.0 (py^{2,6}), 140.2 (py^4), 100.5 (py^{3,5}), 40.4 (t, *J* = 12.4 Hz, *C*$(CH_3)_3$), 28.6 (C(*C*H$_3)_3$).

$^{31}P\{^1H\}$ NMR (δ, CD_2Cl_2, 20ºC): 103.9 (t, $J_{PPt(sat)}$ = 2534 Hz).

[Pt(PNP-BIPOL)Br]CF_3SO_3 (22d)

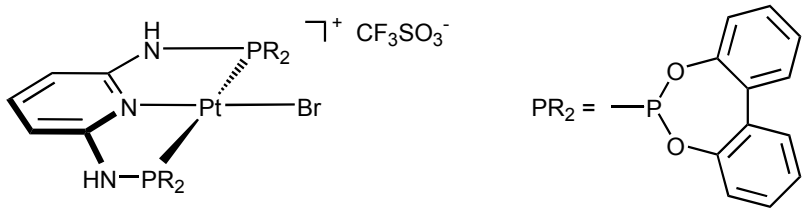

KCF_3SO_3 (27 mg, 0.14 mmol) and $Pt(COD)Br_2$ (50 mg, 0.14 mmol) were added to a solution of **2e** (76 mg, 0.14 mmol) in CH_3CN. The mixture was stirred for 2 h. and filtered. The off-white filtrate was evaporated to dryness and the product was precipitated with Et_2O, collected on a glass frit and washed twice with Et_2O (10 mL).

Yield: 120 mg (89%) off-white solid; $C_{30}H_{21}BrF_3N_3O_7P_2PtS$ (MW: 961.51); 37.48% C, 2.20% H, 4.37% N.

^{1}H NMR (δ, CD_3CN, 20ºC): 9.52 (s, $J_{HPt(sat)}$ = 26.0 Hz, 2H, N*H*), 7.71 (s, 1H, py^4), 7.54-7.26 (m, 16H, Ph), 6.68 (d, *J* = 8.2 Hz, 2H, py^{3,5}).

^{31}P{^{1}H} NMR (δ, CD_3CN, 20ºC): 123.4 (t, $J_{PPt(sat)}$ = 4190 Hz).

[Pt(PNP-^{Me}TAR)Br]CF_3SO_3 (22e)

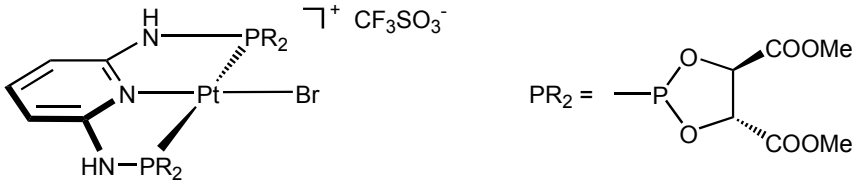

This complex has been prepared analogously to **22a** with KCF_3SO_3 (110 mg, 0.58 mmol), $Pt(COD)Br_2$ (200 mg, 0.58 mmol) and **2g** (368 mg, 0.58 mmol) as the starting materials.

Yield: 510 mg (93%) off-white solid; $C_{18}H_{21}BrF_3N_3O_{15}P_2PtS$ (MW: 945.37); 22.87% C, 2.24% H, 4.44% N.

^{1}H NMR (δ, CD_3CN, 20ºC): 8.93 (s, $J_{HPt(sat}$ = 29.2 Hz, 2H, N*H*), 7.77 (s, 1H, py^4), 6.86 (d, *J* = 8.2 Hz, py^{3,5}), 5.56 - 5.48 (m, 4H, C*H*), 3.90 - 3.84 (m, 12 H, CH_3).

^{13}C{^{1}H} NMR (δ, CD_3CN, 20ºC): 168.5 (*C*O), 166.1 (*C*O), 154.4 (t, *J* = 8.6 Hz, py^{2,6}), 145.8 (py^4), 103.2 (t, *J* = 5.8 Hz, py^{3,5}), 77.6 (*C*H), 76.7 (*C*H), 53.7 (CH_3), 53.5 (CH_3).

^{31}P{^{1}H} NMR (δ, CD_3CN, 20ºC): 131.6 (t, $J_{PPt(sat)}$ = 4286 Hz).

4.7.11 Platinum(II) PCP complexes

[Pt(PCP-Ph)Br] (28a)

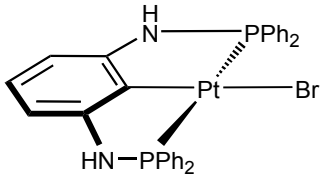

A mixture of $Pt(COD)Br_2$ (50 mg, 0.11 mmol) and **3a** (53 mg, 0.11 mmol) in toluene was heated to 80ºC, and Et_3N (20 µL, 0.13 mmol) was added. The mixture was refluxed overnight, and then filtered while hot. The solvent was removed under vacuum and the pale yellow product was precipitated with Et_2O, collected on a glass frit and washed twice with Et_2O (10 mL).

Yield: 77 mg (93 %) off-white solid; $C_{30}H_{25}BrN_2P_2Pt$ (MW: 750.48); 48.01% C, 3.36% H, 3.73% N.

^{1}H NMR (δ, CD_2Cl_2, 20°C): 7.93 - 7.84 (m, 8H, Ph), 7.50 - 7.41 (m, 12H, Ph), 6.89 (t, *J* = 8.0 Hz, 1H, Ph^4), 6.37 (d, *J* = 8.0 Hz, 2H, Ph^{3,5}), 5.35 (s, $J_{HPt(sat)}$ = 77.6 Hz, 2H, N*H*).

^{13}C{^{1}H} NMR (δ, CD_2Cl_2, 20°C): 153.7 (t, *J* = 12.0 Hz, C^{Ph}), 133.9 (C^{PPh}), 132.3 (t, *J* = 7.6 Hz, C^{PPh}), 131.3 (C^{PPh}), 128.6 (t, *J* = 5.7 Hz, C^{PPh}), 127.2 (t, *J* = 5.7 Hz, C^{Ph}), 103.0 (t, *J* = 7.6 Hz, C^{Ph}).

^{31}P{^{1}H} NMR (δ, CD_2Cl_2, 20°C): 76.1 (t, $J_{PPt(sat)}$ = 3208 Hz).

[Pt(PCP-^{i}Pr)Br] (28b)

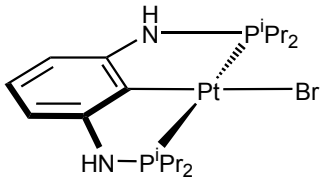

This complex has been prepared analogously to **28a** with $Pt(COD)Br_2$ (50 mg, 0.11 mmol), **3b** (38 mg, 0.11 mmol) and Et_3N (20 µL, 0.13 mmol) as the starting materials.

Yield: 61 mg (91 %) off-white solid; $C_{18}H_{33}BrN_2P_2Pt$ (MW: 614.41); 35.19% C, 5.41% H, 4.56% N.

^{1}H NMR (δ, CD_2Cl_2, 20°C): 6.77 (t, *J* = 7.7 Hz, 1H, Ph^4), 6.18 (d, *J* = 7.7 Hz, 2H, Ph^{3,5}), 4.35 (s, $J_{HPt(sat)}$ = 75.8 Hz, 2H, N*H*), 2.60 – 2.48 (m, *J* = 7.5 Hz, 4H, C*H*$(CH_3)_2$, 1.27 – 1.18 (m, 24H, CH(C*H*$_3$)$_2$).

^{13}C{^{1}H} NMR (δ, CD_2Cl_2, 20°C): 155.2 (t, *J* = 10.7 Hz, C^{Ph}), 128.5 (C^{Ph}), 125.2 (C^{Ph}), 101.6 (t, *J* = 6.6 Hz, C^{Ph}), 27.9 (t, *J* = 16.7 Hz, *C*H$(CH_3)_2$), 16.7 (CH(*C*H$_3$)$_2$).

$^{31}P\{^1H\}$ NMR (δ, CD_2Cl_2, 20°C): 106.6 (t, $J_{PPt(sat)}$ = 3112 Hz).

[Pt(PCP-^{t}Bu)Br] (28c)

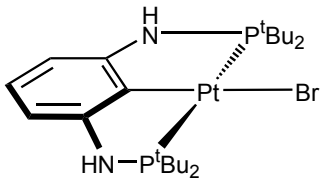

This complex has been prepared analogously to **28a** with $Pt(COD)Br_2$ (50 mg, 0.11 mmol), **3c** (44 mg, 0.11 mmol) and Et_3N (20 μL, 0.13 mmol) as the starting materials.

Yield: 58 mg (79 %) off-white solid; $C_{22}H_{41}BrN_2P_2Pt$ (MW: 670.52); 39.41% C, 6.16% H, 4.18% N.

^1H NMR (δ, CD_2Cl_2, 20°C): 6.86 (t, *J* = 7.9 Hz, 1H, Ph^4), 6.16 (d, *J* = 7.9 Hz, 2H, $Ph^{3,5}$), 4.47 (s, $J_{HPt(sat)}$ = 76.4 Hz, 2H, N*H*), 1.14 (s, 36H, $C(CH_3)_3$).

$^{13}C\{^1H\}$ NMR (δ, CD_2Cl_2, 20°C): 155.7 (t, *J* = 9.8 Hz, C^{Ph}), 134.6 (C^{Ph}), 126.6 (d, *J* = 11.4 Hz, C^{Ph}), 101.1 (t, *J* = 6.3 Hz, C^{Ph}), 39.4 (t, *J* = 13.0 Hz, $C(CH_3)_3$), 28.0 ($C(CH_3)_3$).

$^{31}P\{^1H\}$ NMR (δ, CD_2Cl_2, 20°C): 109.5 (t, $J_{PPt(sat)}$ = 3736 Hz).

4.8 Catalytic Reactions

4.8.1 Iron(II) catalyzed coupling of aromatic aldehydes and EDA

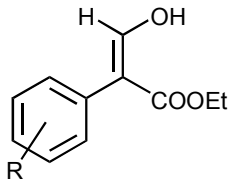

General Procedure: Aldehyde (1 equiv.) and ethyldiazoacetate (1 equiv.) were added to a solution of the catalyst (10 mol%) in CH_3NO_2 (5 mL) at room temperature and the mixture was stirred at this temperature for 16 h. The mixture was then filtered through a plug of silica to remove the catalyst and the product was purified by flash chromatography (silica, CH_2Cl_2).

3-Hydroxy-2-(4-methoxyphenyl)acrylic acid ethyl ester (Table 14, entry 1):

^{1}H NMR (δ, $CDCl_3$, 20°C): 12.05 (d, *J* = 12.6 Hz, 1H, CHO*H*), 7.23 (d, *J* = 12.6 Hz, 1H, C*H*OH), 7.17 (d, *J* = 8.7 Hz, Ph^{2,6}), 6.86 (d, *J* = 8.9 Hz, 2H, Ph^{3,5}), 4.26 (q, *J* = 7.1 Hz, 2H, COOC*H*$_2$CH$_3$), 3.78 (s, 3H, OC*H*$_3$), 1.27 (t, *J* = 7.2 Hz, 3H, COOCH$_2$C*H*$_3$). ^{13}C{^{1}H} NMR (δ, $CDCl_3$, 20°C): 171.8 (*C*OOCH$_2$CH$_3$), 162.8 (*C*HOH), 158.7 (Ph), 130.5 (Ph), 126.4 (Ph), 113.6 (Ph), 108.1 (*C*CHOH), 60.8 (COO*C*H$_2$CH$_3$), 55.1 (O*C*H$_3$), 14.1 (COOCH$_2$*C*H$_3$).

3-Hydroxy-2-(4-fluorophenyl)acrylic acid ethyl ester (Table 14, entry 2):

^{1}H NMR (δ, $CDCl_3$, 20°C): 12.08 (d, *J* = 12.6 Hz, 1H, CHO*H*), 7.25 – 7.17 (m, 3H, C*H*OH and Ph^{2,6}), 6.98 (t, *J* = 8.8 Hz, 2H, Ph^{3,5}), 4.25 (q, *J* = 7.2 Hz, 2H, COOC*H*$_2$CH$_3$), 1.25 (t, *J* = 7.1 Hz, 3H, COOCH$_2$C*H*$_3$). ^{13}C{^{1}H} NMR (δ, $CDCl_3$, 20°C): 171.4 (*C*OOCH$_2$CH$_3$), 163.3 (*C*HOH), 160.0 (Ph), 131.0 (Ph), 127.6 (Ph), 114.9 (Ph), 107.6 (*C*CHOH), 60.9 (COO*C*H$_2$CH$_3$), 14.0 (COOCH$_2$*C*H$_3$).

3-Hydroxy-2-(4-chlorophenyl)acrylic acid ethyl ester (Table 14, entry 3):

^{1}H NMR (δ, $CDCl_3$, 20°C): 12.13 (d, *J* = 12.6 Hz, 1H, CHO*H*), 7.29 – 7.15 (m, 5H, C*H*OH and Ph), 4.27 (q, *J* = 7.2 Hz, 2H, COOC*H*$_2$CH$_3$), 1.27 (t, *J* = 7.2 Hz, 3H, COOCH$_2$C*H*$_3$). ^{13}C{^{1}H} NMR (δ, $CDCl_3$, 20°C): 171.2 (*C*OOCH$_2$CH$_3$), 163.5 (*C*HOH), 132.7 (Ph), 130.6 (Ph), 128.3 (Ph), 107.6 (*C*CHOH), 61.1 (COO*C*H$_2$CH$_3$), 14.1 (COOCH$_2$*C*H$_3$).

3-Hydroxy-2-(4-bromophenyl)acrylic acid ethyl ester (Table 14, entry 4):

^{1}H NMR (δ, $CDCl_3$, 20°C): 12.13 (d, *J* = 12.6 Hz, 1H, CHO*H*), 7.44 (d, *J* = 8.5 Hz, 2H, Ph^{3,5}), 7.27 (d, *J* = 12.6 Hz, 1H, C*H*OH), 7.13 (d, *J* = 8.5 Hz, 2H, Ph^{2,6}), 4.28 (q, *J* = 7.2 Hz, 2H, COOC*H*$_2$CH$_3$), 1.28 (t, *J* = 7.2 Hz, 3H, COOCH$_2$C*H*$_3$). ^{13}C{^{1}H} NMR (δ, $CDCl_3$, 20°C): 171.2 (*C*OOCH$_2$CH$_3$), 163.5 (*C*HOH), 133.0 (Ph), 131.3 (Ph), 131.0 (Ph), 121.0 (Ph), 107.7 (*C*CHOH), 61.1 (COO*C*H$_2$CH$_3$), 14.1 (COOCH$_2$*C*H$_3$).

3-Hydroxy-2-(4-N,N-dimethylaminophenyl)acrylic acid ethyl ester (Table 14, entry 5):

^{1}H NMR (δ, $CDCl_3$, 20°C): 12.00 (d, *J* = 12.6 Hz, 1H, CHO*H*), 7.26 (s, 1H, Ph), 7.19 (d, *J* = 12.6 Hz, C*H*OH), 7.13 (s, 1H, Ph), 6.74 (d, *J* = 7.9 Hz, 2H, Ph), 4.29 (q, *J* = 7.2 Hz, 2H, COOC*H*$_2$CH$_3$), 2.97 (s, 6H, N(C*H*$_3$)$_2$), 1.30 (t, *J* = 7.2 Hz, 3H, COOCH$_2$C*H*$_3$). ^{13}C{^{1}H} NMR (δ, $CDCl_3$, 20°C): 172.1 (*C*OOCH$_2$CH$_3$), 162.3 (*C*HOH), 130.2 (Ph), 129.7 (Ph), 112.9 (Ph), 112.3 (Ph), 108.3 (*C*CHOH), 60.8 (COO*C*H$_2$CH$_3$), 40.6 (N(*C*H$_3$)$_2$), 14.2 (COOCH$_2$*C*H$_3$).

3-Hydroxy-2-(biphenylyl)acrylic acid ethyl ester (Table 14, entry 6):

^{1}H NMR (δ, $CDCl_3$, 20°C): 12.22 (d, *J* = 12.6 Hz, 1H, CHO*H*), 7.65 – 7.58 (m, 4H, Ph), 7.50 – 7.44 (m, 3H, Ph), 7.41 – 7.36 (m, 3H, C*H*OH and Ph), 4.35 (q, *J* = 7.2 Hz, 2H, COOCH_2CH$_3$), 1.34 (t, *J* = 7.1 Hz, 3H, COOCH$_2$CH_3). ^{13}C{^{1}H} NMR (δ, $CDCl_3$, 20°C): 171.6 (*C*OOCH$_2$CH$_3$), 163.5 (*C*HOH), 140.7 (Ph), 139.8 (Ph), 133.1 (Ph), 129.7 (Ph), 128.8 (Ph), 127.3 (Ph), 127.0 (Ph), 126.9 (Ph), 108.3 (*C*CHOH), 61.1 (COO*C*H$_2$CH$_3$), 14.2 (COOCH$_2$*C*H$_3$).

3-Hydroxy-2-(phenyl)acrylic acid ethyl ester (Table 14, entry 7):

^{1}H NMR (δ, $CDCl_3$, 20°C): 12.17 (d, *J* = 12.6 Hz, 1H, CHO*H*), 7.34 – 7.28 (m, 5H, C*H*OH and Ph), 4.30 (q, *J* = 7.2 Hz, 2H, COOCH_2CH$_3$), 1.30 (t, *J* = 7.1 Hz, 3H, COOCH$_2$CH_3). ^{13}C{^{1}H} NMR (δ, $CDCl_3$, 20°C): 171.6 (*C*OOCH$_2$CH$_3$), 163.4 (*C*HOH), 133.8 (Ph), 129.3 (Ph), 128.1 (Ph), 127.0 (Ph), 108.6 (*C*CHOH), 60.9 (COO*C*H$_2$CH$_3$), 14.1 (COOCH$_2$*C*H$_3$).

3-Hydroxy-2-(2-methylphenyl)acrylic acid ethyl ester (Table 14, entry 8):

^{1}H NMR (δ, $CDCl_3$, 20°C): 12.07 (d, *J* = 12.6 Hz, 1H, CHO*H*), 7.25 – 7.11 (m, 5H, C*H*OH and Ph), 4.27 (q, *J* = 7.1 Hz, 2H, COOCH_2CH$_3$), 2.27 (s, 3H, CH_3), 1.25 (t, *J* = 7.2 Hz, 3H, COOCH$_2$CH_3). ^{13}C{^{1}H} NMR (δ, $CDCl_3$, 20°C): 171.6 (*C*OOCH$_2$CH$_3$), 163.1 (*C*HOH), 138.3 (Ph), 133.4 (Ph), 131.1 (Ph), 129.8 (Ph), 127.9 (Ph), 125.7 (Ph), 107.7 (*C*CHOH), 60.7 (COO*C*H$_2$CH$_3$), 20.0 (*C*H$_3$), 14.2 (COOCH$_2$*C*H$_3$).

3-Hydroxy-2-(3-methylphenyl)acrylic acid ethyl ester (Table 14, entry 9):

^{1}H NMR (δ, $CDCl_3$, 20°C): 12.16 (d, *J* = 12.6 Hz, 1H, CHO*H*), 7.29 (d, *J* = 12.6 Hz, C*H*OH), 7.23 – 7.09 (m, 4H, Ph), 4.27 (q, *J* = 7.1 Hz, 2H, COOCH_2CH$_3$), 2.37 (s, 3H, CH_3), 1.30 (t, *J* = 7.2 Hz, 3H, COOCH$_2$CH_3). ^{13}C{^{1}H} NMR (δ, $CDCl_3$, 20°C): 171.7 (*C*OOCH$_2$CH$_3$), 163.3 (*C*HOH), 137.7 (Ph), 134.0 (Ph), 130.1 (Ph), 128.0 (Ph), 127.7 (Ph), 126.6 (Ph), 108.6 (*C*CHOH), 60.9 (COO*C*H$_2$CH$_3$), 21.3 (*C*H$_3$), 14.1 (COOCH$_2$*C*H$_3$).

3-Hydroxy-2-(4-methylphenyl)acrylic acid ethyl ester (Table 14, entry 10):

^{1}H NMR (δ, $CDCl_3$, 20°C): 12.15 (d, *J* = 12.6 Hz, 1H, CHO*H*), 7.28 (d, *J* = 12.6 Hz, C*H*OH), 7.22 – 7.17 (m, 4H, Ph), 4.29 (q, *J* = 7.1 Hz, 2H, COOCH_2CH$_3$), 2.36 (s, 3H, CH_3), 1.29 (t, *J* = 7.1 Hz, 3H, COOCH$_2$CH_3). ^{13}C{^{1}H} NMR (δ, $CDCl_3$, 20°C): 171.8 (*C*OOCH$_2$CH$_3$), 163.1 (*C*HOH), 136.6 (Ph), 131.2 (Ph), 129.3 (Ph), 128.9 (Ph), 108.4 (*C*CHOH), 60.9 (COO*C*H$_2$CH$_3$), 21.0 (*C*H$_3$), 14.1 (COOCH$_2$*C*H$_3$).

3-Hydroxy-2-(3,4-dimethoxyphenyl)acrylic acid ethyl ester (Table 14, entry 11):

^{1}H NMR (δ, $CDCl_3$, 20°C): 12.03 (d, *J* = 12.6 Hz, 1H, CHO*H*), 7.28 (d, *J* = 12.6 Hz, C*H*OH), 6.82 – 6.80 (m, 3H, Ph), 4.28 (q, *J* = 7.2 Hz, 2H, $COOCH_2CH_3$), 3.88 – 3.87 (2 x s, 6H, OCH_3), 1.30 (t, *J* = 7.2 Hz, 3H, $COOCH_2CH_3$). $^{13}C\{^1H\}$ NMR (δ, $CDCl_3$, 20°C): 171.7 ($COOCH_2CH_3$), 162.9 (*C*HOH), 148.4 (Ph), 148.2 (Ph), 126.8 (Ph), 121.6 (Ph), 113.1 (Ph), 110.9 (Ph), 108.2 (*C*CHOH), 60.9 ($COOCH_2CH_3$), 55.8 (OCH_3), 55.8 (OCH_3), 14.2 ($COOCH_2CH_3$).

3-Hydroxy-2-(2,5-dimethoxyphenyl)acrylic acid ethyl ester (Table 14, entry 12):

^{1}H NMR (δ, $CDCl_3$, 20°C): 11.95 (d, *J* = 12.6 Hz, 1H, CHO*H*), 7.18 (d, *J* = 12.6 Hz, C*H*OH), 6.84 – 6.80 (m, 2H, $Ph^{3,4}$), 6.70 (s, 1H, Ph^6), 4.23 (q, *J* = 7.0 Hz, 2H, $COOCH_2CH_3$), 3.75 – 3.72 (6H, OCH_3), 1.22 (t, *J* = 7.1 Hz, 3H, $COOCH_2CH_3$). $^{13}C\{^1H\}$ NMR (δ, $CDCl_3$, 20°C): 171.6 ($COOCH_2CH_3$), 162.8 (*C*HOH), 153.2 (Ph), 152.2 (Ph), 124.2 (Ph), 117.7 (Ph), 113.1 (Ph), 111.6 (Ph), 104.5 (*C*CHOH), 60.5 ($COOCH_2CH_3$), 55.9 (OCH_3), 55.6 (OCH_3), 14.2 ($COOCH_2CH_3$).

4.8.2 Palladium(II) catalyzed Suzuki-Miyaura Coupling

General Procedure: *Pd(II) PNP complexes*: Dioxane (5 mL) was added in a Schlenk flask to a mixture of phenylboronic acid (1.5 equivs.), aryl bromide (1 equiv.), Cs_2CO_3 (2 equivs.) and the corresponding amount of catalyst and the reaction mixture was stirred at 80ºC for 3 h. Upon cooling, the product was purified by flash column chromatography (silica, petroleum ether). *Pd(II) PCP complexes*: Toluene (5 mL) was added in a Schlenk flask to a mixture of phenylboronic acid (1.5 equivs.), aryl bromide (1 equiv.), K_2CO_3 (2 equivs.) and catalyst and the reaction mixture was stirred at 110ºC for 16 h. Upon cooling, the product was purified by flash column chromatography (silica, petroleum ether)

4.8.3 Copper(I) catalyzed synthesis of oxazolines and N-sulfonyl-2-imidazolines

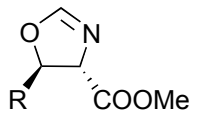

trans

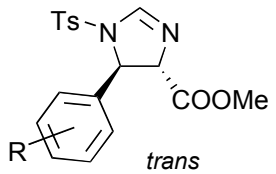

trans

General procedure: *Oxazolines*: Methyl isocyanoacetate (1 equiv.) was added to a mixture of the corresponding amount of catalyst, $^{i}Pr_2EtN$ (10 mol%) and aldehyde (1 equiv.) in CH_2Cl_2 under an argon atmosphere. The reaction mixture was stirred at 40ºC for 2 h. after which it was allowed to cool down to room temperature. The products were isolated from the crude reaction mixture by flash column chromatography (silica, ethyl acetate:hexanes 1:1). *Imidazolines*: The reaction procedure was identical to that for oxazolines with the exception that no base was used.

Table 34, entry 5: ^{1}H NMR (δ, $CDCl_3$, 20°C): 3.84 (s, 3H, COOC*H*$_3$), 4.54 (d, *J* = 6.3 Hz, 1H, C*H*), 6.10 (d, *J* = 6.3 Hz, 1H, C*H*), 7.20 (s, 1H, C*H*), 7.59 (d, *J* = 8.5 Hz, 1H, Ph), 8.20 – 8.13 (m, 2H, Ph).
Table 34, entry 6: ^{1}H NMR (δ, $CDCl_3$, 20°C): 3.78 (s, 3H, COOC*H*$_3$), 4.77 (dd, *J* = 8.7 Hz, *J* = 1.7 Hz, 1H, C*H*), 6.17 (d, *J* = 8.7 Hz, 1H, C*H*), 7.04 – 6.98 (m, 2H, C*H* and Ph), 7.32 – 7.18 (m, 2H, Ph).
Table 36, entry 5: ^{1}H NMR (δ, $CDCl_3$, 20°C): 2.34 (s, 3H, C*H*$_3$), 3.62 (s, 3H, COOC*H*$_3$), 4.59 (d, *J* = 6.3 Hz, 1H, C*H*), 5.48 (d, *J* = 6.3 Hz, 1H, C*H*), 7.23 – 7.19 (m, 3H, Ph), 7.37 – 7.32 (m, 1H, Ph), 7.48 – 7.42 (m, 1H, Ph), 7.56 – 7.52 (m, 1H, Ph), 7.67 (d, *J* = 2.1 Hz, 1H, C*H*), 7.99 (s, 1H, Ph).
Table 36, entry 6: ^{1}H NMR (δ, $CDCl_3$, 20°C): 2.32 (s, 3H, C*H*$_3$), 3.62 (s, 3H, COOC*H*$_3$), 4.71 (dd, *J* = 7.5 Hz, *J* = 1.8 Hz, 1H, C*H*), 5.64 (d, *J* = 7.5 Hz, 1H, C*H*), 7.17 – 7.06 (m 4H, Ph and C*H*), 7.55 – 7.43 (m, 4H, Ph).

4.9 Crystallographic Data

All data were collected on a Bruker Smart CCD area detector diffractometer using graphite-monochromated Mo Kα radiation (λ = 0.71073 Å) and 0.3° ω-scan frames covering a hemisphere or complete spheres of the reciprocal space. Corrections for absorption, $\lambda/2$ effects, and crystal decay were applied[167]. The structures were solved by direct methods using the program SHELXS97[168]. Structure refinement on F^2 was carried out with the program SHELXL97[3]. All non-hydrogen atoms were refined anisotropically. Hydrogen atoms were inserted in idealized positions and were refined riding with the atoms to which they were bonded.

---

[167] Bruker programs: SMART, version 5.054; SAINT, version 6.2.9; SADABS, version 2.10; XPREP, version 5.1; SHELXTL, version 5.1 (Bruker AXS Inc., Madison, WI, 2001).
[168] Sheldrick, G. M. SHELX97: Program System for Crystal Structure Determination; University of Göttingen, Göttingen, Germany, 1997.

	7a·3CH_3CN	**7b**·solv[a]	**7f**
Empirical formula	$C_{41}H_{43}B_2F_8FeN_9P_2$	$C_{23}H_{42}B_2F_8FeN_6P_2$	$C_{23}H_{30}B_2F_8FeN_6O_{12}P_2$
MW [g·mol^{-1}]	953.25	694.04	873.94
Crystal size [mm]	0.72 x 0.24 x 0.18	0.54 x 0.41 x 0.30	0.53 x 0.42 x 0.24
Space group	P21/c (no. 14)	P212121 (no. 19)	P212121 (no. 19)
a [Å]	16.3735(8)	11.0106(5)	8.8343(4)
b [Å]	11.6332(6)	18.6305(8)	11.0454(5)
c [Å]	24.4946(13)	19.4426(8)	35.9063(18)
α [º]	90	90	90
β [º]	99.322(1)	90	90
γ [º]	90	90	90
V [Å^3]	4604.0(4)	3988.3(3)	3503.7(3)
Z	4	4	4
ρ_{calc} [g·cm^{-3}]	1.375	1.156	1.657
T [K]	173(2)	173(2)	173(2)
μ [mm^{-1}] (Mo K_α)	0.470	0.516	0.631
F(000)	1960	1440	1776
θ_{max} [º]	25	27	30
no. of rflns. measd.	46985	48932	52428
no. of unique rflns.	8075	8660	10209
no. of rflns. I > 2σ(I)	6284	8257	9987
no. of params.	602	462	518
R_1 (I > 2σ(I))	0.0500	0.0490	0.0321
R_1 (all data)	0.0683	0.0512	0.0329
wR_2 (all data)	0.1410	0.1366	0.0834
Diff. Four. peaks (min/max) [eÅ^{-3}]	-0.52/0.82	-0.30/0.68	-0.20/0.53

$$R_1 = \frac{\sum \left| |F_o| - |F_c| \right|}{\sum |F_o|} \qquad \omega R_2 = \left[\frac{\sum \omega \left(F_o^2 - F_c^2 \right)}{\sum \omega \left(F_o^2 \right)} \right]^{1/2}$$

[a]Solvent disordered and squeezed with program PLATON (Spek, A. L., 2004). Chemical formula and derived quantities ρ_{calc}, μ, and F(000) are given without solvent contributions.

	8a·solv[a]	**8b**·solv[a]	**8c**
Empirical formula	$C_{89}H_{76}B_2FeN_6P_2$	$C_{44}H_{36}B_2F_8FeN_6P_2$	$C_{58}H_{50}B_2F_8FeN_6P_4$
MW [g·mol^{-1}]	1368.97	940.20	1184.39
Crystal size [mm]	0.62 x 0.42 x 0.40	0.62 x 0.14 x 0.12	0.48 x 0.45 x 0.43
Space group	P-1 (no. 2)	$P2_12_12_1$ (no. 19)	I-43d (no. 220)
a [Å]	11.659(2)	10.9571(5)	25.3728(4)
b [Å]	13.706(3)	14.1550(6)	25.3728(4)
c [Å]	24.476(5)	31.6243(15)	25.3728(4)
α [º]	89.319(4)	90	90
β [º]	79.691(4)	90	90
γ [º]	87.069(4)	90	90
V [Å^3]	3843.0(13)	4904.9(4)	16334.5(4)
Z	2	4	12
ρ_{calc} [g·cm^{-3}]	1.183	1.273	1.445
T [K]	296(1)	173(2)	173(2)
μ [mm^{-1}] (Mo K_α)	0.287	0.439	0.469
F(000)	1436	1920	7296
θ_{max} [º]	25	25	27
no. of rflns. measd.	46708	59833	19617
no. of unique rflns.	13404	8573	2962
no. of rflns. I > 2σ(I)	9921	8025	2465
no. of params.	902	594	200
R_1 (I > 2σ(I))	0.0515	0.0440	0.0449
R_1 (all data)	0.0704	0.0476	0.0606
wR_2 (all data)	0.1422	0.1128	0.1305
Diff. Four. peaks (min/max) [eÅ^{-3}]	-0.36/0.45	-0.30/0.39	-0.23/0.25

$$R_1 = \frac{\sum \left| |F_o| - |F_c| \right|}{\sum |F_o|} \qquad \omega R_2 = \left[\frac{\sum \omega \left(F_o^2 - F_c^2 \right)}{\sum \omega \left(F_o^2 \right)} \right]^{1/2}$$

[a]Solvent disordered and squeezed with program PLATON (Spek, A. L., 2004). Chemical formula and derived quantities ρ_{calc}, μ, and F(000) are given without solvent contributions.

	9b·$(CH_3)_2CO$	**7d**·solv[a]	**10**·CH_3CN
Empirical formula	$C_{25}H_{45}B_2F_8FeN_5O_2P_2$	$C_{35}H_{30}B_2F_8FeN_6O_4P_2$	$C_{37}H_{32}BF_4FeN_7O_4P_2$
MW [g·mol^{-1}]	739.07	890.06	843.30
Crystal size [mm]	0.46 x 0.28 x 0.26	0.54 x 0.38 x 0.34	0.52 x 0.26 x 0.12
Space group	P21/c (no. 14)	P-1 (no. 2)	P-1 (no. 2)
a [Å]	10.8683(9)	12.5467(7)	12.7153(6)
b [Å]	10.4976(8)	18.0244(11)	13.1428(6)
c [Å]	29.963(2)	19.2853(11)	13.1741(6)
α [º]	90	101.294(1)	63.936(1)
β [º]	99.796(2)	99.336(1)	73.814(1)
γ [º]	90	94.203(1)	86.801(1)
V [Å^3]	3368.7(4)	4195.3(4)	1893.6(2)
Z	4	4	2
ρ_{calc} [g·cm^{-3}]	1.457	1.409	1.479
T [K]	173(2)	173(2)	173(2)
μ [mm^{-1}] (Mo K_α)	0.619	0.515	0.553
F(000)	1536	1808	864
θ_{max} [º]	29.96	27	30
no. of rflns. measd.	44797	50294	27966
no. of unique rflns.	9753	18196	10890
no. of rflns. I > 2σ(I)	8247	14787	9367
no. of params.	408	1085	520
R_1 (I > 2σ(I))	0.0374	0.0420	0.0359
R_1 (all data)	0.0470	0.0527	0.0436
wR_2 (all data)	0.0980	0.1237	0.1002
Diff. Four. peaks (min/max) [eÅ^{-3}]		-0.37/0.77	-0.36/0.56

$$R_1 = \frac{\sum \left| |F_o| - |F_c| \right|}{\sum |F_o|} \qquad \omega R_2 = \left[\frac{\sum \omega \left(F_o^2 - F_c^2 \right)}{\sum \omega \left(F_o^2 \right)} \right]^{1/2}$$

[a]Solvent disordered and squeezed with program PLATON (Spek, A. L., 2004). Chemical formula and derived quantities ρ_{calc}, μ, and F(000) are given without solvent contributions.

	12a·$(C_2H_5)_2O$	**15**	**16**
Empirical formula	$C_{21}H_{43}Cl_2FeN_3OP_2$	$C_{23}H_{16}Br_2FeNO_3P$	$C_{32}H_{30}B_2F_8FeN_8P_2$
MW [g·mol^{-1}]	542.27	601.01	818.05
Crystal size [mm]	0.54 x 0.28 x 0.20	0.36 x 0.23 x 0.20	0.45 x 0.35 x 0.27
Space group	P212121 (no. 19)	P2(1)/c	P2(1)/c
a [Å]	9.6583(5)	10.2554(5)	12.170(3)
b [Å]	14.5653(7)	10.9390(5)	11.946(3)
c [Å]	20.2207(10)	19.7572(10)	25.332(5)
α [º]	90	90	90
β [º]	90	93.3060(10)	95.342(4)
γ [º]	90	90	90
V [Å^3]	2844.6(2)	2212.75(19)	3666.8(13)
Z	4	4	4
ρ_{calc} [g·cm^{-3}]	1.266	1.804	1.482
T [K]	173(2)	173(2)	297(2)
μ [mm^{-1}] (Mo K_α)	0.0847	0.71073	0.71073
F(000)	1152	1184	1664
θ_{max} [º]	29.92	30.00	27.00
no. of rflns. measd.	32002	28777	27951
no. of unique rflns.	8261	6221	7967
no. of rflns. I > 2σ(I)	7741	5595	6158
no. of params.	271	296	514
R_1 (I > 2σ(I))	0.0403	0.0422	0.0599
R_1 (all data)	0.0430	0.0484	0.0778
wR_2 (all data)	0.1130	0.0786	0.1579
Diff. Four. peaks (min/max) [eÅ^{-3}]			

$$R_1 = \frac{\sum \left| |F_o| - |F_c| \right|}{\sum |F_o|} \qquad \omega R_2 = \left[\frac{\sum \omega \left(F_o^2 - F_c^2 \right)}{\sum \omega \left(F_o^2 \right)} \right]^{1/2}$$

	17a'·solv[a]	**17c'**·0.5 CH_3OH	**18d**·CH_3OH
Empirical formula	$C_{29}H_{25}Br_2N_3NiP_2$	$C_{43}H_{86}Br_4N_6Ni_2OP_4$	$C_{48}H_{45}BrN_3NiO_8P_3$
MW [g·mol^{-1}]	695.99	1264.04	1023.40
Crystal size [mm]	0.25 x 0.20 x 0.15	0.49 x 0.26 x 0.20	0.70 x 0.42 x 0.03
Space group	P212121 (no. 19)	P-1 (no. 2)	P212121
a [Å]	12.5635(6)	7.8079(4)	15.043(12)
b [Å]	14.9548(7)	7.9355(4)	19.159(12)
c [Å]	18.4417(9)	22.6580(11)	33.21(3)
α [º]	90	80.501(1)	90
β [º]	90	88.178(1)	90
γ [º]	90	80.752(1)	90
V [Å^3]	3464.9(3)	1366.61(12)	9572(12)
Z	4	1	8
ρ_{calc} [g·cm^{-3}]	1.334	1.536	1.420
T [K]	300(2)	173(2)	173(2)
μ [mm^{-1}] (Mo K_α)	2.978	3.767	1.396
F(000)	1392	650	4208
θ_{max} [º]	25	30	23.1
no. of rflns. measd.	36102	25539	11282
no. of unique rflns.	6047	7905	
no. of rflns. I > 2σ(I)	5192	7184	5725
no. of params.	334	280	365
R_1 (I > 2σ(I))	0.0409	0.0218	0.3037
R_1 (all data)	0.0504	0.0253	0.1310
wR_2 (all data)	0.1060	0.0549	0.365
Diff. Four. peaks (min/max) [eÅ^{-3}]	-0.42/0.51	-0.47/0.83	

$$R_1 = \frac{\sum \left| |F_o| - |F_c| \right|}{\sum |F_o|} \qquad \omega R_2 = \left[\frac{\sum \omega \left(F_o^2 - F_c^2 \right)}{\sum \omega \left(F_o^2 \right)} \right]^{1/2}$$

[a]Solvent disordered and squeezed with program PLATON (Spek, A. L., 2004). Chemical formula and derived quantities ρ_{calc}, μ, and F(000) are given without solvent contributions.

	19a·0.5 C_6H_6	**19c**	**20b**
Empirical formula	$C_{33}H_{28}ClN_2NiP_2$	$C_{22}H_{41}ClN_2NiP_2$	$C_{11}H_{19}Cl_2N_2NiP$
MW [g·mol^{-1}]	608.67	489.67	339.86
Crystal size [mm]	0.47 x 0.22 x 0.15	0.58 x 0.25 x 0.05	0.25 x 0.18 x 0.05
Space group	P21/c (no. 14)	Pna21 (no. 33)	P2(1)
a [Å]	9.3016(5)	22.614(2)	11.762(6)
b [Å]	21.4580(12)	7.9747(8)	8.342(5)
c [Å]	15.0813(8)	13.7454(14)	43.56(3)
α [º]	90	90	90
β [º]	99.619(1)	90	92.487(16)
γ [º]	90	90	90
V [Å^3]	2967.8(3)	2478.8(4)	4270(4)
Z	4	4	12
ρ_{calc} [g·cm^{-3}]	1.362	1.312	1.586
T [K]	297(2)	173(2)	173(2)
μ [mm^{-1}] (Mo K_α)	0.877	1.030	0.71073
F(000)	1260	1048	2112
θ_{max} [º]	28	30	22.93
no. of rflns. measd.	20760	17862	21041
no. of unique rflns.	7147	6018	18333
no. of rflns. I > 2σ(I)	3374	5453	5977
no. of params.	352	265	445
R_1 (I > 2σ(I))	0.0391	0.0335	0.1950
R_1 (all data)	0.1026	0.0409	0.3155
wR_2 (all data)	0.0788	0.0821	0.4134
Diff. Four. peaks (min/max) [eÅ^{-3}]	-0.34/0.33	-0.44/0.56	

$$R_1 = \frac{\sum \left| |F_o| - |F_c| \right|}{\sum |F_o|} \qquad \omega R_2 = \left[\frac{\sum \omega \left(F_o^2 - F_c^2 \right)}{\sum \omega \left(F_o^2 \right)} \right]^{1/2}$$

	21c·2 CH_2Cl_2	**21e**·Et_2O·2CH_3CN	**24**·DMF
Empirical formula	$C_{23}H_{45}Cl_6N_3P_2Pd$	$C_{68}H_{58}Cl_2F_6N_8O_{15}P_4Pd_2S_2$	$C_{32}H_{29}ClN_4O_6P_2Pd$
MW [g·mol^{-1}]	744.66	1812.92	769.38
Crystal size [mm]	0.42 x 0.23 x 0.18	0.32 x 0.16 x 0.14	0.22 x 0.20 x 0.18
Space group	Cc (no. 9)	P-1 (no. 2)	P21/c
a [Å]	11.9574(6)	12.9005(18)	9.4778(4)
b [Å]	24.8990(12)	16.118(3)	13.7127(6)
c [Å]	11.8565(6)	20.204(3)	24.2252(10)
α [º]	90.00	90.731(3)	90
β [º]	102.277(2)	107.214(3)	94.642(1)
γ [º]	90.00	113.257(3)	90
V [Å^3]	3449.3(3)	3646.4(10)	3138.1(2)
Z	4	2	4
ρ_{calc} [g·cm^{-3}]	1.434	1.651	1.628
T [K]	173(2)	173(2)	173(2)
μ [mm^{-1}] (Mo K_α)	1.113	0.798	0.831
F(000)	1528	864	1560
θ_{max} [º]	30	25	29.93
no. of rflns. measd.	31983	36241	9598
no. of unique rflns.	10031	12667	
no. of rflns. I > 2σ(I)	9673	9428	7211
no. of params.	318	966	421
R_1 (I > 2σ(I))	0.0296	0.0518	0.0401
R_1 (all data)	0.0309	0.0780	0.0330
wR_2 (all data)	0.0782	0.1369	0.0768
Diff. Four. peaks (min/max) [eÅ^{-3}]	-0.40/0.86	-1.14/1.59	

$$R_1 = \frac{\sum \left\| F_o \right| - \left| F_c \right\|}{\sum \left| F_o \right|} \qquad \omega R_2 = \left[\frac{\sum \omega \left(F_o^2 - F_c^2 \right)}{\sum \omega \left(F_o^2 \right)} \right]^{1/2}$$

	25a·2DMF	**25d**·CH_3CN	**26b**
Empirical formula	$C_{36}H_{39}ClN_4O_2P_2Pd$	$C_{33}H_{27}ClF_3N_3P_2Pd$	$C_{20}H_{33}F_3N_2O_2P_2Pd$
MW [g·mol^{-1}]	763.50	726.37	558.82
Crystal size [mm]	0.40 x 0.27 x 0.23	0.38 x 0.28 x 0.204	0.62 x 0.55 x 0.38
Space group	P212121 (no. 19)	P21/n (no. 14)	P21/n (no. 14)
a [Å]	12.9104(6)	11.1604(5)	12.4771(6)
b [Å]	14.3253(6)	19.9505(9)	14.3627(7)
c [Å]	18.6546(8)	13.6931(6)	13.8741(7)
α [º]	90	90	90
β [º]	90	94.624(1)	94.266(1)
γ [º]	90	90	90
V [Å^3]	3450.1(3)	3038.9(2)	2479.4(2)
Z	4	4	4
ρ_{calc} [g·cm^{-3}]	1.470	1.588	1.497
T [K]	173(2)	173(2)	173(2)
μ [mm^{-1}] (Mo K_α)	0.747	0.851	0.918
F(000)	1568	1464	1144
θ_{max} [º]	30	30	30
no. of rflns. measd.	45267	44927	33847
no. of unique rflns.	9963	8788	7185
no. of rflns. I > 2σ(I)	9661	8429	6630
no. of params.	427	389	281
R_1 (I > 2σ(I))	0.0234	0.0203	0.0263
R_1 (all data)	0.0246	0.0213	0.0290
wR_2 (all data)	0.0628	0.0533	0.0678
Diff. Four. peaks (min/max) [eÅ^{-3}]	-0.31/0.83	-0.55/0.74	-0.61/0.95

$$R_1 = \frac{\sum \left| |F_o| - |F_c| \right|}{\sum |F_o|} \qquad \omega R_2 = \left[\frac{\sum \omega \left(F_o^2 - F_c^2 \right)}{\sum \omega \left(F_o^2 \right)} \right]^{1/2}$$

	28a·CH_2Cl_2·$HNEt_3Br$	**30**	**32a**	**32b**
Empirical formula	$C_{37}H_{43}Br_2Cl_2N_3P_2Pt$	$C_{21}H_{16}Cl_2NOPPd$	$C_{20}H_{20}BF_4N_2PPd$	$C_{14}H_{24}BF_4N_2PPd$
MW [g·mol^{-1}]	1017.49	506.62	512.56	444.53
Crystal size [mm]	0.18 x 0.12 x 0.10		0.45 x 0.25 x 0.24	0.40 x 0.16 x 0.14
Space group	P21/c (no. 14)		P2(1)2(1)2(1)	P2(1)2(1)2(1)
a [Å]	8.7928(5)	10.302(2)	9.9980(4)	10.2776(6)
b [Å]	18.5713(11)	11.329(4)	12.7834(5)	11.9892(7)
c [Å]	24.1001(14)	17.054(3)	15.9105(6)	15.1736(9)
α [º]	90	90	90	90
β [º]	97.161(1)	99.025(7)	90	90
γ [º]	90	90	90	90
V [Å^3]	3904.7(4)	1965.8(9)	2033.50(14)	1869.69(19)
Z	4	4	4	4
ρ_{calc} [g·cm^{-3}]	1.731	1.712	1.674	1.579
T [K]	173(2)	173(2)	100(2)	100(2)
μ [mm^{-1}] (Mo K_α)	5.889	0.71073	0.71073	0.71073
F(000)	1992	1008	1024	896
θ_{max} [º]	30	29.96	30.06	30.09
no. of rflns. measd.	57788	9561	24216	24084
no. of unique rflns.	11370	4879	5986	5516
no. of rflns. I > 2σ(I)	9338	4007	5852	5074
no. of params.	424	244	266	208
R_1 (I > 2σ(I))	0.0293	0.0380	0.0167	0.0279
R_1 (all data)	0.0412	0.0488	0.0171	0.0339
wR_2 (all data)	0.0722	0.1027	0.0432	0.0617
Diff. Four. peaks (min/max) [eÅ^{-3}]	-1.60/1.48			

$$R_1 = \frac{\sum \left| |F_o| - |F_c| \right|}{\sum |F_o|} \qquad \omega R_2 = \left[\frac{\sum \omega \left(F_o^2 - F_c^2 \right)}{\sum \omega \left(F_o^2 \right)} \right]^{1/2}$$